

Alma Mater Studiorum – Università di Bologna

DOTTORATO DI RICERCA IN
SALUTE, SICUREZZA E SISTEMI DEL VERDE

Ciclo 34

Settore Concorsuale: 05/A1 - Botanica

Settore Scientifico Disciplinare: BIO/15 - Biologia Farmaceutica

NATURAL PRODUCT CHEMISTRY AND METABOLOMICS: A ROADMAP
THROUGH CIRCULAR ECONOMY, SUSTAINABLE AGRICULTURE, AND
BIODIVERSITY VALORIZATION

Presentata da: Ilaria Chiocchio

Coordinatore Dottorato

Patrizia Tassinari

Supervisore

Ferruccio Poli

Co-Supervisor

Manuela Mandrone
Daniele Torreggiani

Esame finale anno 2022

Abstract

Inspired by the Sustainable Developmental Goals of the Agenda 2030, this work addressed three topics of pivotal importance in the sustainability era, namely: circular economy, sustainable agriculture, and biodiversity valorization. Natural products chemistry and metabolomics were keys to achieve the following aims: 1) the valorization of waste plant material for circular economy, 2) the achievement of deep knowledge of plant-environment interactions in view of sustainable agriculture, 3) the biodiversity valorization through the investigation of local flora.

The first aim was accomplished by analyzing the phytochemical profile and the bioactivity of neglected plants matrices. Residues of aromatic plants after distillation resulted active against a plant pathogen suggesting a potential reuse of these matrices in agriculture. In addition, by-products of chestnut cultivation proved endowed with *in vitro* neuroprotective properties.

The second aim was achieved by the development of two case studies. In particular, a work was carried out in field to study *Sorghum bicolor* subjected to several environmental and anthropic factors, and the other one in greenhouse exploring *Taxus baccata* responses to different LED lighting. Metabolomics proved successful to identify sorghum biomarkers for crop quality and development and allowed to monitor taxus growth providing useful insights for sustainable agriculture.

To achieve the third aim, spontaneous plants collected in Sardinia were investigated for their antiproliferative activities. Five plants resulted endowed with promising bioactivity thus their phytochemical composition was investigated through NMR spectroscopy. Finally, a focus on chemodiversity was placed by studying *Solanum dulcamara* chemotypes through MS metabolomics which revealed that the chemotypes differed for the leaf steroidal glycoalkaloids.

The overall thesis work underlined the importance of plant specialized metabolites in multiple fields and demonstrated that the study of these molecules aids the sustainable development, enhancing circular economy, sustainable agriculture, and biodiversity valorization. In this context, metabolomics approach resulted particularly interesting.

Table of contents

Introduction.....	1
The Sustainability Era.....	1
The contribute of Natural Products Chemistry to sustainability	4
NMR-based metabolomics: a powerful tool in Natural Products Chemistry.....	6
Objectives and thesis structure.....	7
Chapter 1	
<i>The importance of plant secondary metabolites for circularity</i>	11
1.1. Plant Secondary Metabolites: An Opportunity for Circular Economy	12
1.2. Leaves and Spiny Burs of <i>Castanea sativa</i> from an Experimental Chestnut Grove: Metabolomic Analysis and Anti-Neuroinflammatory Activity.....	61
1.3. From waste to phyto-protection: screening of 37 neglected plant matrices against <i>Clavibacter michiganensis</i> and <i>Pseudomonas syringae</i>	82
Chapter 2	
<i>Achieving sustainable agriculture through smart and innovative growth systems</i>	98
2.1. Metabolomic Study of Sorghum (<i>Sorghum bicolor</i>) to Interpret Plant Behavior under Variable Field Conditions in View of Smart Agriculture Applications	99
2.2. Effects of LED supplemental lighting on the growth and metabolomic profile of <i>Taxus baccata</i> cultivated in a smart greenhouse.....	131
Chapter 3	
<i>Natural products research and chemodiversity as a base for biodiversity protection</i>	160
3.1. Antitumor Potential and Phytochemical Profile of Plants from Sardinia (Italy), a Hotspot for Biodiversity in the Mediterranean Basin	161
3.2. A metabolomic study of leaves and adventitious roots of <i>Solanum dulcamara</i> chemotypes....	187
Conclusions.....	194

Introduction

The Sustainability Era

“Sustainable development is development that meets the needs of the present without compromising the ability of future generations to meet their own needs”. This definition, given by the World Commission on Environment and Development in 1987 [1], can be considered the fundamental idea behind a new era: the era of sustainability [2]. Since 1950 global population has increased extremely fast and consequently also the environmental footprint of mankind has increased [3]. The demand of resources, such as food and energy, with the associated production of wastes and pollution, has reached a tipping point, making urgent a transition from the present model of development to a more sustainable one. This transition implies the cooperation between relevant stakeholders such as governmental bodies, private producing parties, scientists, and non-governmental organizations, and requires policies and actions [4]. In 2015, United Nations adopted the 2030 Agenda, which lists 17 Sustainable Development Goals (SDGs), defining precise targets and indicators to end poverty, protect the planet and improve everyone’s life and prospects, everywhere [5]. Obviously, resources and environment management play a pivotal role in the Agenda. For instance, goal 2 is “zero hunger” and highlights the importance of increasing agricultural productivity and sustainable food production; goal 12 is “responsible consumption and production”, decoupling also economic growth from environmental degradation. Lastly, goals 14 and 15 specifically address the conservation of biodiversity and natural habitats [5].

Sustainable agriculture

In 2017 the estimated undernourished people were 821 million, a number which has been rising since 2014 and most likely will be worsened by the actual COVID pandemic [6]. Changing this trend is one of the great challenges of our time and requires global actions. The global community has defined the following targets to achieve goal 2: universal access to safe and nutritious food; end all forms of malnutrition; double the productivity and incomes of small-scale food producers; sustainable food production and resilient agricultural practices; maintain the genetic diversity in food production; invest in rural infrastructures, agricultural research, technology, and gene banks; prevent

agricultural trade restrictions, market distortions, and export subsidies; ensure stable food commodity markets and timely access to information [5]. Clearly, these targets cannot be achieved without a deep understanding of the complex agricultural ecosystems and require interdisciplinary work of scientists from various research areas, such as agronomy, ecology, sociology, economics, and politics.

With the objective of achieving sustainable agriculture, several strategies have been adopted from the simple adjustment of the crop management to fundamental changes at the farming system level. Lichtfouse et al. [7] described three main strategies: firstly, the substitution strategy which is based on the logic of replacing a farming technique with a more sustainable one, for example, to substitute toxic chemicals with compounds which are less pollutant or less persistent in soil; secondly, the agroecological strategy, which involves the application of ecological concepts such as enhancing biodiversity by intercropping or rotating crops; finally, the global strategy whose principle is to solve agricultural issues at global scale. Other emerging agricultural biotechnologies were recently described by Anderson et al. [8] and are mainly based on genetic and molecular tools to produce transgenic crops resistant to diseases or more tolerant to abiotic stress.

Circular economy

While part of the global population is suffering hunger and malnutrition, another one is dealing with obesity and food wastes. Already in 2011 FAO (Food and Agriculture Organization of the United Nations) estimated that one-third of food (about 1.3 billion tonnes per year) is lost or wasted globally. This is not only an ethical issue but also an environmental one. Together with the food itself, other resources, such as land, water, energy, soil, and seeds are wasted and greenhouse gasses are emitted in vain [9].

In nature there are no wastes, everything is transformed like in a closed-loop, in fact, cycles, such as of water and nutrients, are very common. Basically, this is the idea behind the circular economy: to avoid waste production making it a source for others so closing loops.

Since 2015, the European Commission has adopted the Circular Economy Plan and implemented it in 2020. This strategy presents initiatives aimed at reducing waste production and implementing the SDGs [10], in fact, awareness about this problem was raised also by the United Nations especially in goal 12 of the Agenda 2030.

On one hand, the global waste is expected to grow to 3.40 billion tons by 2050 [11], on the other hand, it has been estimated that moving towards a circular economy Gross Domestic Product in European Union will increase by almost 0.5% by 2030 compared to the baseline case [12]. The measures contained in the Circular Economy Action Plan can help the shift to a more resilient economy providing guidelines for policy and companies. In parallel, also the scientific community is manifesting a growing interest in the topic, as reflected by the number of publications which is raised from less than 200 in 2015 to more than 3100 in 2020 [13]. One notable example of how research can help the implementation of circular economy practices is represented by the valorization of agri-food loss and waste, studying these matrices, and finding potential application in the food, cosmetic, and pharmaceutical industries. In fact, especially waste of plant origin are source of nutrients, enzymes, and bioactive compounds that can be employed in different industrial sectors [14].

Biodiversity

Excessive resources extraction, greenhouse gas emissions, and pollution drastically change ecosystems leading to the loss of biodiversity. Despite some progress made towards sustainable forest management, about 100 million hectares of forest have been lost from 2000 to 2020 and around 1 million of animal and plant species are threatened with extinction [5]. This has profound consequences for human well-being and survival. For example, one consequence of interfering with the natural balance within ecosystems is the occurrence of zoonosis, as also recently shown by the COVID-19 pandemic.

The value of biodiversity for human beings is also emphasized in the following words of United Nations, 34th Session of the Human Rights Council:

“The full enjoyment of human rights, including the rights to life, health, food and water, depends on the services provided by ecosystems. The provision of ecosystem services depends on the health and sustainability of ecosystems, which in turn depend on biodiversity. The full enjoyment of human rights thus depends on biodiversity, and the degradation and loss of biodiversity undermine the ability of human beings to enjoy their human rights.” [15].

Even though the focus on biodiversity is placed in goals 14 and 15 of the Agenda, according to Blicharska et al. [16], biodiversity can contribute to the fulfillment of all the SDGs, either directly or indirectly. In order to counteract the loss of biodiversity it is also

important the establishment of new protected areas; the improvement of regulation, monitoring, and surveillance; combating desertification, illegal fishing, and hunting as well as increasing scientific knowledge [5].

Concerning plants, in addition to provide oxygen, absorbing carbon dioxide, offering food and habitat for many species, they represent a precious source of unique metabolites, also known as secondary metabolites or plant specialized metabolites. Thanks to secondary metabolism, plants can interact with the environment, however, the reason why such extraordinary chemical diversity exists is still debated. One of the most accredited hypotheses is the “interaction diversity” hypothesis, which posits that plants produce numerous compounds because they interact with numerous organisms [17,18]. In this view, secondary metabolites diversity (chemodiversity) can benefit plants in multispecies interactions and the other way around, namely plants grown in a high biodiverse environment likely express higher chemical diversity compared to plants cultivated in a low biodiverse environment, i.e. monoculture. This peculiarity of plants, turns out to be useful also in natural product chemistry, especially in drug discovery [19-21].

In this context, increasing knowledge about plant species, their specific metabolites and their ecological role and potential use, is particularly relevant in biodiversity research, not only for practical and technological purposes but also to increase awareness on the importance of biodiversity and to finally contribute to its preservation.

The contribute of Natural Products Chemistry to sustainability

Natural products chemistry covers the study of chemical compounds produced by living organisms. This research field has led to many innovations, particularly in medicine, where it has been estimated that up to 50% of the approved drugs during the last 30 years are coming from natural products, either directly or indirectly, and many of these are plant-derived [22]. These latter generally belong to secondary metabolites and play different functions in plants, including defense against predators or attraction of pollinators [23]. Over 400 million years, plants have shaped their chemistry and lately, also humans have learned to profit from these precious sources. Phytochemical investigation on *Taxus brevifolia*, *Artemisia annua*, *Galanthus nivalis*, and *Salix alba* resulted in the discovery of taxol, artemisinin, galantamine, and acetylsalicylic acid, providing the basis to treat or even heal diseases as cancer, malaria, Alzheimer’s, or

simple pain and inflammation. Natural products can either be used directly as pharmaceutical agents or serve as lead compounds. Despite other strategies have been adopted in search of new leads, such as high throughput screening systems and combinatorial chemistry, most likely nature will continue to offer a significant portion of these leads [24].

Besides the pharmaceutical field, natural products are also employed for several other purposes. For example, in the food industry carotenoids are used as natural pigments [25], phenolic compounds and terpenes with antimicrobial properties are employed as natural preservatives [26], and terpenes are also used as flavoring and perfuming compounds [27]. Even agriculture can benefit from natural products, which find application as pesticides, herbicides, or are used as starting material or as leads in the synthesis of substances for crop protection [28,29]. In search for new molecules, focusing on understudied plants or conducting research in highly biodiverse areas (which likely return high chemical diversity), is particularly promising. Additionally, nowadays the possibility of recovering bioactive molecules from waste appears very attractive in view of sustainable development.

The extraordinary chemical diversity of secondary metabolites and consequently the wide range of possibilities for their utilization, explain the relevance of natural products chemistry. However, in addition to study single molecules, their chemical structure, and their biological properties, focusing on extracts and their phytochemical patterns is equally important. For example, studying the metabolomic change within an organ or the entire organism in different biotic or abiotic conditions is useful to understand why a plant species produces a peculiar molecule, thus clarifying the biological or ecological role of this latter [30]. Unrevealing the metabolic pathways beyond the natural product of interest, is crucial to develop biotechnological methods for its synthesis [31]. Measuring the change of metabolites triggered by the administration of a natural product is relevant to understand its mechanism of action and its toxicity [32]. All these objectives can be achieved through multidisciplinary work and adopting an “omic” approach, in particular, metabolomics proved successful in different research fields such as drug discovery, evolutionary biology, and chemical ecology.

In conclusion, the study of natural products, especially supported by the metabolomics approach, brought innovation in several disciplines and, in the light of what

described in the previous paragraph, plays an important role in implementing scientific knowledge also in fields such as biodiversity, circular economy, and sustainable agriculture representing the *fil rouge* of this thesis work.

NMR-based metabolomics: a powerful tool in Natural Products Chemistry

The classical phytochemical approach to the study of plant metabolites requires extraction, isolation and purification through chromatographic methods, and structural elucidation using techniques such as nuclear magnetic resonance (NMR) spectroscopy and mass spectrometry (MS). This approach is time-consuming, requires the use of a large quantity of solvents and starting plant material, and revealed some pitfalls when employed for lead compound discovery, such as degradation and isolation of compounds that are already known (replication).

A novel approach is offered by metabolomics, defined as “the area of research which strives to obtain complete metabolic fingerprints, to detect differences between them and to provide hypothesis to explain those differences” [33]. The successful execution of metabolomics applied to natural products chemistry depends primarily on the proper harvesting and sample preparation. The following steps include the analysis of a sufficient number of samples to be compared, the multivariate data analysis, the identification of the biomarkers of interest, the extraction of biological knowledge, and the validation of the generated hypothesis(s) [34].

Since its foundation in the late 1990s, metabolomics has proven to be a valuable tool for the analysis of biological systems and has been used in different fields, including medical science, synthetic biology, medicine, and predictive modeling of plant, animal, and microbial systems [35]. Currently, the main methods used for metabolomic studies rely on NMR or MS coupled with Chromatography (liquid or gas). Each method has its respective advantages and disadvantages. NMR is highly reproducible, fast, quantitative, and avoids samples derivatization treatments. However, its main limitation is its low sensitivity. MS is a highly sensitive technique that can reveal information on thousands of different metabolites. The main challenges associated with MS are reproducibility and compounds identification [36].

Simple and fast sample preparation, short measurement time, advanced data analysis methods, the possibility to determine the structures of known or unknown

compounds using advanced two-dimensional (2D) techniques make the NMR-based metabolomic approach a very powerful tool for the profiling of crude plant extracts and for the rapid identification of bioactive natural products [37]. To date, numerous applications of NMR-based metabolomics have been reported in plants natural products chemistry, such as the quality control of botanicals or foods [38], chemotaxonomy [39], analysis of genetically modified plants [40], interactions between plants and other organisms [41], plant disease diagnosis [42]. Moreover, NMR-metabolomics combined with projection-based multivariate data analysis (PLS-DA, PLS) provides the possibility to link the chemical profile of plant extracts to their bioactivity data [43], offering a valid approach to solve the major challenge in the studies of medicinal plants: to identify the active compounds into a complex biological matrix.

Objectives and thesis structure

This thesis work, inspired by Sustainable Developmental Goals, addresses this topic through three research lines focused on: 1) circular economy, 2) sustainable agriculture, 3) biodiversity. Consequently, the work is structured in three chapters covering the overmentioned subjects and the obtained results.

Chapter one, dedicated to circular economy, includes a bibliographic survey, which was carried out as first step of this work, in order to assess the state of the art about recovery of bioactive compounds from neglected matrices of plant origin. Moreover, this chapter includes two works done on waste plant material, obtained from local industries and providers. These matrices, properly treated and extracted, were investigated by analyzing both the phytochemical profile and their potential biological activities, in order to valorize these products for the use in the pharmaceutical or agrochemical industries. In fact, recovering functional ingredients from easily available and low-cost material contributes to tackling the economic and environmental problem of the disposal of such waste by promoting recycling or re-use, thus enhancing the circular economy.

Chapter 2 addressed the topic of sustainable agriculture, which requires to adopt cultivation techniques that use fewer inputs and resources without drastically reducing yields and keeping the desired standards of safety and quality. This can only be achieved through a deep knowledge of the plants, their needs, and how they relate to biotic and abiotic factors. In this framework, a field experiment was carried out on *Sorghum bicolor*, a crop important especially for its nutritional value. In this study, untargeted

metabolomics was coupled with agrometeorological survey with the aim of studying the metabolomic variation during crop development and in response to environmental and anthropic factors. Pursuing the goal of understanding how the plant shapes its metabolome in relation to the environment, can help to define the most appropriate farming practices and to develop smart agriculture techniques.

A second research about the topic of sustainable agriculture, was focused on a plant of pharmaceutical interest: *Taxus baccata*. In this case, plants were grown in a smart greenhouse experimenting the effects of supplemental LED lighting on plant's growth and metabolome. The 2030 Agenda highlighted also the importance of innovation and technology as well as the need of developing more sustainable farming systems. Indoor cultivation offers several advantages such as the possibility of reducing water supply and pesticides. Moreover, LEDs are considered more environmentally friendly and economically favorable than the conventional lighting, and have safer management and disposal practices [44,45]. Thus, researching in this field opens up new opportunities for improving agriculture sector.

Finally, a focus on biodiversity and the consequent chemodiversity is reported in chapter 3. Plants collected in Sardinia, an island characterized by high biodiversity and notable degree of endemism, were investigated for their potential antiproliferative activity. Subsequently, their phytochemical composition was investigated by NMR. Additionally, another research project was focused on the chemodiversity of steroidal glycosides of *Solanum dulcamara*. As above-mentioned, searching for new leads is likely more successful in area with high biodiversity, in addition achieving a deep knowledge of the endogenous and endemic species contributes to increase consciousness about the importance of protecting the biodiversity of the territory.

References

1. WCED. Our Common Future: Report of the World Commission on Environment and Development. 1987. Available online: <http://www.un-documents.net/our-common-future.pdf>
2. Conte, E. The era of sustainability: Promises, pitfalls and prospects for sustainable buildings and the built environment. *Sustainability* **2018**, *10*(6), 2092.
3. Motesharrei, S., Rivas, J., Kalnay, E., Asrar, G. R., Busalacchi, A. J., Cahalan, R. F., Cane, M.A., Colwell, R.R., Feng, K., Franklin, R.S., Hubacek, K., Miralles-Wilhelm, F., Miyoshi, T., Ruth, M., Sagdeev, R., Shirmohammadi, A., Shukla, J., Srebric, J., Yakovenko, V.M., Zeng, N. Modeling sustainability: population, inequality, consumption, and bidirectional coupling of the Earth and Human Systems. *National Science Review* **2016**, *3*(4), 470–494.
4. Jansen, L. The challenge of sustainable development. *Journal of cleaner production* **2003**, *11*(3), 231–245.
5. United Nation website . Sustainable developmental Goals. Website: <https://www.un.org/sustainabledevelopment/development-agenda/>
6. Food and Agriculture Organization of the United Nations web site. Available online: <http://www.fao.org/food-loss-and-food-waste/flw-data>.
7. Lichtfouse, E., Navarrete, M., Debaeke, P., Souchère, V., Alberola, C., & Ménassieu, J. Agronomy for sustainable agriculture: a review. *Sustainable agriculture* **2009**, 1–7.
8. Anderson, J. A., Gipmans, M., Hurst, S., Layton, R., Nehra, N., Pickett, J., Shah, D.M., Souza, T.L.P.O., Tripathi, L. Emerging agricultural biotechnologies for sustainable agriculture and food security. *Journal of agricultural and food chemistry* **2016**, *64*(2), 383–393.
9. FAO (Food and Agriculture Organization of the United Nations). Food Wastage Footprint: Impacts on Natural Resources–Summary Report; FAO: Rome, Italy, **2013**.
10. European Commission Website. Available online: <https://ec.europa.eu/environment/circular-economy>.
11. World Bank (2018), What a Waste 2.0: A Global Snapshot of Solid Waste Management to 2050.
12. Cambridge Econometrics, Trinomics, and ICF (2018), Impacts of circular economy policies on the labour market.
13. Scopus analyzer. Query string: TITLE-ABS-KEY (circular AND economy). Accessible online: <https://www.scopus.com>.
14. Osorio, L. L. D. R., Flórez-López, E., & Grande-Tovar, C. D. The Potential of Selected Agri-Food Loss and Waste to Contribute to a Circular Economy: Applications in the Food, Cosmetic and Pharmaceutical Industries. *Molecules* **2021**, *26*(2), 515.
15. United Nations Human Rights Council, 34th Session. Available online at: <https://www.cbd.int/financial/2017docs/humanrights.pdf>.
16. Blicharska, M., Smithers, R. J., Mikusiński, G., Rönnbäck, P., Harrison, P. A., Nilsson, M., & Sutherland, W. J. Biodiversity’s contributions to sustainable development. *Nature sustainability*, **2019**, *2*(12), 1083–1093.
17. Whitehead, S. R., Bass, E., Corrigan, A., Kessler, A., & Poveda, K. Interaction diversity explains the maintenance of phytochemical diversity. *Ecology Letters*, **2021**, *24*(6), 1205–1214.
18. Kessler, A., & Kalske, A. Plant secondary metabolite diversity and species interactions. *Annual Review of Ecology, Evolution, and Systematics*, **2018**, *49*, 115–138.
19. Cordell, G. A. Biodiversity and drug discovery—a symbiotic relationship. *Phytochemistry*, **2000**, *55*(6), 463–480.
20. Kingston, D. G. Modern natural products drug discovery and its relevance to biodiversity conservation. *Journal of natural products*, **2011**, *74*(3), 496–511.
21. da Silva Bolzani, V., Valli, M., Pivatto, M., & Viegas, C. Natural products from Brazilian biodiversity as a source of new models for medicinal chemistry. *Pure and Applied Chemistry*, **2012**, *84*(9), 1837–1846.
22. Veeresham, C. Natural products derived from plants as a source of drugs. *Journal of advanced pharmaceutical technology & research*, **2012**, *3*(4), 200.
23. Demain, A.L.; Fang, A. The natural functions of secondary metabolites. In *History of Modern Biotechnology I, Advances in Biochemical Engineering/Biotechnology*; Fiechter, A., Ed.; Springer: Berlin/Heidelberg, Germany, **2000**; Volume 69, pp. 1–39.
24. Cragg, G. M., & Newman, D. J. Natural products: a continuing source of novel drug leads. *Biochimica et Biophysica Acta (BBA)-General Subjects*, **2013**, *1830*(6), 3670–3695.

25. Aberoumand, A. A review article on edible pigments properties and sources as natural biocolorants in foodstuff and food industry. *WJDFS* **2011**, 6(1), 71–78.
26. Gyawali, R., & Ibrahim, S. A. Natural products as antimicrobial agents. *Food control* **2014**, 46, 412–429.
27. Caputi, L., & Aprea, E. Use of terpenoids as natural flavouring compounds in food industry. *Recent patents on food, nutrition & agriculture* **2011**, 3(1), 9–16.
28. Duke, S. O., Dayan, F. E., Romagni, J. G., & Rimando, A. M. Natural products as sources of herbicides: current status and future trends. *Weed Research (Oxford)* **2000**, 40(1), 99–111.
29. Hüter, O. F. Use of natural products in the crop protection industry. *Phytochemistry reviews* **2011**, 10(2), 185–194.
30. Lankadurai, B. P., Nagato, E. G., & Simpson, M. J. Environmental metabolomics: an emerging approach to study organism responses to environmental stressors. *Environmental Reviews* **2013**, 21(3), 180–205.
31. O'Connor, S. E. Engineering of secondary metabolism. *Annual review of genetics* **2015**, 49, 71–94.
32. Zhao, Q., Zhang, J. L., & Li, F. Application of metabolomics in the study of natural products. *Natural products and bioprospecting* **2018**, 8(4), 321–334.
33. Schripsema, J., & Dagnino, D. Metabolomics: Experimental design, methodology and data analysis. *Encyclopedia of Analytical Chemistry: Applications, Theory and Instrumentation* **2006**, 1–17.
34. Wolfender, J. L., Rudaz, S., Hae Choi, Y., & Kyong Kim, H. Plant metabolomics: from holistic data to relevant biomarkers. *Current Medicinal Chemistry* **2013**, 20(8), 1056–1090.
35. Putri, S. P., Nakayama, Y., Matsuda, F., Uchikata, T., Kobayashi, S., Matsubara, A., & Fukusaki, E. Current metabolomics: practical applications. *Journal of bioscience and bioengineering* **2013**, 115(6), 579–589.
36. Wishart, D. S. Emerging applications of metabolomics in drug discovery and precision medicine. *Nature reviews Drug discovery* **2016**, 15(7), 473–484.
37. Kim, H. K., Y. H. Choi, and R. Verpoorte. 'NMR-based plant metabolomics: where do we stand, where do we go?', *Trends Biotechnol* **2011**, 29: 267–75.
38. Mandrone, M., Marincich, L., Chiocchio, I., Petroli, A., Gođevac, D., Maresca, I., & Poli, F. NMR-based metabolomics for frauds detection and quality control of oregano samples. *Food Control* **2021**, 127, 108141.
39. Kim H.K. Choi, Y.H., & Verpoorte, R. Metabolic classification of Ilex species by NMR based metabolomics. *Phytochemistry* **2010**, 71, 773–784.
40. Le Gall G., Colquhoun I.J., Davis A.L., Collins G.J., Verhoeven M.E. Metabolite profiling of tomato (*Lycopersicon esculentum*) using ¹H NMR spectroscopy as a tool to detect potential unintended effects following a genetic modification. *J Agric Food Chem* **2003**, 51, 2447–56.
41. Allwood, J. W., Ellis, D. I., & Goodacre, R. Metabolomic technologies and their application to the study of plants and plant–host interactions. *Physiologia plantarum* **2008**, 132(2), 117–135.
42. Pontes, J. G. M., Ohashi, W. Y., Brasil, A. J., Filgueiras, P. R., Espíndola, A. P. D., Silva, J. S., Poppi, R.J., Coletta-Filho, H.D., Tasic, L. Metabolomics by NMR spectroscopy in plant disease diagnostic: Huanglongbing as a case study. *ChemistrySelect* **2016**, 1(6), 1176–1178.
43. Kashif A., Muzamal I., Yuliana N.D., Lee Y-J., Park S., Han S., Lee J-W, Lee H-S., Verpoorte R., Choi Y.H. Identification of bioactive metabolites against adenosine A1 receptor using NMR-based metabolomics, *Metabolomics* **2013**, 9, 778–785.
44. Bantis, F.; Smirnakou, S.; Ouzounis, T.; Koukounaras, A.; Ntagkas, N.; Radoglou, K. Current status and recent achievements in the field of horticulture with the use of light-emitting diodes (LEDs). *Sci. Hortic.* **2018**, 235, 437–451.
45. Paucek, I., Appolloni, E., Pennisi, G., Quaini, S., Gianquinto, G., & Orsini, F. LED Lighting systems for horticulture: Business growth and global distribution. *Sustainability* **2020**, 12(18), 7516.

Chapter 1

The importance of plant secondary metabolites for circularity

One of the main goals to achieve a sustainable development is represented by the transition from a linear economy to a circular economy. Which role do plant secondary metabolites play in this regard? These molecules proved endowed with numerous biological activities, thus are employed in different industrial sectors such as pharmaceutical, nutraceutical, cosmetic, agricultural. This chapter is dedicated to the valorization of neglected plant matrices through the recovery of valuable compounds and it is structured in three parts. The first part is a review reporting the state of art about the principal classes of plant secondary metabolites, their biological activities and examples of their recovery from wastes and by-products. The second part reports a research work about the metabolomic analysis and anti-neuroinflammatory activity of leaves and spiny burs from an experimental chestnut grove in Emilia-Romagna region. Finally, a screening of plant neglected matrices as antioxidant and anti-phytopathogens is described in the third part of this chapter.

1.1. Plant Secondary Metabolites: An Opportunity for Circular Economy

This review has been published in *Molecules* Journal:

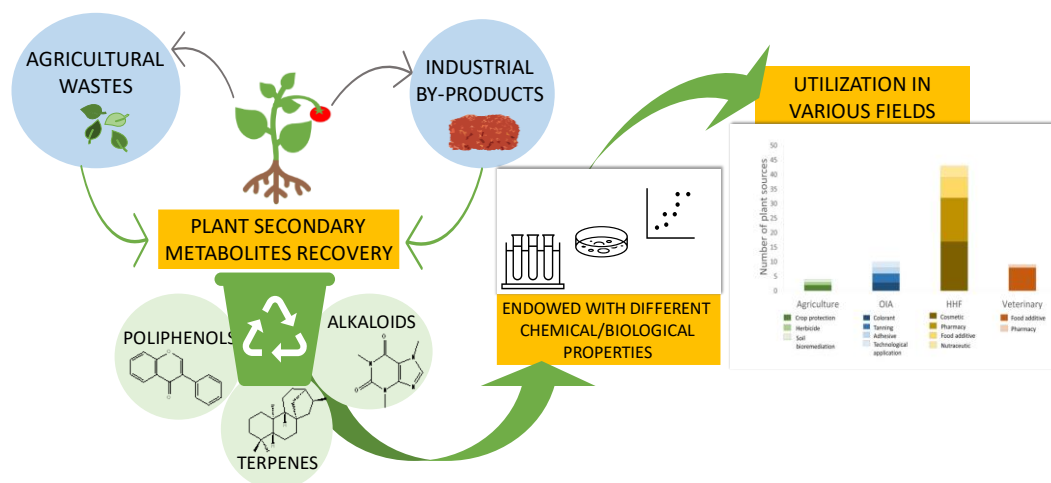
Chiocchio, I.; Mandrone, M.; Tomasi, P.; Marincich, L.; Poli, F. Plant Secondary Metabolites: An Opportunity for Circular Economy. *Molecules* 2021, 26, 495.

<https://doi.org/10.3390/molecules26020495>

Keywords: circular economy; waste valorization; plant by-products; plant secondary metabolites; natural products; bioactivities

Abstract

Moving toward a more sustainable development, a pivotal role is played by circular economy and a smarter waste management. Industrial wastes from plants offer a wide spectrum of possibilities for their valorization, still being enriched in high added-value molecules, such as secondary metabolites (SMs). The current review provides an overview of the most common SM classes (chemical structures, classification, biological activities) present in different plant waste/byproducts and their potential use in various fields. A bibliographic survey was carried out, taking into account 99 research articles (from 2006 to 2020), summarizing all the information about waste type, its plant source, industrial sector of provenience, contained SMs, reported bioactivities, and proposals for its valorization. This survey highlighted that a great deal of the current publications are focused on the exploitation of plant wastes in human healthcare and food (including cosmetic, pharmaceutical, nutraceutical and food additives). However, as summarized in this review, plant SMs also possess an enormous potential for further uses. Accordingly, an increasing number of investigations on neglected plant matrices and their use in areas such as veterinary science or agriculture are expected, considering also the need to implement “greener” practices in the latter sector.



Introduction

According to the United Nations [1], the global population is expected to increase from 7.7 billion (2019) to 9.7 billion in 2050. This prospect raises several concerns about the global consumption of biomass, fossil fuels, metals, and minerals, which should double [2], and annual waste production, following the current trend, will increase by 70% in the next 40 years [3]. Undoubtedly, these premises challenge the move toward amore sustainable development.

In this scenario, wastes and by-products from the food and agricultural industries are gaining international attention, not only for the issues associated with pollution, but also to overcome the paradox of 820 million people suffering from hunger and malnutrition while others are dealing with food over-consumption and related diseases, together with increasing food waste production [4,5]. Moreover, food waste and overproduction imply unnecessary exploitation of the environment and natural resources such as carbon, water, and land. The land footprint estimated by the FAO (Food and Agriculture Organization of the United Nations) in 2013 [6] revealed that almost 30% of the world's agricultural lands are used to produce food that is ultimately lost or wasted, determining additional pollution and greenhouse gases emissions to no actual purpose. Furthermore, food overproduction and bad waste management also have a negative impact on the economy, with money loss at different levels of the supply chain.

Conversely, the reduction of food loss and waste generation has the potential to generate considerable economic value.

ReFED (Rethink Food waste through Economics and Data), a multi-stakeholder nonprofit committed to reducing food waste, identified 27 solutions, which were grouped into three categories: prevention, recovery, and recycling [7]. Although the associated incomes cannot be generalized for all countries, following these solutions, USD 100 billion is expected over 10 years in U.S. According to this program, the solutions focused on preventing waste production account for over 75% of the total, while 23% relate to waste recovery, and only 2% to recycling [5]. This proposal is consistent with the EPA (Environmental Protection Agency) "waste hierarchy," which grades waste prevention as the most preferable option (Figure 1) [8].

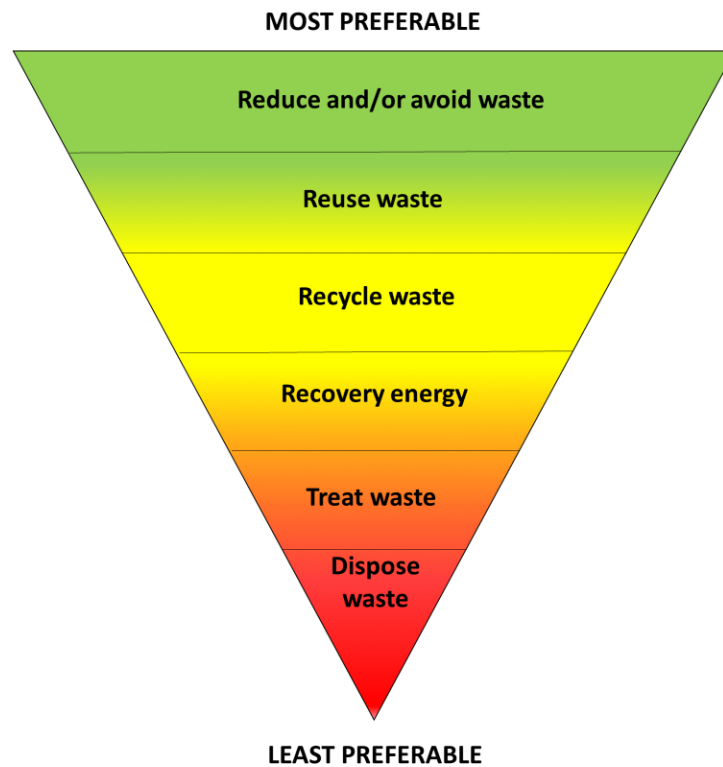


Figure 1. Scheme of the “waste hierarchy” proposed by the EPA [8].

In this scenario, the idea of circular economy took shape, promoting the shift from a linear economic scheme of “take-make-use-dispose” to a circular model, employing reuse, sharing, repair, refurbishment, remanufacturing, and recycling to create a closed-loop system, attempting to minimize the use of resource inputs and the generation of waste, pollution, and carbon emissions [9,10]. In Europe, the most relevant strategy launched in order to attain a sustainable development is the Circular Economy Action Plan, according to which waste materials and energy become input for other industrial processes or regenerative resources for nature (i.e., compost) [11]. In order to facilitate and stimulate the implementation of these guidelines, the scientific community is paying increasing attention to the valorization of industrial and agricultural wastes and by-products, in particular, those derived from plants. These neglected matrices are often manufactured for biofuel production, such as methane or ethanol [12]. However, according to the proposed “waste hierarchy” (Figure 1), energy recovery is a less preferable strategy of waste management, compared to others. Moreover, although biofuel is an alternative to petroleum-derived fuels, its sustainability is quite controversial [13,14].

Actually, the high added-value molecules still contained in plant wastes and byproducts offer a wide spectrum of possibilities for their valorization and reuse, as foreseen by circular economy [15,16]. For example, from agri-food wastes it is still possible to extract macromolecules such as nucleic acids [17], pectin's [18], cellulose material [19], and enzymes such as bromelain, which is derived from pineapple residues and extensively used as a pharmaceutical and meat tenderizer [20]. Primary metabolites (i.e., organic acids, amino acids, carbohydrates) can also be obtained from plant waste material and used for different purposes [21]. Plants in particular produce secondary metabolites (SMs), which are not directly involved in the basic functions of growth, development, and reproduction of the organism, but are essential for long-term survival and play multiple roles, including defense against predators or attraction of pollinators [22]. SMs are endowed with numerous biological activities, making them also extremely important for human health and well-being. Moreover, due to their chemical and biological properties, SMs have also found application in many other fields, serving as pigments, cosmetics, antifeedants and so on [23].

SMs are usually classified according to their biosynthetic pathways in three principal groups: phenolics, terpenes, and alkaloids [24]. These phytochemicals are characterized by enormous chemical and biological diversity and, in addition to being species-specific and organ-specific, their production depends on many biotic and abiotic factors.

One of the most common examples of SM recovery from plant by-products is from fruit peel generated from industrial processes [25], as in the case of citrus peel, from which essential oils [26] as well as phenolic compounds [27] are extracted. Phenolic acids, flavonols, and catecholamines are obtained also from banana peel [28], while carotenoids such as lycopene are usually obtained from tomato peel and other industrial tomato byproducts [29].

Interestingly, SMs are potentially present in all plant organs, offering several possibilities for the valorization of wastes from plant cultivation. In fact, in the agricultural sector, only a few plant organs are harvested and fully consumed, generating numerous wastes at different levels of the supply chain. In this context, scientific investigations aimed at identifying the bioactive compounds contained in these neglected matrices play a pivotal role in laying the basis for their valorization.

Aimed at facilitating and encouraging research projects focused on plant wastes/byproducts and circular economy implementation, the current review provides an overview of the most common SMs present in plant matrices, their classification and bioactivities, and the consequent potential application in different fields of the waste material containing these compounds. Consequently, in this work 99 publications (from 2006 to 2020) focused on plant waste/by-product valorization were reviewed and tabulated in order to schematize the state of the art on this topic and offer the opportunity to easily extrapolate information for the design of new studies on neglected plant material and its reuse in a circular economy perspective.

Polyphenols

Chemical Structure and Classification

Polyphenols are one of the largest and most complex classes of SMs produced by plants, derived from shikimate biosynthesis pathway, which provides precursors for aromatic molecules. Based on the biosynthetic pathway, the number of aromatic rings, carbon atoms, and hydroxyl groups, they are divided into different sub-classes such as: simple phenols, phenolic acids, flavonoids and tannins (Figure 2).

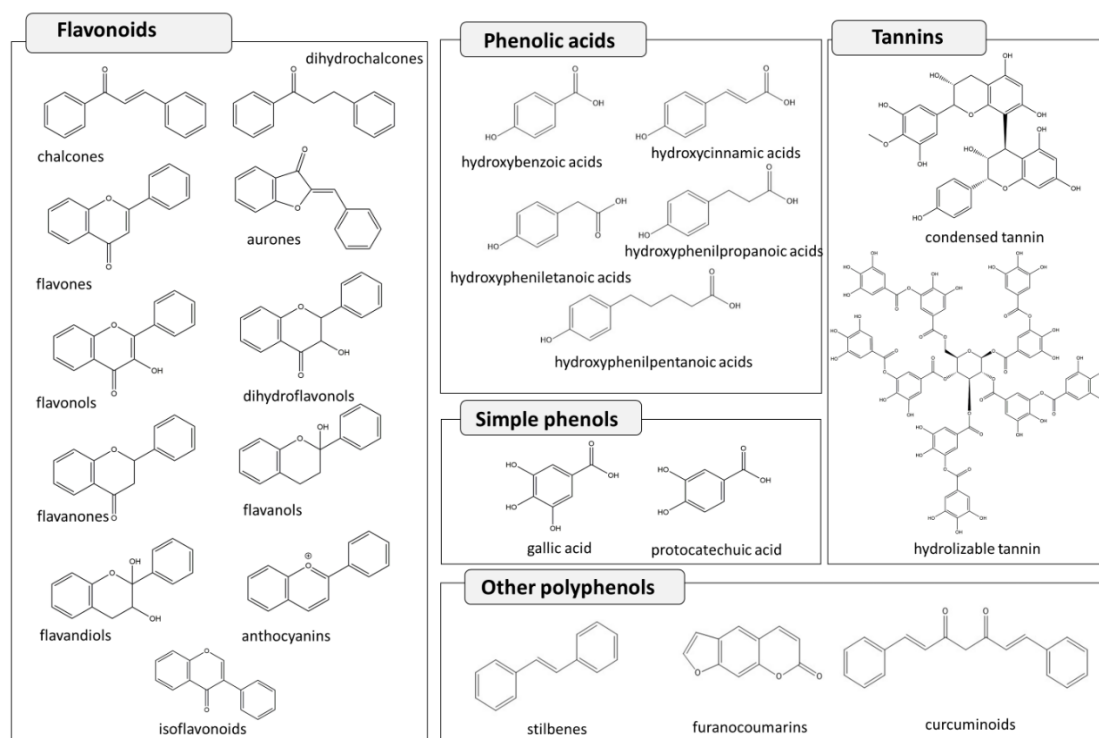


Figure 2. Examples of polyphenols, basic nucleus and classification.

Simple phenols are constituted by a single benzenic ring (C₆) linked to a hydroxyl group such as resorcinol, orcinol, catechol, guaiacol, hydroquinone, and phloroglucinol.

Phenolic acids present a carboxylic group among the substituents on the benzene ring, and they are generally divided into benzoic acid derivatives (C₆-C₁) (i.e., gallic acid, vanillic acid, syringic acid) and hydroxycinnamic derivatives (C₆-C₃) (i.e., caffeic acid, ferulic acid and coumaric acid).

Flavonoids (C₆-C₃-C₆) are generally constituted by two benzenic rings (A ring and B ring) linked by a chain made of three carbons, often condensed into a pyranic ring (C ring). Given their complexity, flavonoids are divided into other sub-classes such as: chalcones, dihydrochalcones, aurones, flavones, flavonols, dihydroflavonol, flavanones, flavanol, flavandiol or leucoanthocyanidin, anthocyanidin, bioflavonoids. Moreover, flavonoids exist in the aglycone form or as glycoside derivatives [30].

Tannins are high molecular weight polyphenols, usually distinct into condensed tannins (proanthocyanidins), which are polymers constituted by flavonoids units, and hydrolysable tannins characterized by a monosaccharide, normally D-glucose, esterified with one or more molecules of gallic acid (gallotannins), or ellagic acid (ellagitannins). Hydrolysable tannins are more labile in acid, alkali, or hot water than condensed tannins [30].

Distribution in Plants and Biological Activities

Polyphenols are widely distributed in all plant organs [31]. In general, phenolic acids are found in seeds, leaves, roots, and stems [32], while flavonoids are prominently found in aerial parts, and tannins in roots, bark, and seeds [33].

This heterogeneous group of SMs plays different roles in plants. For instance, flavonoids confer color to the flowers, attracting insects and promoting pollination [34]; some polyphenols are deterrents for herbivores [35], others are very important for Unprotections for their antioxidant properties [36,37].

Polyphenols, especially flavonoids, are considered important molecules for the human diet and, consequently, are often proposed as ingredients in food supplements and nutraceuticals. In fact, in addition to being antioxidant agents, they are endowed with several other biological activities [38]. For instance, flavonoids were proven active as

anti-inflammatory[39], anticancer [40,41], antihypertensive [42], microcirculation improving[43], and hypolipidemic agents [44]. They proved also interesting as active ingredients in the cosmetic field [45–47] and as natural dyes [48].

Phenolic acids are naturally found in fruits and vegetables, and are endowed with a wide spectrum of bioactivities such as: antidepressant [49], antihypertensive [50], anti-inflammatory [51], neuroprotective [51], antihyperglycemic [52], anticancer and antidiarrheal[53].

Regarding tannins, they are used in the veterinary field as anthelmintic and antimicrobial agents [54,55], as well as in the leather industry for their tanning properties[56]. However, tannins should be used carefully, since in addition to their health promoting properties, some toxic effects have also been reported [57,58]. Moreover, although tannin-rich ingredients are often added to ruminants' feed, there is still a lack of information about the interaction between hydrolysable tannins and ruminants' gastrointestinal microbiota. The fate of hydrolysable tannin metabolites derived from gastrointestinal microbial activity in the animal is still underexplored. It is known that some metabolites derived from hydrolysable tannins (i.e., pyrogallol) have adverse effects on gastrointestinal microbiota and the host animal [59]. These data point out the need of deeper investigation on tannin uses and effects, taking into account that risks and benefits depend on the specific situation and concentration used.

Polyphenols from Agro-Industrial Wastes and By-Products

Polyphenols being present in a wide spectrum of plant organs, they are easily found in numerous agro-industrial wastes/by-products, offering several possibilities for their valorization. First of all, an excellent polyphenol source is represented by the main byproducts of wine production, namely: pomace, skins, and seeds. In particular, molasses seeds have a high flavonoids content, and molasses pomace is rich in tannins [60]. Grape pomace contains gallic acid, syringic acid, vanillic acid, catechin, isoquercitrin, and epicatechin [61]. The presence of these antioxidant metabolites [60,61] makes the wine byproducts useful additives for ruminant feed [62]. In addition to the antioxidant potential, pomace also shows anti-cholesterol activity [63], while tannins from pomace are also used as wood adhesive [64].

Another polyphenol source is olive pomace [65], a by-product of the olive oil supply chain. This matrix is rich in tyrosol and its derivatives, and it also contains flavonoids such as rutin, apigenin, luteolin, taxifolin, diosmetin, and quercetin, and phenolic acids such as cinnamic, p-coumaric, caffeic, vanillic, and ferulic acid [66,67]. Due to its polyphenol content, olive pomace is also added to ruminant feed [68].

Moreover, olive wastewater contains polyphenols such as hydroxytyrosol [69,70], whose antioxidant and antibacterial properties make it a useful ingredient for cosmetic formulations [71].

Juice industry by-products such as pomace, skins, and seeds are another potential source of polyphenols. Among them, apple pomace is an example [72], since it contains catechin, epicatechin, chlorogenic acid, procyanidin B2, phlorizin, and gallic acid [73].

Among by-products derived from juice production, noteworthy are also strawberries, blueberries, carrots, and pears. In particular, black currants and chokeberries are the richest in anthocyanins, which are suitable ingredients for animal feed [74,75] and textile dyes [76].

Polyphenol-rich wastes derive also from agricultural remains after harvesting [75], canning, and liquor industries [77].

Regarding the aromatic herb industry, basil, sage, and rosemary generate several kind of wastes resulting from pruning, packaging, or distillation processes. It was proved that wastewater from the distillation of these herbs contains important metabolites such as glycosylated flavonoids and caffeic acid derivatives, above all, rosmarinic acid [78]. Wastewater generated from aescin (a saponin from horse chestnuts) production contains kaempferol and quercetin [79].

By-products containing polyphenols are also generated from the production of soluble coffee. For example, coffee grounds, which is the principal by-product, contain many polyphenols such as condensed tannins [80], chlorogenic acid, p-coumaric acid, ferulic acid, rutin, naringin, resveratrol [81]. By virtue of these SMs, coffee grounds proved active to inhibit seed germination [82]. Another by-product from this supply chain is the silver skin, a thin tegument covering coffee beans that is removed in the roasting process. Silverskin is rich in chlorogenic acid derivatives such as dicaffeoylquinic acids and feruloylquinic acids [83–85].

Regarding the agricultural sector, chestnuts wastes from *Castanea sativa* Miller, such as spiny burs, are noteworthy for their polyphenol content [86–89], including gallic acid and ellagic acid derivatives, together with glycosylated flavonoid [90,91]. By-products derived from chestnut flour production such as chestnut peels are sources of polyphenols, in particular, tannins [86,88,92]. For this reason, chestnut spiny burs and peels are valuable as natural antioxidants and often used in animal feed [86]. Also bud pomace of *C. sativa* contains cinnamic acids, benzoic acids, flavonols, and catechin [93]. Regarding *C. sativa* cultivation for wood production, the principal waste is the bark, which is also an important source of tannins [94], similar to other tree barks [95].

Several other polyphenol-rich by-products are known, such as Cocoa shell, the waste of chocolate production, which contains catechin, epicatechin, and gallic acid [96]; the waste of black tea, which shows antioxidant and antimicrobial activity [97]; melon peels, which contain a great amount of polyphenols [98]; larch bark, a source proanthocyanin B7, a well-known antioxidant [99]; and maize bran containing ferulic acid [100].

Terpenes

Chemical Structure and Classification

Terpenes, also termed terpenoids or isoprenoids, constitute a large family of natural products extremely diversified in their structure, functions, and properties. Terpenes derive from mevalonic acid biosynthetic pathway. However, since their decomposition generates isoprene units (C₅), this compound has been defined as terpene's basic constituent. For this reason, these SMs are classified based on the number of isoprene units present in their structure, and generally condensed head-to-tail. Following this rule they are divided into hemiterpenes (C₅H₈), monoterpenes (C₅H₈)₂, sesquiterpenes (C₅H₈)₃, diterpenes (C₅H₈)₄, sesterterpenes (C₅H₈)₅, triterpenes (C₅H₈)₆, etc. [101] (Figure 3).

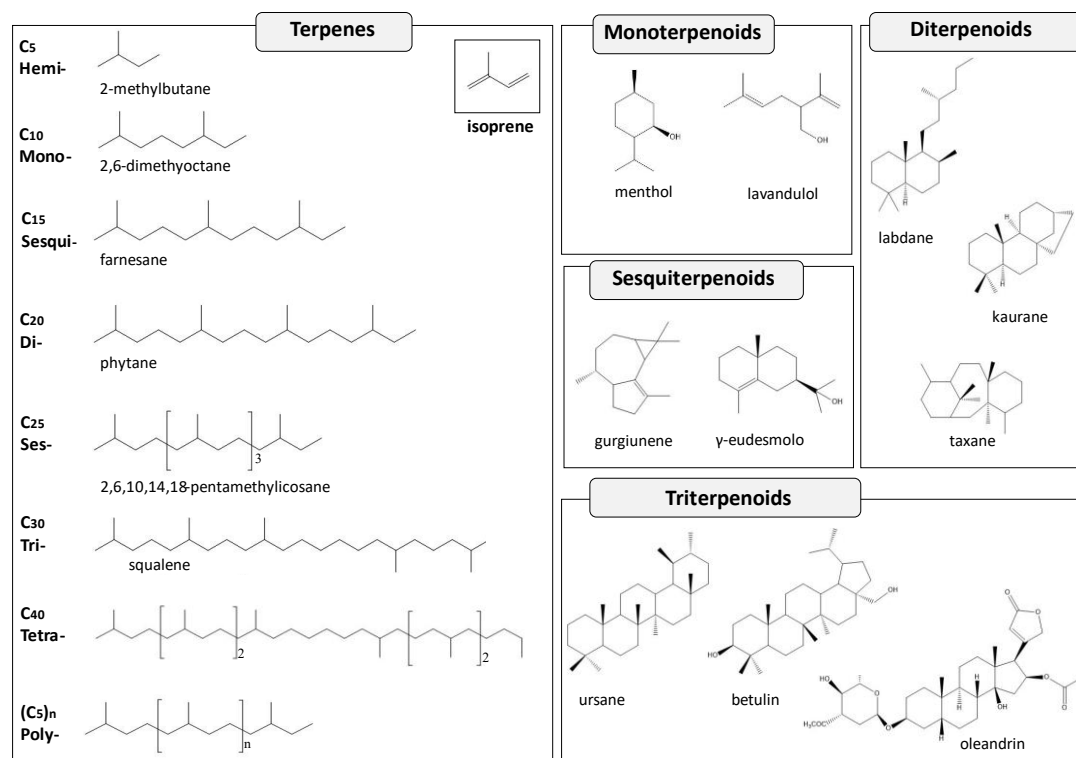


Figure 3. Some examples of terpene chemical structures and classification according to the number of isoprene units contained in the structure.

The broader term of terpenoids is applied to terpene-related molecules that, in addition to isoprene units, contain other substituents, for instance, oxygenated functional groups [102]. Many other natural substances, such as alkaloids, phenolics, and vitamins, despite deriving from biosynthetic pathways other than mevalonate (i.e., acetate or shikimate), are sometimes classified as meroterpenoids since they present isoprenic moieties in their structure.

Hemiterpenes are quite rare; one example is isoprene itself, which is a volatile compound present in several plants, especially trees. Monoterpenes are generally responsible for essential oils fragrance, some examples are: limonene, borneol, camphor, pinene, cineole, menthol, thymol, carvacrol. Diterpenes have as a precursor geranylgeranyl diphosphate; examples are phytol, which forms the lateral chains of chlorophylls, and taxol isolated from *Taxus brevifolia* Nutt, which is an important natural antitumor agent. Other renowned diterpenes are labdanes, which are the major components of the resin produced by plants of the Cistaceae family [103], and the gibberellins, important phytohormones regulating plant growth and development [104]. Squalene is triterpenes' precursor, deriving from numerous compounds, including

tetracyclic triterpenes like dammarenes, and pentacyclic triterpenes like lupanes and oleanes. The latter are often found in saponin skeletons, where they are glycosylated with one or more sugar moieties. Saponins are phytogetic biosurfactants, which induce foam formation in aqueous solution, reducing the viscosity of heavy crude oil-in-water emulsions [105]. Triterpenic saponins are found in numerous plants, the most renowned among them are *Saponaria officinalis* L. (soapwort), *Quillaja saponaria* Molina, and *Gypsophila arrostii* Guss. [106], which were, in fact, traditionally used for their soap properties. Saponins are classified on the basis of the differences occurring in their aglycone structure or sugar moiety. For example, on the basis of the sugar moiety they are classified into mono, bi, and tridesmosidic. The type of aglycone and the number of linked sugar residues determine the foam properties and the entity of adsorption at the interface [107].

Steroids can be considered modified triterpenes containing the lanosterol tetracyclic system without the two methyl substituents in C-4 and C-14 positions. Cholesterol is the basic structure of this class. They can be found also as saponins (steroidal saponins), such as cardioactive glycosides.

Tetraterpenes include carotenoids, while high molecular weight isoprenoid polymers (higher than C₄₀) are found in natural rubbers produced, for example, by trees belonging to the Euphorbiaceae and Sapotaceae families [108].

Distribution in Plants and Biological Activities

Terpenes may serve a wide spectrum of functions in plants, including attracting pollinators or protecting injured tissues from herbivores, insects, and parasites attack. According to this biological role various monoterpenes are toxic to insects [109], fungi [110], and bacteria [111]. In addition, steroidal saponins such as cardenolides are toxic to many animals through their inhibition of Na⁺/K⁺-ATPases. However, the same property makes them useful as therapeutic agents, in carefully regulated doses, to slow down and strengthen the heartbeat.

Due to their numerous bioactivities, terpenes find various applications in several industrial sectors, such as pharmaceutical, food, cosmetic, perfumery, and agricultural, and are used as drugs, food supplements, flavors, fragrances, biopesticides, etc.

First of all, the peculiar fragrance of many monoterpenes, present principally in aromatic plant essential oils, makes this class of compounds extremely important for food, aromatherapy, and perfumes. In addition to the fragrance, monoterpenes from essential oils, such as thymol, thymine, and carvacrol (found principally in plants belonging to the Lamiaceae family) proved interesting also for their numerous biological activities, for instance, their potential in the treatment of disorders affecting respiratory, nervous, and cardiovascular systems, and as antimicrobial and antioxidant agents [112].

Also labdane-type diterpenes are useful for the perfume industry, finding application as fixatives in high-end perfumes. Specifically, a fixative is a material with low volatility that provides long-term scent, aids in mixing with the other materials, and extends the shelf life of the perfume. The resin obtained from some plants of the Cistaceae family is one of the most common sources of labdane diterpenes used as perfume fixatives [113].

Saponins are extremely important for the food industry. In fact, many of the processed foods, including baked goods, ice creams, sauces, desserts, and drinks, contain dispersions such as emulsions and foams used to stabilize, determine, and control texture and rheological properties of these products. Saponins, due to their amphiphilic properties, proved to stabilize food emulsions with less sensitivity to pH, ionic strength, and high temperatures (up to 90 °C) than currently used emulsifiers [114]. Moreover, the increasing consumer demand for plant-based and sustainable emulsifiers and foaming agents makes saponins much requested for the food industry nowadays.

Despite saponins being toxic at high dosages, small quantities have been approved as food additives. The two main commercial sources are *Q. saponaria* from Chile, whose saponins have a prominently triterpenoid structure, and *Yucca schidigera* Roetzl ex Ortgies from Mexico, which contains saponins with a steroid structure [106].

Moreover, saponins at low dosage also showed numerous biological activities important for human healthcare, which are summarized in several review papers [115–117]; most relevant among them are the anticancer, cholesterol-lowering, and antiviral properties [118–121]. Some examples of the therapeutic potential of triterpenic saponins are provided by boswellic and betulinic acids. In fact, the extracts of the resin obtained from incense trees (*Boswellia serrata* Roxb.), containing the pentacyclic triterpenoid boswellic acid, have been employed as an anti-inflammatory drug [122], and the clinical

trials on gum-resin from *B. serrata* have shown an improvement in the symptoms in patients with osteoarthritis and rheumatoid arthritis [123,124]. Betulinic acid, a naturally occurring pentacyclic triterpene, exhibited a high variety of biological activities [125], including potent antiviral effects [126].

Moreover, saponins are antimicrobial agents active also against bacteria and fungi invading plants [127,128]. The mechanism of these activities is likely based on saponins' ability to form complexes with sterols present in the membrane of microorganisms and to cause, consequently, membrane perturbation [129,130]. Saponins also exert insecticidal [131] and molluscicidal [132] activities, as well as allelopathic activity toward different plant species [133]. These properties, together with their biological role in plant defense, confer to saponins an enormous potential as natural biopesticides useful for "green" agriculture practices. For example, Trdá et al. [134] found that saponin aescin, in addition to its antifungal effect against crop pathogens, is also able to activate plant immunity (in two different plant species) and to provide salicylic acid-dependent resistance against both fungal and bacterial pathogens.

In the pharmaceutical industry, terpenes are used as excipients to enhance skin penetration of active principles [135] and as therapeutic agents endowed with numerous bioactivities including, as mentioned above, chemo-preventive, antimicrobial, antifungal, antiviral, antihyperglycemic, analgesic, anti-inflammatory, and antiparasitic activities [110,111,118,122]. Among the pharmaceuticals, the anticancer paclitaxel and antimalarial artemisinin are two of the most renowned terpene-based drugs.

Terpenes and Terpenoids from Agro-Industrial Wastes and By-Products

Due to their numerous bioactivities, terpenes are particularly interesting in the context of waste requalification. Monoterpenes such as thymol and carvacrol are still present in discrete amounts in several by-products derived both from essential oil distillation and from the harvesting of some aromatic plants. For instance, the solid waste residues left after the distillation of leaves and stems of Mexican oregano (*Poliomintha longiflora* A. Gray) contain thymol and carvacrol, and are, as a result, endowed with antimicrobial activity [136]. Similarly, the monoterpenes limonene and nerol were found in fennel (*Foeniculum vulgare* Mill.) horticultural wastes [137].

The inedible part (stones, husks, kernels, seeds) from the fruit processing supply chain constitutes a huge portion of the consequent solid waste, which remains underexploited. For example, about one-third of citrus fruit production is industrially processed, with more than 80% used for orange juice production, which generates a huge amount of peel waste [138]. Orange essential oil mostly contains the monoterpene dlimonene (3.8% of orange peel dry weight) [139,140]. This molecule has been used as an ingredient in bio-based functional food, as preservatives for food [141], as well as in cosmetics and aromatherapy massage [142,143].

Moreover, the presence of d-limonene, an anti-fungal and antibacterial agent, makes orange oil a useful ingredient also for bio-pesticide formulations [144]. Finally, it is interesting to notice that waste orange peel, in addition to d-limonene, contains also other bioactive terpenes like linalool, and myrcene [145]. Besides orange peel, these terpenes can be found also in the peel of other citrus fruits such as lemon and several lime species [146], providing a good basis for the exploitation of this kind of wastes.

Regarding diterpenes, more than one million tons a year [147] of residue is produced after steam distillation of pine resin to recover the volatile fraction called turpentine. The consequent by-product is the gum rosin, which is a mixture of resin acids (90–95%) and other neutral compounds. The resin acids, most of which are isomers of each other, can be classified into two main categories: abietic-type (including abietic, neoabietic, palustric, and levopimaric), and pimaric-type (including pimaric, isopimaric, and sandaracopimaric) [148]. Gum rosin is a high-value-added residue, in fact, it is a natural alternative to fossil-based polymers obtained from the heating and evaporation of pine resin [149], as well as a producer of organocatalysts to promote complicated asymmetric industrial synthesis [150].

Several waste matrices contain saponins, which offer an enormous potential for their valorization. An example is provided by sisal (*Agave sisalana* Perrine), which is the main hard fiber produced worldwide. From its leaves, only the hard fibers (3–5% of total weight) are removed. The remaining 95–97% of the biomass is considered sisal waste, although it contains steroidal saponins, potentially useful for foods, cosmetics, and pharmaceuticals formulations, as well as for soil bioremediation [151].

Saponins from onion skin were found useful as a new natural emulsifier to formulate oil-in-water nanoemulsions by a high-pressure homogenizer [152].

Triterpenic acids such as oleanolic, betulinic, and ursolic acids provide another example of high-value terpenes that can be extracted from agricultural wastes prior to burning for energy production.

For example, oleanolic acid is found in agroforestry waste streams, such as in olive trees (*Olea europaea* L.), from which tons of wastes and by-products are generated on annual basis, including olive wood and leaves, cake, pomace, kernel, paste. During the production process, assuming a maximum content up to 3.1% of oleanolic acid in the leaves of *O. europaea*, a large amount of this high-value compound can potentially be extracted, contributing to the integrated valorization of the olive oil production chain [153]. In this context, the terpenes contained in the ethanol extract of olive milled residue showed anti-allergic activity on the cell line of rat basophilic leukemia, supporting the potential valorization of this other olive by-product [154].

Humulus lupulus L. (hops) flowers are used to preserve and give flavor to beer, while hops leaves are usually discarded as a waste. However, hops leaves contain β -caryophyllene, phytol, fatty acids, terpenes, and C5-ring bitter compounds, and the oil obtained from the leaves contains bitter acids, in particular cohumulinic, dehydrocohumulinic, and humulinic acid, possessing antibacterial activity [155].

Melon (*Cucumis melo* L.) is one of the most popular fruit cultivated in tropical countries and is industrially processed to obtain a wide spectrum of products such as juices, jams, dehydrated pulp, and salads or snacks, with consequent generation of a large number of by-products. However, these matrices (prominently pulp, seed, and peel) are still a good source of carotenoids (C40 tetraterpenoid pigments) like β -carotene, lutein, β -cryptoxanthin, phytoene, violaxanthin, neoxanthin, and zeaxanthin [156]. These substances are used to develop health-promoting functional food since they play an important role in eye photoprotection (provitamin A), improving immune functions, and preventing chronic diseases [157].

Alkaloids

Chemical Structure and Classification

A large number (more than 10,000 molecules) of plant SMs are classified as alkaloids [158]. The presence of nitrogen in the structure is the peculiar chemical feature

of alkaloids. However, due to the huge structural diversity, alkaloid classification is extremely challenging. More recent classifications are based on carbon skeletons and/or biochemical precursor. However, this requires compromises in borderline cases, for example, the alkaloid nicotine (from *Nicotiana* spp.), which contains a pyridine fragment from nicotinamide and a pyrrolidine part from ornithine, could be correctly assigned to two different classes [108].

Historically, alkaloids have been defined as metabolites containing one or more nitrogen atom(s) within heterocyclic ring(s) [159]. However, N-containing compounds where the N atom is not heterocyclic, such as hordenine, ephedrine, colchicine and capsaicin, were further included into this SM group and classified as proto-alkaloids or amino-alkaloids. For this reason heterocyclic N-containing compounds are often regarded as “true alkaloids.” Since “true alkaloids” biosynthetically derive from amino acids, they are classified on the basis of the biogenetic origin (Figure 4).

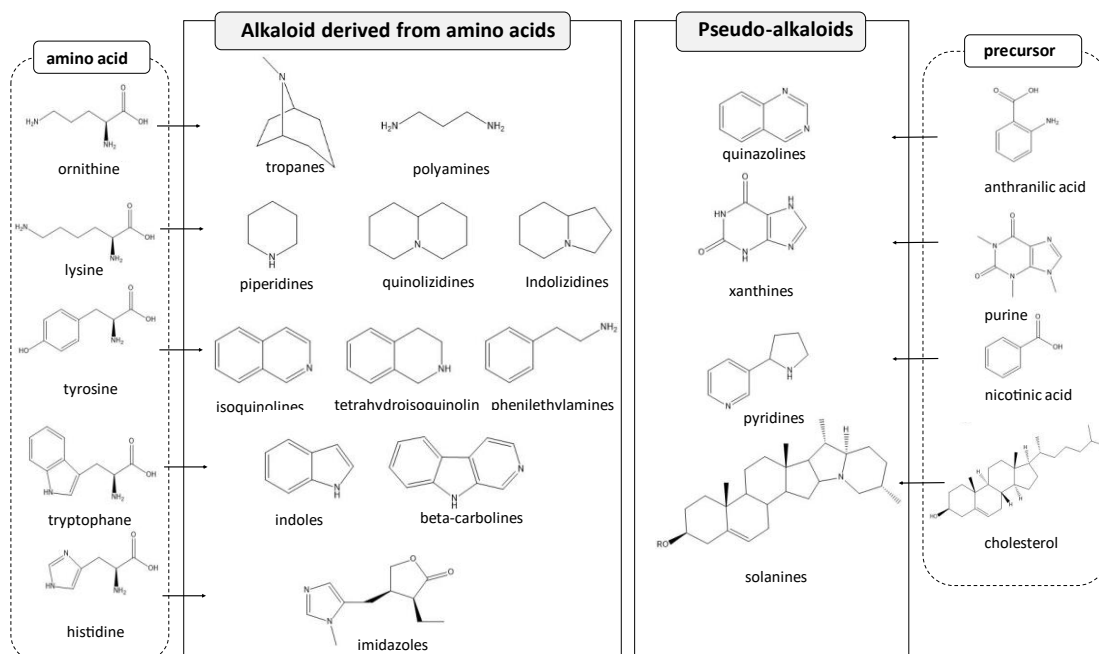


Figure 4. Examples of alkaloids (basic skeletons) and their precursors.

In particular, the majority of them derive from ornithine, leucine, lysine, tyrosine, tryptophan, histidine, and phenylalanine. More specifically, pyrrole alkaloids derive from leucine; pyrrolidine, tropane, and pyrrolizidine alkaloids from ornithine; quinolizidine, and indolizidine alkaloids derive from lysine; catecholamines, isoquinoline,

tetrahydroisoquinoline, and benzyltetrahydroisoquinoline alkaloids originate from tyrosine; indolamines, indole, carboline, quinoline, pyrrolindole and ergot alkaloids come from tryptophan; and imidazole alkaloids from histidine.

As the “true alkaloids,” proto-alkaloids derive from amino acids, and on this basis they are subsequently divided into phenylethylamino alkaloids, pyrrolizidine alkaloids, terpenoid indole alkaloids.

Following this classification criterion, another class of alkaloid, namely “pseudoalkaloids,” was constituted, including compounds that do not originate from amino acids, while having a nitrogen atom inserted into the molecule by transamination or amination reactions (Figure 4). This latter class includes aromatic alkaloids, ephedra alkaloids, purine alkaloids, sesquiterpene alkaloids such as isoprenoid alkaloids including mono- (from geraniol), di- (from geranylgeranyl-PP), and triterpene (from cholesterol) derivatives, these latter called steroidal alkaloids [158].

Regarding steroidal “pseudo-alkaloids,” they are often glycosylated (glycoalkaloids). These peculiar compounds are produced in more than 350 plant species, mainly from Solanaceae and Liliaceae families [160]. They consist of a C₂₇ cholestane skeleton (aglycone), where the –OH in position -3 is glycosylated by one to five monosaccharides, such as D-glucose, D-galactose, D-xylose and L-rhamnose.

Other peculiar alkaloids are the polyamine alkaloids (derivatives of putrescine, spermidine, and spermine), peptide and cyclopeptide alkaloids [161,162].

Distribution in Plants and Biological Activities

Alkaloids are an enormous group of phytochemicals of ecological importance, and possess a number of toxicological, pharmacological, nutritional, and cosmetic activities. Alkaloids are extremely abundant in flowering plants (Angiospermae), with a wide distribution in all organs such as leaves, flowers, seeds, roots, stems, fruits, bark, and bulbs. However, the presence and the distribution of these metabolites depend on the phase of plant life cycle, and strongly vary according to plant species, which produce different types of alkaloids, accumulated in various organs [163,164].

Alkaloids play numerous roles in plants, due to their involvement in defense [165–167], allelopathy [168], seed dispersal, and pollinator attraction [169,170].

Consistent with their defensive role, the highest alkaloid content is often found in plant reproductive organs [171]. In fact, many alkaloids are toxic to different organisms, protecting plants from pathogens and preventing non-specialist herbivore grazing [165,167]. In contrast, other alkaloids are essential for plant–pollinator interactions, increasing the number of pollinator visits, thus favoring plant reproduction [169,170]. Alkaloids have been historically used as drugs, and they remain very important in this context [172]; an example is provided by morphine from poppy straw, which is one of the most used analgesics today.

The biological activities of the principal sub-classes of alkaloids have been well summarized by Debnath et al. [159]. To cite some examples, quinine and quinidine, two quinolone alkaloids obtained from the bark of *Cinchona officinalis* L. (Rubiaceae), are very important historically used antimalarial drugs [173]; ephedrine, an adrenergic amine from the plants of genus *Ephedra* (Ephedraceae family), is used in many pharmaceutical preparations such as bronchodilators for asthmatic and allergic conditions, and to prevent low blood pressure during spinal anesthesia [174]; vinblastine and vincristine, two indole alkaloids extracted from *Catharanthus roseus* (L.) G. Don (Apocynaceae) [175], are renowned antitumor drugs.

Many other alkaloids have been studied for their promising bioactivities, for example, catuabine, a tropane alkaloid obtained from the bark of *Trichilia catigua* A. Juss. (Meliaceae) is endowed with antidepressant-like effects on the forced swim model of depression in mice and rats [176]; berberine, occurring in roots and stem-bark of different species of *Berberis* (Berberidaceae), showed anti-diabetic effect in rodent models of insulin resistance [177], and anti-hypertensive, anti-inflammatory, antioxidant, antidepressant, hepatoprotective activity, and anti-cancer activity [178,179].

Moreover, since some alkaloids possess psychotropic properties, they have found a role in social and ceremonial activities, as well as being important for popular spices and drinks, like the alkaloid caffeine, which is present in coffee [180]. Specifically, caffeine is a methyl-xanthine alkaloid, and its most important biological sources are *Coffea arabica* L. and *Camelia sinensis* (L.) Kuntze (leaves) (Theaceae). Caffeine is the most widely consumed stimulant drug in the world. It is also used in cold medications, analgesics, slimming agents, and cosmetics.

Moreover, consistent with their defense role, many alkaloids exhibit insecticidal [181,182], and fungicidal activity. For example, a piperidine alkaloid, piperonaline, isolated from the hexane fraction of *Piper longum* L., showed potent fungicidal activity against the phytopathogen *Puccinia recondita* [183]; *Coptis japonica* (Thunb.) Makino extracts and the contained alkaloids (isoquinoline alkaloids, berberine chloride, palmatine iodide, and coptisine chloride) expressed fungicidal activities against several phytopathogens, namely: *Botrytis cineria*, *Erysiphe graminis*, *Phytophthora infestans*, *Puccinia recondita*, *Pyricularia grisea*, and *Rhizoctonia solani* in *in vivo* plant models [184].

Relevant in this context are also the alkaloids produced by the Solanaceae family, which have an enormous potential to deliver new chemicals for crop protection. In fact, more and more of these compounds, or mixtures of them, are being identified as pest control agents, especially against insects, fungi, and mites [185]. The Solanaceae family belongs to the most important plant taxa, particularly in terms of food production (i.e., tomatoes and potatoes). Tomato and potato are the best known and most widely used plants of this group, and they constitutively synthesize low levels of many different glycoalkaloids. These natural toxicants (stress metabolites) have insecticidal and fungicidal properties and, since naturally occurring pesticides are often biosynthesized when plants are under stress, injuries on plant tissues promote the synthesis of higher concentrations of these compounds.

Alkaloids from Agro-Industrial Wastes and By-Products

The neglected matrices containing alkaloids have a high requalification potential by virtue of the numerous bioactivities possessed by these metabolites.

For instance, caffeine, a methyl-xanthine alkaloid, besides being an important ingredient for energy drink industry, it is also relevant for cosmetics. Caffeine is, in fact, used for cellulitis reduction [186,187], and to prevent skin aging through both antioxidant activity and inhibition of skin remodeling enzymes [188].

Among the industrial by-products, a source of caffeine is represented by spent coffee grounds (from coffee bars), which still have an amount of caffeine in the range of 5.99- 11.50 mg/g of dry matter [189].

Another source of methyl-xanthines (including caffeine and theobromine) are cocoa shells [96,190]. This is of particular interest, considering that the high amount of cocoa bean shell produced per year is generally disposed as waste and underutilized as fuel for boilers, animal feed, or fertilizer [191].

Another class of alkaloids, extremely relevant in view of waste valorization, is represented by glycoalkaloids, mainly produced by plants of the Solanaceae family. The major components of the glycoalkaloid family are α -solanine and α -chaconine found in potato plants (*Solanum tuberosum* L.), and solasonine and solamargine found in eggplants (*Solanum melongena* L.), whereas α -tomatine and dehydrotomatine are spirosolane-type glycoalkaloids found in tomato plants (*Lycopersicon esculentum* Mill.) [185].

These compounds are agrochemically important, in fact, their defensive role in plants makes many of them (i.e., α -tomatine, α -chaconine, α -solanine, and various *Solanum* spp. extracts) endowed with insecticidal activity against various insect species. In particular, both α -chaconine and α -solanine decrease insect feeding, delay their development, affect reproduction, and alter insect enzyme activity [185].

Although the majority of the toxicity studies have been focused on tomatoes and potatoes due to the economic importance and availability of these species, acute toxicity to insects has also been reported in plant extracts belonging to other genera, such as Piper, Datura, and Withania [185]. Notably, from *Datura stramonium* L. it is possible to extract a great variety of bioactive alkaloids, saponins, sterols, and polyphenols. This plant, as well as several other plants containing alkaloids, is often considered an agricultural waste [155], since it is invasive and its presence in cultivated fields is undesired.

Potato peels, a by-product of the industrial production of potato fries, chips, and flour, are a significant part of the annual worldwide production of about 1.3 billion tons of food waste [192]. In this context, alkaloids extracted from potato peels proved to be antioxidant [193] and antiprotozoal against pathogenic *Trichomonad* strains that infect humans, farm animals, and felines [192].

Alkaloids from plant wastes have been also tested for biological activities eventually useful for human healthcare, for instance, tomato (*L. esculentum*, Solanaceae) leaves alkaloids proved promising for Alzheimer disease treatment [194].

Extraction Techniques

Conventional Extraction Procedures and New Prospective for Solvents

Natural products are characterized by great diversity, which implies the necessity to develop specific extraction methods according to the starting raw material and selected metabolite(s). Generally, the raw matrix is subjected to an air drying process, dried in an oven or freeze-dried, and subsequently ground to create a homogeneous sample before the extraction [195–197]. Sometimes, before polyphenol extraction, the matrix is defatted with a non-polar solvent like n-hexane [70].

One of the most common extraction methods is solid–liquid extraction using water or organic solvents [65,84]. In some cases the extraction is performed through a Soxhlet extractor, which allows an efficient recycle of the solvent, which can be used in small amounts to extract a significant quantity of plant material [195,198].

If the starting material is a liquid, as for wastewaters, a liquid–liquid extraction, for instance, using ethyl acetate, is preferable [70,71]. Liquid/liquid partition has often been employed also to extract alkaloids and terpenes [199].

Sometimes the extraction can be facilitated by acidic or basic conditions under heating, as in the case of tannins, which can be extracted by maceration under reflux, using aqueous solvents, slightly alkaline at 85 °C. In particular, hydrolysable tannins are well extracted using a blend of 1% NaOH for 240 min, while condensed tannins are extracted with a blend of 1% Na₂SO₃ for 960 min [92].

Essential oils are obtained by stem distillation, which extracts preferentially volatile monoterpenes, while resins, which are generally more enriched in diterpenes, are extracted using organic solvents.

However, toxic solvents, like n-hexane or methanol, are unsuitable to extract products conceived for food or health uses. An option is to replace methanol with ethanol, which makes safer and “greener” the process. For example, an excellent polyphenol yield is obtained through maceration in a hydro-alcoholic blend of 50 or 60% ethanol for 30 min at a temperature between 60° and 80 °C, under reflux or simply under continuous stirring at room temperature [61,189].

However, in search of more efficient and environmental friendly alternatives to extract high-value molecules, ionic liquids (ILs) and natural deep eutectic solvents (NADES) have been proposed [200].

ILs are ionic species (organic salts), fluids or solids at room temperature, consisting of an organic cation (i.e., ammonium, imidazolium, pyridinium, phosphonium) and an anion (i.e., bromide, chloride, tetrafluoroborate, hexafluorophosphate). Due to their ionic nature, ILs possess negligible vapor pressure and high solvation ability, and they offer a wide spectrum of extraction abilities and selectivity [201]. Compounds such as flavonoids, alkaloids, phenolics, terpenoids, phenylpropanoids, and polysaccharides have been successfully extracted by ILs [202]. Moreover, recently, the possibility of using aqueous solutions of ILs instead of their pure forms led to a substantial improvement in their extraction efficiency and cost reduction. These solvents have already been used for the extraction of waste from natural products. For instance, solutions of surface-active ILs in water were used to efficiently extract triterpenic acids from apple peels [203], oleanolic acid from *O. europaea* [138], anthocyanins from grape pomace and peel of eggplant [204,205].

Natural deep eutectic solvents (NADES) are considered as a specific class of liquids present in living cells, where they play an important role in biosynthesis, transport, and storage of compounds with intermediate polarity [206]. NADES are composed of hydrogen bond donors (HBDs) and hydrogen bond acceptors (HBAs) mixed together. The usual HBAs are nontoxic quaternary ammonium salts or amino acids, while HBDs are organic acids or carbohydrates. Alcohol, amine, aldehyde, ketone, and carboxylic groups can be used as both HBAs and HBDs. There are a huge number of natural metabolites, which can be combined to prepare NADES, making the latter a high versatility tailormade class of solvents. NADES have numerous favorable properties, they are liquid state within a wide temperature range, manifest chemical and thermal stability, are nonflammable and non-volatile, nontoxic as well as having sustainable “green” properties. On this basis, NADES have been used to extract a wide range of natural compounds, including phenolics, alkaloids, saponins, anthraquinones, terpenoids, polyunsaturated fatty acids, and photosynthetic pigments [207,208]. NADES and their perspectives in the agri-food sector were extensively reviewed by Mišan et al. [206]. Regarding the employment of NADES in the extraction of plant-driven industrial wastes, they have been used to efficiently obtain phenols from by-products of the olive oil industry, and the onion, tomato, potato, orange, and pear canning industries [209,210].

Non-Conventional Extraction Methods

Different extraction methods have been proposed in order to shorten, improve, and obtain greener procedures for natural metabolite extraction. Several works have been dedicated to summarize these techniques and their use to extract bioactive metabolites from natural wastes [211,212]. Ultrasonic-assisted extraction (UAE) is an effective extraction technique for a wide range of compounds from different types of matrices. Due to the cavitation effects leading to cell wall disruption the release of the target compound(s) from the biomass is favored [213]. In addition, ultrasounds also use the oxidative energy of radicals created during sonolysis to make more efficient the extraction process [214].

This results in a shortening of the extraction process with low consumption of solvents and high product yields. This method has been used to efficiently extract different classes of metabolites from several plants [213].

Microwave-assisted extraction (MAE) reduces extraction time with a minor consumption of solvents and minimum degradation of target compounds. It is based on microwave energy, which heats the solvents and increases the internal pressure inside the cell, helping the disruption of the cellular wall and the release of active compounds to the solvent [215]. Combined with inert atmosphere to avoid polyphenol degradation, this is a sustainable technique [216] that allows to work at high temperature (150 °C), obtaining very good yields of extracts endowed with a high antioxidant power [217]. This method can be optimized using a solution at pH 12, which facilitates the extraction of polyphenols [195].

Supercritical fluid technology (SFT) is based on supercritical fluids, among them the most used is supercritical carbon dioxide (CO₂), generated by increasing the pressure and the temperature of the liquid/gas above the critical point. These fluids have liquid-like solvent power and gas-like diffusivity, resulting optimal to extract compounds from plant matrices, and yield solvent-free extracts by the reduction of CO₂ pressure, which allows to easily remove it. This technique has been extensively applied to extract plant metabolites from waste. For instance, STF was used to efficiently extract tocopherols and carotenoids rich oil guava seeds, which are endowed with good antioxidant activity [218].

Supercritical fluid extraction (SFE) was proven not suitable for polyphenol extraction [198], however it could be useful in a first phase where fatty acids are removed

from the matrix, and polyphenols might be extracted subsequently with the help of a co-solvent [197].

Among the green technologies, pressurized liquid extraction (PLE), also called accelerated solvent extraction (ASE), is a fully automated technique that combines high temperature and pressure with the use of liquid solvents. This technique proved efficient to extract different matrices such as food [219] medicinal plants [220], and environmental samples [221]. PLE improves extraction yield, significantly reducing time and solvent consumption, [222] and it can be used to extract molecules of different polarity, such as phenolic compounds, carotenoids, and essential oils [222]. An optimized PLE protocol for the extraction of water-soluble molecules is represented by hydrothermal extraction, which uses water at high temperature and high pressure and has been employed to extract spent coffee grounds [223].

Trends in Publications Focused on Plant Wastes Valorization

The number of scientific publications dealing with the valorization of waste derived from plants have notably increased in the last three years (Figure 5) [224]. This trend reflects the rising global interest in circular economy and requalification of neglected plant matrices.

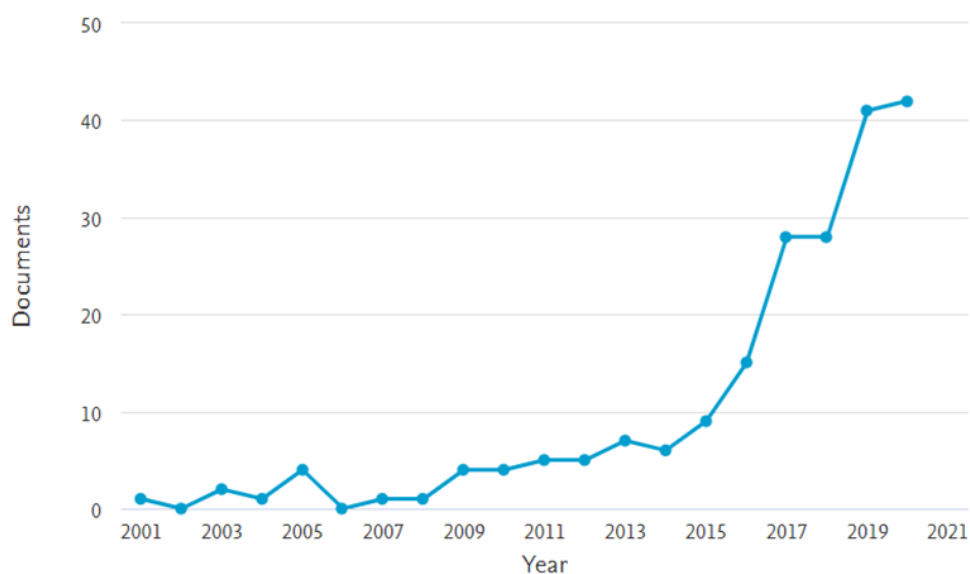


Figure 5. Trend of scientific publications from 2001 to 2020 reported by Scopus using as a query string: TITLE-ABS-KEY (plant AND by-products AND waste AND valorization).

This review carried out a bibliographic survey, taking into account 99 scientific articles on this topic published from 2006 to 2020. Table 1 summarizes the information about waste type, its plant source, industrial sector of provenience, contained secondary metabolites, reported bioactivity, and potential use for its valorization. The survey included 64 plants generating wastes, mainly derived from the food and beverage industries, followed by the herbal, agriculture, and forestry industries, and only one report was dedicated to a plant waste from the perfume industry. Moreover, according to this survey, wastes from 16 plant species originated from more than one industrial sector. This is easily understandable taking into account that the majority of the industrial products undergo different steps in the production chain. For example, different kinds of wastes are generated from *Castanea sativa* cultivated for nuts production, and these wastes originate at different level of the production chain. In particular, spiny burs are the main agricultural residue from tree cultivation, while husks are discarded by the food industry when producing chestnut flour. The beverage industry generates also a considerable amount of wastes/by-products from plant origin, most prominent among them fruit pomace and or/peel. Nevertheless, a conspicuous number of wastes are also produced during the previous steps of the supply chain, namely, the fruit production itself leads to several agricultural residues. An example is provided by the wine production chain, where grape pomace is the main final waste, even though the cultivation of *Vitis vinifera* L. itself generates residuals like green prunings. In this case, as highlighted also by our survey, due to their content in polyphenols, flavonoids, and tannins, grape pomace and skin are strongly valorized by-products (12 publications were focused on the requalification of these wastes). However, as pointed out by Acquadro et al. [225], green pruning might be exploited for its phenolic content.

Focusing on the specific classes of SMs considered in the examined papers, polyphenols emerged as the most investigated one. Out of 64 plants mentioned in the reviewed articles, the generic presence of polyphenols was reported in 31 of them. Moreover, several investigations were focused also on specific polyphenol sub-classes, such as flavonoids (found in 21 plants) and phenolic acids (found in 18 plants).

Conversely, terpenes and alkaloids resulted as less investigated; in fact, they were mentioned as important compounds in only 12 and 7 plant species, respectively. In the

context of waste valorization, the main bioactivity related to polyphenols was the in vitro antioxidant activity, which is common also to terpenes [29] and alkaloids [189]; this encourages further works dedicated to these latter classes of plant metabolites, often contained in wastes/by-products.

According to this bibliographic survey, terpene saponins resulted as the less explored metabolite from plant waste matrices. Their presence was, in fact, reported only in waste constituted by onion skin and *A. sisalana* leaves. As mentioned above, saponins have numerous applications and bioactivities, among them their possible use in soil bioremediation. Moreover, this survey pointed out that only few waste matrices were studied for their potential use in the agriculture sector (Figure 6).

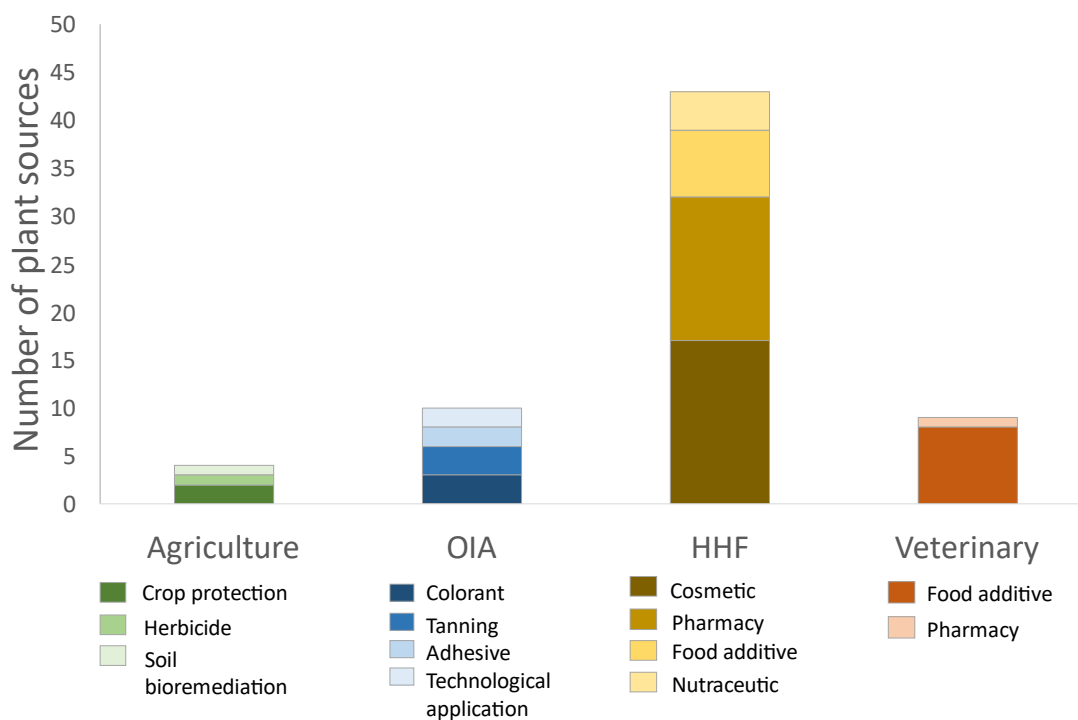


Figure 6. Number of plant matrices investigated for potential application in four different areas: agriculture, OIA (Other Industrial Applications), HHF (Human Healthcare and Food), and veterinary science. The graphic summarizes the results of our bibliographic survey (from 2006 to 2020).

In particular, *Anacardium occidentale* L. nut shells and *Castanea sativa* burs proved good sources of molecules endowed with pesticide and anti-fungal properties, respectively. On this basis they could find application as crop protection agents. Spent coffee ground showed allelopathic activity, which is useful for herbicide products. As it

is evident in Figure 6, the majority of plant wastes were valorized proposing potential exploitation in the area here called “human healthcare and food” (HHF) (including cosmetic, pharmaceutical, nutraceutical, and food additive use). However, since plant SMs are endowed with a wide range of chemical and biological properties (as summarized in this review), it is expected that, following the actual trend, wastes and byproducts of plant origin will be increasingly investigated also for their potential use in other areas of application, especially in agriculture, considering the need to implement “greener” practices in this sector.

Table 1. Summary of the results emerging from the survey. The table reports: plant species from which the waste is generated, the industrial sector manufacturing the plant material, the nature of the produced waste, the class of secondary metabolites found in the waste material, the bioactivity possessed by waste extract(s), the potential use for waste valorization, and the corresponding reference source of all the information reported in a line. If no biological activity was investigated, or no potential valorization in a specific field was proposed, the wording “not specified” (n. s.) has been inserted in the corresponding cell.

Plant species¹	Waste producer Industry	Waste type	Contained secondary metabolites	Reported bioactivity	Potential use for waste valorization	References
<i>Acacia mangium</i> Willd.	Forestry	bark	tannins	n. s.	leather tanning	[56]
<i>Aesculus hippocastanum</i> L.	Herbal industry	wastewaters	flavonoids	n. s.	n. s.	[79]
<i>Agave sisalana</i> Perrine	Fiber Industry	leaves	saponins	n. s.	cosmetic, pharmacy soil bioremediation	[151]
<i>Allium cepa</i> L.	Food	peel	flavonoids, saponins	antiobesity	pharmacy	[44]
				surface activity	food additive	[152]
				photoprotection	cosmetic	[226]
<i>Allium sativum</i> L.	Food	n. s.	flavonoids	photoprotection	cosmetic	[226]
<i>Aloe barbadensis</i> Mill.	Agriculture	roots	anthraquinones	antiviral	pharmacy	[227, 228]
<i>Anacardium occidentale</i> L.	Food	nut shell liquid (CNSL), testa, cashew apple, and cashew apple bagasse	phenolic acids, alkaloids, tannins	pesticide, larvicide, antitermite, dye, anti-cancer, anti-bacterial, antioxidant, neurotransmitter, etc.	colorant crop protection pharmacy	[229]
<i>Ananas comosus</i> (L.) Merr.	Food	core and skin	polyphenols	antioxidant <i>in vitro</i>	food additive	[230]
	Food	skin and husks		antioxidant <i>in vitro</i>	feed additive	[231]

<i>Arachis hypogaea</i> L.			phenolic acids, flavonoids polyphenols	antibacterial	pharmacy	
<i>Aronia melanocarpa</i> (Michx.) Elliot	Beverage	pomace	flavonoids	antioxidant <i>in vitro</i>	feed additive	[74]
<i>Camellia sinensis</i> (L.) Kuntze	Food	black tea waste	polyphenols	antioxidant <i>in vitro</i> antibacterial	cosmetic, food additive, pharmacy	[97]
<i>Castanea sativa</i> Mill.	Agriculture and Food	burs	polyphenols	fungicides, enzyme inhibitor and antioxidant <i>in vitro</i>	cosmetic, crop protection, food additive, pharmacy	[86-90]
		leaves		enzyme inhibitor, antitumoral and antioxidant <i>in vitro</i>		[86-88]
		bud		n. s.		[93]
		husks		enzyme inhibitor antioxidant <i>in vitro</i>		[86, 88]
		husks and bark	tannins	n. s.	cosmetic, pharmacy, industrial application	[92, 94]
<i>Citrus spp.</i>	Food and Beverage	peel and pulp	flavonoids, essential oil, phenolic acid	antioxidant <i>in vitro</i> , anti-inflammatory <i>in vitro</i> , antitumoral	cosmetic, food additive, pharmacy	[27, 226, 228]
<i>Citrus x bergamia</i> (Risso) Risso & Poit.	Herbal Industry	peel	flavonoids	antibacterial	pharmacy	[228, 232]
<i>Citrus x sinensis</i> (L.) Osbeck	Beverage	peel	essential oil	n. s.	n. s.	[233]

<i>Coffea</i> spp.	Beverage and Food	spent coffee grounds and silver skin	polyphenols and alkaloids	antioxidant <i>in vitro</i>	cosmetic, food additive, nutraceutical, pharmacy	[80, 81, 84, 189]
		spent coffee grounds	n.s.	anti-pollutants		[234]
		spent coffee grounds	polyphenols	allelopathic activity	herbicide	[82]
<i>Coffea arabica</i> L.	Food	silver skin	polyphenols	antioxidant <i>in vitro</i>	n. s.	[85]
<i>Cucumis melo</i> L.	Food and Beverage	peel	polyphenols	antioxidant <i>in vitro</i>	cosmetic, nutraceutical, food additive, pharmacy	[98]
<i>Cucurbita</i> spp.	Food	peel, seeds and fruits not suitable for human consumption	terpenes and phenolic acids	improvement of meat, milk, or eggs	feed additive	[235]
<i>Curcuma longa</i> L.	Agriculture	leaves	terpenes	anti-inflammatory <i>in vivo</i> and <i>in vitro</i>	pharmacy	[236]
<i>Cynara scolymus</i> L.	Food	floral stems	polyphenols, flavonoids, tannins	antioxidant <i>in vitro</i> , antibacterial, anti-denaturing protein, antidiabetic <i>in vivo</i> and anti-hyperlipidemic <i>in vivo</i>	nutraceutical	[237]
	Agriculture	bracts of the heads			cosmetic	[75]
<i>Datura stramonium</i> L.	Agriculture	leaves and flowers	terpenes	antibacterial	pharmacy	[155]
<i>Daucus carota</i> L.	Beverage	pomace	terpenes	antioxidant <i>in vitro</i>	feed additive	[74]

<i>Foeniculum vulgare</i> Mill.	Herbal Industry	seeds solid residue from distillation	flavonoids and polyphenols	antibacterial and antioxidant <i>in vitro</i>	food additive	[228, 238]
	Agriculture	leaves, inflorescence and pseudo stems	terpenes	antioxidant <i>in vitro</i>	n. s.	[137]
<i>Fragaria</i> spp.	Beverage	pomace	flavonoids	antioxidant <i>in vitro</i>	feed additive	[74]
<i>Humulus lupulus</i> L.	Beverage	leaves and flowers	terpenes	antibacterial	pharmacy	[155]
<i>Hyssopus officinalis</i> L.	Herbal Industry	solid distillation residue	phenolic acids	antioxidant <i>in vitro</i>	food additive	[228, 239]
<i>Ilex paraguariensis</i> A.St.-Hil.	Beverage	exhausted leaves	terpenes, flavonoids, polyphenols	antioxidant <i>in vitro</i>	n. s.	[240]
<i>Juglans</i> spp.	Agriculture and Food	husks	tannins, flavonoids, terpenes, phenolic acids, anthraquinones, naphthoquinones	removal of hazardous materials, antioxidant <i>in vitro</i> , antibacterial, anti-platelet, cytotoxic	cosmetic, pharmacy	[241]
					colorant	
<i>Larix kaempferi</i> (Lamb.) Carrière	Forestry	bark	flavonoids	enzyme inhibitor	cosmetic	[99]
<i>Lavandula x intermedia</i> Emeric ex Loisel.	Perfume Industry	solid distillation residue	flavonoids, polyphenols, phenolic acids	antioxidant <i>in vitro</i>	n. s.	[228, 242]
<i>Lycopersicon esculentum</i> Mill.	Agriculture	leaves	polyphenols and alkaloids	enzyme inhibitor	pharmacy	[194]

<i>Lycopersicon lycopersicum</i> (L.) H.Karst.	Food	peel	polyphenols	antioxidant <i>in vitro</i>	cosmetic, food additive, pharmacy	[75]
<i>Malus spp.</i>	Beverage	pomace	flavonoids and polyphenols	antioxidant <i>in vitro</i> , additive	cosmetic, food additive, pharmacy	[74, 75, 217]
<i>Malus domestica</i> (Suckow) Borkh.	Food and Beverage	pomace	flavonoids and phenolic acids	antioxidant <i>in vitro</i> , photoprotection	cosmetic, feed additive	[74, 226]
<i>Mangifera indica</i> L.	Food	pomace	polyphenols	photoprotection	cosmetic	[226]
<i>Ocimum basilicum</i> L.	Food and Herbal Industry	oil distillation wastewaters	polyphenols	antioxidant <i>in vitro</i>	cosmetic, food additive, nutraceutical, pharmacy	[78, 228, 243]
<i>Olea europaea</i> L.	Food	distillation wastewater, pomace, leaves	polyphenols	antioxidant <i>in vitro</i> , antibacterial, decrease lipolysis	cosmetic, food additive, nutraceutical, pharmacy	[69-71, 153, 226, 244]
		leaves, fruit milled waste	terpenes	antiallergic	nutraceutical, pharmacy	[153, 154]
		pomace	polyphenols	antioxidant <i>in vitro</i> , improvement of gut microbiota	feed additive	[68]
<i>Pinus spp.</i>	Forestry	resin	terpenes	improve thermal stability of bio-based materials	technological application	[149]
				organocatalyst		[150]
<i>Pinus pinaster</i> Aiton	Agriculture	bark	tannins	Tanning	leather tanning	[95]

<i>Poliomintha longiflora</i> A. Gray	Herbal Industry	solid distillation residue	polyphenols, phenolic acids, acids, terpenes	antibacterial and antioxidant <i>in vitro</i>	n. s.	[136, 228]
<i>Prunus avium</i> (L.) L.	Food	peel and stems	polyphenols	antioxidant <i>in vitro</i> , enzyme inhibitor and photoprotection	cosmetic	[245]
<i>Prunus cerasus</i> L.	Food and Beverage	cherry liquor pomace, pomace and seeds	polyphenols	antioxidant <i>in vitro</i>	cosmetic, nutraceutical	[77, 246, 247]
		stems, leaves, pomace and seeds	terpenes	antibacterial	nutraceutical	
<i>Prunus dulcis</i> (Mill.) D. A. Webb	Agriculture and Food	husks skins and blanching water	polyphenols and flavonoids	antibacterial, antioxidant <i>in vitro</i>	pharmacy, technological application	[248]
<i>Punica granatum</i> L.	Food and Beverage	peel, arils, mesocarp and pulp	polyphenols	antioxidant <i>in vitro</i> , antibacterial, photoprotection	cosmetic	[226, 249-253]
<i>Pyrus</i> spp.	Beverage	pomace	polyphenols	antioxidant <i>in vitro</i>	cosmetic	[75]
<i>Quercus suber</i> L.	Forestry	by-product of bark processing	phenolic acids and tannins	antioxidant <i>in vitro</i>	cosmetic	[254]
<i>Ribes nigrum</i> L.	Beverage	pomace	tannins and flavonoids	dyes, antioxidant <i>in vitro</i>	feed additive	[74]
			phenolic acids and flavonoids	enzyme inhibitor, antioxidant <i>in vitro</i>	cosmetic	[48, 255]
<i>Salvia officinalis</i> L.	Herbal industry and Food	oil distillation wastewaters	polyphenols	antioxidant <i>in vitro</i>	n. s.	[78]

<i>Salvia officinalis</i> subsp. <i>Lavandulifolia</i> (Vahl) Gams	Herbal Industry	solid distillation residue	phenolic acids	antioxidant <i>in vitro</i>	cosmetic, food additive	[228, 256]
<i>Salvia rosmarinus</i> Spenn.	Herbal Industry	solid distillation residue	polyphenols and phenolic acids	antioxidant <i>in vitro</i>	food additive	[228, 257]
		oil distillation wastewaters	terpenes and polyphenols	antioxidant <i>in vitro</i>	n. s.	[78]
<i>Santolina</i> <i>chamaecyparissus</i> L.	Herbal Industry	solid distillation residue	phenolic acids	antioxidant <i>in vitro</i>	pharmacy	[228, 239]
<i>Satureja montana</i> L.	Herbal Industry	solid distillation residue	phenolic acids	antioxidant <i>in vitro</i>	pharmacy	[228, 239]
<i>Solanum</i> <i>lycopersicum</i> L.	Food	pomace	terpenes	antioxidant <i>in vitro</i> , photoprotection, chemioprevention	cosmetic, nutraceutical	[29, 226]
<i>Solanum</i> <i>tuberosum</i> L.	Food	peel	polyphenols and alkaloids	antioxidant <i>in vitro</i>	n. s.	[193]
		peel		anti-trichomonads	pharmacy	[192]
<i>Solidago virgaurea</i> L.	Herbal industry	dried herb	polyphenols	antioxidant <i>in vitro</i>	cosmetic, food additive	[75]
<i>Sophora flavescens</i> Aiton	Herbal Industry	all plants	flavonoids and alkaloids	anti-inflammatory <i>in</i> <i>vitro</i>	pharmacy	[258]
	Agriculture	seeds	alkaloids	antioxidant <i>in vitro</i> and antibacterial	n. s.	[259]
	Food	bean shell	phenolic acids	antioxidant <i>in vitro</i>	food additive	[195]

<i>Theobroma cacao</i> L.			polyphenols and alkaloids		n. s.	[190]
			flavonoids and alkaloids		n. s.	[96]
<i>Thymus mastichina</i> (L.) L.	Herbal Industry	solid distillation residue	phenolic acids	antioxidant <i>in vitro</i>	n. s..	[228, 256]
<i>Ugni molinae</i> Turcz	Food and Herbal Industry	seeds	polyphenols	antibacterial	n. s.	[260]
<i>Vaccinium myrtillus</i> L.	Beverage	pomace	flavonoids	Dyes	colorant	[76]
<i>Vitis labrusca</i> L.	Beverage	pomace	polyphenols	n. s.	nutraceutical	[250, 261]
<i>Vitis vinifera</i> L.	Agriculture	green pruning	polyphenols	antioxidant <i>in vitro</i>	cosmetic, nutraceutical, pharmacy	[225]
	Beverage	seeds pomace and stems	flavonoids, polyphenols	antioxidant <i>in vitro</i> , antibacterial		[225, 250, 262-265]
		pomace	flavonoids, polyphenols	antioxidant <i>in vitro</i> , photoprotection, cholesterol-lowering activities		[61, 63, 226, 250, 251, 261, 264, 266]
		pomace	polyphenols, tannins, flavonoids, saponins	antioxidant <i>in vivo</i> , anthelmintic	feed additive, pharmacy	[62, 267]
		pomace	tannins	adhesive properties	adhesive	[64]
<i>Zea mays</i> L.	Agriculture	maize bran	phenolic acids	n. s.	n. s.	[100]

¹Plant scientific names have been updated following the World Checklist of Vascular Plants (WCVP 2020) [268].

References

1. United Nations. *World Population Prospects 2019*; United Nations: New York, NY, USA, 2019.
2. OECD. *Global Material Resources Outlook to 2060: Economic Drivers and Environmental Consequences*; OECD Publishing: Paris, France, 2019.
3. Kaza, S.; Yao, L.; Bhada-Tata, P.; Van Woerden, F. *What a Waste 2.0: A Global Snapshot of Solid Waste Management to 2050*; Urban Development; World Bank: Washington, DC, USA, 2018; p. 168.
4. Mirabella, N.; Castellani, V.; Sala, S. Current options for the valorization of food manufacturing waste: A review. *J. Clean. Prod.* **2014**, *65*, 28–41.
5. FAO (Food and Agriculture Organization of the United Nations). *The State of Food and Agriculture 2019*; FAO: Rome, Italy, 2019.
6. FAO (Food and Agriculture Organization of the United Nations). *Food Wastage Footprint: Impacts on Natural Resources—Summary Report*; FAO: Rome, Italy, 2013.
7. ReFED (Rethink Food Waste through Economics and Data). *A Roadmap to Reduce US Food Waste by 20 Percent*; ReFED: Berkeley, CA, USA, 2016.
8. The NSW Environment Protection Authority Website. Available online: <https://www.epa.nsw.gov.au/your-environment/recycling-and-reuse/warr-strategy/the-waste-hierarchy> (accessed on 1 October 2020).
9. Barreiro-Gen, M.; Lozano, R. How circular is the circular economy? Analysing the implementation of circular economy in organisations. *Bus. Strateg. Environ.* **2020**, *29*, 3484–3494.
10. Morseletto, P. Targets for a circular economy. *Resour. Conserv. Recy.* **2020**, *153*, 104553.
11. European Commission Website. Available online: <https://ec.europa.eu/environment/circular-economy/> (accessed on 9 January 2021).
12. Momayez, F.; Karimi, K.; Taherzadeh, M.J. Energy recovery from industrial crop wastes by dry anaerobic digestion: A review. *Ind. Crop. Prod.* **2019**, *129*, 673–687.
13. Solomon, B.D. Biofuels and sustainability. *Ann. N. Y. Acad. Sci.* **2010**, *1185*, 119–134.
14. Baudry, G.; Delrue, F.; Legrand, J.; Pruvost, J.; Vallée, T. The challenge of measuring biofuel sustainability: A stakeholder-driven approach applied to the Fr.0ench case. *Renew Sust. Energ. Rev.* **2017**, *69*, 933–947.
15. Ben-Othman, S.; Jöudu, I.; Bhat, R. Bioactives from Agri-Food Wastes: Present Insights and Future Challenges. *Molecules* **2020**, *25*, 510.
16. Sagar, N.A.; Pareek, S.; Sharma, S.; Yahia, E.M.; Lobo, M.G. Fruit and vegetable waste: Bioactive compounds, their extraction, and possible utilization. *Compr. Rev. Food Sci. Food Saf.* **2018**, *17*, 512–531.
17. Bosco, F.; Casale, A.; Gribaudo, G.; Mollea, C.; Malucelli, G. Nucleic acids from agro-industrial wastes: A green recovery method for fire retardant applications. *Ind. Crop. Prod.* **2017**, *108*, 208–218.
18. Nagel, A.; Winkler, C.; Carle, R.; Endress, H.U.; Rentschler, C.; Neidhart, S. Processes involving selective precipitation for the recovery of purified pectins from mango peel. *Carbohydr. Polym.* **2017**, *174*, 1144–1155.
19. Ibrahim, M.M.; El-Zawawy, W.K.; Jüttke, Y.; Koschella, A.; Heinze, T. Cellulose and microcrystalline cellulose from rice straw and banana plant waste: Preparation and characterization. *Cellulose* **2013**, *20*, 2403–2416.
20. Banerjee, S.; Ranganathan, V.; Patti, A.; Arora, A. Valorisation of pineapple wastes for food and therapeutic applications. *Trends Food Sci. Tech.* **2018**, *82*, 60–70.
21. Patsalou, M.; Menikea, K.K.; Makri, E.; Vasquez, M.I.; Drouza, C.; Koutinas, M. Development of a citrus peel-based biorefinery strategy for the production of succinic acid. *J. Clean. Prod.* **2017**, *166*, 706–716.
22. Demain, A.L.; Fang, A. The natural functions of secondary metabolites. In *History of Modern Biotechnology I, Advances in Biochemical Engineering/Biotechnology*; Fiechter, A., Ed.; Springer: Berlin/Heidelberg, Germany, 2000; Volume 69, pp. 1–39.
23. Kabera, J.N.; Semana, E.; Mussa, A.R.; He, X. Plant secondary metabolites: Biosynthesis, classification, function and pharmacological properties. *J. Pharm. Pharmacol.* **2014**, *2*, 377–392.
24. Bourgaud, F.; Gravot, A.; Milesi, S.; Gontier, E. Production of plant secondary metabolites: A historical perspective. *Plant Sci.* **2001**, *161*, 839–851.

25. Pathak, P.D.; Mandavgane, S.A.; Kulkarni, B.D. Fruit peel waste: Characterization and its potential uses. *Curr. Sci.* **2017**, *113*, 444–454.
26. Mahato, N.; Sharma, K.; Sinha, M.; Cho, M.H. Citrus waste derived nutra-/pharmaceuticals for health benefits: Current trends and future perspectives. *J. Funct. Foods* **2018**, *40*, 307–316.
27. Singh, B.; Singh, J.P.; Kaur, A.; Singh, N. Phenolic composition, antioxidant potential and health benefits of citrus peel. *Food Res. Int.* **2020**, 109–114.
28. Vu, H.T.; Scarlett, C.J.; Vuong, Q.V. Phenolic compounds within banana peel and their potential uses: A review. *J. Funct. Foods* **2018**, *40*, 238–248.
29. Szabo, K.; Cătoi, A.F.; Vodnar, D.C. Bioactive compounds extracted from tomato processing by-products as a source of valuable nutrients. *Plant Foods Hum. Nutr.* **2018**, *73*, 268–277.
30. Bravo, L. Polyphenols: Chemistry, Dietary Sources, Metabolism, and Nutritional Significance. *Nutr. Rev.* **1998**, *56*, 317–333.
31. Harborne, J.B. General procedures and measurement of total phenolics. In *Methods in Plant Biochemistry*; Academic Press Limited: Cambridge, MA, USA, 1989; Volume 1, pp. 1–28.
32. Robbins, R.J. Phenolic Acids in Foods: An Overview of Analytical Methodology. *J. Agric. Food Chem.* **2003**, *51*, 2866–2887.
33. Tuominen, A.; Toivonen, E.; Mutikainen, P.; Salminen, J.P. Defensive strategies in Geranium sylvaticum. Part 1: Organ-specific distribution of water-soluble tannins, flavonoids and phenolic acids. *Phytochemistry* **2013**, *95*, 394–407.
34. He, Q.; Shen, Y.; Wang, M.; Huang, M.; Yang, R.; Zhu, S.; Wang, L.; Xu, Y.; Wu, R. Natural variation in petal color in *Lycoris longituba* revealed by anthocyanin components. *PLoS ONE* **2011**, *6*, e22098.
35. Boeckler, G.A.; Gershenzon, J.; Unsicker, S.B. Phenolic glycosides of the Salicaceae and their role as anti-herbivore defenses. *Phytochemistry* **2011**, *72*, 1497–1509.
36. Agati, G.; Azzarello, E.; Pollastri, S.; Tattini, M. Flavonoids as antioxidants in plants: Location and functional significance. *Plant Sci.* **2012**, *196*, 67–76.
37. Landry, L.G.; Chapple, C.C.; Last, R.L. Arabidopsis mutants lacking phenolic sunscreens exhibit enhanced ultraviolet-B injury and oxidative damage. *Plant Physiol.* **1995**, *109*, 1159–1166.
38. Pengfei, L.; Tiansheng, D.; Xianglin, H.; Jianguo, W. Antioxidant properties of isolated isorhamnetin from the sea buckthorn marc. *Plant Foods Hum. Nutr.* **2009**, *64*, 141–145.
39. Jang, J.H.; Lee, S.H.; Jung, K.; Yoo, H.; Park, G. Inhibitory effects of myricetin on lipopolysaccharide-induced neuroinflammation. *Brain Sci.* **2020**, *10*, 32.
40. Tavsan, Z.; Kayalı, H.A. Flavonoids showed anticancer effects on the ovarian cancer cells: Involvement of reactive oxygen species, apoptosis, cell cycle and invasion. *Biomed. Pharmacother.* **2019**, *116*, 109004.
41. Rosa, L.D.S.; Jordão, N.A.; Da Costa Pereira Soares, N.; DeMesquita, J.F.; Monteiro, M.; Teodoro, A.J. Pharmacokinetic, antiproliferative and apoptotic effects of phenolic acids in human colon adenocarcinoma cells using in vitro and in silico approaches. *Molecules* **2018**, *23*, 2569.
42. Hou, S.Z.; Xu, S.J.; Jiang, D.X.; Chen, S.X.; Wang, L.L.; Huang, S.; Lai, X.P. Effect of the flavonoid fraction of *Lithocarpus polystachyus* Rehd. on spontaneously hypertensive and normotensive rats. *J. Ethnopharmacol.* **2012**, *143*, 441–447.
43. Mastantuono, T.; Di Maro, M.; Chiurazzi, M.; Battiloro, L.; Muscariello, E.; Nasti, G.; Starita, N.; Colantuoni, A.; Lapi, D. Rat pial microvascular changes during cerebral blood flow decrease and recovery: Effects of cyanidin administration. *Front. Physiol.* **2018**, *9*, 540.
44. Bae, C.R.; Park, Y.K.; Cha, Y.S. Quercetin-rich onion peel extract suppresses adipogenesis by down-regulating adipogenic transcription factors and gene expression in 3T3-L1 adipocytes. *J. Sci. Food Agric.* **2014**, *94*, 2655–2660.
45. Shin, S.W.; Jung, E.; Kim, S.; Kim, J.H.; Kim, E.G.; Lee, J.; Park, D. Antagonizing effects and mechanisms of afzelin against UVB-induced cell damage. *PLoS ONE* **2013**, *8*, e61971.
46. Lianza, M.; Mandrone, M.; Chiocchio, I.; Tomasi, P.; Marincich, L.; Poli, F. Screening of ninety herbal products of commercial interest as potential ingredients for phytocosmetics. *J. Enzyme Inhib. Med. Chem.* **2020**, *35*, 1287–1291.
47. Chiocchio, I.; Mandrone, M.; Sanna, C.; Maxia, A.; Tacchini, M.; Poli, F. Screening of a hundred plant extracts as tyrosinase and elastase inhibitors, two enzymatic targets of cosmetic interest. *Ind. Crop. Prod.* **2018**, *122*, 498–505.
48. Rose, P.M.; Cantrill, V.; Benohoud, M.; Tidder, A.; Rayner, C.M.; Blackburn, R.S. Application of anthocyanins from blackcurrant (*Ribes nigrum* L.) fruit waste as renewable hair dyes. *J. Agric. Food Chem.* **2018**, *66*, 6790–6798.

49. Barauna, S.C.; Delwing-Dal Magro, D.; Brueckheimer, M.B.; Maia, T.P.; Sala, G.A.B.N.; Döhler, A.W.; Campestrini Harger, M.; Machado de Melo, D.F.; De Gasper, A.L.; Debiassi Alberton, M.; et al. Antioxidant and antidepressant-like effects of *Eugenia catharinensis* D. Legrand in an animal model of depression induced by corticosterone. *Metab. Brain Dis.* **2018**, *33*, 1985–1994.
50. Agunloye, O.M.; Oboh, G.; Ademiluyi, A.O.; Ademosun, A.O.; Akindahunsi, A.A.; Oyagbemi, A.A.; Omobowale, T.O.; Ajibade, T.O.; Adedapo, A.A. Cardio-protective and antioxidant properties of caffeic acid and chlorogenic acid: Mechanistic role of angiotensin converting enzyme, cholinesterase and arginase activities in cyclosporine induced hypertensive rats. *Biomed. Pharmacother.* **2019**, *109*, 450–458.
51. Zaitone, S.A.; Ahmed, E.; Elsherbiny, N.M.; Mehanna, E.T.; El-Kherbetawy, M.K.; ElSayed, M.H.; Alshareef, D.; Moustafa, Y.M. Caffeic acid improves locomotor activity and lessens inflammatory burden in a mouse model of rotenone-induced nigral neurodegeneration: Relevance to Parkinson's disease therapy. *Pharmacol. Rep.* **2019**, *71*, 32–41.
52. Sanchez, M.B.; Miranda-Perez, E.; Verjan, J.C.G.; Barrera, M.D.L.A.F.; Perez-Ramos, J.; Alarcon-Aguilar, F.J. Potential of the chlorogenic acid as multitarget agent: Insulin-secretagogue and PPAR α/γ dual agonist. *Biomed. Pharmacother.* **2017**, *94*, 169–175.
53. Frauches, N.S.; do Amaral, T.O.; Largueza, C.B.D.; Teodoro, A.J. Brazilian myrtaceae fruits: A review of anticancer proprieties. *J. Pharm. Res. Int.* **2016**, *12*, 1–15.
54. Del Carmen Acevedo-Ramírez, P.M.; Hallal-Calleros, C.; Flores-Pérez, I.; Alba-Hurtado, F.; Mendoza-Garfías, M.B.; del Campo, N.C.; Barajas, R. Anthelmintic effect and tissue alterations induced in vitro by hydrolysable tannins on the adult stage of the gastrointestinal nematode *Haemonchus contortus*. *Vet. Parasitol.* **2019**, *266*, 1–6.
55. Redondo, L.M.; Chacana, P.A.; Dominguez, J.E.; Fernandez Miyakawa, M.E.D. Perspectives in the use of tannins as alternative to antimicrobial growth promoter factors in poultry. *Front. Microbiol.* **2014**, *5*, 118.
56. Mutiar, S.; Asben, A. Quality of Leather Using Vegetable Tannins Extract of *Acacia Mangium* Bark from Waste of Industrial Plantation. In *IOP Conference Series: Earth and Environmental Science*; IOP Publishing Ltd.: West Sumatera, Indonesia, 2018; Volume 327, pp. 13–14.
57. Labieniec, M.; Gabryelak, T. Effects of tannins on Chinese hamster cell line B14. *Mutat. Res. Genet. Toxicol. Environ. Mutagen.* **2003**, *539*, 127–135.
58. Labieniec, M.; Gabryelak, T.; Falcioni, G. Antioxidant and pro-oxidant effects of tannins in digestive cells of the freshwater mussel *Unio tumidus*. *Mutat. Res. Genet. Toxicol. Environ. Mutagen.* **2003**, *539*, 19–28.
59. Lotfi, R. A commentary on methodological aspects of hydrolysable tannins metabolism in ruminant: A perspective view. *Lett. Appl. Microbiol.* **2020**, *71*, 466–478.
60. Gülcü, M.; Uslu, N.; Özcan, M.M.; Gökmen, F.; Özcan, M.M.; Banjanin, T.; Gezgin, S.; Dursun, N.; Geçgel, Ü.; Ceylan, D.A.; et al. The investigation of bioactive compounds of wine, grape juice and boiled grape juice wastes. *J. Food Process. Preserv.* **2019**, *43*, e13850.
61. Moldovan, M.L.; Iurian, S.; Puscas, C.; Silaghi-Dumitrescu, R.; Hanganu, D.; Bogdan, C.; Vlase, L.; Oniga, I.; Benedec, D.A. Design of Experiments strategy to enhance the recovery of polyphenolic compounds from *Vitis vinifera* by-products through heat reflux extraction. *Biomolecules* **2019**, *9*, 529.
62. Ishida, K.; Kishi, Y.; Oishi, K.; Hirooka, H.; Kumagai, H. Effects of feeding polyphenol-rich winery wastes on digestibility, nitrogen utilization, ruminal fermentation, antioxidant status and oxidative stress in wethers. *Anim. Sci. J.* **2015**, *86*, 260–269.
63. Ferri, M.; Bin, S.; Vallini, V.; Fava, F.; Michelini, E.; Roda, A.; Minnucci, G.; Bucchi, G.; Tassoni, A. Recovery of polyphenols from red grape pomace and assessment of their antioxidant and anti-cholesterol activities. *New Biotechnol.* **2016**, *33*, 338–344.
64. Ping, L.; Pizzi, A.; Guo, Z.D.; Brosse, N. Condensed tannins extraction from grape pomace: Characterization and utilization as wood adhesives for wood particleboard. *Ind. Crop. Prod.* **2011**, *34*, 907–914.
65. Nunes, M.A.; Páscoa, R.N.; Alves, R.C.; Costa, A.S.; Bessada, S.; Oliveira, M.B.P. Fourier transform near infrared spectroscopy as a tool to discriminate olive wastes: The case of monocultivar pomaces. *Waste Manag.* **2020**, *103*, 378–387.
66. Peralbo-Molina, A.; Priego-Capote, F.; Luque de Castro, M.D. Tentative identification of phenolic compounds in olive pomace extracts using liquid chromatography–tandem mass spectrometry with a quadrupole–quadrupole–time-of-flight mass detector. *J. Agric. Food Chem.* **2012**, *60*, 11542–11550.

67. Cea Pavez, I.; Lozano-Sánchez, J.; Borrás-Linares, I.; Nuñez, H.; Robert, P.; Segura-Carretero, A. Obtaining an Extract Rich in Phenolic Compounds from Olive Pomace by Pressurized Liquid Extraction. *Molecules* **2019**, *24*, 3108.
68. Mannelli, F.; Cappucci, A.; Pini, F.; Pastorelli, R.; Decorosi, F.; Giovannetti, L.; Mele, M.; Minieri, S.; Conte, G.; Pauselli, M.; et al. Effect of different types of olive oil pomace dietary supplementation on the rumen microbial community profile in *Comisana ewes*. *Sci. Rep.* **2018**, *8*, 1–11.
69. De Toffoli, A.; Monteleone, E.; Bucalossi, G.; Veneziani, G.; Fia, G.; Servili, M.; Zanoni, B.; Pagliarini, E.; Toschi, G.; Dinnella, C. Sensory and chemical profile of a phenolic extract from olive mill waste waters in plant-based food with varied macro-composition. *Food Res. Int.* **2019**, *119*, 236–243.
70. El-Abbassi, A.; Kiai, H.; Hafidi, A. Phenolic profile and antioxidant activities of olive mill wastewater. *Food Chem.* **2012**, *132*, 406–412.
71. Aissa, I.; Kharrat, N.; Aloui, F.; Sellami, M.; Bouaziz, M.; Gargouri, Y. Valorization of antioxidants extracted from olive mill wastewater. *Biotechnol. Appl. Biochem.* **2017**, *64*, 579–589.
72. Sudha, M.L.; Baskaran, V.; Leelavathi, K. Apple pomace as a source of dietary fiber and polyphenols and its effect on the rheological characteristics and cake making. *Food Chem.* **2007**, *104*, 686–692.
73. Krawitzky, M.; Arias, E.; Peiro, J.M.; Negueruela, A.I.; Val, J.; Oria, R. Determination of color, antioxidant activity, and phenolic profile of different fruit tissue of Spanish ‘Verde Doncella’ apple cultivar. *Int. J. Food Prop.* **2014**, *17*, 2298–2311.
74. Pieszka, M.; Gogol, P.; Pietras, M.; Pieszka, M. Valuable components of dried pomaces of chokeberry, black currant, strawberry, apple and carrot as a source of natural antioxidants and nutraceuticals in the animal diet. *Ann. Anim. Sci.* **2015**, *15*, 475–491.
75. Peschel, W.; Sánchez-Rabaneda, F.; Diekmann, W.; Plescher, A.; Gartzía, I.; Jiménez, D.; Lamuela-Raventós, R.; Buxaderas, S.; Codina, C. An industrial approach in the search of natural antioxidants from vegetable and fruit wastes. *Food Chem.* **2006**, *97*, 137–150.
76. Phan, K.; Van Den Broeck, E.; Van Speybroeck, V.; De Clerck, K.; Raes, K.; De Meester, S. The potential of anthocyanins from blueberries as a natural dye for cotton: A combined experimental and theoretical study. *Dyes Pigment* **2020**, *176*, 108180.
77. Maurício, E.M.; Rosado, C.; Duarte, M.P.; Fernando, A.L.; Díaz-Lanza, A.M. Evaluation of industrial sour cherry liquor wastes as an ecofriendly source of added value chemical compounds and energy. *Waste Biomass Valorization* **2020**, *11*, 201–210.
78. Celano, R.; Piccinelli, A.L.; Pagano, I.; Roscigno, G.; Campone, L.; De Falco, E.; Russo, M.; Rastrelli, L. Oil distillation wastewaters from aromatic herbs as new natural source of antioxidant compounds. *Food Res. Int.* **2017**, *99*, 298–307.
79. Kapusta, I.; Janda, B.; Szajwaj, B.; Stochmal, A.; Piacente, S.; Pizza, C.; Franceschi, F.; Franz, C.; Oleszek, W. Flavonoids in horse chestnut (*Aesculus hippocastanum*) seeds and powdered waste water byproducts. *J. Agric. Food Chem.* **2007**, *55*, 8485–8490.
80. Mussatto, S.I.; Ballesteros, L.F.; Martins, S.; Teixeira, J.A. Extraction of antioxidant phenolic compounds from spent coffee grounds. *Sep. Purif. Technol.* **2011**, *83*, 173–179.
81. Ramón-Gonçalves, M.; Gómez-Mejía, E.; Rosales-Conrado, N.; León-González, M.E.; Madrid, Y. Extraction, identification and quantification of polyphenols from spent coffee grounds by chromatographic methods and chemometric analyses. *Waste Manag.* **2019**, *96*, 15–24.
82. Sant’Anna, V.; Biondo, E.; Kolchinski, E.M.; da Silva, L.F.S.; Corrêa, A.P.F.; Bach, E.; Brandelli, A. Total polyphenols, antioxidant, antimicrobial and allelopathic activities of spent coffee ground aqueous extract. *Waste Biomass Valorization* **2017**, *8*, 439–442.
83. Bessada, S.M.; Alves, R.C.; Costa, A.S.; Nunes, M.A.; Oliveira, M.B.P. Coffea canephora silverskin from different geographical origins: A comparative study. *Sci. Total Environ.* **2018**, *645*, 1021–1028.
84. Regazzoni, L.; Saligari, F.; Marinello, C.; Rossoni, G.; Aldini, G.; Carini, M.; Orioli, M. Coffee silver skin as a source of polyphenols: High resolution mass spectrometric profiling of components and antioxidant activity. *J. Funct. Foods* **2016**, *20*, 472–485.
85. Bresciani, L.; Calani, L.; Bruni, R.; Brighenti, F.; Del Rio, D. Phenolic composition, caffeine content and antioxidant capacity of coffee silverskin. *Food Res. Int.* **2014**, *61*, 196–201.
86. Zamuz, S.; López-Pedrouso, M.; Barba, F.J.; Lorenzo, J.M.; Domínguez, H.; Franco, D. Application of hull, bur and leaf chestnut extracts on the shelf-life of beef patties stored under MAP: Evaluation of their impact on physicochemical properties, lipid oxidation, antioxidant, and antimicrobial potential. *Food Res. Int.* **2018**, *112*, 263–273.

87. Vella, F.M.; De Masi, L.; Calandrelli, R.; Morana, A.; Laratta, B. Valorization of the agro-forestry wastes from Italian chestnut cultivars for the recovery of bioactive compounds. *Eur. Food Res. Technol.* **2019**, *245*, 2679–2686.
88. Flórez-Fernández, N.; Torres, M.D.; Gómez, S.; Couso, S.; Domínguez, H. Potential of Chestnut Wastes for Cosmetics and Pharmaceutical Applications. *Waste Biomass Valorization* **2019**, *11*, 1–10.
89. Pinto, D.; Braga, N.; Rodrigues, F.; Oliveira, M.B.P.P. Castanea sativa bur: An undervalued by-product but a promising cosmetic ingredient. *Cosmetics* **2017**, *4*, 50.
90. Esposito, T.; Celano, R.; Pane, C.; Piccinelli, A.L.; Sansone, F.; Picerno, P.; Zaccardelli, M.; Aquino, R.P.; Mencherini, T. Chestnut (*Castanea sativa* Miller.) burs extracts and functional compounds: UHPLC-UV-MS profiling, antioxidant activity, and inhibitory effects on phytopathogenic fungi. *Molecules* **2019**, *24*, 302.
91. Chioocchio, I.; Prata, C.; Mandrone, M.; Ricciardiello, F.; Marrazzo, P.; Tomasi, P.; Angeloni, C.; Fiorentini, D.; Malaguti, M.; Poli, F.; et al. Leaves and Spiny Burs of *Castanea Sativa* from an Experimental Chestnut Grove: Metabolomic Analysis and Anti- Neuroinflammatory Activity. *Metabolites* **2020**, *10*, 408.
92. Aires, A.; Carvalho, R.; Saavedra, M.J. Valorization of solid wastes from chestnut industry processing: Extraction and optimization of polyphenols, tannins and ellagitannins and its potential for adhesives, cosmetic and pharmaceutical industry. *Waste Manag.* **2016**, *48*, 457–464.
93. Turrini, F.; Donno, D.; Boggia, R.; Beccaro, G.L.; Zunin, P.; Leardi, R.; Pittaluga, A.M. An innovative green extraction and reuse strategy to valorize food supplement by-products: *Castanea sativa* bud preparations as case study. *Food Res. Int.* **2019**, *115*, 276–282.
94. Comandini, P.; Lerma-García, M.J.; Simó-Alfonso, E.F.; Toschi, T.G. Tannin analysis of chestnut bark samples (*Castanea sativa* Mill.) by HPLC-DAD-MS. *Food Chem.* **2014**, *157*, 290–295.
95. Seabra, I.J.; Chim, R.B.; Salgueiro, P.; Braga, M.E.; de Sousa, H.C. Influence of solvent additives on the aqueous extraction of tannins from pine bark: Potential extracts for leather tanning. *J. Chem. Technol. Biotechnol.* **2018**, *93*, 1169–1182.
96. Grillo, G.; Boffa, L.; Binello, A.; Mantegna, S.; Cravotto, G.; Chemat, F.; Dizhbite, T.; Lauberte, L.; Telysheva, G. Cocoa bean shell waste valorisation; extraction from lab to pilot-scale cavitation reactors. *Food Res. Int.* **2019**, *115*, 200–208.
97. Üstündağ, Ö.G.; Erşan, S.; Özcan, E.; Özcan, G.; Kayra, N.; Ekinçi, F.Y. Black tea processing waste as a source of antioxidant and antimicrobial phenolic compounds. *Eur. Food Res. Technol.* **2016**, *242*, 1523–1532.
98. Vella, F.M.; Cautela, D.; Laratta, B. Characterization of polyphenolic compounds in cantaloupe melon by-products. *Foods* **2019**, *8*, 196.
99. Kakumu, Y.; Yamauchi, K.; Mitsunaga, T. Identification of chemical constituents from the bark of *Larix kaempferi* and their tyrosinase inhibitory effect. *Holzforchung* **2019**, *73*, 637–643.
100. Tilay, A.; Bule, M.; Kishenkumar, J.; Annapure, U. Preparation of ferulic acid from agricultural wastes: Its improved extraction and purification. *J. Agric. Food Chem.* **2008**, *56*, 7644–7648.
101. Guimarães, A.G.; Serafini, M.R.; Quintans-Júnior, L.J. Terpenes and derivatives as a new perspective for pain treatment: A patent review. *Expert Opin. Ther. Pat.* **2014**, *24*, 243–265.
102. Schwab, W.; Fuchs, C.; Huang, F.C. Transformation of terpenes into fine chemicals. *Eur. J. Lipid Sci. Technol.* **2013**, *115*, 3–8.
103. Salomé-Abarca, L.F.; Mandrone, M.; Sanna, C.; Poli, F.; van der Hondel, C.A.; Klinkhamer, P.G.; Choi, Y.H. Metabolic variation in *Cistus monspeliensis* L. ecotypes correlated to their plant-fungal interactions. *Phytochemistry* **2020**, *176*, 112402.
104. Fleet, C.M.; Sun, T.P. A DELLAcate balance: The role of gibberellin in plant morphogenesis. *Curr. Plant Biol.* **2005**, *8*, 77–85.
105. Hajimohammadi, R.; Hosseini, M.; Amani, H.; Najafpour, G.D. Production of saponin biosurfactant from *Glycyrrhiza glabra* as an agent for upgrading heavy crude oil. *J. Surfactants Deterg.* **2016**, *19*, 1251–1261.
106. Gonzalez, P.J.; Sörensen, P.M. Characterization of saponin foam from *Saponaria officinalis* for food applications. *Food Hydrocoll.* **2020**, *101*, 105541.
107. Toppel, J.; Gies, K.; Harbaum-Piayda, B.; Steffen-Heins, A.; Drusch, S. Composition of *Quillaja* saponin extract affects lipid oxidation in oil-in-water emulsions. *Food Chem.* **2017**, *221*, 386–394.
108. Dewick, P.M. *Medicinal Natural Products: A Biosynthetic Approach*; John Wiley & Sons: New York, NY, USA, 2002.
109. Lee, S.; Peterson, C.J.; Coats, J.R. Fumigation toxicity of monoterpenoids to several stored product insects. *J. Stored Prod. Res.* **2003**, *39*, 77–85.

110. Hammer, K.A.; Carson, C.F.; Riley, T.V. Antifungal activity of the components of *Melaleuca alternifolia* (tea tree) oil. *J. Appl. Microbiol.* **2003**, *95*, 853–860.
111. Friedman, M.; Henika, P.R.; Mandrell, R.E. Bactericidal activities of plant essential oils and some of their isolated constituents against *Campylobacter jejuni*, *Escherichia coli*, *Listeria monocytogenes*, and *Salmonella enterica*. *J. Food Prot.* **2002**, *65*, 1545–1560.
112. Salehi, B.; Mishra, A.P.; Shukla, I.; Sharifi-Rad, M.; Contreras, M.D.M.; Segura-Carretero, A.; Sharifi-Rad, J. Thymol, thyme, and other plant sources: Health and potential uses. *Phytother. Res.* **2018**, *32*, 1688–1706.
113. Raimundo, J.R.; Frazão, D.F.; Domingues, J.L.; Quintela-Sabarís, C.; Dentinho, T.P.; Anjos, O.; Delgado, F. Neglected Mediterranean plant species are valuable resources: The example of *Cistus ladanifer*. *Planta* **2018**, *248*, 1351–1364.
114. McClements, D.J.; Gumus, C.E. Natural emulsifiers—Biosurfactants, phospholipids, biopolymers, and colloidal particles: Molecular and physicochemical basis of functional performance. *Adv. Colloid Interface Sci.* **2016**, *234*, 3–26.
115. del Hierro, J.N.; Herrera, T.; Fornari, T.; Reglero, G.; Martin, D. The gastrointestinal behavior of saponins and its significance for their bioavailability and bioactivities. *J. Funct. Food* **2018**, *40*, 484–497.
116. Rehan, M.; Mir, S.A. Structural diversity, natural sources, and pharmacological potential of plant-based saponins with special focus on anticancer activity: A review. *Med. Chem. Res.* **2020**, *29*, 1707–1722.
117. Singh, B.; Singh, J.P.; Singh, N.; Kaur, A. Saponins in pulses and their health promoting activities: A review. *Food Chem.* **2017**, *233*, 540–549.
118. Jesch, E.D.; Carr, T.P. Food ingredients that inhibit cholesterol absorption. *Prev. Nutr. Food Sci.* **2017**, *22*, 67–80.
119. Marrelli, M.; Conforti, F.; Araniti, F.; Statti, G.A. Effects of saponins on lipid metabolism: A review of potential health benefits in the treatment of obesity. *Molecules* **2016**, *21*, 1404.
120. Vinarova, L.; Vinarov, Z.; Atanasov, V.; Pantcheva, I.; Tcholakova, S.; Denkov, N.; Stoyanov, S. Lowering of cholesterol bioaccessibility and serum concentrations by saponins: In vitro and in vivo studies. *Food Funct.* **2015**, *6*, 501–512.
121. Zhao, Y.L.; Cai, G.M.; Hong, X.; Shan, L.M.; Xiao, X.H. Anti-hepatitis B virus activities of triterpenoid saponin compound from potentilla anserine L. *Phytomedicine* **2008**, *15*, 253–258.
122. Anthoni, C.; Laukoetter, M.G.; Rizken, E. Mechanism underlying the anti-inflammation actions of boswellic acid derivatives in experimental colitis. *Am. J. Physiol. Gastrointest. Liver Physiol.* **2006**, *290*, G1131–G1137.
123. Poeckel, D.; Tausch, L.; Altmann, A.; Feißt, C.; Klinkhardt, U.; Graff, J.; Werz, O. Induction of central signalling pathways and select functional effects in human platelets by β -boswellic acid. *Br. J. Pharmacol.* **2005**, *146*, 514–524.
124. Poeckel, D.; Tausch, L.; George, S.; Jauch, J.; Werz, O. 3-O-acetyl -11-keto-boswellic acid decreases basal intracellular Ca²⁺ levels and inhibits agonist-induced Ca²⁺ mobilization and mitogen-activated protein kinase activation in human monocyte cells. *J. Pharmacol. Exp. Ther.* **2006**, *316*, 224–232.
125. Singh, B.; Sharma, R.A. Plant terpenes: Defense responses, phylogenetic analysis, regulation and clinical applications. *3 Biotech* **2015**, *5*, 129–151.
126. Alakurtti, S.; Mäkelä, T.; Koskimies, S.; Yli-Kauhaluoma, J. Pharmacological properties of the ubiquitous natural product betulinic acid. *Eur. J. Pharm. Sci.* **2006**, *29*, 1–13.
127. Hoagland, R.E.; Zablutowicz, R.M.; Reddy, K.N. Studies of the phytotoxicity of saponins on weed and crop plants. In *Saponins Used in Food and Agriculture*; Waller, G.R., Yamasaki, K., Eds.; Springer: Boston, MA, USA, 1996; Volume 405, pp. 57–73.
128. Moses, T.; Papadopoulou, K.K.; Osbourn, A. Metabolic and functional diversity of saponins, biosynthetic intermediates and semi-synthetic derivatives. *Crit. Rev. Biochem. Mol.* **2014**, *49*, 439–462.
129. Augustin, J.M.; Kuzina, V.; Andersen, S.B.; Bak, S. Molecular activities, biosynthesis and evolution of triterpenoid saponins. *Phytochemistry* **2011**, *72*, 435–457.
130. Sreij, R.; Dargel, C.; Schweins, R.; Prévost, S.; Dattani, R.; Hellweg, T. Aescin-cholesterol complexes in DMPC model membranes: A DSC and temperature-dependent scattering study. *Sci. Rep.* **2019**, *9*, 1–15.
131. Nielsen, J.K.; Nagao, T.; Okabe, H.; Shinoda, T. Resistance in the plant, *Barbarea vulgaris*, and counter-adaptations in flea beetles mediated by saponins. *J. Chem. Ecol.* **2010**, *36*, 277–285.

132. Huang, H.C.; Liao, S.C.; Chang, F.R.; Kuo, Y.H.; Wu, Y.C. Molluscicidal saponins from *Sapindus mukorossi*, inhibitory agents of golden apple snails, *Pomacea canaliculata*. *J. Agric. Food Chem.* **2003**, *51*, 4916–4919.
133. Waller, G.R.; Jurzysta, M.; Thorne, R.L.Z. Allelopathic activity of root saponins from alfalfa (*Medicago sativa* L.) on weeds and wheat. *Bot. Bull. Acad. Sinica* **1993**, *34*, 1–11.
134. Trdá, L.; Janda, M.; Macková, D.; Pospíchalová, R.; Dobrev, P.; Burketová, L.; Matušinsky, P. Dual Mode of the Saponin Aescin in Plant Protection: Antifungal Agent and Plant Defense Elicitor. *Front. Plant Sci.* **2019**, *10*, 1448.
135. Fox, L.T.; Gerber, M.; Plessis, J.D.; Hamman, J.H. Transdermal drug delivery enhancement by compounds of natural origin. *Molecules* **2011**, *16*, 10507–10540.
136. Cid-Pérez, T.S.; Ávila-Sosa, R.; Ochoa-Velasco, C.E.; Rivera-Chavira, B.E.; Nevárez-Moorillón, G.V. Antioxidant and antimicrobial activity of Mexican Oregano (*Poliomintha longiflora*) essential oil, hydrosol and extracts from waste solid residues. *Plants* **2019**, *8*, 22.
137. Cautela, D.; Vella, F.M.; Castaldo, D.; Laratta, B. Characterization of essential oil recovered from fennel horticultural wastes. *Nat. Prod. Res.* **2019**, *33*, 1964–1968.
138. Negro, V.; Mancini, G.; Ruggeri, B.; Fino, D. Citrus waste as feedstock for bio-based products recovery: Review on limonene case study and energy valorization. *Bioresour. Technol.* **2016**, *214*, 806–815.
139. Pourbafrani, M.; Forgács, G.; Horváth, I.S.; Niklasson, C.; Taherzadeh, M.J. Production of biofuels, limonene and pectin from citrus wastes. *Bioresour. Technol.* **2010**, *101*, 4246–4250.
140. Ciriminna, R.; Lomeli-Rodriguez, M.; Cara, P.D.; Lopez-Sanchez, J.A.; Pagliaro, M. Limonene: A versatile chemical of the bioeconomy. *Chem. Commun.* **2014**, *50*, 15288–15296.
141. Fitzgerald, C.; Hossain, M.; Rai, D.K. Waste/By-Product Utilisations. In *Innovative Technologies in Beverage Processing*; John Wiley & Sons; Wiley-Blackwell: Hoboken, NJ, USA, 2017; Volume 7, pp: 297–309.
142. Edris, A.E. Pharmaceutical and therapeutic potentials of essential oils and their individual volatile constituents: A review. *Phytother. Res.* **2007**, *21*, 308–323.
143. González-Molina, E.; Domínguez-Perles, R.; Moreno, D.A.; García-Viguera, C. Natural bioactive compounds of *Citrus limon* for food and health. *J. Pharm. Biomed. Anal.* **2010**, *51*, 327–345.
144. Hollingsworth, R.G. Limonene, a citrus extract, for control of mealybugs and scale insects. *J. Econ. Entomol.* **2005**, *98*, 772–779.
145. Meneguzzo, F.; Brunetti, C.; Fidalgo, A.; Ciriminna, R.; Delisi, R.; Albanese, L.; Ferrini, F. Real-Scale Integral Valorization of Waste Orange Peel via Hydrodynamic Cavitation. *Processes* **2019**, *7*, 581.
146. Lota, M.L.; de Rocca Serra, D.; Tomi, F.; Jacquemond, C.; Casanova, J. Volatile components of peel and leaf oils of lemon and lime species. *J. Agric. Food Chem.* **2002**, *50*, 796–805.
147. Celli, A.; Colonna, M.; Gandini, A.; Gioia, C.; Lacerda, T.M.; Vannini, M. Polymers from monomers derived from biomass. In *Chemicals and Fuels from Bio-Based Building Blocks*; Cavani, F., Albonetti, S., Basile, F., Gandini, A., Eds.; Wiley-VCH: Weinheim, Germany, 2016; pp. 297–308.
148. Llevot, A.; Grau, E.; Carlotti, S.; Grelier, S.; Cramail, H. Dimerization of abietic acid for the design of renewable polymers by ADMET. *Eur. Polym. J.* **2015**, *67*, 409–417.
149. Aldas, M.; Pavon, C.; López-Martínez, J.; Arrieta, M.P. Pine Resin Derivatives as Sustainable Additives to Improve the Mechanical and Thermal Properties of Injected Moulded Thermoplastic Starch. *Appl. Sci.* **2020**, *10*, 2561.
150. Meninno, S. Valorization of Waste: Sustainable Organocatalysts from Renewable Resources. *ChemSusChem* **2020**, *13*, 439–468.
151. Ribeiro, B.D.; Barreto, D.W.; Coelho, M.A.Z. Use of micellar extraction and cloud point preconcentration for valorization of saponins from sisal (*Agave sisalana*) waste. *Food Bioprod. Process.* **2015**, *94*, 601–609.
152. Dahlawi, S.M.; Nazir, W.; Iqbal, R.; Asghar, W.; Khalid, N. Formulation and characterization of oil-in-water nanoemulsions stabilized by crude saponins isolated from onion skin waste. *RSC Adv.* **2020**, *10*, 39700–39707.
153. Cláudio, A.F.M.; Cognigni, A.; de Faria, E.L.; Silvestre, A.J.; Zirbs, R.; Freire, M.G.; Bica, K. Valorization of olive tree leaves: Extraction of oleanolic acid using aqueous solutions of surface-active ionic liquids. *Sep. Purif. Technol.* **2018**, *204*, 30–37.
154. Kishikawa, A.; Amen, Y.; Shimizu, K. Anti-allergic triterpenes isolated from olive milled waste. *Cytotechnology* **2017**, *69*, 307–315.

155. Campalani, C.; Chioggia, F.; Amadio, E.; Gallo, M.; Rizzolio, F.; Selva, M.; Perosa, A. Supercritical CO₂ extraction of natural antibacterials from low value weeds and agro-waste. *J. CO₂ Util.* **2020**, *40*, 101–198.
156. Gómez-García, R.; Campos, D.A.; Aguilar, C.N.; Madureira, A.R.; Pintado, M. Valorization of melon fruit (*Cucumis melo* L.) byproducts: Phytochemical and Biofunctional properties with Emphasis on Recent Trends and Advances. *Trends Food Sci. Technol.* **2020**, *25*, 1–22.
157. Arscott, S.A. Food sources of carotenoids. In *Carotenoids and Human Health*; Humana Press: Totowa, NJ, USA, 2013; pp. 3–19.
158. Aniszewski, T. *Alkaloids: Chemistry, Biology, Ecology, and Applications*, 2nd ed.; Elsevier: Amsterdam, The Netherlands, 2015.
159. Debnath, B.; Singh, W.S.; Das, M.; Goswami, S.; Singh, M.K.; Maiti, D.; Manna, K. Role of plant alkaloids on human health: A review of biological activities. *Mater. Today Chem.* **2018**, *9*, 56–72.
160. Roddick, J.G. Steroidal glycoalkaloids: Nature and consequences of bioactivity. *Adv. Exp. Med. Biol.* **1996**, *404*, 277–295.
161. Guggisberg, A.; Hesse, M. Putrescine, spermidine, spermine, and related polyamine alkaloids. In *The Alkaloids: Chemistry and Pharmacology*; Academic Press: New York, NY, USA, 1984; Volume 22, pp. 85–188.
162. Tschesche, R.; Kausmann, E.U. *Alkaloids: Chemistry and Physiology*, 1st ed.; Academic Press: Cambridge, Massachusetts, 1975; pp. 165–205.
163. Bednarz, H.; Roloff, N.; Niehaus, K. Mass spectrometry imaging of the spatial and temporal localization of alkaloids in Nightshades. *J. Agric. Food Chem.* **2019**, *67*, 13470–13477.
164. van Dam, N.M.; Vuister, L.W.; Bergshoeff, C.; de Vos, H.; Van der Meijden, E.D. The “Raison D’être” of pyrrolizidine alkaloids in *Cynoglossum officinale*: Deterrent effects against generalist herbivores. *J. Chem. Ecol.* **1995**, *21*, 507–523.
165. Mattocks, A.R. Toxicity of pyrrolizidine alkaloids. *Nature.* **1968**, *217*, 723–728.
166. Steppuhn, A.; Gase, K.; Krock, B.; Halitschke, R.; Baldwin, I.T. Nicotine’s defensive function in nature. *PLoS Biol.* **2004**, *2*, e217.
167. Trigo, J.R. Effects of pyrrolizidine alkaloids through different trophic levels. *Phytochem. Rev.* **2011**, *10*, 83–98.
168. Liu, D.L.; Lovett, J.V. Biologically active secondary metabolites of barley. II. Phytotoxicity of barley allelochemicals. *J. Chem. Ecol.* **1993**, *19*, 2231–2244.
169. Kessler, D.; Bhattacharya, S.; Diezel, C.; Rothe, E.; Gase, K.; Schöttner, M.; Baldwin, I.T. Unpredictability of nectar nicotine promotes outcrossing by hummingbirds in *Nicotiana attenuata*. *Plant J.* **2012**, *71*, 529–538.
170. Mustard, J.A. Neuroactive nectar: Compounds in nectar that interact with neurons. *Arthropod Plant Interact.* **2020**, *14*, 151–159.
171. Prada, F.; Stashenko, E.E.; Martínez, J.R. LC/MS study of the diversity and distribution of pyrrolizidine alkaloids in *Crotalaria* species growing in Colombia. *J. Sep. Sci.* **2020**, *43*, 4322–4337.
172. Newman, D.J.; Cragg, G.M. Natural products as sources of new drugs over the nearly four decades from 01/1981 to 09/2019. *J. Nat. Prod.* **2020**, *83*, 770–803.
173. D’Alessandro, S.; Scaccabarozzi, D.; Signorini, L.; Perego, F.; Ilboudo, D.P.; Ferrante, P.; Delbue, S. The use of antimalarial drugs against viral infection. *Microorganisms* **2020**, *8*, 85.
174. Ma, G.; Bavadekar, S.A.; Davis, Y.M.; Lalchandani, S.G.; Nagmani, R.; Schaneberg, B.T.; Feller, D.R. Pharmacological effects of ephedrine alkaloids on human α 1- and α 2-adrenergic receptor subtypes. *J. Pharmacol. Exp. Ther.* **2007**, *322*, 214–221.
175. Ronghe, M.; Burke, G.A.A.; Lowis, S.P.; Estlin, E.J. Remission induction therapy for childhood acute lymphoblastic leukaemia: Clinical and cellular pharmacology of vincristine, corticosteroids, L-asparaginase and anthracyclines. *Cancer Treat. Rev.* **2001**, *27*, 327–337.
176. Campos, M.M.; Fernandes, E.S.; Ferreira, J.; Santos, A.R.; Calixto, J.B. Antidepressant-like effects of *Trichilia catigua* (Catuaba) extract: Evidence for dopaminergic-mediated mechanisms. *Psychopharmacology* **2005**, *182*, 45–53.
177. Turner, N.; Li, J.Y.; Gosby, A.; To, S.W.C.; Cheng, Z.; Miyoshi, H.; Taketo, M.M.; Cooney, G.J.; Kraegen, E.W.; James, D.E.; et al. Berberine and its more biologically available derivative, dihydroberberine, inhibit mitochondrial respiratory complex I: A mechanism for the action of berberine to activate AMP-activated protein kinase and improve insulin action. *Diabetes* **2008**, *57*, 1414–1418.
178. Amritpal, S.; Sanjiv, D.; Navpreet, K.; Jaswinder, S. Berberine: Alkaloid with wide spectrum of pharmacological activities. *J. Nat. Prod.* **2010**, *3*, 64–75.

179. Palmieri, A.; Scapoli, L.; Iapichino, A.; Mercolini, L.; Mandrone, M.; Poli, F.; Gianni, A.B.; Baserga, C.; Martinelli, M. Berberine and *Tinospora cordifolia* exert a potential anticancer effect on colon cancer cells by acting on specific pathways. *Int. J. Immunopathol. Pharmacol.* **2019**, *33*, 2058738419855567.
180. Crozier, A.; Clifford, M.; Ashihara, H. *Plant Secondary Metabolites: Occurrence, Structure and Role in the Human Diet*; Blackwell: Oxford, UK, 2006.
181. Liu, Z.L.; Liu, Q.Z.; Du, S.S.; Deng, Z.W. Mosquito larvicidal activity of alkaloids and limonoids derived from *Evodia rutaecarpa* unripe fruits against *Aedes albopictus* (Diptera: Culicidae). *Parasitol. Res.* **2012**, *111*, 991–996.
182. Yang, Y.C.; Lee, S.G.; Lee, H.K.; Kim, M.K.; Lee, S.H.; Lee, H.S. A piperidine amide extracted from *Piper longum* L. fruit shows activity against *Aedes aegypti* mosquito larvae. *J. Agric. Food Chem.* **2002**, *50*, 3765–3767.
183. Yogendra, K.N.; Dhokane, D.; Kushalappa, A.C.; Sarmiento, F.; Rodriguez, E.; Mosquera, T. StWRKY8 transcription factor regulates benzylisoquinoline alkaloid pathway in potato conferring resistance to late blight. *Plant Sci.* **2017**, *256*, 208–216.
184. Lee, C.H.; Lee, H.J.; Jeon, J.H.; Lee, H.S. In vivo antifungal effects of *Coptis japonica* root-derived isoquinoline alkaloids against phytopathogenic fungi. *J. Microbiol. Biotechnol.* **2005**, *15*, 1402–1407.
185. Chowański, S.; Adamski, Z.; Marciniak, P.; Rosiński, G.; Büyükgüzel, E.; Büyükgüzel, K.; Falabella, P.; Scranio, L.; Ventrella, E.; Lelario, F.; et al. A review of bioinsecticidal activity of Solanaceae alkaloids. *Toxins*, **2016**, *8*, 60.
186. Bertin, C.; Zunino, H.; Pittet, J.C.; Beau, P.; Pineau, P.; Massonneau, M.; Robert, C.; Hopkins, J. A double-blind evaluation of the activity of an anti-cellulite product containing retinol, caffeine, and ruscogenine by a combination of several non-invasive methods. *J. Cosmet. Sci.* **2001**, *52*, 199–210.
187. Velasco, M.V.R.; Tano, C.T.N.; Machado-Santelli, G.M.; Consiglieri, V.O.; Kaneko, T.M.; Baby, A.R. Effects of caffeine and siloxanetriol alginate caffeine, as anticellulite agents, on fatty tissue: Histological evaluation. *J. Cosmet. Dermatol.* **2008**, *7*, 23–29.
188. Eun Lee, K.; Bharadwaj, S.; Yadava, U.; Gu Kang, S. Evaluation of caffeine as inhibitor against collagenase, elastase and tyrosinase using in silico and in vitro approach. *J. Enzyme Inhib. Med. Chem.* **2019**, *34*, 927–936.
189. Panusa, A.; Zuurro, A.; Lavecchia, R.; Marrosu, G.; Petrucci, R. Recovery of natural antioxidants from spent coffee grounds. *J. Agric. Food Chem.* **2013**, *61*, 4162–4168.
190. Okiyama, D.C.; Soares, I.D.; Cuevas, M.S.; Crevelin, E.J.; Moraes, L.A.; Melo, M.P.; Oliveira, A.L.; Rodrigues, C.E. Pressurized liquid extraction of flavanols and alkaloids from cocoa bean shell using ethanol as solvent. *Food Res. Int.* **2018**, *114*, 20–29.
191. Arlorio, M.; Coisson, J.D.; Travaglia, F.; Varsaldi, F.; Miglio, G.; Lombardi, G.; Martelli, A. Antioxidant and biological activity of phenolic pigments from *Theobroma cacao* hulls extracted with supercritical CO₂. *Food Res. Int.* **2005**, *38*, 1009–1014.
192. Friedman, M.; Huang, V.; Quiambao, Q.; Noritake, S.; Liu, J.; Kwon, O.; Chintalapati, S.; Young, J.; Levin, C.E.; Tam, C.; et al. Potato peels and their bioactive glycoalkaloids and phenolic compounds inhibit the growth of pathogenic trichomonads. *J. Agric. Food Chem.* **2018**, *66*, 7942–7947.
193. Wu, Z.G.; Xu, H.Y.; Ma, Q.; Cao, Y.; Ma, J.N.; Ma, C.M. Isolation, identification and quantification of unsaturated fatty acids, amides, phenolic compounds and glycoalkaloids from potato peel. *Food Chem.* **2012**, *135*, 2425–2429.
194. Figueiredo-Gonzalez, M.; Valentao, P.; Andrade, P.B. Tomato plant leaves: From by-products to the management of enzymes in chronic diseases. *Ind. Crop. Prod.* **2016**, *94*, 621–629.
195. Mellinas, C.; Ramos, M.; Jiménez, A.; Garrigós, M.C. Recent Trends in the Use of Pectin from Agro-Waste Residues as a Natural- Based Biopolymer for Food Packaging Applications. *Materials* **2020**, *13*, 673.
196. Xu, M.; Ran, L.; Chen, N.; Fan, X.; Ren, D.; Yi, L. Polarity-dependent extraction of flavonoids from citrus peel waste using a tailor-made deep eutectic solvent. *Food Chem.* **2019**, *297*, 124970.
197. Aizpurua-Olaizola, O.; Ormazabal, M.; Vallejo, A.; Olivares, M.; Navarro, P.; Etxebarria, N.; Usobiaga, A. Optimization of supercritical fluid consecutive extractions of fatty acids and polyphenols from *Vitis vinifera* grape wastes. *J. Food Sci.* **2015**, *80*, E101–E107.
198. Manna, L.; Bugnone, C.A.; Banchemo, M. Valorization of hazelnut, coffee and grape wastes through supercritical fluid extraction of triglycerides and polyphenols. *J. Supercrit. Fluids* **2015**, *104*, 204–211.
199. Takla, S.S.; Shawky, E.; Hammada, H.M.; Darwish, F.A. Green techniques in comparison to conventional ones in the extraction of Amaryllidaceae alkaloids: Best solvents selection and parameters optimization. *J. Chromatogr. A* **2018**, *1567*, 99–110.

200. Chemat, F.; Vian, M.A. Alternative Solvents for Natural Products Extraction. In *Green Chemistry and Sustainable Technology*; Springer-Verlag: Berlin/Heidelberg, Germany, 2014.
201. Passos, H.; Freire, M.G.; Coutinho, J.A. Ionic liquid solutions as extractive solvents for value-added compounds from biomass. *Green Chem.* **2014**, *16*, 4786–4815.
202. Ventura, S.P.; e Silva, F.A.; Quental, M.V.; Mondal, D.; Freire, M.G.; Coutinho, J.A. Ionic-liquid-mediated extraction and separation processes for bioactive compounds: Past, present, and future trends. *Chem. Rev.* **2017**, *117*, 6984–7052.
203. De Faria, E.L.P.; Shabudin, S.V.; Cláudio, A.F.M.; Válega, M.; Domingues, F.M.J.; Freire, C.S.R.; Silvestre, A.J.D.; Freire, M.G. Aqueous solutions of surface-active ionic liquids: Remarkable alternative solvents to improve the solubility of triterpenic acids and their extraction from biomass. *ACS Sustain. Chem. Eng.* **2017**, *5*, 7344–7351.
204. Fan, C.; Li, N.; Cao, X.; Wen, L. Ionic liquid-modified countercurrent chromatographic isolation of high-purity delphinidin-3-rutinoside from eggplant peel. *J. Food Sci.* **2020**, *85*, 1132–1139.
205. Lima, Á.S.; Soares, C.M.F.; Paltram, R.; Halbwirth, H.; Bica, K. Extraction and consecutive purification of anthocyanins from grape pomace using ionic liquid solutions. *Fluid Ph. Equilibria* **2017**, *451*, 68–78.
206. Mišan, A.; Nađpal, J.; Stupar, A.; Pojić, M.; Mandić, A.; Verpoorte, R.; Choi, Y.H. The perspectives of natural deep eutectic solvents in agri-food sector. *Crit. Rev. Food Sci. Nutr.* **2020**, *60*, 2564–2592.
207. Jeong, K.M.; Jin, Y.; Han, S.Y.; Kim, E.M.; Lee, J. One-step sample preparation for convenient examination of volatile monoterpenes and phenolic compounds in peppermint leaves using deep eutectic solvents. *Food Chem.* **2018**, *251*, 69–76.
208. Jablonský, M.; Šima, J. Phytomass Valorization by Deep Eutectic Solvents-Achievements, Perspectives, and Limitations. *Crystals* **2020**, *10*, 800.
209. De los Ángeles Fernández, M.; Espino, M.; Gomez, F.J.; Silva, M.F. Novel approaches mediated by tailor-made green solvents for the extraction of phenolic compounds from agro-food industrial by-products. *Food Chem.* **2018**, *239*, 671–678.
210. Panzella, L.; Moccia, F.; Nasti, R.; Marzorati, S.; Verotta, L.; Napolitano, A. Bioactive phenolic compounds from agri-food wastes: An update on green and sustainable extraction methodologies. *Front. Nutr.* **2020**, *7*, 60.
211. Roselló-Soto, E.; Koubaa, M.; Moubarik, A.; Lopes, R.P.; Saraiva, J.A.; Boussetta, N.; Barba, F.J. Emerging opportunities for the effective valorization of wastes and by-products generated during olive oil production process: Non-conventional methods for the recovery of high-added value compounds. *Trends. Food Sci. Technol.* **2015**, *45*, 296–310.
212. Burlini, I.; Sacchetti, G. Secondary Bioactive Metabolites from Plant-Derived Food Byproducts through Ecopharmacognostic Approaches: A Bound Phenolic Case Study. *Plants* **2020**, *9*, 1060.
213. Roselló-Soto, E.; Galanakis, C.M.; Brnčić, M.; Orlien, V.; Trujillo, F.J.; Mawson, R.; Barba, F.J. Clean recovery of antioxidant compounds from plant foods, by-products and algae assisted by ultrasounds processing. Modeling approaches to optimize processing conditions. *Trends. Food Sci. Technol.* **2015**, *42*, 134–149.
214. Chemat, F.; Cravotto, G. *Microwave-Assisted Extraction for Bioactive Compounds*; Springer: New York, NY, USA, 2013.
215. Barba, F.J.; Puértolas, E.; Brnčić, M.; Nedelchev Panchev, I.; Dimitrov, D.A.; Athès-Dutour, V.; Moussa, M.; Souchon, I. Emerging extraction. In *Food Waste Recovery: Processing Technologies and Industrial Techniques*; Galanakis, C., Ed.; Academic Press: Cambridge, MA, USA, 2015; pp. 249–272.
216. Plazzotta, S.; Ibarz, R.; Manzocco, L.; Martín-Belloso, O. Optimizing the antioxidant biocompound recovery from peach waste extraction assisted by ultrasounds or microwaves. *Ultrason. Sonochem.* **2020**, *63*, 104954.
217. Casazza, A.A.; Pettinato, M.; Perego, P. Polyphenols from apple skins: A study on microwave-assisted extraction optimization and exhausted solid characterization. *Sep. Purif. Technol.* **2020**, *240*, 116640.
218. Kapoor, S.; Gandhi, N.; Tyagi, S.K.; Kaur, A.; Mahajan, B.V.C. Extraction and characterization of guava seed oil: A novel industrial byproduct. *Lebensm. Wiss. Technol.* **2020**, *132*, 109882.
219. Carabias-Martínez, R.; Rodríguez-Gonzalo, E.; Revilla-Ruiz, P.; Hernández-Méndez, J. Pressurized liquid extraction in the analysis of food and biological samples. *J. Chromatogr. A* **2005**, *1089*, 1–17.
220. Benthin, B.; Danz, H.; Hamburger, M. Pressurized liquid extraction of medicinal plants. *J. Chromatogr. A* **1999**, *837*, 211–219.
221. Schantz, M.M. Pressurized liquid extraction in environmental analysis. *Anal. Bioanal. Chem.* **2006**, *386*, 1043–1047.

222. Mustafa, A.; Turner, C. Pressurized liquid extraction as a green approach in food and herbal plants extraction: A review. *Anal. Chim. Acta* **2011**, *703*, 8–18.
223. Wu, C.T.; Agrawal, D.C.; Huang, W.Y.; Hsu, H.C.; Yang, S.J.; Huang, S.L.; Lin, Y.S. Functionality analysis of spent coffee ground extracts obtained by the hydrothermal method. *J. Chem.* **2019**, doi:10.1155/2019/4671438.
224. Scopus Preview. Available online: <https://www.scopus.com/term/analyzer.uri?sid=a812e38dc2896c675cc2befb7b3d7df8&origin=result&list&src=s&s=TITLE-ABS-KEY+%28+plant+AND+by-products+AND+waste+AND+valorization%29&sort=plf-f&sdt=a&sot=a&sl=65&count=204&analyzeResults=Analyze+results&txGid=ad7a147decc8a12b718c1490e34a2899> (accessed on 19 November 2020).
225. Acquadro, S.; Appleton, S.; Marengo, A.; Bicchi, C.; Sgorbini, B.; Mandrone, M.; Gai, F.; Peiretti, P.G.; Cagliero, C.; Rubiolo, P. Grapevine Green Pruning Residues as a Promising and Sustainable Source of Bioactive Phenolic Compounds. *Molecules* **2020**, *25*, 464.
226. Simitzis, P.E. Agro-industrial by-products and their bioactive compounds—An ally against oxidative stress and skin aging. *Cosmetics* **2018**, *5*, 58.
227. Borges-Argaez, R.; Chan-Balan, R.; Cetina-Montejo, L.; Ayora-Talavera, G.; Sansores-Peraza, P.; Gomez-Carballo, J.; Caceres-Farfan, M. In vitro evaluation of anthraquinones from Aloe vera (*Aloe barbadensis* Miller) roots and several derivatives against strains of influenza virus. *Ind. Crop. Prod.* **2019**, *132*, 468–475.
228. Saha, A.; Basak, B.B. Scope of value addition and utilization of residual biomass from medicinal and aromatic plants. *Ind. Crop. Prod.* **2020**, *145*, 111979.
229. Sharma, P.; Gaur, V.K.; Sirohi, R.; Larroche, C.; Kim, S.H.; Pandey, A. Valorization of cashew nut processing residues for industrial applications. *Ind. Crop. Prod.* **2020**, *152*, 112550.
230. Sepúlveda, L.; Romaní, A.; Aguilar, C.N.; Teixeira, J. Valorization of pineapple waste for the extraction of bioactive compounds and glycosides using autohydrolysis. *Innov. Food Sci. Emerg. Technol.* **2018**, *47*, 38–45.
231. Toomer, O.T. A comprehensive review of the value-added uses of peanut (*Arachis hypogaea*) skins and by-products. *Crit. Rev. Food Sci.* **2020**, *60*, 341–350.
232. Mandalari, G.; Bennett, R.N.; Bisignano, G.; Trombetta, D.; Saija, A.; Faulds, C.B.; Gasson, M.J.; Nabad, A. Antimicrobial activity of flavonoids extracted from bergamot (*Citrus bergamia* Risso) peel, a byproduct of the essential oil industry. *J. Appl. Microbiol.* **2007**, *103*, 2056–2064.
233. Gavahian, M.; Chu, Y.H.; Mousavi Khaneghah, A. Recent advances in orange oil extraction: An opportunity for the valorisation of orange peel waste a review. *Int. J. Food Sci. Technol.* **2019**, *54*, 925–932.
234. Pujol, D.; Liu, C.; Gominho, J.; Olivella, M.À.; Fiol, N.; Villaescusa, I.; Pereira, H. The chemical composition of exhausted coffee waste. *Ind. Crop. Prod.* **2013**, *50*, 423–429.
235. Valdez-Arjona, L.P.; Ramírez-Mella, M. Pumpkin Waste as Livestock Feed: Impact on Nutrition and Animal Health and on Quality of Meat, Milk, and Egg. *Animals* **2019**, *9*, 769.
236. Kumar, A.; Agarwal, K.; Singh, M.; Saxena, A.; Yadav, P.; Maurya, A.K.; Yadav, A.; Tandon, S.; Chanda, D.; Bawankule, D.U. Essential oil from waste leaves of *Curcuma longa* L. alleviates skin inflammation. *Inflammopharmacology* **2018**, *26*, 1245–1255.
237. Mejri, F.; Baati, T.; Martins, A.; Selmi, S.; Serralheiro, M.L.; Falé, P.L.; Rauter, A.; Casabianca, H.; Hosni, K. Phytochemical analysis and in vitro and in vivo evaluation of biological activities of artichoke (*Cynara scolymus* L.) floral stems: Towards the valorization of food by-products. *Food Chem.* **2020**, *333*, 127506.
238. Sayed-Ahmad, B.; Straumīte, E.; Šabovics, M.; Krūma, Z.; Merah, O.; Saad, Z.; Hijazi, A.; Talou, T. Effect of addition of fennel (*Foeniculum vulgare* L.) on the quality of protein bread. Proceedings of the Latvian Academy of Sciences, Section B. Natural, Exact, and Applied Sciences. *J. Latvian Acad. Sci.* **2017**, *71*, 509–514.
239. Ortiz-de Elguea-Culebras, G.; Berruga, M.I.; Santana-Méridas, O.; Herraiz-Peñalver, D.; Sánchez-Vioque, R. Chemical Composition and Antioxidant Capacities of Four Mediterranean Industrial Essential Oils and Their Resultant Distilled Solid By-Products. *Eur. J. Lipid Sci. Technol.* **2017**, *119*, 1700242.
240. Gullón, B.; Eibes, G.; Moreira, M.T.; Herrera, R.; Labidi, J.; Gullón, P. Yerba mate waste: A sustainable resource of antioxidant compounds. *Ind. Crop. Prod.* **2018**, *113*, 398–405.

241. Jahanban-Esfahlan, A.; Ostadrahimi, A.; Tabibiazar, M.; Amarowicz, R. A comprehensive review on the chemical constituents and functional uses of walnut (*Juglans* spp.) husk. *Int. J. Mol. Sci.* **2019**, *20*, 3920.
242. Torras-Claveria, L.; Jauregui, O.; Bastida, J.; Codina, C.; Viladomat, F. Antioxidant activity and phenolic composition of lavandin (*Lavandula x intermedia* Emeric ex Loiseleur) waste. *J. Agric. Food Chem.* **2007**, *55*, 8436–8443.
243. Pagano, I.; Sánchez-Camargo, A.D.P.; Mendiola, J.A.; Campone, L.; Cifuentes, A.; Rastrelli, L.; Ibañez, E. Selective extraction of high-value phenolic compounds from distillation wastewater of basil (*Ocimum basilicum* L.) by pressurized liquid extraction. *Electrophoresis* **2018**, *39*, 1884–1891.
244. King, A.J.; Griffin, J.K.; Roslan, F. In vivo and in vitro addition of dried olive extract in poultry. *J. Agric. Food Chem.* **2014**, *62*, 7915–7919.
245. Agulló-Chazarra, L.; Borrás-Linares, I.; Lozano-Sánchez, J.; Segura-Carretero, A.; Micol, V.; Herranz-López, M.; Barrajón-Catalán, E. Sweet Cherry Byproducts Processed by Green Extraction Techniques as a Source of Bioactive Compounds with Antiaging Properties. *Antioxidants* **2020**, *9*, 418.
246. Yılmaz, F.M.; Görgüç, A.; Karaaslan, M.; Vardin, H.; Ersus Bilek, S.; Uygun, Ö.; Bircan, C. Sour cherry by-products: Compositions, functional properties and recovery potentials—A review. *Crit. Rev. Food Sci. Nutr.* **2019**, *59*, 3549–3563.
247. Piccirillo, C.; Demiray, S.; Ferreira, A.S.; Pintado, M.E.; Castro, P.M. Chemical composition and antibacterial properties of stem and leaf extracts from Ginja cherry plant. *Ind. Crop. Prod.* **2013**, *43*, 562–569.
248. Prgomet, I.; Gonçalves, B.; Dominguez-Perles, R.; Santos, R.; Saavedra, M.J.; Aires, A.; Pascual-Seva, N.; Barros, A. Irrigation deficit turns almond by-products into a valuable source of antimicrobial (poly) phenols. *Ind. Crop. Prod.* **2019**, *132*, 186–196.
249. Kharchoufi, S.; Licciardello, F.; Siracusa, L.; Muratore, G.; Hamdi, M.; Restuccia, C. Antimicrobial and antioxidant features of ‘Gabsi’ pomegranate peel extracts. *Ind. Crop. Prod.* **2018**, *111*, 345–352.
250. Andrade, M.A.; Lima, V.; Silva, A.S.; Vilarinho, F.; Castilho, M.C.; Khwaldia, K.; Ramos, F. Pomegranate and grape by-products and their active compounds: Are they a valuable source for food applications? *Trends Food Sci. Technol.* **2019**, *86*, 68–84.
251. Legua, P.; Forner-Giner, M.Á.; Nuncio-Jáuregui, N.; Hernández, F. Polyphenolic compounds, anthocyanins and antioxidant activity of nineteen pomegranate fruits: A rich source of bioactive compounds. *J. Funct. Foods* **2016**, *23*, 628–636.
252. Fischer, U.A.; Carle, R.; Kammerer, D.R. Identification and quantification of phenolic compounds from pomegranate (*Punica granatum* L.) peel, mesocarp, aril and differently produced juices by HPLC-DAD–ESI/MSn. *Food Chem.* **2011**, *127*, 807–821.
253. Alexandre, E.M.; Silva, S.; Santos, S.A.; Silvestre, A.J.; Duarte, M.F.; Saraiva, J.A.; Pintado, M. Antimicrobial activity of pomegranate peel extracts performed by high pressure and enzymatic assisted extraction. *Food Res. Int.* **2019**, *115*, 167–176.
254. Carriço, C.; Ribeiro, H.M.; Marto, J. Converting cork by-products to ecofriendly cork bioactive ingredients: Novel pharmaceutical and cosmetics applications. *Ind. Crop. Prod.* **2018**, *125*, 72–84.
255. Plainfossé, H.; Trinel, M.; Verger-Dubois, G.; Azoulay, S.; Burger, P.; Fernandez, X. Valorisation of *Ribes nigrum* L. Pomace, an Agri-Food By-Product to Design a New Cosmetic Active. *Cosmetics* **2020**, *7*, 56.
256. Sanchez-Vioque, R.; Izquierdo-Melero, M.E.; Quilez, M.; Herraiz-Penalver, D.; Santana-Méridas, O.; Jordan, M.J. Solid Residues from the Distillation of *Salvia lavandulifolia* Vahl as a Natural Source of Antioxidant Compounds. *J. Am. Oil Chem. Soc.* **2018**, *95*, 1277–1284.
257. Navarrete, A.; Herrero, M.; Martín, A.; Cocero, M.J.; Ibañez, E. Valorization of solid wastes from essential oil industry. *J. Food Eng.* **2011**, *104*, 196–201.
258. Ma, H.; Huang, Q.; Qu, W.; Li, L.; Wang, M.; Li, S.; Chu, F. In vivo and in vitro anti-inflammatory effects of *Sophora flavescens* residues. *J. Ethnopharmacol.* **2018**, *224*, 497–503.
259. Weng, Z.; Guo, S.; Qian, D.; Zhu, Z.; Zhang, S.; Li, A.; Lei, Z.; Duan, J. *Sophora flavescens* Seed as a promising high potential byproduct: Phytochemical characterization and bioactivity evaluation. *Ind. Crop. Prod.* **2017**, *109*, 19–26.
260. Cabrera-Barjas, G.; Quezada, A.; Bernardo, Y.; Moncada, M.; Zúñiga, E.; Wilkens, M.; Giordano, A.; Nestic, A.; Delgado, N. Chemical composition and antibacterial activity of red murta (*Ugni molinae* Turcz.) seeds: An undervalued Chilean resource. *J. Food Meas. Charact.* **2020**, *14*, 1–12.
261. Ribeiro, L.F.; Ribani, R.H.; Francisco, T.M.G.; Soares, A.A.; Pontarolo, R.; Haminiuk, C.W.I. Profile of bioactive compounds from grape pomace (*Vitis vinifera* and *Vitis labrusca*) by spectrophotometric, chromatographic and spectral analyses. *J. Chromatogr. B* **2015**, *1007*, 72–80.

262. Poveda, J.M.; Loarce, L.; Alarcón, M.; Díaz-Maroto, M.C.; Alañón, M.E. Revalorization of winery by-products as source of natural preservatives obtained by means of green extraction techniques. *Ind. Crop. Prod.* **2018**, *112*, 617–625.
263. Leal, C.; Gouvinhas, I.; Santos, R.A.; Rosa, E.; Silva, A.M.; Saavedra, M.J.; Barros, A.I. Potential application of grape (*Vitis vinifera* L.) stem extracts in the cosmetic and pharmaceutical industries: Valorization of a by-product. *Ind. Crop. Prod.* **2020**, *154*, 112675.
264. Pantelić, M.M.; Zagorac, D.Č.D.; Davidović, S.M.; Todić, S.R.; Bešlić, Z.S.; Gašić, U.M.; Tešić, Z.L.; Natić, M.M. Identification and quantification of phenolic compounds in berry skin, pulp, and seeds in 13 grapevine varieties grown in Serbia. *Food Chem.* **2016**, *211*, 243–252.
265. Maier, T.; Schieber, A.; Kammerer, D.R.; Carle, R. Residues of grape (*Vitis vinifera* L.) seed oil production as a valuable source of phenolic antioxidants. *Food Chem.* **2009**, *112*, 551–559.
266. Farhadi, K.; Esmailzadeh, F.; Hatami, M.; Forough, M.; Molaie, R. Determination of phenolic compounds content and antioxidant activity in skin, pulp, seed, cane and leaf of five native grape cultivars in West Azerbaijan province, Iran. *Food Chem.* **2016**, *199*, 847–855.
267. Soares, S.C.S.; De Lima, G.C.; Laurentiz, A.C.; Féboli, A.; Dos Anjos, L.A.; de Paula Carlis, M.S.; Filardi, R.D.S.; de Laurentiz, R.D.S. In vitro anthelmintic activity of grape pomace extract against gastrointestinal nematodes of naturally infected sheep. *Int. J. Vet. Sci.* **2018**, *6*, 243–247.
268. World Checklist of Vascular Plants. Available online: <https://wcvp.science.kew.org/> (accessed on 14 December 2020).

1.2. Leaves and Spiny Burs of *Castanea sativa* from an Experimental Chestnut Grove: Metabolomic Analysis and Anti-Neuroinflammatory Activity

This article has been published in *Metabolites* Journal:

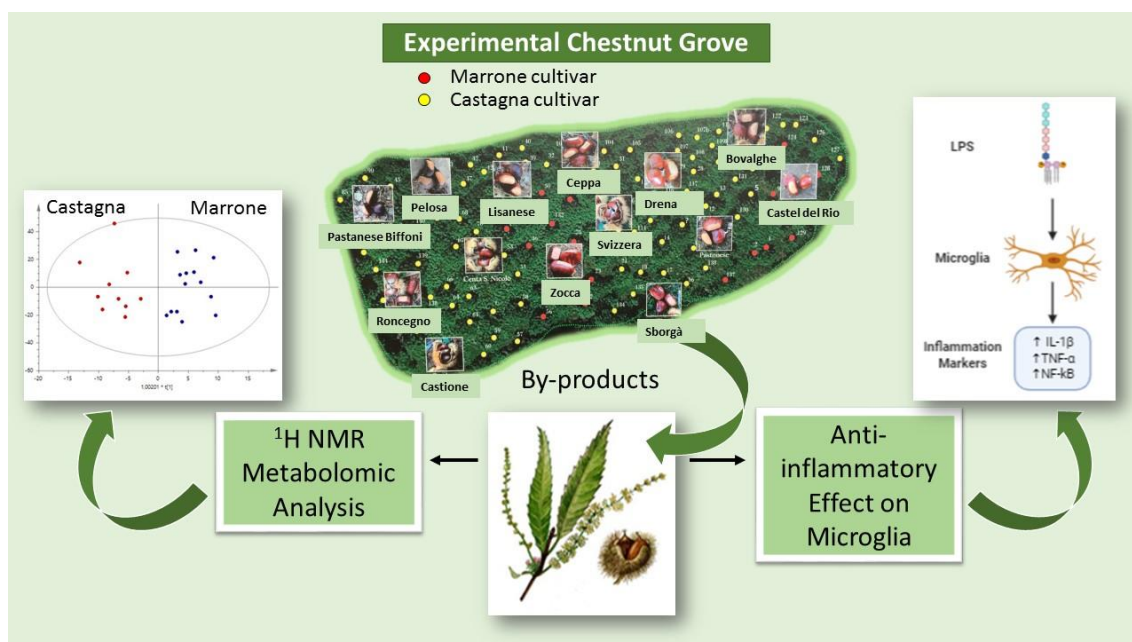
Chiocchio, I., Prata, C., Mandrone, M., Ricciardiello, F., Marrazzo, P., Tomasi, P., Angeloni, C., Fiorentini, D., Malaguti, M., Poli, F., Hrelia, S. Leaves and spiny burs of *Castanea Sativa* from an experimental chestnut grove: Metabolomic analysis and anti-neuroinflammatory activity. *Metabolites*, 2020, 10(10), 408.

<https://doi.org/10.3390/metabo10100408>

Keywords: ¹H NMR-based Metabolomics; neuroinflammation; flavonoids; Castanea sativa; waste valorization

Abstract

Castanea sativa cultivation has been present in Mediterranean regions since ancient times. In order to promote a circular economy, it is of great importance to valorize chestnut groves' by-products. In this study, leaves and spiny burs from twenty-four *Castanea* trees were analyzed by ^1H NMR metabolomics to provide an overview of their phytochemical profile. The Orthogonal Projections to Latent Structures Discriminant Analysis (OPLS-DA) performed on these data allowed us to distinguish 'Marrone' from 'Castagna', since the latter were generally more enriched with secondary metabolites, in particular, flavonoids (astragalin, isorhamnetin glucoside, and myricitrin) were dominant. Knowing that microglia are involved in mediating the oxidative and inflammatory response of the central nervous system, the potential anti-inflammatory effects of extracts derived from leaves and spiny burs were evaluated in a neuroinflammatory cell model: BV-2 microglia cells. The tested extracts showed cytoprotective activity (at 0.1 and 0.5 mg/mL) after inflammation induction by 5 $\mu\text{g/mL}$ lipopolysaccharide (LPS). In addition, the transcriptional levels of IL-1 β , TNF- α , and NF- κB expression induced by LPS were significantly decreased by cell incubation with spiny burs and leaves extracts. Taken together, the obtained results are promising and represent an important step to encourage recycling and valorization of chestnut byproducts, usually considered "waste".



Introduction

Castanea sativa Mill. (Fagaceae) is widespread in the Mediterranean region, where, since ancient times, its cultivation for timber and nut production has played a pivotal role in local sustenance and economy. In the last decade, increasing attention has been given to the chestnut waste that is generated yearly, which has a negative impact on both the environment and economy [1,2]. In fact, farmers tend to burn spiny burs, a maintenance practice, which could be avoided by adopting more sustainable solutions [1–3]. In this context, the implantation of circular economy practices, based on valorization of a crop's waste material, plays a pivotal role. Regarding chestnut by-products, Costa-Trigo and co-workers suggested the application of chestnut burs extract for the production of culture media suitable for the growth of a wide range of microorganisms [4]. Moreover, chestnut shells of an Italian cultivar “Marrone di Roccadaspide” PGI (Protected Geographical Indication) were found to be endowed with antioxidant activity linked to their high content of tannins [5]. The abundance of total phenols and hydrolysable tannins confers to chestnut grove by-products interesting anti-inflammatory activity, as demonstrated by the ability of *Castanea* shell extracts to reduce the levels of cytokines and other biomarkers of inflammation in several experimental models [6–11].

The present study was carried out on leaves and spiny burs of *Castanea sativa* collected from trees growing in the experimental chestnut grove of Granaglione, situated on the Apennines Mountains in Emilia-Romagna [12,13], where a number of different cultivars of *C. sativa*, are cultivated and studied. In order to first obtain an overview of the phytochemical composition of the samples, their ¹H NMR metabolomic profiles were measured.

Metabolomics relies on untargeted analysis protocols handled with multivariate data treatment. This workflow has already been applied successfully in several areas of research, from human diagnostics and epidemiology to the plant sciences [14]. In this latter field of study, metabolomics was successful at facilitating the identification of the active components of medicinal plants [15], studying plant ecotypes and biological features [16,17], and controlling food and botanical quality, both in terms of nutraceutical/biological properties and fraud detection [18,19].

Since the analyzed samples were classified as ‘Castagna’ and ‘Marrone’ by pomological analysis, the obtained metabolomic data were also treated by chemometrics in order to explore the occurrence of differences between these two groups.

Moreover, with the view of valorizing *Castanea* by-products, the potential cytoprotective and anti-inflammatory roles of leaves and spiny burs extracts were investigated. In fact, according to previous studies, *Castanea* by-products are able to decrease oxidative stress [20] and consequently they could be promising in counteracting chronic degenerative diseases. Inflammation represents a feature of all chronic degenerative diseases, among which neurodegenerative diseases are considered a real threat to human health. It has been suggested that a cascade of processes collectively called neuroinflammation, which involves support cells called glia, contributes to neurodegeneration [21]. In particular, the activation of the neuroimmune cells, microglia, into proinflammatory states is an effective endogenous defense that protects the central nervous system (CNS) against microorganisms and injuries. It is usually a positive mechanism that aims to eliminate threats and restore homeostasis [22]. However, chronically activated and proliferating microglia promote the neuroinflammatory state by releasing cytokines and reactive oxygen and nitrogen species, ultimately causing oxidative damage to the neurons [23]. Growing experimental evidence suggests that controlling microglia activation may have protective effects against neurodegenerative diseases [24].

Therefore, the most phytochemically diverse samples, according to metabolomic analysis, were tested in a cellular model of microglia (BV-2 cells) to evaluate their potential neuroprotective and anti-inflammatory activities.

Hence, the overall objective of this study was to upgrade phytochemical knowledge on *Castanea* and its biological properties, with a particular attention to provide a basis for the valorization of chestnut grove waste material.

Results and Discussion

Metabolomic Analysis

In order to compare the phytochemical profiles of ‘Castagna’ and ‘Marrone’, the Orthogonal Projections to Latent Structures Discriminant Analysis (OPLS-DA) was built.

This is a powerful multivariate data modeling tool that provides insights into separations between experimental groups based on high-dimensional spectral measurements, i.e., from NMR. In this case, it was built using bucketed ^1H NMR spectra as the x variables, and ‘Castagna’ and ‘Marrone’ (Figure 1A) as the discriminant classes, as identified by pomological analysis. Three components maximized the explained 87.5% of the variation in the data set (given by $R^2x(\text{Cum})$), $R^2y(\text{Cum})$ was 84.8%, while the obtained $Q^2(\text{Cum})$ was 73.1%, indicating good model predictability (Q^2 must be equal or higher than 50%). The model was further validated by the permutation test, giving $R^2(\text{Cum}) = 84.8\%$ and $Q^2(\text{Cum}) = 73.1\%$, and CV-ANOVA resulting in $p = 0.41 \times 10^{-3}$ and $F = 7.68$. The overall parameters proved that the developed model was not only interpretable but also predictive and, thus, able to discriminate ‘Castagna’ from ‘Marrone’ on the basis of the leaves’ phytochemical profile.

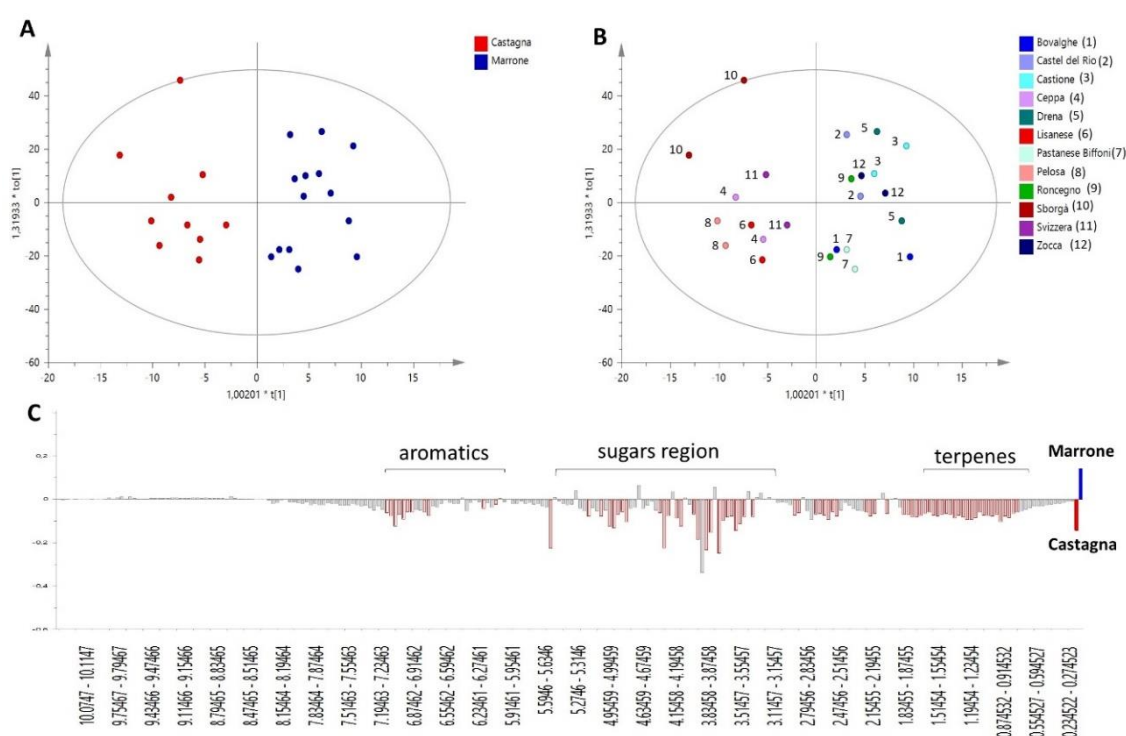


Figure 1. OPLS-DA model performed on ^1H NMR profiles of different *C. sativa* cultivars, discriminating ‘Castagna’ and ‘Marrone’ on the basis of leaf metabolome. (A) Score scatter plot colored according to model’s given classes; (B) Score Scatter plot colored according to the different cultivars analyzed (reported in the legend), each cultivar is represented by samples collected from two different trees; (C) Predictive loading plot is a schematic representation of bucketed ^1H NMR spectra, indicating the most important ^1H NMR signals contributing to the discrimination of ‘Castagna’ (in red on the negative axis of the plot) from ‘Marrone’ (on the positive axis of the plot).

It is worth noting that for each class, samples collected from two different trees of the same specific cultivar were analyzed, and they generally showed a reproducible metabolome, indicated by their closeness in the score of the scatter plot of the model (Figure 1B).

S-plot, loading plot, and VIP (Variable Influence on Projection) plot (not shown) of the OPLS-DA model explain the relationships between x variables (^1H NMR signals) and given classes, in this case, ‘Castagna’ and ‘Marrone’. Thus, these plots were used to provide information on metabolites peculiar to a specific *Castanea* cultivar and important for its metabolomics-based distinction and identification.

‘Marrone’ leaves were characterized by small amounts of all metabolites, as highlighted by Figure 1C, where the highest intensity of the general spectral signals was found for ‘Castagna’ samples. Glucose and quinic acid were the only two metabolites showing a slight increasing trend in ‘Marrone’, but based on standard deviation calculated on VIP plot results, it is clear that this observation is not generalizable for all ‘Marrone’ samples; therefore, these metabolites are not trustworthy markers of distinction for ‘Marrone’.

Specifically, several aromatic signals were found to be less concentrated in ‘Marrone’, among them, two doublets at δ 5.95 and 6.03 with coupling constants around 2.2 Hz, which are generally characteristic of flavonoid protons situated on aromatic ring B [25]. They increased linearly with other aromatic signals and a doublet at δ 0.8, which is potentially related to the methyl group of rhamnose that is a common sugar moiety of several glycosylated flavonoids.

The results obtained from this model made essential further studies aimed at characterizing the main flavonoids contained in leaves.

The highest content of flavonoids was revealed, by ^1H NMR analysis, in the EtOAc fraction that was derived from the liquid–liquid partition of an extract obtained by pooling all samples. Thus, this fraction was further fractionated by column chromatography. Three main flavonoids were chemically characterized through NMR and MS analysis. Mono and bi-dimensional NMR experiments allowed to elucidate the substitution pattern of the B ring (Table S1 and Figures S1–S4), while MS provided the molecular weights. On this basis, the identified flavonoids were astragalin $[\text{M-H}]^-$ ion at m/z 447, isorhamnetin glucoside $[\text{M-H}]^-$ ion at m/z 477, and myricitrin $[\text{M-H}]^-$ ion at m/z 463

(Figure 2). The presence of astragalín and isorhamnetín in *C. sativa* leaves was already reported [26]. Moreover, astragalín was also found in *C. sativa* burs and flowers [27,28] and isorhamnetín glucoside was found in flowers [29]. Various glycosides of myricetin, kaempferol, and isorhamnetín were also found in *C. sativa* and *C. crenata* flowers [28–30].

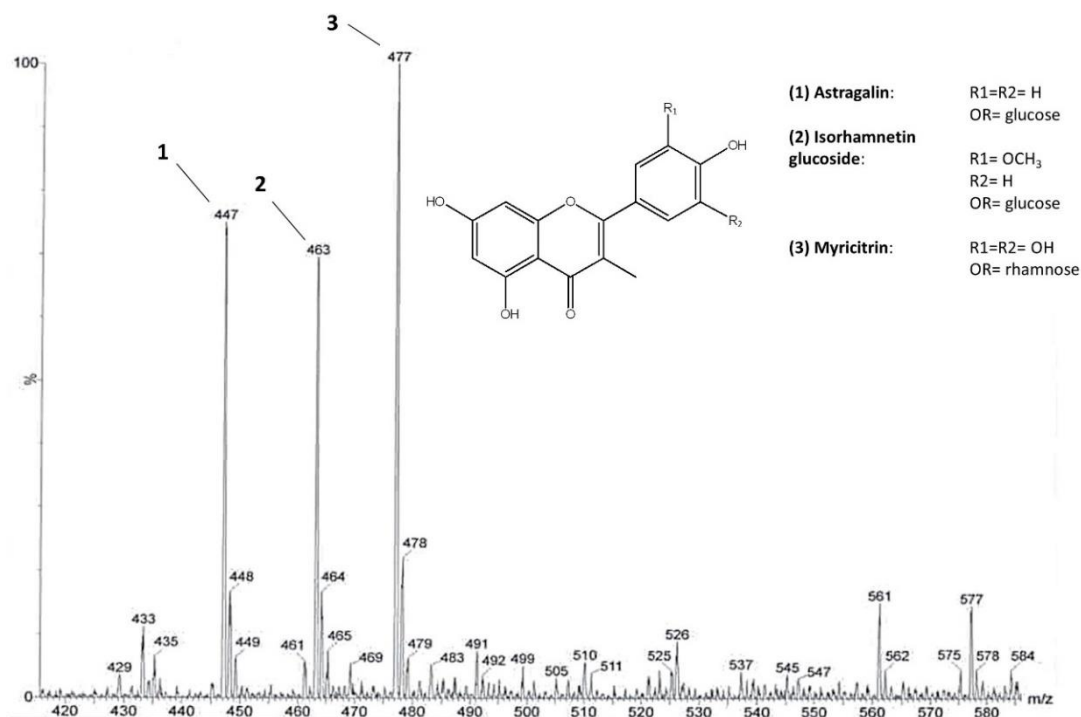


Figure 2. The main flavonoid glycosides identified in *C. sativa* leaves. ESI-MS spectrum of the flavonoid fraction obtained after direct infusion. Molecular ions at m/z 447, 477, and 463 belong to astragalín (1), isorhamnetín glucoside (2), and myricitrín (3), respectively.

Spiny burs hydroalcoholic extracts were investigated through ¹H NMR profiling. In contrast to the variation seen in the extracts from leaves, no specific metabolomics variation could be associated to ‘Castagna’ and ‘Marrone’ spiny burs. Compared to leaves (Figure 3A), this organ was less rich in secondary metabolites. Glucose and quinic acid were the most abundant compounds (Figure 3B). However, the aromatic region of the spectrum also showed numerous signals, potentially ascribable to tannins, which were

previously reported to be contained in this plant material [27].

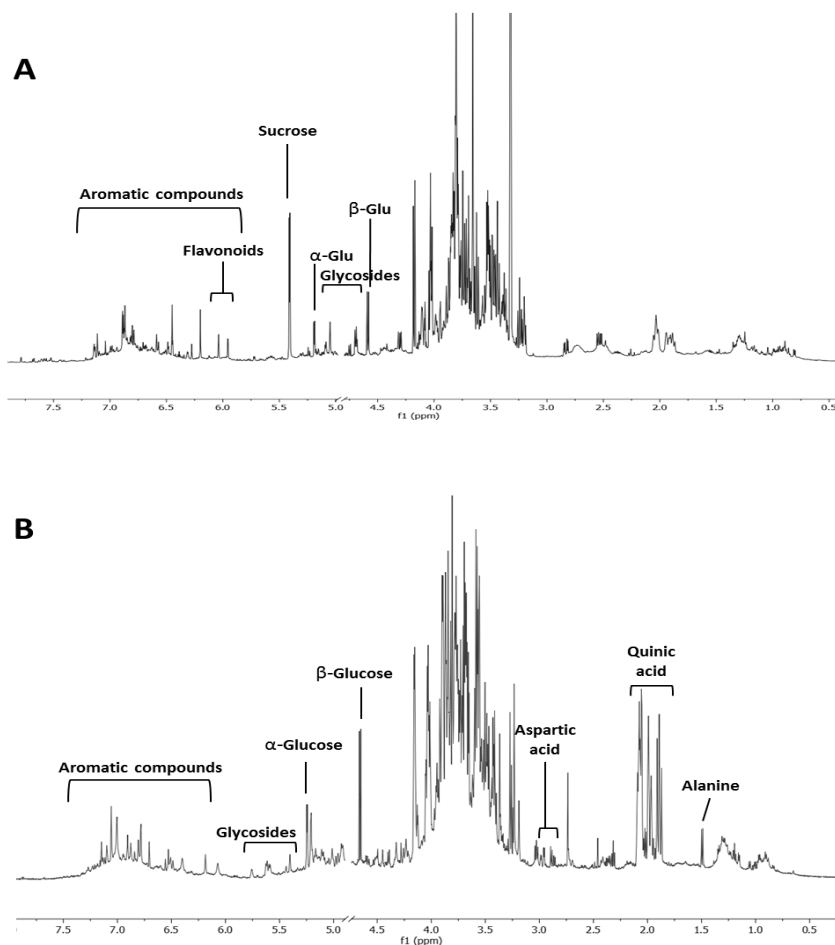


Figure 3. ¹H NMR profiling of *C. sativa* of representative leaves (A) and spiny burs (B) hydroalcoholic extract

Effects of Chestnut Extracts on Cell Viability in Microglia BV-2 Cells

Since it has been demonstrated that the BV-2 microglia cell line is a valid model system to study inflammation, and its response to lipopolysaccharide (LPS) is comparable to that of primary microglia [31], this cell model was chosen to study the potential anti-inflammatory and neuroprotective role of different extracts from chestnut by-products.

The potential cytotoxicity of different extracts from leaves and spiny burs, obtained as described in the Materials and Methods section, was tested in the BV-2 cell line. Cells were incubated with increasing concentrations of extracts (0.1–1 mg/mL) for 24 h, and then their viability was evaluated by MTT assay (Figure 4). Results show that, in several cases, the highest concentration of extracts tested (1 mg/mL) significantly reduced BV-2

viability. Extract concentrations ranging from 0.1 to 0.5 mg/mL did not affect cell viability compared to control cells. Therefore, this range of concentration was used in the subsequent experiments in order to evaluate potential cytoprotective and anti-inflammatory activities exerted by the extracts.

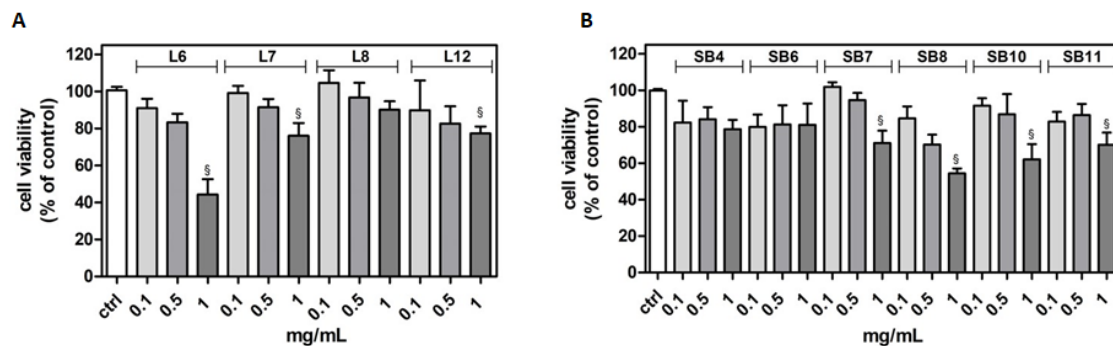


Figure 4. Effect of different extracts from chestnut by-products on the viability of BV-2 cells. BV-2 cells were incubated for 24 h with increasing concentrations (0.1, 0.5, 1.0 mg/mL) of extracts from chestnut leaves L (panel **A**) and spiny burs SB (panel **B**). Viability was evaluated by MTT test, as reported in the Materials and Methods section. Results are expressed as means \pm SD of three independent experiments. Statistical analysis was performed by Bonferroni multiple comparison test following one-way ANOVA. § $p < 0.05$, significantly different from control cells.

Cytoprotective Effects of Chestnut Extracts in the Presence of Inflammatory Stress

To evaluate the possible cytoprotective role of the chestnut extracts against inflammatory stress, BV-2 cells were incubated with the different chestnut extracts in the presence or absence of LPS, as an inflammation inducer [32], and assessed for cell viability by MTT test, as reported in Figure 5.

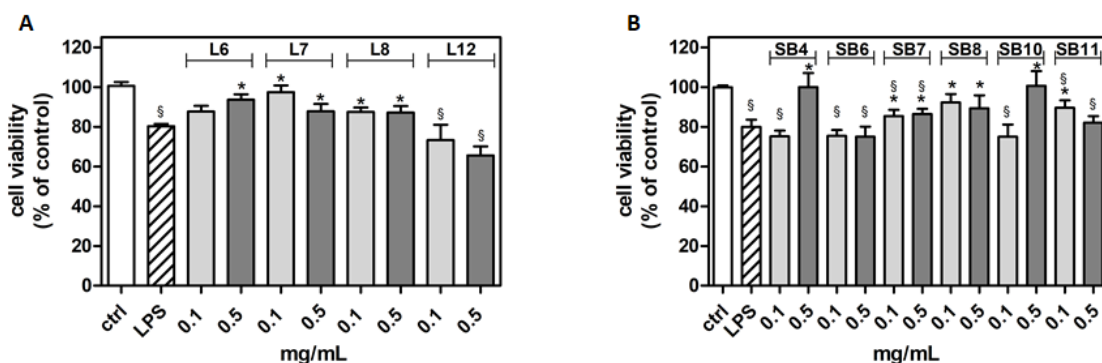


Figure 5. The effect of different extracts from chestnut by-products on the viability of BV-2 cells treated with lipopolysaccharide (LPS). BV-2 cells were incubated for 3 h with increasing concentrations (0.1, 0.5

mg/mL) of extracts from chestnut leaves L (panel **A**) and spiny burs SB (panel **B**), then 0.5 $\mu\text{g/mL}$ LPS was added and the cells were incubated for a total of 24 h. Viability was evaluated by MTT test, as reported in the Materials and Methods section. Results are expressed as means \pm SD of three independent experiments. Statistical analysis was performed by Bonferroni multiple comparison test following one-way ANOVA; § $p < 0.05$, significantly different from control cells; * $p < 0.05$, significantly different from LPS-treated cells.

The results show that many of the tested chestnut leaves extracts are able to exert a significant protective effect following LPS-generated inflammatory stress, with the exception of L12 (“Zocca”), which showed no significant differences from that of LPS-treated cells. Notably, according to the metabolomic analysis, L12 also showed a lower flavonoid content compared to that of the other samples tested. These data might suggest the importance of flavonoids in cytoprotective and anti-inflammatory activities, as it has been reported by Spagnuolo et al. [33]. However, other plant constituents, such as tannins and coumarins, might also counteract inflammation [34,35]. For instance, a coumarin endowed with anti-inflammatory activity was found in the inner shell of chestnuts (*Castanea crenata*) [36].

Anti-Inflammatory Effects of Chestnut Extracts

As reported by Henn et al. [31], after exposure to LPS, BV2 cells show a broad response of gene activation, and many of the activated genes correspond to inflammatory mediators, such as IL-1 β and TNF- α . These inflammatory mediators play an important role in the pathological processes of neurodegenerative diseases, as detailed in the review by Smith et al. [37]. To verify this observation in our model system, cells were treated with 0.5 $\mu\text{g/mL}$ LPS for 21 h then subjected to RT-PCR analysis using specific primers for the detection of inflammatory markers. Results in Figure 6 confirm that LPS caused an increase in the transcriptional levels of IL-1 β and TNF- α , highlighting the amplitude of the response of LPS-treated BV2 cells with respect to controls.

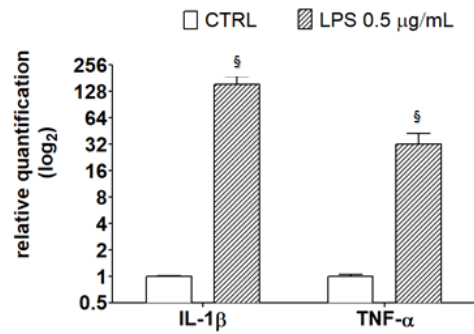


Figure 6. Transcriptional level of inflammatory markers in LPS-treated BV-2 cells. BV-2 cells were incubated with LPS (0.5 μg/mL) for 21 h; then, RNA was extracted, reverse-transcribed to cDNA, and analyzed by RT-PCR using specific primers for IL-1β and TNF-α, as described in the Materials and Methods section. Results are expressed as means ± SD of three independent experiments. Statistical analysis was performed by Bonferroni multiple comparison test following one-way ANOVA. § $p < 0.05$, significantly different from control cells.

In order to ascertain whether chestnut extracts are able to exert their protective effect at the transcriptional level, BV-2 cells pretreated with chestnut extracts were exposed to LPS, as previously reported, then mRNA quantification of the inflammatory markers was evaluated by RT-PCR (Figure 7).

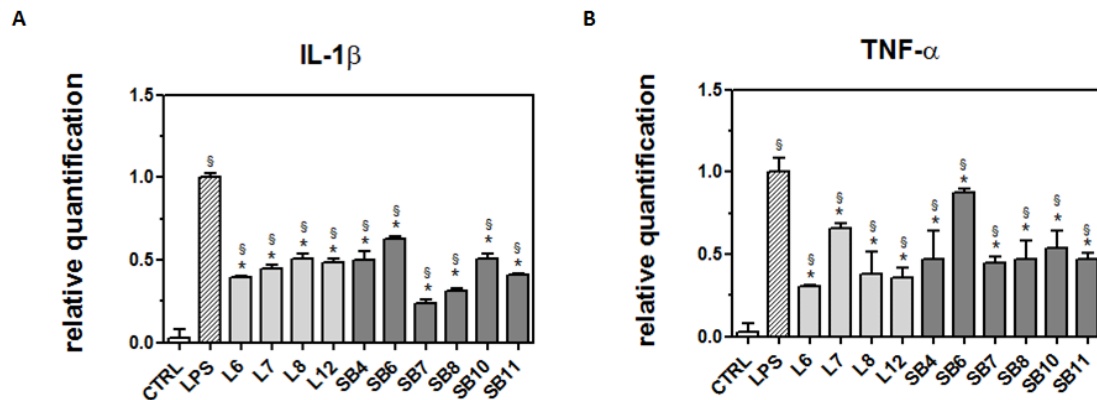


Figure 7. Protective effect of extracts from chestnut by-products on the transcriptional level of inflammatory markers in LPS-treated BV-2 cells. BV-2 cells were incubated for 3 h with 0.5 mg/mL extracts from chestnut leaves (L) and spiny burs (SB); then, 0.5 μg/mL LPS was added and the cells were incubated for a total of 24 h. Cells were then subjected to RNA extraction and analyzed by RTPCR using specific primers for IL-1β (panel A) and TNF-α (panel B), as described in the Materials and Methods section. Results are expressed as means ± SD of three independent experiments. Statistical analysis was performed by Bonferroni multiple comparison test following one-way ANOVA. § $p < 0.05$, significantly different from control cells; * $p < 0.05$, significantly different from LPS-treated cells.

As shown in Figure 7A, all chestnut extracts tested at the concentration of 0.5 mg/mL were able to significantly decrease mRNA levels of IL-1 β , a potent pro-inflammatory cytokine that is crucial for host-defense responses to infection and injury.

In addition, all the tested extracts were also able to reduce the mRNA level of TNF- α , as reported in Figure 7B. Since it has been reported that TNF- α can induce necrotic or apoptotic cell death [38], it is conceivable that these results agree with the observed protective effect exerted by the chestnut extracts on BV-2 viability.

The signaling pathway involving the transcription factor NF- κ B is considered a typical proinflammatory pathway, largely based on the activation of NF- κ B by pro-inflammatory agents and on the role of NF- κ B in the expression of pro-inflammatory genes including cytokines, chemokines, and adhesion molecules [39]. For this reason, the expression of this protein in LPS-stimulated BV-2 cells was evaluated in the absence and presence of chestnut extracts. Results obtained by Western blot analysis and reported in Figure 8 reveal that different tested chestnut extracts, with the exceptions of L6 (“Lisanese”), SB6 (“Lisanese”), and SB7 (“Pastanese Biffoni”), are able to significantly decrease the LPS-induced expression of NF- κ B.

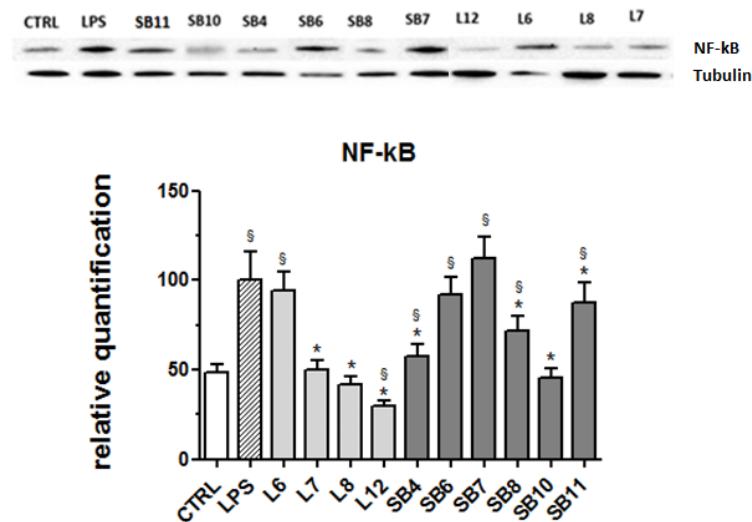


Figure 8. Effect of extracts from chestnut by-products on the NF- κ B expression in LPS-treated BV-2 cells. BV-2 cells were incubated for 3 h with 0.5 mg/mL of extracts from chestnut leaves L or spiny burs SB; then, 0.5 μ g/mL LPS was added and the cells were incubated for 21 h. Cells were then lysed and the proteins were extracted, separated by SDS-PAGE, transferred to a nitrocellulose membrane, and immunoassayed using anti-NF- κ B and anti-tubulin antibodies, as described in the Materials and Methods section. Results are expressed as means \pm SD of three independent experiments. Statistical analysis was

performed by Bonferroni multiple comparison test following one-way ANOVA. § $p < 0.05$, significantly different from control cells; * $p < 0.05$, significantly different from LPS-treated cells.

Materials and Methods

Chemicals and Materials

Deuterium oxide ($\text{H}_2\text{O}-d_2$, 99.90% D) and $\text{MeOH}-d_4$ (99.80% D) were purchased from Eurisotop (Cambridge Isotope Laboratories, Inc, Saint-Aubin, France). Ultra-low Endotoxin FBS was obtained from Euroclone (Euroclone, Milan, Italy). Mini-PROTEAN[®] TGX. precast gels 4–20%, Precision Plus Protein. Unstained Standards, Clarity. Western ECL Substrate and DC[™] protein assay were purchased from Bio-Rad Laboratories (Hercules, California, United States). Primary antibodies against Nf- κ B were purchased from Millipore (Merck Millipore, Burlington, MA, USA). Standard 3-(trimethylsilyl)-propionic-2,2,3,3- d_4 acid sodium salt (TMSP), sodium phosphate dibasic anhydrous sodium phosphate monobasic anhydrous, Dulbecco's modified Eagle medium (DMEM), penicillin, streptomycin, glutamine, lipopolysaccharide (LPS) from *Escherichia coli* serotype O127:B8, 3-(4,5-dimethylthiazol-2-yl)-2,5-diphenyl tetrazolium bromide (MTT), and all the other solvents and chemicals were purchased from Sigma-Aldrich Co. (St. Louis, MO, USA).

Sampling and NMR Metabolomics

Samples were collected during October 2018 in the experimental grove of Granaglione (Bologna, Italy, 44.1589851, 10.90389823). About twenty leaves were collected from each tree, immediately frozen in liquid nitrogen, then stored at -80°C until they were freeze-dried, ground, and kept in a fridge at 4°C before the analysis. Spiny burs were dried in a stove at 60°C , ground, and stored at room temperature. Pomological analysis was performed by Dr. Luca Dondini from the University of Bologna.

Thirty milligrams of freeze-dried and powdered leaves or spiny burs material were extracted using 1 mL of a bland (1:1) $\text{MeOH}-d_4/\text{H}_2\text{O}-d_2$ (containing 0.1 M phosphate buffer and 0.01% of TMSP standard). Samples were exposed to ultrasonic waves in a water bath (TransSonic TP 690, Elma, Germany) at a frequency of 35 kHz for 30 min and subsequently centrifuged for 20 min at $1700 \times g$ (Eppendorf Centrifuge 5804R, Hamburg,

Germany); the supernatant (700 μ L) was then separated from the pellet and transferred into NMR tubes.

Pre-Purification of Flavonoids from Leaves

The following procedure was designed according to Mandrone et al. [15] with slight modifications.

Seventy-eight grams of powdered chestnut leaves, obtained from all twenty-five lots, were extracted with 1 L of MeOH/H₂O (1:1). After 30 min of sonication, the extract was centrifuged for 20 min (2469 \times g). Then, it was filtered on a Büchner funnel and dried by a rotary evaporator at 40°C (R215, Büchi, Flawil, Switzerland).

The extract was suspended in 250 mL of H₂O and 50 mL of MeOH and subsequently extracted by liquid/liquid partition with 250 mL of hexane, chloroform, ethyl acetate, and n-butanol (four times for each solvent).

Dried Et-FR (200 mg) was sub-fractionated by an MPLC instrument (Reveleris[®], Büchi, Flawil, Switzerland) equipped with a UV-detector and fraction collector and by using a C18 column (4 g) at a flow rate of 8 mL/min to collect fractions for UV peaks and setting the UV-Vis detector at 210 nm, 260 nm, and 350 nm. The extract was eluted with a gradient of H₂O with 0.1% of TFA (solvent A) and MeOH (solvent B). Initial conditions were 5% followed by a linear increase of 5–25% B in 2 min, isocratic elution with 25% B for 5 min, increase to 60% B in 2 min, 60% B for 15 min, increase of 60–70% B in 2 min, 70% B for 15 min, increase of 70–100% B in 2 min, and finally 100% B for 5 min. This procedure resulted in thirteen fractions (from FR1 to FR13). Fraction FR6 contained a mixture of different flavonoids.

NMR and MS Spectra Measurement

¹H NMR spectra, J-resolved (J-res), ¹H-¹H homonuclear, and inverse detected ¹H-¹³C correlation experiments were recorded at 25°C on a Varian Inova 600 MHz NMR instrument (600 MHz operating at the ¹H frequency) equipped with an indirect triple resonance probe. CD₃OD was used for an internal lock. For ¹H NMR profiling, the relaxation delay was 2.0 s, observed pulse 5.80 μ s, number of scans 256, acquisition time 16 min, and spectral width 9595.78 Hz (corresponding to δ 16.0). For the aqueous

samples, a presaturation sequence (PRESAT) was used to suppress the residual H₂O signal at δ 4.83 (power = -6dB, presaturation delay 2 s).

ESI-MS analyses were performed by direct injection of MeOH solutions of the compounds using a WATERS ZQ 4000 (Milford, MA, USA) mass spectrometer. 3.5.

NMR Processing and Multivariate Data Treatment

Free induction decays (FIDs) were Fourier transformed, and the resulting spectra were phased, baseline-corrected, and calibrated to TMS at δ 0.0. Spectral intensities were reduced to integrated regions of equal width (δ 0.04) corresponding to the region from δ 0.0 to 10.0, with scaling on standard at δ 0.0 using the NMR Mestrenova software (Mestrelab Research, Santiago de Compostela, Spain). The analysis of the ¹H NMR profiles was performed based on an in-house library and comparison with the literature [17,25].

The regions of δ 4.9–4.8 and 3.34–3.26 were excluded from the analysis of the aqueous samples because of the residual solvents' signals. For multivariate analysis, the model OPLS-DA (Orthogonal Partial Least Squares Discriminant Analysis) was developed using SIMCA-P+ software (v. 15.0, Umetrics, Umeå, Sweden). Data were normalized for standard (at δ 0.0) and subjected to Pareto scaling. The model was evaluated by the goodness of fit ($R^2x(\text{Cum})$) and goodness of prediction ($Q^2(\text{Cum})$), together with the parameters given by the cross validation tests: permutation test (performed using 30 permutations) and CV-ANOVA [40].

Cell Culture

BV-2 murine microglial cells were kindly provided by Prof. Elisabetta Blasi (University of Modena and Reggio Emilia, Modena, Italy) and were cultured in DMEM supplemented with 10% heat inactivated Ultra-low Endotoxin FBS (Euroclone, Milano, Italy), L-glutamine (1%), and streptomycin (1%) in a humidified incubator maintained at 37 °C and 5% CO₂, according to Blasi et al. [41].

Cell Viability

Cell viability was evaluated by the MTT assay as previously reported [42]. BV-2 cells were treated with increasing concentrations of extracts from chestnut by-products

(0.1–1 mg/mL) for 3 h in 96-well plates and then 0.5 µg/mL LPS was added and the co-treatment prolonged until 24 h. At the end of the treatments, the exhausted medium was eliminated and the MTT solution was added. The blue-violet formazan salt crystals that formed were dissolved with DMSO. The absorbance at 595 nm was measured using a multiwell plate reader (VICTOR3 Multilabel Counter; PerkinElmer, Wellesley, MA, USA).

RT-PCR Analysis

The transcriptional level of inflammatory markers was evaluated by RT-PCR as previously reported [42].

After 3 h of treatment with extracts from chestnut by-products (0.5 mg/mL) and 21 h co-treatment with LPS (0.5 µg/mL), total RNA was extracted from BV-2 cells using an RNeasy Mini kit (Qiagen). RNA quantification was performed using a NanoVue spectrophotometer and mRNA was reversetranscribed into cDNA using iScript cDNA synthesis kit (Bio-Rad). The PCR was carried out in a total volume of 10 µL containing cDNA, SsoAdvanced SYBR Green mix (Bio-Rad), and primers, according to manufacturer's instructions.

(IL-1_β: FW_GTTCCCATTAGACAACACTGCACTACAG
RV_GTCGTTGCTTGGTTCTCCTTGTA; TNF-α:
FW_CCCCAAAGGGATGAGAAGTTC RV_CCTCCACTTGGTGGTTTGCT;
GAPDH*:
FW_ACCACAGTCCATGCCATCACRV_TCCACCACCCTGTTGCTGTA;
*reference control)

Western Blot Analysis

The protein expression of NF-κB was evaluated by Western Blotting as previously reported [43].

After 3 h treatment with extracts from chestnut by-products (0.5 mg/mL) and 21 h co-treatment with LPS (0.5 µg/mL), BV-2 cells (250,000 cells/well) were washed with ice-cold PBS and lysed with RIPA buffer containing a protease and phosphatase inhibitor mixture. Protein concentration of the lysates was determined by Bio-Rad DC protein assay. Proteins (10 µg per lane) were electrophoretically separated on precast gels (Bio-

Rad—Laboratories Inc.) and transferred to nitrocellulose membranes. Then, the nitrocellulose membranes were blocked and incubated overnight with primary antibodies (anti-NF- κ B or anti-Tubulin I as internal normalizer) at 4°C. Nitrocellulose membranes were washed with T-TBS and incubated at room temperature for 1 h with secondary antibodies in T-TBS. Chemiluminescence detection was performed using Clarity Western ECL substrate. Bands were acquired with a CCD imager (ChemiDoc MP System, Bio-Rad) and relative densitometric analyses were performed using Image Lab analysis software (Bio-Rad).

Conclusions

In this study, leaves and spiny burs of *Castanea sativa* from the experimental chestnut grove of Granaglione (Italy) were subjected to phytochemical analysis and tested for potential neuroprotective and anti-inflammatory activities.

The ¹H NMR-metabolomic analysis performed on ‘Marrone’ and ‘Castagna’ leaves showed that it was possible to distinguish these two classes of samples on the basis of some phytochemical features. In particular, ‘Marrone’ was characterized by lower amounts of all the metabolites, and specifically aromatic compounds, in particular flavonoids, namely, astragalin, isorhamnetin glucoside, and myricitrin, identified by means of NMR and MS experiments. The developed multivariate data model (OPLS-DA), based on the leaves metabolomic profile, might be useful in support of the pomological analysis commonly performed to distinguish ‘Marrone’ and ‘Castagna’, or to discriminate among them when nuts are not available.

With the aim of valorizing the by-products of the experimental chestnut grove, the potential neuroprotective effect of leaves and spiny burs were evaluated in a microglial model. The most current research is focused on the development of neuroprotective therapies aimed at contrasting neuroinflammation at the glial level [44].

On this basis, the effects of extracts on BV-2 cell viability were assayed. Afterwards, their protective activity was assessed in the microglia model exposed to LPS, an inducer of inflammation.

Deepening the study, the effect of extracts on the transcriptional levels of some genes that are protagonists of the inflammatory process, namely IL-1 β , TNF- α , and NF- κ B, were also evaluated.

Despite the differences found in the metabolomic profiles, leaves and spiny burs of both ‘Marrone’ and ‘Castagna’ at concentrations of 0.1 and 0.5 mg/mL all showed interesting cytoprotective and anti-inflammatory activity on microglia cells, also reducing the expression of the abovementioned genes.

These results represent an important step to encourage the recycling and valorization of *Castanea* by-products, favoring the circular economy and reducing the environmental impact related to management of chestnut grove waste.

Further studies are ongoing to deeply investigate the metabolites that are active in counteracting neuroinflammation.

Supplementary Materials: available online at <http://www.mdpi.com/2218-1989/10/10/408/s1>.

References

1. Aires, A.; Carvalho, R.; Saavedra, M.J. Valorization of solid wastes from chestnut industry processing: Extraction and optimization of polyphenols, tannins and ellagitannins and its potential for adhesives, cosmetic and pharmaceutical industry. *Waste Manag.* **2016**, *48*, 457–464.
2. Braga, N.; Rodrigues, F.; Oliveira, M.B. Castanea sativa by-products: A review on added value and sustainable application. *Nat. Prod. Res.* **2015**, *29*, 1–18.
3. Squillaci, G.; Apone, F.; Sena, L.M.; Carola, A.; Tito, A.; Bimonte, M.; De Lucia, A.; Colucci, G.; La Cara, F.; Morana, A. Chestnut (*Castanea sativa* Mill.) industrial wastes as a valued bioresource for the production of active ingredients. *Process Biochem.* **2018**, *64*, 228–236.
4. Costa-Trigo, I.; Otero-Penedo, P.; Outeiriño, D.; Paz, A.; Domínguez, J.M. Valorization of chestnut (*Castanea Sativa*) residues: Characterization of different materials and optimization of the acid-hydrolysis of chestnut burrs for the elaboration of culture broths. *Waste Manag.* **2019**, *87*, 472–484.
5. Cerulli, A.; Napolitano, A.; Masullo, M.; Hošek, J.; Pizza, C.; Piacente, S. Chestnut shells (Italian Cultivar “Marrone Di Roccaspide” PGI): Antioxidant activity and chemical investigation with in depth LC-HRMS/MSn rationalization of tannins. *Food Res. Int.* **2020**, *129*, 108787.
6. Jung, B.S.; Lee, N.K.; Na, D.S.; Yu, H.H.; Paik, H.D. Comparative analysis of the antioxidant and anticancer activities of chestnut inner shell extracts prepared with various solvents. *J. Sci. Food Agric.* **2016**, *96*, 2097–2102.
7. Sorice, A.; Siano, F.; Capone, F.; Guerriero, E.; Picariello, G.; Budillon, A.; Ciliberto, G.; Paolucci, M.; Costantini, S.; Volpe, M.G. Potential anticancer effects of polyphenols from chestnut shell extracts: Modulation of cell growth, and cytokinomic and metabolomic profiles. *Molecules* **2016**, *21*, 1411.
8. Vella, F.M.; Laratta, B.; La Cara, F.; Morana, A. Recovery of bioactive molecules from chestnut (*Castanea sativa* Mill.) by-products through extraction by different solvents. *Nat. Prod. Res.* **2018**, *32*, 1022–1032.
9. Lenzi, M.; Malaguti, M.; Cocchi, V.; Hrelia, S.; Hrelia, P. *Castanea sativa* Mill. bark extract exhibits chemopreventive properties triggering extrinsic apoptotic pathway in Jurkat cells. *BMC Complement. Altern. Med.* **2017**, *17*, 251.
10. Chiarini, A.; Micucci, M.; Malaguti, M.; Budriesi, R.; Ioan, P.; Lenzi, M.; Fimognari, C.; Gallina Toschi, T.; Comandini, P.; Hrelia, S. Sweet chestnut (*Castanea sativa* Mill.) bark extract: Cardiovascular activity and myocyte protection against oxidative damage. *Oxidative Med. Cell. Longev.* **2013**.
11. Sangiovanni, E.; Piazza, S.; Vrhovsek, U.; Fumagalli, M.; Khalilpour, S.; Masuero, D.; Di Lorenzo, C.; Colombo, L.; Mattivi, F.; De Fabiani, E.; et al. A bio-guided approach for the development of a chestnut-based proanthocyanidin-enriched nutraceutical with potential anti-gastritis properties. *Pharmacol. Res.* **2018**, *134*, 145–155.
12. Regione Emilia-Romagna Website. 2019 Congress about the Experimental Chestnut Grove and the Valorization of Chestnut Cultivation in Emilia-Romagna Region. Available online: <https://agricoltura.regione.emilia-romagna.it/convegni/2019/innovazione-e-valorizzazione-della-castanicoltura-emiliano-romagnola/castagno-magnani> (accessed on 3 March 2020).
13. Alto Reno Terme Website. Description and Maps of the Experimental Chestnut Grove. Available online: <https://www.discoveraltorenoterme.it/varano-didactic-chestnut-park/> (accessed on 3 March 2020).
14. Wolfender, J.-L.; Marti, G.; Thomas, A.; Bertrand, S. Current approaches and challenges for the metabolite profiling of complex natural extracts. *J. Chromatogr. A* **2015**, *1382*, 136–164.
15. Mandrone, M.; Coqueiro, A.; Poli, F.; Antognoni, F.; Choi, Y.H. Identification of a collagenase-inhibiting flavonoid from *Alchemilla vulgaris* using NMR-Based metabolomics. *Planta Med.* **2018**, *84*, 941–946.
16. Salomé-Abarca, L.F.; Mandrone, M.; Sanna, C.; Poli, F.; van der Hondel, C.A.; Klinkhamer, P.G.; Choi, Y.H. Metabolic variation in *Cistus monspeliensis* L. ecotypes correlated to their plant-fungal interactions. *Phytochemistry* **2020**, *176*, 112402.
17. Mandrone, M.; Antognoni, F.; Aloisi, I.; Potente, G.; Poli, F.; Cai, G.; Faleri, C.; Parrotta, L.; Del Duca, S. Compatible and incompatible pollen-styles interaction in *Pyrus communis* L. show different transglutaminase features, polyamine pattern and metabolomics profiles. *Front. Plant Sci.* **2019**, *10*, 741.
18. Anđelković, B.; Vujisić, L.; Vučković, I.; Tešević, V.; Vajs, V., & Gođevac, D. Metabolomics study of Populus type propolis. *J. Pharm. Biomed. Anal.* **2017**, *135*, 217–226.

19. Callao, M.P.; Ruisánchez, I. An overview of multivariate qualitative methods for food fraud detection. *Food Control* **2018**, *86*, 283–293.
20. Barreira, J.C.; Ferreira, I.C.; Oliveira, M.B.P.; Pereira, J.A. Antioxidant activities of the extracts from chestnut flower, leaf, skins and fruit. *Food Chem.* **2008**, *107*, 1106–1113.
21. Wolf, S.A.; Boddeke, H.W.; Kettenmann, H. Microglia in physiology and disease. *Ann. Rev. Physiol.* **2017**, *79*, 619–643.
22. Glass, C.K.; Saijo, K.; Winner, B.; Marchetto, M.C.; Gage, F.H. Mechanisms underlying inflammation in neurodegeneration. *Cell* **2010**, *140*, 918–934.
23. Tarawneh, R.; Galvin, J.E. Potential future neuroprotective therapies for neurodegenerative disorders and stroke. *Clin. Geriatr. Med.* **2010**, *26*, 125–147.
24. Perry, V.H.; Holmes, C. Microglial priming in neurodegenerative disease. *Nat. Rev. Neurol.* **2014**, *10*, 217–224.
25. Mandrone, M.; Scognamiglio, M.; Fiorentino, A.; Sanna, C.; Cornioli, L.; Antognoni, F.; Bonvicini, F.; Poli, F. Phytochemical profile and α -glucosidase inhibitory activity of Sardinian *Hypericum scruglii* and *Hypericum hircinum*. *Fitoterapia* **2017**, *120*, 184–193.
26. Munekata, P.E.S.; Franco, D.; Trindade, M.A.; Lorenzo, J.M. Characterization of phenolic composition in chestnut leaves and beer residue by LC–DAD–ESI–MS. *LWT Food Sci. Technol.* **2016**, *68*, 52–58.
27. Esposito, T.; Celano, R.; Pane, C.; Piccinelli, A.L.; Sansone, F.; Picerno, P.; Zaccardelli, M.; Aquino, R.P.; Mencherini, T. Chestnut (*Castanea sativa* Miller.) burs extracts and functional compounds: UHPLC–UV–HRMS profiling, antioxidant activity, and inhibitory effects on phytopathogenic fungi. *Molecules* **2019**, *24*, 302.
28. Carocho, M.; Barros, L.; Bento, A.; Santos-Buelga, C.; Morales, P.; Ferreira, I.C.F.R. Castanea sativa Mill. flowers amongst the most powerful antioxidant matrices: A phytochemical approach in decoctions and infusions. *BioMed Res. Int.* **2014**.
29. Barros, L.; Tiago, C.; Montserrat, D.; Silva, S.; Oliveira, R.; Carvalho, A.M.; Henriques, M.; Santos-buelga, C.; Ferreira, I.C. Characterization of phenolic compounds in wild medicinal flowers from Portugal by HPLC–DAD–ESI/MS and evaluation of antifungal properties. *Ind. Crops Prod.* **2013**, *44*, 104–110.
30. Tuyen, P.T.; Xuan, T.D.; Khang, D.T.; Ahmad, A.; Quan, N.V.; Anh, T.; Thi, T.; Anh, L.H.; Minh, T.N. Phenolic compositions and antioxidant properties in bark, flower, inner skin, kernel and leaf extracts of *Castanea crenata* Sieb. et Zucc. *Antioxidants* **2017**, *6*, 31.
31. Henn, A.; Lund, S.; Hedtjärn, M.; Schrattenholz, A.; Pörzgen, P.; Leist, M. The suitability of BV2 cells as alternative model system for primary microglia cultures or for animal experiments examining brain inflammation. *ALTEX* **2009**, *26*, 83–94.
32. Han, Q.; Yuan, Q.; Meng, X.; Huo, J.; Bao, Y.; Xie, G. 6-Shogaol attenuates LPS-induced inflammation in BV2 microglia cells by activating PPAR-. *Oncotarget* **2017**, *8*, 42001–42006.
33. Spagnuolo, C.; Moccia, S.; Russo, G.L. Anti-inflammatory effects of flavonoids in neurodegenerative disorders. *Eur. J. Med. Chem.* **2018**, *153*, 105–115.
34. Azab, A.; Nassar, A.; Azab, A.N. Anti-inflammatory activity of natural products. *Molecules* **2016**, *21*, 1321.
35. Ferlazzo, N.; Cirmi, S.; Calapai, G.; Ventura-Spagnolo, E.; Gangemi, S.; Navarra, M. Anti-inflammatory activity of Citrus bergamia derivatives: Where do we stand? *Molecules* **2016**, *21*, 1273.
36. Cho, D.Y.; Ko, H.M.; Kim, J.; Kim, B.W.; Yun, Y.S.; Park, J.I.; Ganesan, P.; Lee, J.T.; Choi, D.K. Scoparone inhibits LPS-simulated inflammatory response by suppressing IRF3 and ERK in BV-2 microglial cells. *Molecules* **2016**, *21*, 1718.
37. Smith, J.A.; Das, A.; Ray, S.K.; Banik, N.L. Role of pro-inflammatory cytokines released from microglia in neurodegenerative diseases. *Brain Res. Bull.* **2012**, *87*, 10–20.
38. Idriss, H.T.; Naismith, J.H. TNF- α and the TNF receptor superfamily: Structure-function relationship(s). *Microsc. Res. Tech.* **2000**, *50*, 184–195.
39. Pugazhenthii, S.; Zhang, Y.; Bouchard, R.; Mahffey, G. Induction of an inflammatory loop by interleukin-1 β and tumor necrosis factor- α involves NF-kB and STAT-1 in differentiated human neuroprogenitor cells. *PLoS ONE* **2013**, *8*, e69585.
40. Malzert-Fréon, A.; Hennequin, D.; Rault, S. Partial least squares analysis and mixture design for the study of the influence of composition variables on lipidic nanoparticle characteristics. *J. Pharm. Sci.* **2010**, *99*, 4603–4615.
41. Blasi, E.; Barluzzi, R.; Bocchini, V.; Mazzolla, R.; Bistoni, F. Immortalization of murine microglial cells by a v-raf/v-myc carrying retrovirus. *J. Neuroimmunol.* **1990**, *27*, 229–237.

42. Wandjou, J.G.N.; Lancioni, L.; Barbalace, M.C.; Hrelia, S.; Papa, F.; Sagratini, G.; Vittori, S.; dall'Acqua, S.; Caprioli, G.; Beghelli, D.; et al. Comprehensive characterization of phytochemicals and biological activities of the Italian ancient apple 'Mela Rosa dei Monti Sibillini'. *Food Res. Int.* **2020**, *137*, 109422.
43. Ko, W.; Sohn, J.H.; Jang, J.H.; Ahn, J.S.; Kang, D.G.; Lee, H.S.; Kim, J.S.; Kim, Y.C.; Oh, H. Inhibitory effects of alternanamide on inflammatory mediator expression through TLR4-MyD88-mediated inhibition of NF- κ B and MAPK pathway signaling in lipopolysaccharide-stimulated RAW264.7 and BV2 cells. *Chem. Biol. Interact.* **2016**, *244*, 16–26.
44. Du, L.; Zhang, Y.; Chen, Y.; Zhu, J.; Yang, Y.; Zhang, H.L. Role of microglia in neurological disorders and their potentials as a therapeutic target. *Mol. Neurobiol.* **2017**, *54*, 7567–7584.

1.3. From waste to phyto-protection: screening of 37 neglected plant matrices against *Clavibacter michiganensis* and *Pseudomonas syringae*

Chiocchio, I., Mandrone, M., Tacchini, M., Poli, F.

Manuscript in preparation

Introduction

The old economic approach, based on the logic of “make, use, dispose”, is no longer sustainable and needs to be counteracted. One of the current alternatives is represented by the circular economy, which aims to close loops in industrial systems by minimizing waste and by-products and turning them into resources [1]. The transition to a circular economy system requires actions and policy, the European Commission adopted the first circular economy action plan in 2015 and a new one in 2019 [2], which lists key products such as electronics, plastics, and food wastes.

In order to implement this strategy, in the past two decades, the scientific community has been paying growing attention also to the valorization of industrial and agricultural wastes of plant origin [3,4]. These biological matrices are particularly interesting since they are source of high-value compounds such as secondary metabolites. Plant secondary metabolites are endowed with numerous biological activities making them useful in different fields such as cosmetic, nutraceutical, pharmaceutical, food additives, antifeedant [5]. According to a recent review work [6] the majority of the studies published between 2006 and 2020 deals with the potential use of neglected plant matrices as a source of bioactive molecules for human health care, while there are only a few reports about the use of these sources in agricultural field.

The agriculture itself is one of the most challenged sectors for sustainable development. Indeed, population growth and the consequent rising demand for food require increasingly higher yields. However, lands are limited and overharvesting has caused several environmental problems such as depletion and pollution of water, hydrologic modifications, emission of greenhouse gasses, degradation of soil quality and fertility due to the use of fertilizers and pesticides [7,8]. Hence, more sustainable farming techniques need to be implemented and adopted. In this context, plant derived compounds represent a valuable alternative to the use of synthetic compounds.

The present work aims at investigating whether neglected plant matrices can be used as sources of anti-phytopathogens, favoring both circular economy and sustainable agriculture. To this purpose 37 samples including agricultural residues, pest plants, herbal and food industry by-products were tested against strains of *Pseudomonas syringae* pv.

syringae ATCC 19310 and *Clavibacter michiganensis* subsp. *nebraskense* ATCC 27822. In addition, *in vitro* antioxidant activity of the samples was also determined. Finally, preliminary information about the phytochemical composition of the most active samples were obtained through ¹H NMR profiling and by measuring total phenolics and flavonoids content. *Pseudomonas syringae* pv *syringae* van Hall (ATCC 19310) was chosen as Gram-negative bacteria because it is the most polyphagous in the *P. syringae* complex that primarily affects woody and herbaceous host plants. Alongside this microorganism, the bacterium *Clavibacter michiganensis* subsp. *nebraskense* (ATCC 27822) was chosen, as it is a Gram-positive bacterium that affects the maize plant (the third most cultivated cereal in the world with an increasing cultivation trend [9]) during all its growth stages.

Materials and methods

Chemicals

All reagents were purchased from Sigma Aldrich (Milano, Italy), except the deuterated solvents, which were purchased from Eurisotop (Cambridge, UK).

Plant material and sample treatment

Thirty-seven neglected plant matrices classified as agricultural waste and by-products (crops residues and pest plants), residue from herbal industry (distillation residues), and residues from food industry (by-products belonging to 31 plant species) (Table 1) were obtained between 2018 and 2019. The matrices were provided by local producers (Emilia-Romagna region, Italy) including farmers, herbalists, and winemakers and vouchers of the dried plant material were deposited in Department of Pharmacy and Biotechnology, University of Bologna (via Irnerio 42, Bologna, Italy). Solid wastes from distillation, grape pomace and almond exocarp were freeze dried, while the other plant matrices were dried at 40 °C in stove. After the drying process, all samples were grounded and stored in the dark and at room temperature.

Extracts preparation

Extracts were prepared as described by *Cappadone et al.* [10] with slight modifications. Briefly, 120 mg of dried and powdered plant material underwent ultrasonic assisted extraction for 30 min using 6 mL of MeOH/H₂O (1:1). Subsequently, samples were centrifuged (2469 x g) for 20 min and each supernatant was separated from the pellet and divided into four tubes. Solvent was evaporated in vacuum concentrator (Savant SpeedVac SPD210, Thermo Fisher Scientific, Waltham, Massachusetts, United States) in order to yield the crude extracts. Aliquots of the extracts were in turn used for ¹H NMR profiling, antioxidant, and antimicrobial activity.

Total phenolic content and total flavonoid content

Total polyphenol and flavonoid content and antioxidant activity were measured on the extracts before evaporating the solvent, the supernatant was separated from the pellet and directly tested.

The total phenolic and total flavonoid content of the extracts were assessed by means of spectrophotometric methods using the spectrophotometer Victor™ X3 PerkinElmer (Waltham, Massachusetts, United States) as described by *Chiocchio et al.* [11] with slight modifications. The crude extracts were diluted in methanol (1:1) and tested in duplicate for each assay. Gallic acid and rutin were used to build the calibration curves which were used to calculate by interpolation the total phenolic content and total flavonoid content, respectively. Thus, total phenolic content was expressed as mg of gallic acid equivalent (GAE) per g of dried plant material and total flavonoid content was expressed as mg rutin equivalent (RE) per g of dried plant material.

Total antioxidant activity

In vitro antioxidant activity of the extracts was determined using the DPPH free radical scavenging assay as described by *Marrelli et al.* [12] with slight modifications. Crude extracts were diluted in methanol in order to test different concentrations (ranging from 1.25 to 1000 µL/mL in the assay). 50 µL of sample solutions were added to 700 µL of a DPPH methanol solution (50 mM). After 20 min at room temperature, absorbances (Abs) were measured at 517 nm and the percentage of antioxidant activity was calculated using the following formula:

$$\text{Antiradical activity \%} = ((\text{control Abs} - \text{sample Abs}) / \text{control Abs}) \times 100.$$

Methanol was used as negative control, Trolox (Tr) at different concentrations (ranging from 50 to 500 μM) was used as a positive control and Tr IC_{50} was used for the calculation of Trolox equivalents. Total antioxidant activity was expressed as mg of Trolox equivalent (TE) per mL of extract.

Antibacterial Activity

The antibacterial activity has been evaluated against phytopathogenic bacteria to preliminarily verify phytoiatric properties. *Pseudomonas syringae* pv. *syringae* ATCC 19310 and *Clavibacter michiganensis* subsp. *nebraskense* ATCC 27822 were used to determine MIC (Minimum Inhibitory Concentration) through microdilution method using 96-well microtiter plates. Bacterial cultures were incubated overnight at 26 °C and 28 °C, respectively, in Tryptic Soy Broth (OXOID Ltd., Hampshire, UK). One hundred μL of sterile medium were used together with 100 μL of sample to perform serial dilutions of extracts previously dissolved in fresh medium (50 mg/mL of stock solution), into all micro-wells. One-hundred microliters of bacterial culture standardized to 2×10^7 CFU/mL were added to the wells and incubated at 26 °C and 28 °C for 24 h. After the incubation period, 40 μL of water solution (20 mg/mL) of 2,3,5-triphenyl-tetrazolium chloride (Sigma-Aldrich, St. Louis, USA) were added to each well and then incubated for 30 min: microbial growth was evaluated by microplate reader (680XR, Bio Rad, Laboratories, Inc., Hercules, CA, USA) at 415 nm. Thymol (concentration range 0.0625-0.5 $\mu\text{g}/\text{mL}$) was used as a positive control. All determinations were made in triplicate.

NMR and ESI-MS analysis

For ^1H NMR profiling each extract was solubilized in deuterated solvents obtaining a final concentration equal to 5 mg/mL. The solvent used was a mixture (1:1) of phosphate buffer (90 mM; pH 6.0) in $\text{H}_2\text{O}-d_2$ containing 0.01% trimethylsilylpropionic-2,2,3,3- d_4 acid sodium salt (TMSP) and $\text{MeOH}-d_4$.

^1H NMR spectra were recorded at 25°C on a Varian Inova 600 MHz NMR instrument (600 MHz operating at the ^1H frequency) equipped with an indirect triple resonance probe. Methanol- d_4 was used for internal lock. Each ^1H -NMR spectrum consisted of 256 scans (corresponding to 16 min) with the relaxation delay (RD) of 2 s, acquisition time 0.707 s, and spectral width of 9595.8 Hz (corresponding to δ 16.0). A

presaturation sequence (PRESAT) was used to suppress the residual water signal at δ 4.83 (power = -6dB, presaturation delay 2 s). The spectra were manually phased and baseline corrected, and calibrated to the internal standard trimethyl silyl propionic acid sodium salt (TMSP) at δ 0.0 using Mestrenova software (Mestrelab Research, Spain). Compounds identification was based on an in-house library and comparison with literature data [13].

For ESI-MS analyses, extracts were dissolved in MeOH, and analyzed by WATERS ZQ 4000 (Milford, MA USA) mass spectrometer. in negative and/or positive ion modes according to the more ionizable chemical groups of samples. A direct infusion of 20 μ L/ min, source temperature of 80 °C and desolvation (nitrogen) gas (flow rate of 200 L/h) were common parameters used in both positive and negative ion modes. Capillary potential and source cone were 3.54 Kv and 20 V in positive ion mode, and 2.53 Kv and 30 V in negative ion mode. The mass range was from 0 to 1000 m/z.

Statistical analysis

Values were expressed as the mean \pm SD of one experiment performed in duplicate. Statistical analyses were performed using Graph Pad Prism 4 software (La Jolla, CA, USA). Samples were compared by one-way analysis of variance (ANOVA), followed by Tukey's honestly significant difference (HSD) post-hoc test, considering significant differences at *P* values < 0.05.

Table 1. Plant neglected matrices investigated in this work, their source (plant scientific and common name and plant part), and used tag are reported together with the type of waste/by-product. Plant scientific names have been updated following the World Checklist of Vascular Plants [14].

Scientific name	Common name	Plant part	Type of waste/by-product	Sample tag	Voucher number
<i>Abutilon theophrasti</i> Medik.	Velvetleaf	Aerial parts	Pest plant	Ath	WST25

<i>Achillea millefolium</i> L.	Common yarrow	Aerial parts	Solid waste from distillation	Acm	WST35
<i>Allium cepa</i> L.	Onion	Dry aerial parts	Agricultural residue	Ace	WST1
<i>Artemisia absinthium</i> L.	Wormwood	Aerial parts	Solid waste from distillation	Ara	WST36
<i>Beta vulgaris</i> L.	Sugar beet	Aerial parts	Agricultural residue	Bvu	WST10
<i>Camelina sativa</i> (L.) Crantz	Camelina	Dry aerial parts	Agricultural residue	Csa	WST2
<i>Castanea sativa</i> Mill.	Chestnut	Pericarp	Food Industry by-products	Csp	WST16
		Spiny burs	Agricultural residue	Csr	WST3
<i>Cicer arietinum</i> L.	Chickpea	Aerial parts	Agricultural residue	Car	WST11
<i>Cichorium intybus</i> L.	Chicory	Apical flowering aerial parts	Pest plant	Cia	WST22
		Basal flowering aerial parts	Pest plant	Cib	WST23
<i>Cucurbita pepo</i> L.	Courgette	Leaves	Agricultural residue	Cpe	WST12
		Aerial parts	Agricultural residue	Cpi	WST15
<i>Cupressus sempervirens</i> L.	Cupressus	Leaves	Solid waste from distillation	Css	WST26

<i>Echinochloa crus-galli</i> (L.) P.Beauv.	Cockspur	Flowering aerial parts	Pest plant	Ecg	WST24
<i>Erigeron canadensis</i> L.	Horseweed	Aerial parts	Pest plant	Eca	WST21
<i>Helianthus annuus</i> L.	Sunflower	Leaves	Agricultural residue	Han	WST4
<i>Helichrysum italicum</i> (Roth) G. Don	Curry plant	Aerial parts	Solid waste from distillation	Hei	WST27
<i>Laurus nobilis</i> L.	Laurel	Leaves	Solid waste from distillation	Lan	WST28
<i>Lavandula angustifolia</i> Mill.	Lavander	Aerial parts	Solid waste from distillation	Laa	WST37
<i>Melissa officinalis</i> L.	Lemon balm	Aerial parts	Solid waste from distillation	Meo	WST29
<i>Origanum vulgare</i> L.	Oregano	Stems	Food Industry by- products	Orv	WST19
<i>Phaseolus vulgaris</i> L.	Bean	Husks	Food Industry by- products	Pvb	WST18
		Aerial parts	Agricultural residue	Pvu	WST13
<i>Prunus amygdalus</i> Batsch	Almond	Exocarp	Food Industry by- products	Pam	WST17
<i>Rosa damascena</i>	Damask rose	Buds	Solid waste from distillation	Rod	WST30

<i>Salvia officinalis</i> L.	Sage	Aerial parts	Solid waste from distillation	Sco	WST33
<i>Salvia rosmarinus</i> Schleid.	Rosemary	Aerial parts	Solid waste from distillation	Sar	WST31
<i>Salvia sclarea</i> L.	Clary sage	Aerial parts	Solid waste from distillation	Sas	WST32
<i>Solanum lycopersicum</i> L.	Tomato	Basal leaves	Agricultural residue	Sly	WST14
<i>Solanum tuberosum</i> L.	Potato	Leaves	Agricultural residue	Stu	WST8
<i>Sorghum bicolor</i> (L.) Moench	Sorghum	Leaves	Agricultural residue	Sbl	WST6
		Roots	Agricultural residue	Sbr	WST7
		Stems	Agricultural residue	Sbf	WST5
<i>Thymus vulgaris</i> L.	Common thyme	Aerial parts	Solid waste from distillation	Tvu	WST34
<i>Triticum aestivum</i> L.	Wheat	Dry aerial parts	Agricultural residue	Tae	WST9
<i>Vitis vinifera</i> L.	Grape	Pomace	Food Industry by-products	Vvi	WST20

Results

The tests performed on a 96-well plate in microplate reader against the Gram-negative bacterium (*P. syringae* pv *syringae*) did not show any noteworthy activities, while thymol, already well known in the literature for its antibacterial capacity, exhibited a MIC value of 62.5 µg/mL and Heliocuire S, a terpenic formulate of copper hydroxide

used against bacterial diseases of horticultural crops, ornamental plants and fruit trees, showed a MIC value of 2.625 $\mu\text{L}/\text{mL}$. Regarding the results on Gram-positive bacterium (*C. michiganensis* subsp. *nebraskense*), extracts from 5 plant wastes showed antibacterial activities with MICs ranging from 125 to 1000 $\mu\text{g}/\text{mL}$. Interestingly, all the active matrices were solid residues from distillation, namely *Salvia sclarea* L., *Salvia rosmarinus* Schleid, *Salvia officinalis* L., *Cupressus sempervirens* L., and *Helichrysum italicum* (Roth) G. Don. The extracts deriving from plants belonging to the genus *Salvia*, showed a modest antibacterial activity with MICs ranging between 500 and 1000 $\mu\text{g}/\text{mL}$ (Table 2). However, the best result was exerted by the extract of *Helichrysum italicum* which showed a MIC of 125 $\mu\text{g}/\text{mL}$, higher only than thymol (thymol MIC = 62.5 $\mu\text{g}/\text{mL}$, Heliocuvire S MIC=0.65625 $\mu\text{l}/\text{mL}$).

The results showed that Gram-negative bacteria were less sensitive than Gram-positive bacteria, possibly because of the different bacterial wall characteristics that distinguish bacteria in Gram staining.

Antioxidant activity ranged from 0.3 to 5 mg of Trolox equivalent per mL of plant extract, and extract of *Castanea sativa* (pericarp), *Rosa damascena* (buds post-distillation), *Prunus amygdalus* (exocarp) were the most powerful ones (Fig. 1).

Table 2. Total flavonoid content, total polyphenol content, *in vitro* antioxidant activity and antibacterial activity against *C. michiganensis*.

Scientific name	Sample tag	mg RE/g (DW)	mg GAE/g (DW)	mg TE/mL of extract	MIC ($\mu\text{g}/\text{mL}$)
<i>Abutilon theophrasti</i> Medik.	Ath	13.73 \pm 0.46	18.06 \pm 0.57	0.95 \pm 0.17	-
<i>Achillea millefolium</i> L.	Acm	14.54 \pm 0.48	25.81 \pm 0	0.85 \pm 0.07	-
<i>Allium cepa</i> L.	Ace	1.36 \pm 0.05	2.94 \pm 0	-	-
<i>Artemisia absinthium</i> L.	Ara	16.18 \pm 0.54	29.26 \pm 3.16	0.89 \pm 0.02	-
<i>Beta vulgaris</i> L.	Bvu	3.99 \pm 0.13	6.32 \pm 0.4	-	-

<i>Camelina sativa</i> (L.) Crantz	Csa	0.55 ± 0.02	2.48 ± 0.16	-	-
<i>Castanea sativa</i> Mill.	Csp	4.78 ± 0.16	43.97 ± 1.7	4.76 ± 0.16	-
	Csr	6.23 ± 0.21	30.73 ± 0.76	1.65 ± 0.11	-
<i>Cicer arietinum</i> L.	Car	7.92 ± 0.26	10.04 ± 0.56	-	-
<i>Cichorium intybus</i> L.	Cia	0.35 ± 0.01	4.67 ± 0.02	-	-
	Cib	18.86 ± 0.63	25.26 ± 1.39	1.22 ± 0.07	-
<i>Cucurbita pepo</i> L.	Cpe	13.21 ± 0.44	16.45 ± 0.23	-	-
	Cpi	19.88 ± 0.66	17.35 ± 1.1	0.71 ± 0.08	-
<i>Cupressus sempervirens</i> L.	Css	8.25 ± 0.27	36.39 ± 0.12	2.14 ± 0.11	1
<i>Echinochloa crus-galli</i> (L.) P.Beauv.	Ecg	16.4 ± 0.55	15.95 ± 1.2	-	-
<i>Erigeron canadensis</i> L.	Eca	36.12 ± 1.2	31.68 ± 0.16	1.75 ± 0.14	-
<i>Helianthus annuus</i> L.	Han	5.12 ± 0.17	13.66 ± 0.62	-	-
<i>Helichrysum italicum</i> (Roth) G. Don	Hei	41.19 ± 1.37	37.55 ± 0.55	2.58 ± 0.36	0.125
<i>Laurus nobilis</i> L.	Lan	12.79 ± 0.43	29.87 ± 1.01	-	-
<i>Lavandula angustifolia</i> Mill.	Laa	15.26 ± 0.51	37.52 ± 0.29	1.92 ± 0.07	-
<i>Melissa officinalis</i> L.	Meo	10.53 ± 0.35	36.49 ± 0.75	2.38 ± 0.46	-
<i>Origanum vulgare</i> L.	Orv	4.82 ± 0.16	18.01 ± 0.94	0.56 ± 0	-
<i>Phaseolus vulgaris</i> L.	Pvb	4.34 ± 0.14	6.11 ± 0.18	-	-
	Pvu	20.35 ± 0.68	19.04 ± 0.17	0.51 ± 0	-

<i>Prunus amygdalus</i> Batsch	Pam	3.66 ± 0.12	42.38 ± 0.31	5.1 ± 0.07	-
<i>Rosa damascena</i>	Rod	35.34 ± 1.18	43.96 ± 1.5	4.77 ± 0.12	-
<i>Salvia officinalis</i> L.	Sco	26.6 ± 0.89	38.53 ± 0.95	1.85 ± 0.11	0.5
<i>Salvia rosmarinus</i> Schleid.	Sar	22.9 ± 0.76	39.83 ± 0.43	2.03 ± 0.26	0.5
<i>Salvia sclarea</i> L.	Sas	17.03 ± 0.57	19.9 ± 0.37	0.48 ± 0.01	1
<i>Solanum lycopersicum</i> L.	Sly	19.35 ± 0.65	25.88 ± 0.4	1.06 ± 0.01	-
<i>Solanum tuberosum</i> L.	Stu	2.02 ± 0.07	5.98 ± 0.96	-	-
<i>Sorghum bicolor</i> (L.) Moench	Sbl	8.97 ± 0.3	16.12 ± 2.75	0.34 ± 0.01	-
	Sbr	2.78 ± 0.09	10.96 ± 0.01	-	-
	Sbf	1.41 ± 0.05	5.85 ± 0.08	-	-
<i>Thymus vulgaris</i> L.	Tvu	42.91 ± 1.43	42.05 ± 1.91	1.91 ± 0.03	-
<i>Triticum aestivum</i> L.	Tae	4.13 ± 0.14	5.95 ± 0.35	-	-
<i>Vitis vinifera</i> L.	Vvi	6.24 ± 0.21	29.36 ± 1.74	1.23 ± 0.02	-

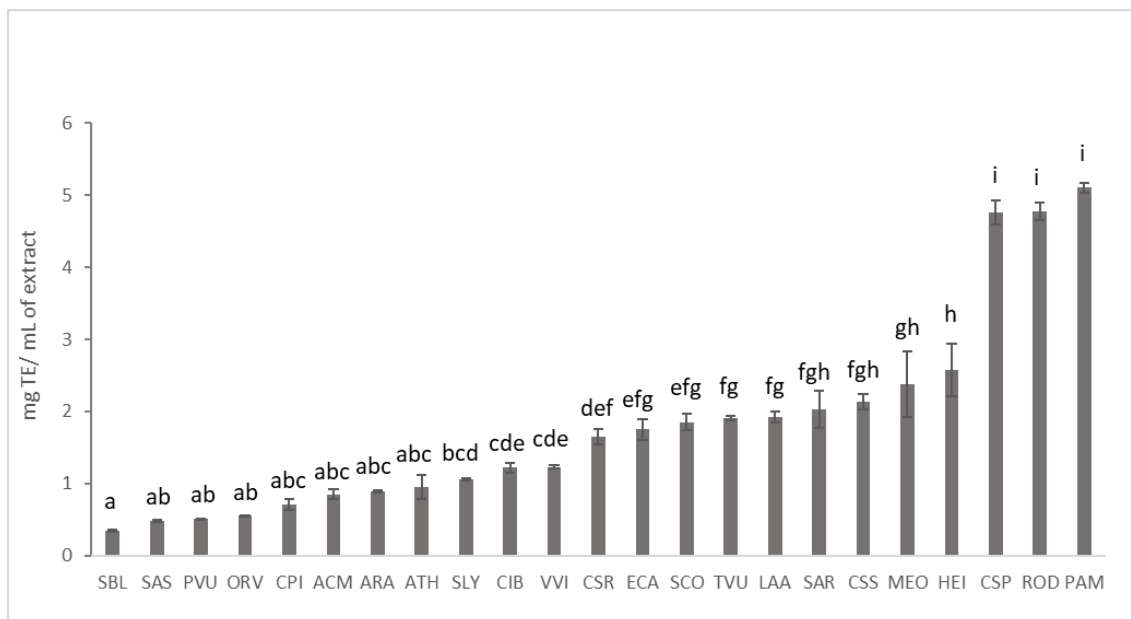


Figure 1. Antioxidant activity measured by DPPH assay. Different letters within the same assay indicate significant differences in ANOVA test ($P < 0.05$). Results are expressed as means \pm SD of three independent experiments.

All plant extract were analyzed for their total phenolic and flavonoid content. Total phenolic content ranged from 2 to 44 mg of gallic acid equivalent (GAE) per g of dried plant material (Fig. 2A), while total flavonoid content ranged from 0 to 43 mg of rutin equivalent (RE) per g of dried plant material (Fig. 2B). Except few samples having very low phenolics and flavonoids content, namely CSA, ACE, and CIA (below 5 mg GAE/g and 5 mg RE/g), most of the examined matrices resulted still valuable source of these antioxidant compounds.

Notably, these three matrices CSP, ROD, and PAM are also the richest in phenolic compounds consistently with the renowned antioxidant capacity associated to these phytochemicals. While ROD showed also high content of flavonoids, the flavonoid content of CSP and PAM was quite low (4.8 and 3.7 mg RE/g).

Interestingly, the samples that showed activity, are rich in polyphenols being all in the upper half of Fig. 1A, all exceeding 20 mg GAE/g plant material (DW).

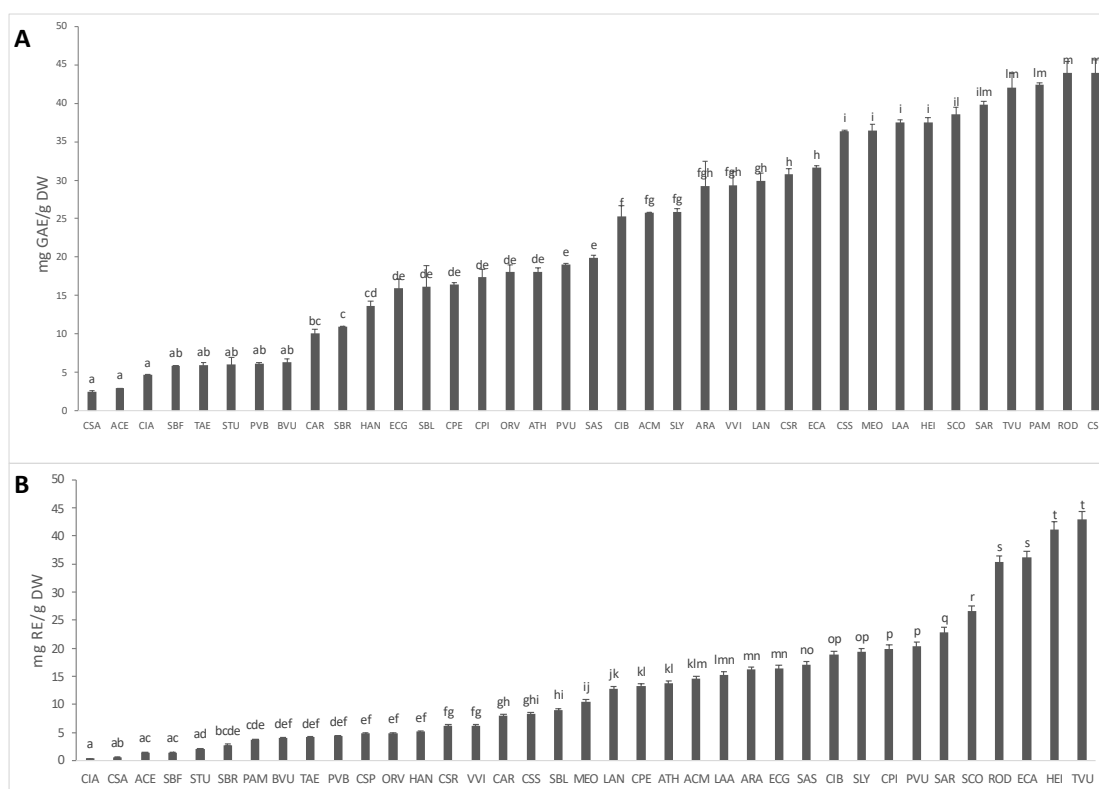


Figure 2. **A)** Total phenolic content; **2B)** Total flavonoid content. Different letters within the same assay indicate significant differences in ANOVA test ($P < 0.05$). Results are expressed as means \pm SD of three independent experiments.

Samples showing significant antibacterial activity were analyzed by ^1H NMR profiling in order to obtain an overview of their main phytochemicals (Figure 3). The analysis showed in all plant extracts belonging to the genus *Salvia* the presence of rosmarinic acid, which alone does not show a MIC value at the concentrations tested (from 0.125 to 1 mg/mL), but that, thanks to its recognized antibacterial activity [15], could act in synergy with other molecules present in the extracts to exert the recorded activity.

Interestingly, the amount of rosmarinic acid in the waste from *S. sclarea* is lower than the other two species, while this sample was found particularly rich in sclareol, a diterpene generally found in the essential oil of this plant.

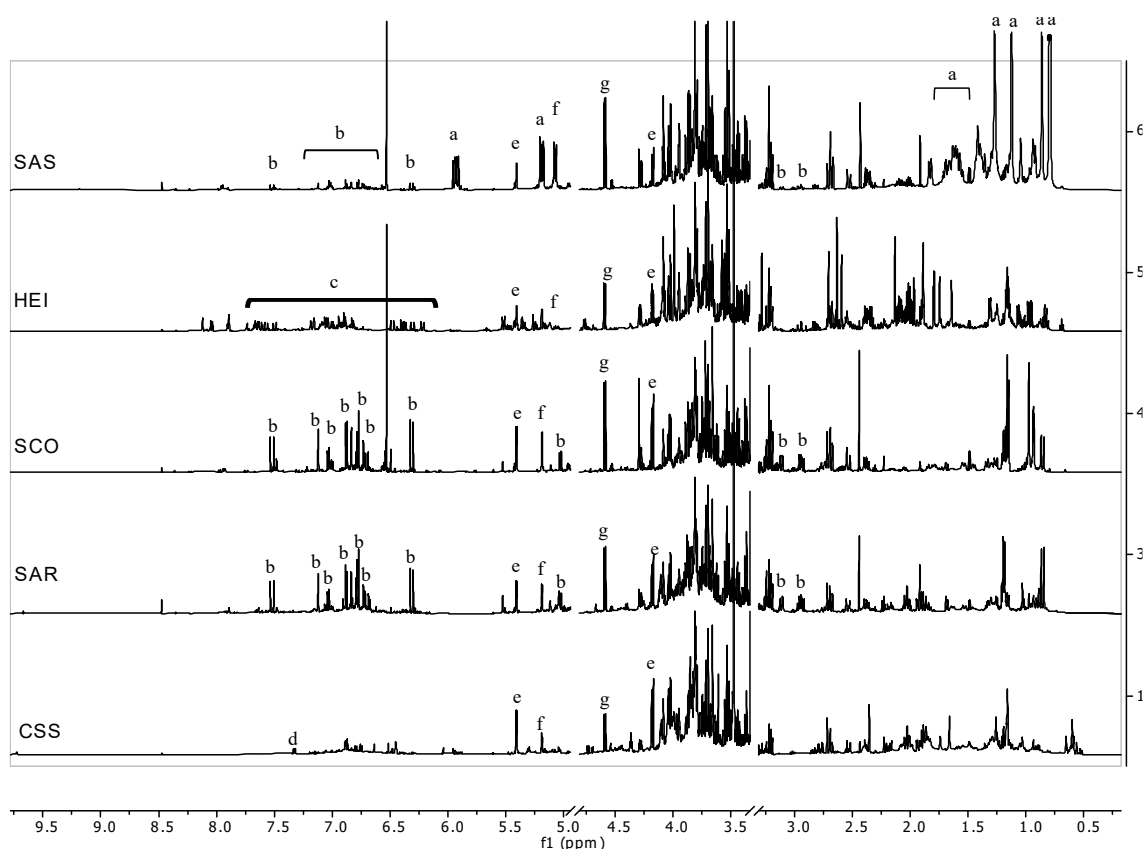


Figure 3. ^1H NMR fingerprinting of the active extracts. a=sclareol, b=rosmarinic acid, c=hydroxycinnamic acids, d=shikimic acid, e=sucrose, f= α -glucose, g= β -glucose.

Another active matrix was the solid residue from the distillation of *C. sempervirens* whose ^1H NMR profile showed the presence of shikimic acid along with other unknown aromatic and aliphatic compounds (at low concentration). Finally, the most powerful antibacterial sample was the extract of *Helichrysum italicum* which resulted rich in hydroxycinnamic acids. This latter data was confirmed also by MS analysis.

Conclusions

This screening of plants neglected matrices allowed to find 5 out of 37 samples active against strains of Gram-positive bacterium *C. michiganensis* subsp. *nebraskense*. The active samples were extracts obtained from the solid wastes after distillation process lighting the potential of plant material to be further used after the extraction of essential oils. In addition, 23 samples proved to exert *in vitro* antioxidant activity by means of DPPH assay. The measured total phenolic and flavonoid content showed that most of the samples contained these compounds and the ^1H NMR analysis carried out on the antibacterial extract revealed that 3 out of 5 samples, all belonging to *Salvia* genus,

contained rosmarinic acid. Other detected compounds were shikimic acid, sclareol, and hydroxycinnamic acids. This preliminary chemical information combined with the exerted biological activities, made the investigated plant matrices a valuable source of functional ingredients providing a basis for their utilization in various fields, especially agriculture.

References

1. Stahel, W. R. The circular economy. *Nature News* **2016**, 531(7595), 435.
2. European Commission Website. Available online: https://ec.europa.eu/environment/topics/circular-economy/first-circular-economy-action-plan_it.
3. Rico, X., Gullón, B., Alonso, J. L., & Yáñez, R. Recovery of high value-added compounds from pineapple, melon, watermelon and pumpkin processing by-products: An overview. *Food Research International* **2020**, 132, 109086.
4. Pleissner, D., Qi, Q., Gao, C., Rivero, C. P., Webb, C., Lin, C. S. K., & Venus, J. Valorization of organic residues for the production of added value chemicals: A contribution to the bio-based economy. *Biochemical Engineering Journal* **2016**, 116, 3–16.
5. Chinou, I. Primary and secondary metabolites and their biological activity. *Chromatographic Science Series* **2008**, 99, 59.
6. Chiocchio I., Mandrone, M., Tomasi, P., Marincich, L., & Poli, F. Plant Secondary Metabolites: An Opportunity for Circular Economy. *Molecules* **2021**, 26(2), 495.
7. Jordan, N., Boody, G., Broussard, W., Glover, J. D., Keeney, D., McCown, B. H., ... & Wyse, D. Sustainable development of the agricultural bio-economy. *Science-New York Then Washington* **2007**, 316(5831), 1570.
8. Gouda, S., Kerry, R. G., Das, G., Paramithiotis, S., Shin, H. S., & Patra, J. K. Revitalization of plant growth promoting rhizobacteria for sustainable development in agriculture. *Microbiological research* **2018**, 206, 131–140.
9. World agricultural production website. Available online: <http://www.worldagriculturalproduction.com/crops/corn.aspx>
10. Cappadone, C., Mandrone, M., Chiocchio, I., Sanna, C., Malucelli, E., Bassi, V., Picone, G., & Poli, F. Antitumor potential and phytochemical profile of plants from sardinia (Italy), a hotspot for biodiversity in the mediterranean basin. *Plants* **2020**, 9(1), 26.
11. Chiocchio, I., Mandrone, M., Sanna, C., Maxia, A., Tacchini, M., & Poli, F. J. I. C. Screening of a hundred plant extracts as tyrosinase and elastase inhibitors, two enzymatic targets of cosmetic interest. *Industrial crops and products* **2018**, 122, 498–505.
12. Marrelli, M., Russo, N., Chiocchio, I., Statti, G., Poli, F., & Conforti, F. Potential use in the treatment of inflammatory disorders and obesity of selected wild edible plants from Calabria region (Southern Italy). *South African Journal of Botany* **2020**, 128, 304–311.
13. Mandrone, M., Marincich, L., Chiocchio, I., Petroli, A., Godevac, D., Maresca, I., & Poli, F. NMR-based metabolomics for frauds detection and quality control of oregano samples. *Food Control* **2021**, 127, 108141.
14. World Checklist of Vascular Plants. Available online: <https://wcvp.science.kew.org/> (accessed on 19 May 2021).
15. Silvia Moreno, Tamara Scheyer, Catalina S. Romano, & Adria´ N A. Vojnov. Antioxidant and antimicrobial activities of rosemary extracts linked to their polyphenol composition. *Free Radical Research*, February **2006**; 40(2): 223–231

Chapter 2

Achieving sustainable agriculture through smart and innovative growth systems

Agriculture is constantly challenged by specific needs such as growing plants resistant to pathogens, having high productivity, yielding high quality products, and being at the same time low-demanding in terms of resources. Achieving these objectives in a sustainable way requires increasing efforts, especially in extending the basic knowledge of plants and their interactions with the environment. In this context, the present chapter reports two case studies (two different plants and growth systems were chosen), which investigated the metabolomic responses of plants to various environmental and anthropic factors.

The first research was focused on *Sorghum bicolor* grown in 12 diverse fields. This plant is drought-tolerant and heat-tolerant representing an important food crop in arid regions. The aim of the work was to investigate the metabolome variations in the different fields with the ultimate goal of favoring the development of smart agriculture techniques.

Additionally, the potential of growing plants in a smart greenhouse was explored in a second research. In this case, *Taxus baccata*, a plant important for its bioactive metabolites, was grown under different LED lighting and the consequent biometric and metabolomic variations were measured.

2.1. Metabolomic Study of Sorghum (*Sorghum bicolor*) to Interpret Plant Behavior under Variable Field Conditions in View of Smart Agriculture Applications

This article has been published in *Journal of Agriculture and Food Chemistry*:

Mandrone, M., Chiochio, I., Barbanti, L., Tomasi, P., Tacchini, M., & Poli, F. Metabolomic Study of Sorghum (*Sorghum bicolor*) to Interpret Plant Behavior under Variable Field Conditions in View of Smart Agriculture Applications. *Journal of Agricultural and Food Chemistry* 2021, 69(3), 1132-1145.

<https://doi.org/10.1021/acs.jafc.0c06533>

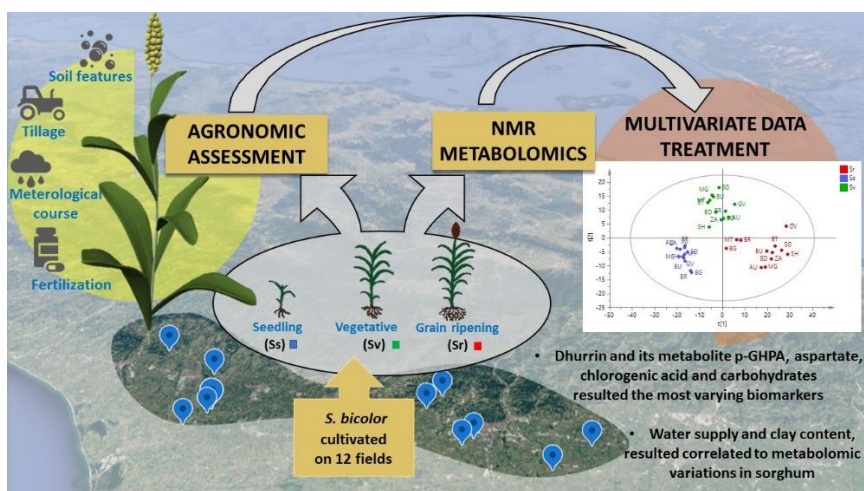
Keywords: smart agriculture; NMR metabolomics; quality control; Sorghum bicolor; dhurrin

Reprinted with permission from [J. Agric. Food Chem. 2021, 69, 3, 1132–1145].
Copyright [2021] American Chemical Society.

<http://pubs.acs.org/articlesonrequest/AOR-UU92PXIMYXGSXR2VAW3A>

Abstract

To tackle the urgency of smarter crop management, the complex nature of agricultural ecosystems needs to be better understood, employing and combining different techniques and technologies. In this study, untargeted metabolomics and agro-meteorological survey were coupled to study the variation of *Sorghum bicolor* (L.) Moench metabolome during crop development, in response to environmental and anthropic factors. Twelve crop fields in the Emilia-Romagna region, Italy, were monitored and sampled at different stages, seedling (Ss), advanced vegetative (Sv), and ripening (Sr), and subjected to ¹H NMR-based metabolomics. The analytical method developed resulted to be successful to quickly analyze different sorghum organs. Dhurrin, a cyanogenic glucoside, resulted to be a biomarker of crop quality and development, and several insights into its turnover and functions were obtained. In particular, p-glucosyloxy-2-hydroxyphenylacetic acid was identified, for the first time, as the main metabolite accumulated in sorghum at Sr, after gradual dhurrin neutralization. During plant life, fertilization and biotic and abiotic stress reflected peculiar metabolomic profiles. Water supply and soil features (i.e., clay content) were correlated to metabolomic variations, affecting dhurrin (and related metabolites), amino acids, organic acids, and carbohydrate content. Increase in chlorogenic acid was registered in consequence of predator attacks. Moreover, grain from three fields presented traces of dhurrin and the lowest antioxidant potential, which resulted in poor grain quality. Metabolomics turned out to be a promising tool in view of smart agriculture for monitoring plant growth status and applying appropriate agricultural practices since the early stage of crop development.



Introduction

Population growth, climate change, and the urgent demand for safe, nutritious, and sufficient food worldwide challenge agriculture to intensify production, while concurrently lowering the food environmental footprint [1]

To tackle this demand, it is increasingly important to deeply understand the complexity of agricultural ecosystems. In order to achieve this goal, techniques and technologies from many disciplines (biotechnology, agronomy, phytochemistry, microbiology, engineering, and information technology) need to be jointly employed [2]

The analysis of big data through an inductive (hypothesis-generating) approach, which leads to advances in various fields, is also expected to enable farmers and companies in the agricultural sector to improve their efficiency in a sustainable way [3]. For instance, considering that most agricultural processes (*i.e.*, crop choice, sowing schedule, growth, and harvest management) depend on the weather, it is of general interest to study how shifts in the weather regimes determine crop variability at regional levels. Thus, advanced and accurate information on weather variables and their quantitative relations to crop processes need to be implemented [4]. In this framework, untargeted metabolomics coupled with agro-climatic studies could represent a valuable tool to obtain information on the variation of crop metabolome in response to environmental and anthropic factors. Metabolomics, which often relies on untargeted analysis protocols, whose data are handled with multivariate techniques (inductive approach), has already been applied successfully in several areas of research, ranging from human diagnostics and epidemiology to plant sciences [5]. In the latter field, this approach resulted to be particularly helpful in facilitating the identification of active principles in medicinal plants [6-8] and for food and botanical quality control, in terms of both nutraceutical/biological properties and fraud detection [9,10].

This work is focused on *Sorghum bicolor* (L.) Moench, belonging to the Poaceae family and Andropogoneae tribe. Of the large intraspecific variation, we addressed sorghum genotypes suited for grain production, that is, those featuring low plants with large panicles, which are grown as cereals for food and/or feed uses. More specifically, this work focuses on commercial sorghum hybrids producing white (actually pale) grain, that is, whose kernels are devoid of tannins and anthocyanins, and are, therefore, better suited for a vast array of food/feed uses.

The relevant role played by sorghum in global agriculture makes it an important crop to be investigated through metabolomic approaches. Sorghum is the fifth most important cereal in the world; thanks to its good drought resistance, it is intensively cultivated in Africa, Asia, and southwest USA [11] and is regarded with growing interest in other warm temperate areas of the world. The EU plays a minor role in grain sorghum cultivation: the crop is concentrated in the central Mediterranean areas, with the two major producing countries, France and Italy (approximately 70,000 and 50,000 ha, respectively). However, the cultivation of sorghum for food preparation is recently increasing in Italy and other Mediterranean countries because of its lack of gluten [12] and its recognized high nutritional value [13]. Nevertheless, sorghum also produces a cyanogenic glycoside (dhurrin), whose content varies depending on the plant stage and growth conditions [14], and because of its toxicity, it must be kept extremely low at harvest.

With these premises, 12 sorghum crop fields in Emilia-Romagna (Italy) were studied from an agronomic and metabolomic viewpoint. In particular, plant samples were harvested at three different stages: seedlings (Ss), advanced vegetative phase (Sv), and grain maturity (Sr), and subjected to ^1H NMR-based metabolomic analysis. Thus, the relationships among the metabolome, crop parameters, and organs were investigated through multivariate data treatment. The antioxidant activity of the grain was also measured.

On this basis, the present study was aimed to detect the variations of sorghum metabolome associated with growth stage, plant organ, and environmental/crop management factors. Consequently, the NMR-based metabolomic approach was here used also for the broad-spectrum quality control of sorghum grain. The final purpose was to better understand the sorghum metabolome and its response to environment, collecting data potentially useful for implementing smart agriculture practices. Particular attention was given to specific agricultural practices or environmental features, which could positively affect sorghum grain in terms of yield and quality.

Materials and Methods

Sorghum fields

In 2017, a survey was run on commercial sorghum crops in the Emilia-Romagna region, the largest sorghum-producing area of Italy. Twelve fields cultivated with sorghum hybrids producing white grain were selected between 44°07' and 44°38' N, and between 11°06' and 12°07' E, in the plain area of the region (nine fields; elevation not exceeding 30 m above sea level) or in the footsteps of the Apennine mountains (three fields at an average elevation of 116 m above sea level) (Figure 1). The map of the fields was created in QGIS 2.18.20 (QGIS Development Team, 2016) using the DEM file provided by ISPRA [15] and the shape file provided by ISTAT [16].

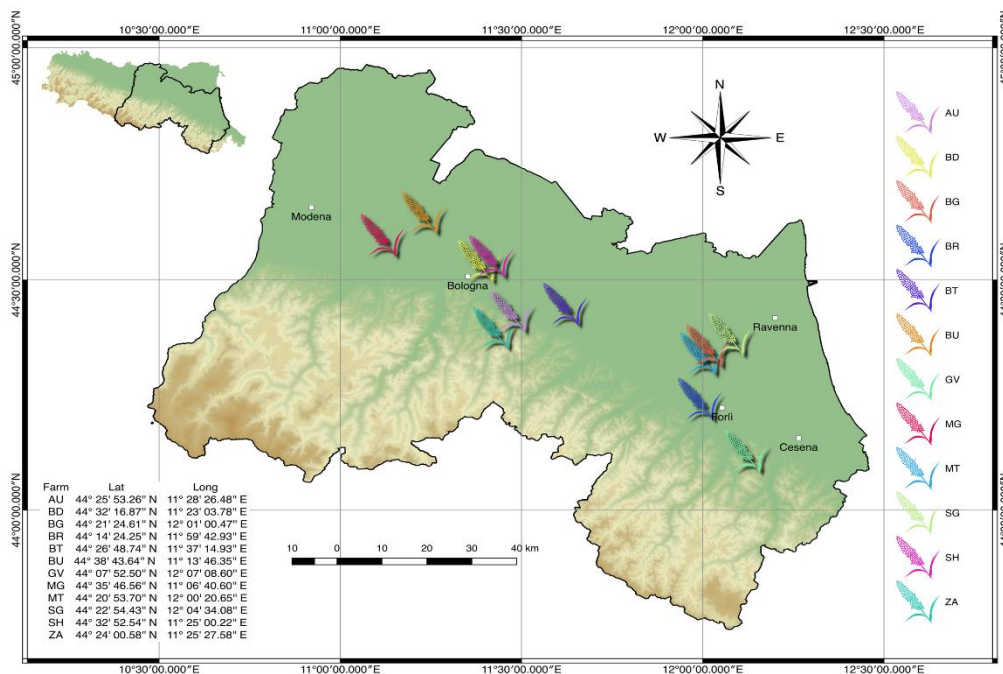


Figure 1. Location of the 12 sorghum fields addressed in this study within the Emilia-Romagna region (Italy). The map of the fields was created in QGIS 2.18.20 (QGIS Development Team, 2016) using the DEM file provided by ISPRA and the shape file provided by ISTAT.

Sorghum cultivation is fully mechanized in Italy, that is, all operations are carried out with agricultural machinery. Fertilization and weed, pest, and disease control, in most cases, are based on mineral fertilizers and chemical plant protection products. All crop interventions, their timing, and the products used in the 12 fields were annotated, from soil tillage (autumn 2016) to crop maturity (summer 2017). The 12 fields were managed

under rain-fed conditions, that is, without irrigation. This is the standard practice for the sorghum crop in the surveyed area.

The course of weather during the crop season (minimum and maximum temperature, precipitation, and relative humidity) was obtained from the regional network of meteorological stations [17]. Principal soil characteristics such as texture, pH, organic carbon (OC) content at 0–30 cm depth, clay content, silt, and clay content were obtained from specific regional maps [18]. The shallow water table depth during sorghum growth was obtained from the same online source [18].

Crop evapotranspiration (ET_C), representing the evapotranspiration of the specific crop under nonlimiting water supply [19], was assessed based on the reference evapotranspiration (ET_0) calculated with the Hargreaves method [20]. The relationship between the actual water supply (precipitation) and potential consumption (ET_C) was investigated as an indicator of potential drought for the crop.

Sorghum in the 12 fields was seeded in the early spring: the average seeding date was April 5, corresponding to 95 ± 5.1 days from the beginning of the year. Sorghum cycle from seeding to harvest lasted an average 127.5 ± 4.9 days after seeding (DAS).

Plant and soil sampling

Sorghum samples were collected at three relevant plant stages: seedling (Ss) (26.2 ± 6.1 DAS), booting–initial heading, that is, advanced vegetative stage (Sv) (76.4 ± 5.4 DAS), and grain ripening (Sr) (111.0 ± 5.1 DAS).

At the first sampling (average date, May 1), 40 seedlings were taken from an area of approximately 10 m^2 . Plants were extracted from soil and immediately frozen in liquid nitrogen, then stored at $-80 \text{ }^\circ\text{C}$ until being freeze-dried, and kept in fridge at $4 \text{ }^\circ\text{C}$ before the analysis.

At the second sampling (average date, June 20), 20 plants were collected from a nearby area and partitioned into stems and leaves. The stems and leaves were immediately frozen in liquid nitrogen and titrated as described for seedlings.

At the third sampling, (average date, July 25), 20 plants were collected from a nearby area and partitioned into stems, leaves, and panicles. The vegetative organs were managed as previously described, whereas the grain from the panicle was dried in a stove at $40 \text{ }^\circ\text{C}$, ground, and stored under dark conditions. Additional panicle samples were taken on 0.9 m^2 crop areas per two replicates, and the grain recovered was weighed and

subjected to moisture assessment. Based on these data, the final grain yield per unit crop surface (Mg ha^{-1}) at the reference moisture (14%) was determined. The test weight, that is, the apparent volumetric mass (g L^{-1}) of the grain, was also determined.

Grain yield and test weight at harvest were subjected to Pearson's correlations with a series of agro-environmental parameters including tillage depth (TD), organic fertilization, mineral N supply, seeding date, length of the growth period, clay content, OC, $\text{ET}_C - P$, P/ET_C , and the depth of the shallow water table in July (WTD).

Soil samples at the depth of 0–0.3 m were also collected at the same three times of plant sampling. They were oven-dried ($105\text{ }^\circ\text{C}$ for 48 h) to determine soil humidity at the beginning (H-ini), middle (H-mid), and end of the sorghum growth season (H-late).

Chemicals

Deuterium oxide (D_2O , 99.90% D), CD_3OD (99.80% D), and CDCl_3 with 0.03% TMS (99.80% D) were purchased from Eurisotop (Cambridge Isotope Laboratories, Inc., France). Standard 3-(trimethylsilyl)-propionic-2,2,3,3- d_4 acid sodium salt (TMSP), sodium phosphate dibasic anhydrous, sodium phosphate monobasic anhydrous, and all the other solvents and chemicals were purchased from Sigma-Aldrich Co. (St. Louis, MO, USA).

Extract preparation for NMR analysis

In all cases, samples representative of each field were obtained by pooling material from all the individuals collected on the same field. A 30 mg of freeze-dried and powdered seedlings, leaves, or stem material were extracted using 1 mL of a bland (50:50) $\text{CD}_3\text{OD}/\text{D}_2\text{O}$ (containing 0.1 M phosphate buffer and 0.01% of TMSP standard). The extracts were sonicated for 30 min and subsequently centrifuged for 20 min at 17,000g, and the supernatant (700 μL) was then separated from the pellet and transferred into NMR tubes.

For grain metabolomics, 50 mg of the dried and ground material was subjected to ultrasound-assisted (20 min) extraction in 0.8 mL of CDCl_3 . Then, 0.8 mL of the bland (50:50) $\text{CD}_3\text{OD}/\text{D}_2\text{O}$ (containing 0.1 M phosphate buffer and 0.01% of TMSP standard) was added, and the samples were subjected to additional sonication for 20 min and subsequently centrifuged for 20 min at 17,000g. The obtained supernatant was constituted by a biphasic mixture: 400 μL of the chloroform phase was mixed with 200 μL of CDCl_3

containing TMS standard (0.03%) and transferred into NMR tubes, whereas 600 μ L of aqueous phase was directly transferred into NMR tubes to be analyzed by NMR separately. All metabolomic analyses have been performed during 2017 and 2018.

Dhurrin, p-GPHA, and Chlorogenic Acid Prepurification and Structure Elucidation

Freeze-dried leaves at Sr (1.2 g) underwent ultrasound-assisted extraction with 60 mL of CH₃OH/H₂O (50:50). The mixture was centrifuged for 20 min at 2469g, and then the supernatant was filtered on a Büchner funnel and evaporated using a rotary evaporator under a reduced pressure below 40 °C. The resulting dried extract (200 mg) was dissolved in a proper volume of water and methanol and chromatographed using a C18 column (4 g) by an MPLC instrument (Reveleris, Büchi, Switzerland) equipped with a UV detector and a fraction collector. The extract was eluted with a gradient of H₂O (solvent A) and MeOH (solvent B) starting from 5% B and reaching 100% B in 25 min, followed by isocratic elution with 100% B for an additional 5 min. The flow rate was 15 mL min⁻¹. This resulted in 19 subfractions (from F1 to F19). Dhurrin was obtained in F3 (see the Supporting Information for NMR assignment) and *p*-glucosyloxy-2-hydroxyphenylacetic acid (*p*-GPHA) in F2.

Freeze-dried leaves at Sv (3 g) underwent ultrasound-assisted extraction with 180 mL of CH₃OH/H₂O (80:20) two times. The mixture was centrifuged for 20 min at 2469g, and then the supernatant was filtered on a Büchner funnel and evaporated using a rotary evaporator under a reduced pressure below 40 °C. The resulting dried extract (700 mg) was dissolved in 50 mL of H₂O and 50 mL of CHCl₃; then, the mixture was transferred into a separating funnel to carry out a liquid–liquid partition using 50 mL of CHCl₃ another two times. The water fractions were combined and dried in the rotary evaporator, yielding 600 mg of crude extract. A 300 mg of this extract was solubilized in a minimum volume of H₂O and chromatographed using a Sephadex column (180 cm \times 2.5 cm internal diameter filled with 210 g of Sephadex LH-20 and 890 mL of CH₃OH). Methanol was used as the eluent, and the flow rate was 1 mL min⁻¹. A total of 17 fractions were collected, and chlorogenic acid was obtained from fraction 10 (see the Supporting Information for NMR and MS data).

p-GPHA (D₂O, 600 MHz): δ 7.39 (d, 2, J = 8.6 Hz, H-4, H-8), 7.09 (d, 2, J = 8.6 Hz, H-5, H-7), 5.02 (d, 1, J = 7.7 Hz, H-1'), 4.89 (s, 1, H-2), 3.88 (dd, 1, J = 12.6, 2.3 Hz, H-6'b), 3.71 (dd, 1, J = 12.6, 5.9 Hz, H-6'a), 3.56 (qd, 1, J = 8.8, 6.2, 2.4 Hz, H-5'), 3.50

(dd, 1, $J = 8.4, 3.9$ Hz, H-2'), 3.47 (t, 1, $J = 10.3$ Hz, H-3'), 3.42 (t, 1, $J = 9.4$ Hz, H-4'); ^{13}C NMR (CD_3OD , 150 MHz): δ 179.4 (CO, C-1), 155.8 (CO, C-6), 134.8 (C, C-3), 128.3 (CH, C-5, C-7), 116.5 (CH, C-4, C-8), 100.5 (CO, C-1'), 76.09 (CH, C-3'), 76.08 (CH, C-5'), 73.3 (CO, C-2), 73.26 (CH, C-2'), 69.72 (CH, C-4'), 66.83 (CH_2 , C-6'a, C-6'b). Positive ESI-MS m/z : 353 $[\text{M} + \text{Na}]^+$, 369 $[\text{M} + \text{K}]^+$, calculated as 330.29 for $\text{C}_{14}\text{H}_{18}\text{O}_9$. Negative ESI-MS m/z : 329 $[\text{M} - \text{H}]^-$.

NMR and MS Spectra Measurement

The ^1H NMR spectra, J -resolved, ^1H - ^1H homonuclear, and inverse-detected ^1H - ^{13}C correlation experiments were recorded at 25 °C on a NMR instrument Varian Inova (Milan, Italy), operating at the ^1H frequency of 600 MHz, equipped with an indirect triple resonance probe. CD_3OD was used as an internal lock for polar extracts and CDCl_3 for chloroform extracts. For ^1H NMR profiling, the relaxation delay was 2.0 s, observed pulse 5.80 μs , number of scans 256, acquisition time 16 min, and spectral width 9595.78 Hz (corresponding to δ 16.0). For the aqueous samples, a presaturation sequence (PRESAT) was used to suppress the residual H_2O signal at δ 4.83 (power = -6 dB, presaturation delay 2 s). ESI-MS analyses were performed by the direct injection of MeOH solutions of the compounds using a Waters ZQ 4000 (Milford, MA USA) mass spectrometer.

NMR Processing and Multivariate Data Treatment

Free induction decays were Fourier-transformed, and the resulting spectra were phased, baseline-corrected, and calibrated to TMS at δ 0.0, which was also used as a standard for semiquantitative analysis. Spectral intensities were reduced to the integrated regions of equal width (δ 0.04), corresponding to the region from δ 0.0 to 10.0, with the scaling on standard at δ 0.0 using the NMR MestReNova 12 software (Mestrelab Research, Santiago de Compostela, Spain). The analysis of ^1H NMR profiles was performed based on an in-house library and comparison with the literature [21-23].

The regions of δ 5–4.5 and 3.34–3.30 were excluded from the analysis of the aqueous samples because of the residual solvent signals, whereas, for the same reason, the region at δ 7.3 was excluded from the analysis of the chloroform fractions. For multivariate analysis, the models (PCA, PLS-DA, OPLS, and OPLS-DA) were developed using SIMCA-P+ software (v. 15.0, Umetrics, Umeå, Sweden). Data were subjected to Pareto scaling. The supervised models were evaluated by the goodness of fit [R^2Y (cum)]

and goodness of prediction [Q^2 (cum)], together with the parameters given by the permutation test (performed using 100 permutations)[24]. The coefficients obtained are reported in Table S1 of the Supporting Information. OPLS-DA and PLS-DA were further validated by cross-validated (CV)-ANOVA. For Ss, nine independent OPLS models were built using the altitude, ET_C – P, organic fertilizer supply, mineral N supply, OC, clay content, silt content, H-ini, and TD in turn as the y variable. A total of 10 independent OPLS models were developed for both stems and leaves at Sv, using the abovementioned variables with the addition of H-mid. Lastly, for Sr leaves, stems, and grain, H-late and WTD were also considered.

β-Carotene Bleaching Assay and Statistical Analysis

Sorghum grain samples were obtained by sonication (20 min) of 30 mg of grain powder in 1 mL of MeOH/H₂O (50:50), followed by centrifugation for 10 min. The supernatants were evaporated in a SpeedVac system (SpeedVac SPD 101b 230, Savant, Italy) to yield the crude extracts. Stock solutions at concentrations of 120, 60, 30, and 15 μg mL⁻¹ were prepared. Water was used as the negative control, whereas Trolox stock solutions (from 50 to 500 μM) were used to build the IC₅₀ curve of positive control. The assay was developed following the method described by Mandrone *et al.* [2017]. The samples were analyzed in triplicate, and the analysis was repeated three times. One-way ANOVA was performed by GraphPad Prism 4 software (La Jolla, CA, USA). Tukey's post-hoc test was used, and differences at $p < 0.05$ were considered significant.

Results

Environmental traits

Soil texture in the 12 fields ranged from being loamy to silty-clayey. The average sand, silt, and clay contents were 23.8 ± 8.3 , 46 ± 3.9 , and $30.2 \pm 8.9\%$, respectively. The pH was always mildly alkaline (~7.5), as that of most soils in the area. Organic carbon was quite low (average, 9.5 ± 3.4 g kg⁻¹), which is also a typical feature in the surveyed area. Therefore, the soils had a prevailing mineral composition and were supplemented with specific doses of minerals and, sometimes (4 cases out of 12), organic fertilizers to support plant growth.

In Figure 2A the course of weather during the crop season is represented according to Bagnouls and Gaussen [25], that is, plotting for each month the average temperature versus precipitation, the latter in a double scale (right y axis) with respect to the former (left y axis), and reference evapotranspiration is also included. Based on the cited authors, the months during which double-scaled precipitation falls below the average temperature represent the dry periods of the year. This, in 2017, occurred in June and especially July, that is, during the drought-sensitive reproductive stage. The difference between the natural water supply (P) and potential demand from the atmosphere (ET_0) is even more remarkable. This means that plants grown under a rain-fed regime underwent a severe water deficit, despite good precipitation restoring soil moisture at the beginning of the crop cycle, and the potential contribution from the shallow water table.

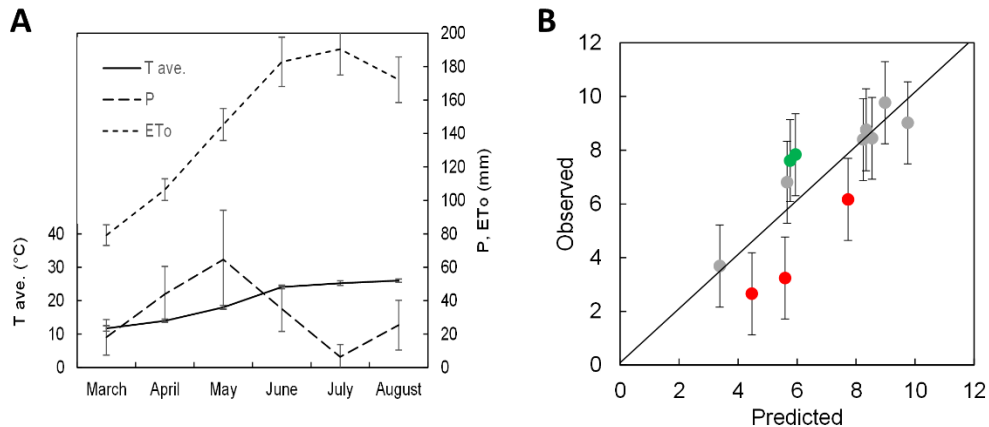


Figure 2. (A) Average temperature (T_{ave}), precipitation (P), and reference evapotranspiration (ET_0) during the sorghum crop season. Vertical bars indicate \pm standard deviation. (B) Predicted grain yield values based on multiple regression involving water table depth and N supply vs observed values. Vertical bars indicate \pm standard error of the estimate. Data points away from the iso-yield bisecting line by more than the standard error are highlighted in red (predicted > observed) or green (predicted < observed).

Grain Yield and Its Relationship with Agro-Environmental Parameters

Grain yield varied in a wide range from a minimum of below 3 Mg ha⁻¹ in a hilly site (GV) to a maximum of almost 10 Mg ha⁻¹ in the fertile lowland (MT) (Table 1). The hot and dry weather of the 2017 crop season may have enhanced intrinsic differences among fields. Test weight, which expresses the degree of grain filling during maturation, varied in a much tighter range: from a minimum of 688 g L⁻¹ to a maximum of 757 g L⁻¹.

Table 1. Grain Yield and Test Weight in the 12 Sorghum Fields (Average \pm Standard Deviation)

farm	grain yield (Mg ha ⁻¹)	test weight (g L ⁻¹)
ZA	3.2 \pm 0.2	700 \pm 80
AU	6.8 \pm 0.5	688 \pm 57
BD	8.4 \pm 1.2	762 \pm 1
SH	8.4 \pm 0.1	705 \pm 31
MG	7.8 \pm 0.9	752 \pm 1
BU	8.8 \pm 0.1	653 \pm 64
BT	9.0 \pm 0.7	745 \pm 9
MT	9.8 \pm 0.5	701 \pm 82
BG	7.6 \pm 2.2	636 \pm 16
SG	6.2 \pm 0.2	757 \pm 4
GV	2.7 \pm 0.2	656 \pm 5
BR	3.7 \pm 0.6	696 \pm 23

The agro-environmental parameters varied remarkably among the 12 fields (Table 2). The fields were all tilled to a relevant depth (0.3–0.45 m). The organic fertilization consisted of livestock manure (BT, MG) or slurry (AU), sometimes in association with a previous lucerne ley (BT, MG). This led to a composite score for organic fertilization ranging from zero, in most cases, to a maximum of 3 in BT. The N supply with mineral fertilizers ranged from a minimum of 92 kg of N ha⁻¹ (BR) to a maximum of 230 kg of N ha⁻¹ (MT). The length of the growing season from seeding to grain ripening varied in a relatively narrow range (120–135 days), owing to similar thermal course and similar (medium and medium–late) sorghum hybrids being cultivated in all fields. The clay content in the soil varied from a minimum of 19% (MT) to a maximum of 47% (BT).

Organic C also varied from a minimum of 0.6% (BT) to a maximum of 1.8% (SG). $ET_C - P$, that is, potential water demand (ET_C) versus supply (P), outlined a relevant water deficit in the growth season: from 270 mm (AU) to 402 mm (BR) of seasonal gap between the plant potential uses and actual availability. Another way of expressing the same concept, the ratio of precipitation to crop evapotranspiration (P/ET_C), indicates that precipitation covered from 17% (BT) to 48% (AU) of plant potential uses. This means that more than 50% of potential uses was not covered by precipitation or could only rely on other sources (previous soil water reserve and the shallow water table). Lastly, WTD during the month of July was either below the limit for detection (3 m depth) or between 1.9 m (BT) and 2.67 m (MT and BG).

Table 2. Agro-Environmental Parameters in the 12 Crop Fields^a.

Farm	Tillage depth (m)	Organic fert. (scale 0-3)	N supply (kg ha ⁻¹)	Seeding date (DOY)	Growth length (d)	Clay (% dw)	OC (% dw)	ET _C -P (mm)	P/ET _C (%)	WTD (m)
ZA	0.45	0	159	94	135	26	1.0	334	39	>3
AU	0.30	1	161	94	120	35	0.6	270	48	>3
BD	0.30	0	161	96	125	26	0.6	376	33	2.15
SH	0.45	1	170	104	120	33	1.1	363	34	2.15
MG	0.35	2	138	97	125	45	1.2	440	29	2.66
BU	0.35	0	184	96	135	28	1.1	449	27	2.37
BT	0.40	3	184	83	130	47	0.6	449	17	1.90
MT	0.30	0	230	95	125	19	0.9	454	24	2.67
BG	0.35	0	133	96	130	20	1.2	492	21	2.67
SG	0.45	1	161	90	125	25	1.8	485	17	2.32
GV	0.30	1	125	98	130	25	0.7	397	26	>3
BR	0.30	0	92	101	130	33	0.9	402	25	>3

^aDOY, day of the year; ET_C , crop evapotranspiration; P , precipitation; OC, organic carbon; WTD, water table depth in July.

The relationships between the agro-environmental and yield parameters are reported in Table 3. Grain yield outlined the significant correlations with the amount of N supplied with mineral fertilizers and WTD in July. Test weight, which is intrinsically less important from a financial viewpoint, was not significantly related to any agro-environmental parameter, nor was it related to yield. Additionally, no significant relationship was observed between the two parameters expressing water deficit ($ET_C - P$ and P/ET_C) on one side and the two grain attributes on the other side.

Table 3. Pearson's Correlations between Agro-Environmental and Yield Parameters in the 12 Fields^a.

	Grain yield	Test weight	Tillage depth	Organic fert.	N supply	Seeding date	Growth length	Clay	OC	ET _c - P	P/ET _c
Test weight	0.24										
Tillage depth	-0.01	0.27									
Organic fert.	0.19	0.45	0.26								
N supply	0.70	0.17	0.16	0.06							
Seeding date	-0.22	-0.36	-0.21	-0.52	-0.38						
Growth length	-0.36	-0.38	0.07	-0.24	-0.16	-0.21					
Clay	0.15	0.45	0.13	0.82	-0.14	-0.27	-0.16				
OC	-0.03	0.12	0.57	-0.12	-0.08	0.08	0.00	0.22			
ET _c - P	0.32	0.02	0.10	0.08	0.10	-0.26	0.30	0.16	0.50		
P/ET _c	-0.17	-0.10	-0.12	-0.22	-0.02	0.35	-0.31	0.06	0.36	-0.93	
WTD	0.71	0.49	0.39	0.40	0.46	-0.36	-0.17	0.27	0.08	0.38	-0.41

^a $r \geq |0.58|$, significant at $P \leq 0.05$; $r \geq |0.71|$, significant at $P \leq 0.01$ ($n = 12$).

The multiple stepwise regression of the crop management and environmental factors on grain yield resulted in the following equation

$$\text{Grain yield} = 9.349825 + 0.013165 * \text{water table depth} + 0.014968 * \text{N supply}; R^2 = 0.67^{**}$$

It is perceived from this equation that the two factors singularly best-related with yield (Table 3) were also interacting, contributing to explain a good share (67%) of the total yield variation among the 12 fields.

Based on this equation, predicted grain yield values were plotted versus the values observed (Figure 2B). Seven fields out of the twelve fell near the iso-yield bisecting line, meaning that the predicted and observed grain yield did not diverge significantly. Two fields in the medium–high range (MG and BG) exhibited a higher observed yield than the

predicted yield, implying a better crop husbandry by the farmer or some unidentified factor determining this result. Lastly, three fields outlined lower observed values than predicted values (ZA, SG, and GV): the field in the medium yield range (SG) (observed and predicted of 6.2 and 7.7 Mg ha⁻¹, respectively) suffered a severe hailstorm at the beginning of the reproductive stage, which can explain the result; the other two cases in the low yield range (ZA and GV) featured a poor crop husbandry or some unidentified factor for this outcome.

Metabolomic Analysis of Leaves and Stems

Seedling Analysis

The untargeted ¹H NMR-based metabolomic analysis pointed out the differentiation of sorghum growing on diverse fields (Figure 3). The diagnostic signals of all identified metabolites are reported in Table S2, and the exemplificative spectra are shown in Figure 4.

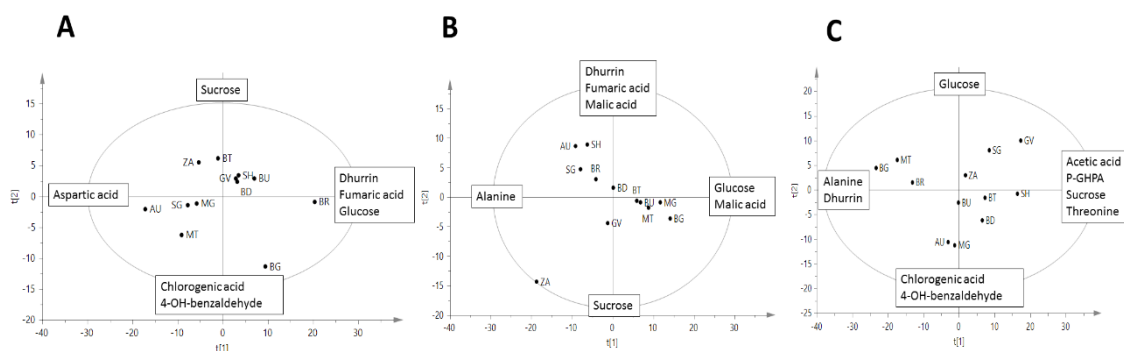


Figure 3. ¹H NMR-based PCA score scatterplot of sorghum at three different growth stages: (A) Ss (seedling stage)—dhurrin, glucose, and fumaric acid increase along the positive side of component *t*[1], whereas aspartic acid follows an inverted trend, increasing on the negative side of *t*[1]. Sucrose increases along the positive side of component *t*[2], whereas *p*-HBA and chlorogenic acid increase on the negative side of *t*[2]; (B) leaves at Sv (advanced vegetative stage)—dhurrin and fumaric acid increase on the positive side of *t*[2] with a trend opposite to that of sucrose; glucose increases on the positive side of *t*[1] with a trend opposite to that of alanine; malic acid increases on the positive side of both *t*[1] and *t*[2]; (C) leaves at Sr (grain ripening)—*p*-GHPA, sucrose, acetic acid, and threonine increase along the positive side of component *t*[1], whereas alanine and dhurrin follow an inverted trend, increasing on the negative side of *t*[1]. Glucose increases along the positive side of component *t*[2], whereas *p*-HBA and chlorogenic acid increase on the negative side of *t*[2].

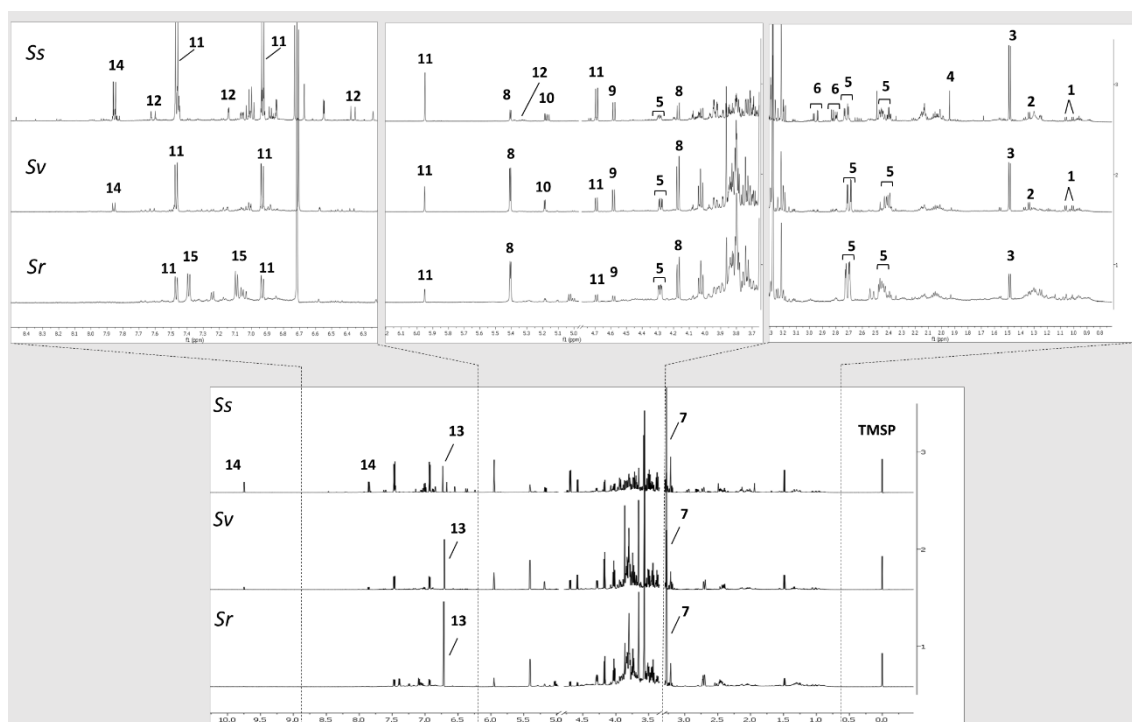


Figure 4. ^1H NMR full spectra of representative samples of sorghum leaves (collected on the SG field) at Ss, Sv, and Sr. Residual solvent signals have been removed; TMS = standard. Numbers indicate the diagnostic signals of the most varied metabolites: 1 = valine, 2 = threonine, 3 = alanine, 4 = acetate, 5 = malic acid, 6 = aspartic acid, 7 = glycine betaine, 8 = sucrose, 9 = β -glucose, 10 = α -glucose, 11 = dhurrin, 12 = chlorogenic acid, 13 = fumaric acid, 14 = *p*-HBA, and 15 = *p*-GHPA.

According to the PCA performed on samples at Ss (Figure 3A), dhurrin, 4-hydroxybenzaldehyde (*p*-HBA), and chlorogenic acid were identified as the most varying secondary metabolites, whereas, among the primary metabolites, glucose, sucrose, fumaric acid, and aspartic acid were the most relevant for sample discrimination (loading plots of the models are given in Figures S1–S3). From NMR profiling, it is observed that dhurrin resulted to be the most abundant secondary metabolite produced at Ss, with the concentration ranging from 35 to 101 mg g^{-1} of dried weight (DW).

BG and BR exhibited a peculiarly diverse metabolomic profile, both being characterized by a higher amount of dhurrin compared to the other samples. Furthermore, BR also showed increased glucose and fumaric acid, whereas BG was particularly enriched in chlorogenic acid and *p*-HBA. Moreover, the PCA revealed an inverted trend between aspartic acid and dhurrin concentration in plants at Ss.

Late Vegetative Stage Analysis

Leaves and stems at Sv were first analyzed separately by building two independent PCA models. Dhurrin was found in both stems and leaves, and in this stage, another aromatic compound was visible in the spectra. It was then isolated and identified (by NMR and MS analysis) as *p*-GPHA. Moreover, at this stage, in contrast to Ss, aspartate did not significantly contribute to the diversification among the leaf samples, and it was no more correlated to the decrease in dhurrin concentration.

With regard to leaves at Sv, sucrose content also resulted to be an important factor of discrimination among samples, together with aliphatic amino acids, fumaric acid, and dhurrin (Figure 3B). The model placed ZA as an outlier because of its high content of chlorogenic acid, *p*-GPHA, and acetate.

One of the most varying metabolites in the stems at Sv resulted to be glucose, increasing linearly with aspartate, aliphatic amino acids, and dhurrin (Figure S4A), while showing a trend opposite to that of chlorogenic acid. This latter metabolite resulted to be peculiarly abundant also in ZA stems.

In order to deepen the metabolomic differences among stems and leaves at Sv, a supervised model OPLS-DA was developed (Figure S4B), classifying samples according to plant organs. This analysis highlighted that stems at Sv were generally characterized by a higher concentration of primary metabolites, except for alanine and fumaric acid. On the other hand, leaves at Sv resulted to be more enriched in secondary metabolites, especially dhurrin. Generally, the metabolite trends observed for the leaves and stems at Sv were not overlapping, with some exceptions: SH, which expressed a high level of dhurrin in both leaves and stems at Sv; GV, which showed a high content of sucrose in both leaves and stems; and ZA, characterized by the accumulation of chlorogenic acid in both organs.

Ripeness Stage Analysis

Different metabolomic profiles were also observed for sorghum leaves at Sr (Figure 3C). Once again, dhurrin ranked among the most varied metabolites, as it followed an inverted trend versus *p*-GPHA, whereas aspartic acid was no more detectable in the leaves at this stage.

BG, MT, and BR leaves at Sr were found to be more similar in their metabolome, characterized by higher amounts of dhurrin and alanine, in contrast to GV and SH, where

these two compounds were strongly decreased in spite of increased *p*-GPHA, threonine, and sucrose. Lastly, AU and MG showed an increment in *p*-HBA and chlorogenic acid.

For the stems at Sr, the most varying metabolites were acetic acid, fatty acids, carbohydrates (glucose and sucrose), malic acid, and glycine betaine (Figure S4C).

As observed at Sv, the metabolome of stems and leaves did not follow the same variation trend. Noteworthy, BG leaves were the poorest in terms of sucrose content, whereas its stems were among the richest.

The differences between leaves and stems at Sr were more deeply investigated through the OPLS-DA model (Figure S4D). This analysis clearly showed that the leaves at Sr have a higher content of the main metabolites except for malate and fumarate, which are more concentrated in the stems.

Assessment of Metabolomic Variation during Plant Development

In order to highlight the variations in the metabolome of different organs during sorghum ontogeny, all data previously obtained on leaves at different stages were summarized in another PLS-DA model, where the given classes were the three stages of harvesting. Similarly, an OPLS-DA model was built to compare the stems at Sv and Sr.

The PLS-DA score scatterplot (Figure 5A) highlighted the peculiar variations, which occurred in leaf metabolome during sorghum growth. In particular, dhurrin, *p*-HBA, chlorogenic acid, glucose, alanine, threonine, and aspartate content decreased progressively from the seedling to the ripening stage. On the other hand, *p*-GPHA, glycine betaine, fumaric acid, sucrose, and malic acid followed the opposite trend, reaching the highest concentration in the leaves at Sr. Based on this, the developed model pointed out that BG, MG, and MT leaves at Sr possessed a metabolome closer to the leaves at Sv.

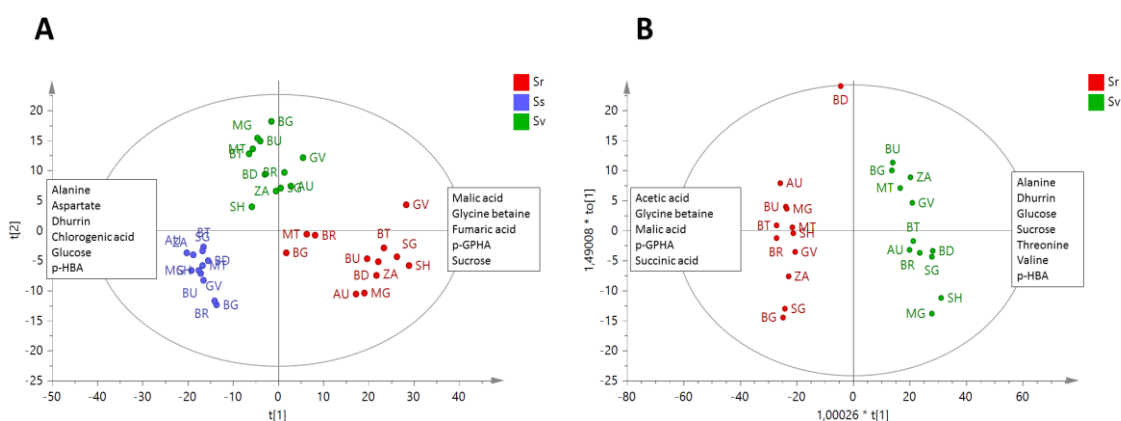


Figure 5. ^1H NMR-based (A) PLS-DA score scatterplot comparing Ss and leaves at Sv and Sr. Leaves of MT, BR, and BG are more closely related between the two stages, in particular for their concentration of dhurrin which increases along the negative side of component $t[1]$. From the permutation test, $R^2 = 0.916$; $Q^2 = 0.893$; p (CV-ANOVA) = 1.26×10^{-23} ; F (CV-ANOVA) = 40.19. (B) OPLS-DA of stems at Sv and Sr; BD presents a peculiar profile because of the high concentration of an unknown aromatic compound. From the permutation test, $R^2 = 0.94$; $Q^2 = 0.898$; p (CV-ANOVA) = 3.75×10^{-9} ; F (CV-ANOVA) = 41.67.

Variable influence on projection (VIP) values of the model were also investigated. Variables having VIP values over 1.0 are generally considered as the most significant in terms of contribution to group separation. Accordingly, in the developed PLS-DA model, metabolites with a VIP cutoff value over 1.0 were: glycine betaine (2.92), sucrose (2.44), dhurrin (2.24), malic acid (2.08), chlorogenic acid (1.91), *p*-GPHA (1.56), *p*-HBA (1.46), and threonine (1.16), as listed in Table S3.

The OPLS-DA model (Figure 5B) built to compare stems at Sv and Sr showed, as in the case of leaves, that dhurrin and *p*-HBA tend to decrease during plant life, with the consequent increase of *p*-GPHA. Moreover, stems at Sv showed the highest content of aliphatic amino acids (alanine, valine, and threonine) and sugars (glucose and sucrose). On the other hand, stems at Sr exhibited an increased amount of organic acids (malate, succinate, and acetate) and glycine betaine.

In this case, metabolites with a VIP cutoff value over 1.0 were: glycine betaine (2.28), glucose (2.07), and sucrose (1.67), as listed in Table S3.

This model also stressed the peculiarity of BD stems at Sr because of the presence of an unknown aromatic compound (spectral signals at δ 7.9, 8.2, and 8.4). Moreover, it showed a low content of succinate, similar to the stems of plants at Sv.

Grain Metabolomics and Antioxidant Properties

Grain collected from the 12 fields were analyzed using a biphasic protocol of extraction, which led to the obtainment of two fractions analyzed separately. As the metabolite content of grain is quite low compared to the content in leaves and stems, this extraction procedure was required in order to concentrate grain metabolites (especially secondary metabolites such as dhurrin), making them detectable and quantifiable by ^1H NMR.

No differences were found among the metabolomes of the lipophilic fractions (data not shown), which appeared to be mainly constituted of fatty acids, whereas the hydrophilic extracts contained the metabolites of interest and were differing among each other.

Dhurrin traces were still found in some samples (ranging from 10 to 76 $\mu\text{g g}^{-1}$ DW). As shown by PCA (Figure 6A), grain of BG was the most enriched in dhurrin, together with *p*-GPHA. Moreover, SG grain showed the highest amount of sucrose, MT the highest amount of malic acid, whereas BR and AU showed the highest amounts of alanine, aspartic acid, and glucose (loading plots of the model are given in Figure S6).

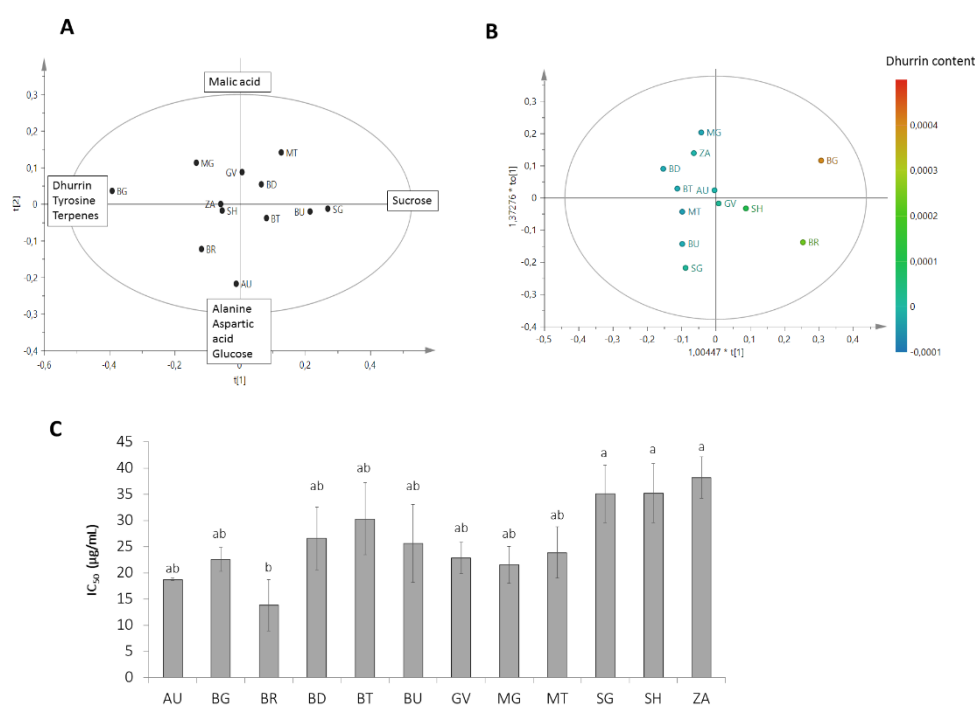


Figure 6. Analysis of sorghum grain. (A) ^1H NMR-based metabolomic PCA score scatterplot showing sucrose increasing along the positive side of component $t[1]$, whereas dhurrin, tyrosine, and terpenes follow an inverted trend, increasing on the negative side of $t[1]$. Malic acid increases along the positive side of component $t[2]$; alanine, aspartic acid, and glucose increase on the negative side of $t[2]$. (B) OPLS based on the intensity of dhurrin diagnostic signal (at δ 5.95) used as y variable. (C) Antioxidant activity based on BCB test and subjected to ANOVA test; different letters indicate significantly different values at $p < 0.05$.

Dietary exposure to elevated levels of some cyanogenic glycosides in the edible parts of crop plants has the potential to cause acute cyanide poisoning, constituting a health risk for humans and domestic animals [16,26]. Owing to the fact that the presence of dhurrin compromises grain quality, in order to highlight the occurrence of this metabolite in the sorghum grain, an OPLS model was built (Figure 6B) using dhurrin concentration as the y variable, which is represented by the intensity of the spectral bin at δ 5.91–5.95, referring to dhurrin diagnostic proton (H-2) in the α position in the nitrile group.

This model allowed us to better visualize that BG, BR, and SH grain still presented traces of dhurrin, whereas the other fields presented no dhurrin at all, resulting in better grain quality.

However, among the better quality samples, there were still some differences, and they could be divided into three groups: one composed by MG and ZA; another by MT, BD, MT, AU, and BT; and the last one by BU and SG. The last group contained high amounts of sucrose but lower contents of all the other metabolites. The group comprising MG and ZA was characterized by more lipids and aliphatic amino acids such as valine. The group composed by all the remaining fields presented high glucose and malic acid, trigonelline, and some aromatic compounds.

β -carotene bleaching (BCB) assay was performed to assess the grain antioxidant properties. All grain, especially BR, were found to actively inhibit the *in vitro* peroxidation of lipids; the statistical analysis highlighted a lower antioxidant potential for SH, SG, and ZA, with no significant differences among them (Figure 6C).

Correlation between Agro-Environmental Parameters and Metabolomic Profiles

Different supervised models (OPLS) were built to establish significant correlations between the variations in sorghum metabolome and the monitored agro-environmental parameters, which were used in turn as *y* variables of the related model, where *x* variables were again the bucketed signals of ^1H NMR spectra.

The *S*-plot, associated to a specific OPLS model, indicated which specific metabolites varied in correlation to the surveyed agro-environmental variable used as *y* (Figures 7 and S6).

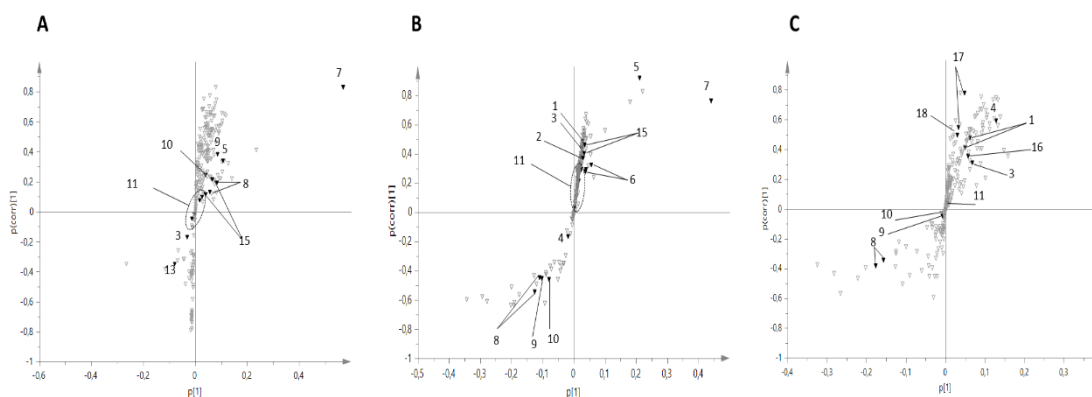


Figure 7. *S*-Plot obtained from different OPLS models using clay as the *y* variable. (A) Effect of clay (Cl) variations on the metabolome of Sr leaves, (B) Sr stems, (C) Sr grain: 1 = valine, 2 = threonine, 3 = alanine, 4 = acetate, 5 = malic acid, 6 = aspartic acid, 7 = glycine betaine, 8 = sucrose, 9 = β -glucose, 10 = α -glucose, 11 = dhurrin, 12 = chlorogenic acid, 13 = fumaric acid, 14 = *p*-HBA, 15 = *p*-GHPA, 16 = lipids, 17 = aromatics, and 18 = trigonelline.

For Ss and Sv leaves, no correlation could be established among variations in the metabolome and the surveyed agro-environmental parameters. Conversely, specific soil features (silt content, H-ini, and OC) were found to be correlated to the variation of Sv stem metabolome. In particular, OC was directly related to the glucose, glycine betaine, aspartate, valine, and threonine content of Sv stems. Sucrose content decreased at raising OC and increased at raising silt content. This latter variable, in turn, showed an inverted relation with acetate and dhurrin. A general increase in the whole metabolome was associated to the highest levels of H-ini, with a remarkable increment of sucrose, glucose, and aliphatic amino acids (aspartate, valine, and threonine).

The only parameter found to be correlated to the stems at Sr was the clay content, whereas for the leaves at Sr, together with clay, water deficit ($ET_C - P$) and TD were also correlated to the metabolomic variations. In the case of Sr stems, malic acid, fumaric acid, glycine betaine, *p*-GPHA, alanine, aspartic acid, and threonine increased together with clay, whereas sucrose and glucose were inversely related to this parameter. For leaves at Sr, increased clay and TD were generally associated with the increase of all metabolites, most prominently sucrose. The highest variation of dhurrin and alanine in Sr leaves was associated to $ET_C - P$ with an inverted trend to glucose, malic acid, and *p*-GPHA.

With regard grain, the models were built after excluding BG, which was clearly too different from the other samples, probably because of delayed ripening. The grain metabolome resulted to be influenced by $ET_C - P$, WTD, and clay, whereas no correlation was established with the panicle weight and grain yield.

$ET_C - P$ resulted to be negatively correlated with alanine, glucose, valine, and acetate, whereas it scarcely affected sucrose. WTD was positively correlated with sucrose and aromatics (δ 6.59–6.67), possibly flavonoids, and negatively correlated with glucose, alanine, and valine. Clay content was negatively correlated with sucrose and malic acid, whereas it positively correlated with aromatics, alanine, valine, and acetate.

The analyzed parameters were not strictly related to dhurrin content, even though this compound resulted to be little increased under increasing $ET_C - P$.

Discussion

The metabolomic analysis allowed us to identify the most prominent metabolites in diverse sorghum organs, their variation during plant growth, and the diversification of plant metabolome under different crop conditions.

Dhurrin is one of the most peculiar secondary metabolites produced by sorghum, and the results of this work provide new insights into its biological role, the variations of its content during plant development, as well as some aspects of its turnover pathway (Figure 8).

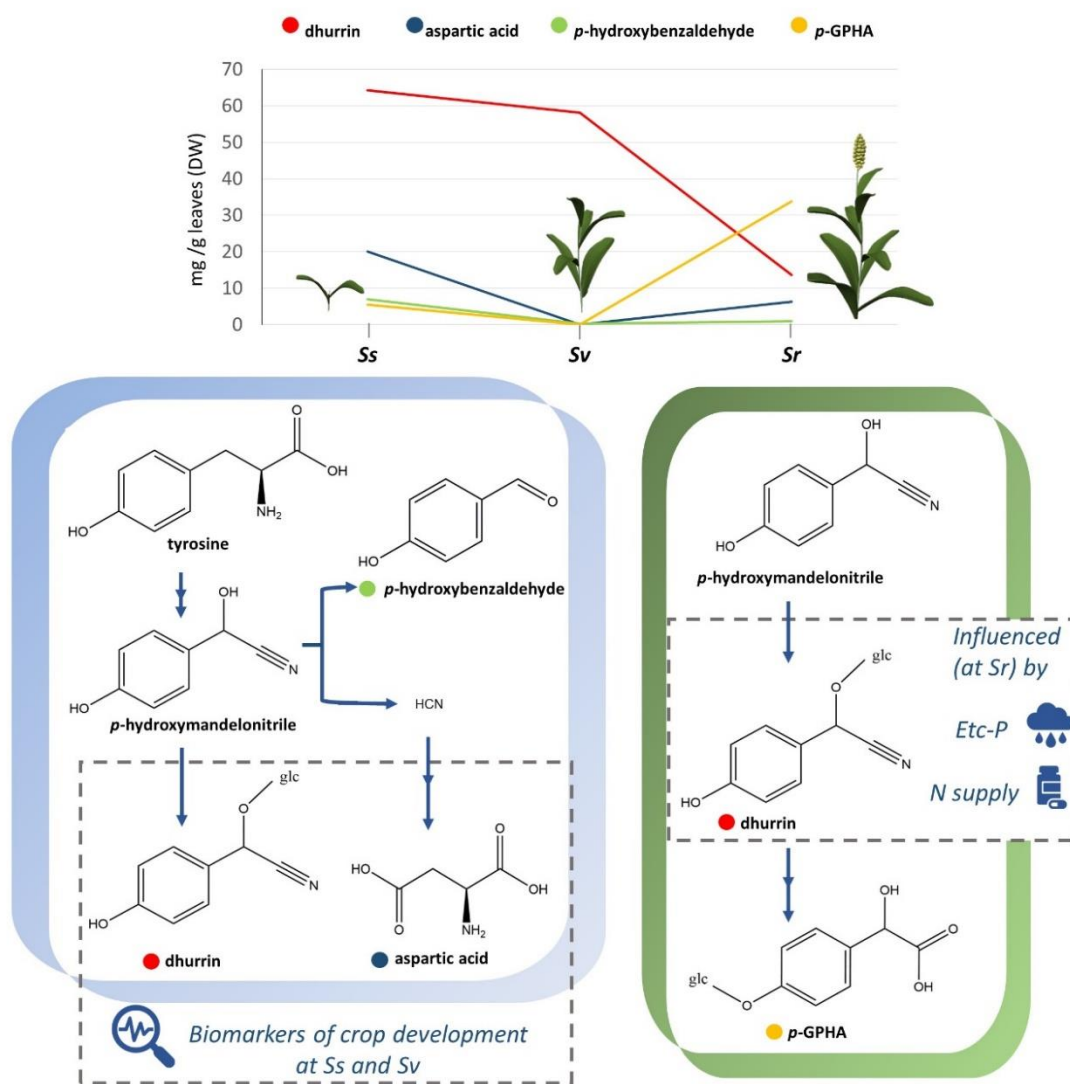


Figure 8. Schematic representation of dhurrin and related metabolite pathways and variations (in leaves) during plant development. The variation trend reflects in different catabolic pathways underwent by dhurrin. On this basis, the levels of dhurrin and aspartic acid in Ss and Sv are the biomarkers of crop development. At Sr, dhurrin content resulted to be affected by overfertilization and water depletion.

Dhurrin is a cyanogenic glycoside, a class of metabolites that, upon tissue disruption, are hydrolyzed by endogenous β -glucosidases into cyanohydrin aglycone, which in turn releases the toxic hydrogen cyanide (HCN) [27].

In this work, dhurrin was found to be particularly abundant at Ss. This is consistent with its defensive role as a deterrent against insects and generalist herbivores [28,29], a function particularly important during the early stage of plant life. On the other hand, dhurrin, as other cyanogenic glycosides, may serve additional functions, such as resistance against abiotic stresses and nitrogen storage/buffer [30,31]. The latter role might be important, especially during ripening processes; in fact, assimilation of nitrogen from the soil in cereals is often insufficient to supply the developing grain; thus, a complementary nutrient is made available through dhurrin remobilization from the leaf tissue [30].

Moreover, according to the analysis performed on plants at Ss, it is observed that when aspartic acid increases, dhurrin decreases. These data support the dhurrin turnover pathway proposed by previous studies [32,33], according to which dhurrin is hydrolyzed to form the intermediate *p*-hydroxymandelonitrile (*p*-HMN), which is then converted into *p*-HBA and HCN. As a mechanism of detoxification, the released HCN is incorporated into β -cyanoalanine, to be finally converted into asparagine and aspartic acid, with a concomitant release of ammonia. Thus, according to the results of our study, when the dhurrin concentration decreases, aspartate production increases. Nevertheless, this trend was observed at Ss, whereas at Sr, a lowered dhurrin content in all organs (leaves, stems, and grain) was associated to the accumulation of *p*-GPHA, instead of aspartic acid. This latter amino acid was not even found in Sr leaves, stems, and grain. Moreover, in this stage, *p*-HBA was also no more detected.

To the best of our knowledge, this is the first report of *p*-GPHA occurrence in sorghum and of its accumulation as the main metabolite after dhurrin catabolism. In contrast to Ss, when dhurrin was converted into aspartate and HCN was neutralized in NH_3 , at Sr, dhurrin underwent a different turnover pathway, probably avoiding the release of HCN. Nielsen *et al.* [30] proposed two putative dhurrin turnover pathways in sorghum grain, one culminating in the production of dhurrin acid and the other in *p*-glycosyloxyphenylacetic acid (*p*-GPA). According to our results, none of them is the most prominent

final metabolite of dhurrin pathways in sorghum at Sr, whereas the metabolomic analysis suggested *p*-GPHA as the main metabolite resulting from dhurrin turnover. Considering the structure similarity of *p*-GPHA, dhurrin acid, and *p*-GPA, the latter two could be the intermediates from which *p*-GPHA is finally obtained.

Besides the aspects related to dhurrin catabolism, the overall metabolomic picture obtained from the seedling analysis suggested three different trends among the 12 sorghum fields. Four out of them showed the lowest content of dhurrin and *p*-HBA (with the resulting glutamate increase). These crop fields were possibly turning into a different development stage, characterized by a decrease of sucrose and glucose, which were likely used as carbon sources for the growth. An opposite trend was observed for two crop fields (BG and BR), which were characterized by the highest concentration of dhurrin. Interestingly, this peculiar metabolomic profile showed at Ss by BG and BR was associated to a delayed trend of development, which became evident at the final stage of the survey (Sr).

However, BG seedlings showed a very peculiar profile, diverging from BR. In fact, BG was also characterized by an extremely high concentration of *p*-HBA and chlorogenic acid. These metabolomic features could not only be related to delayed plant development but also to a reaction against predators. In fact, if *p*-HMN is converted into *p*-HBA, instead of dhurrin, HCN is consequently released as an eventual defensive strategy [34]. The increment of chlorogenic acid is an additional evidence of a predator response, as this compound is already known to be involved in plant defense [35].

The other six fields at Ss were characterized by sucrose accumulation, which might indicate a more quiescent metabolic activity, characterized by sucrose storage. During Sv, when dhurrin and *p*-HBA decreased, an increment of sucrose was once more registered. In this stage, BG and GV leaves were differing from the others for their increased sugar content and decrease of all other metabolites. Specifically, in GV, both glucose and sucrose increased, whereas in BG, only sucrose was highly concentrated. The highest content of dhurrin was found in SH leaves, whereas ZA leaves revealed a peculiar profile, with a high concentration of chlorogenic acid. In this stage, aphids were visible on ZA leaves, corroborating chlorogenic acid as defense against predator attack.

The progressive decrease of dhurrin during plant development was clearly evidenced by the PLS-DA model, comparing leaves at Ss, Sv, and Sr (Figure 5A). This

model showed how three crops at Sr (MT, BR, and BG) still presented high amounts of dhurrin in their leaves and, generally, metabolomic features similar to the leaves at Sv. Among these three fields, BR and BG also showed a significant concentration of dhurrin in their grain, which is an established biomarker of low ripeness degree in sorghum [30]. Conversely, in the case of MT, dhurrin was not found in the grain. These data remind that dhurrin is not only a biomarker of low ripeness degree but is also involved in other plant physiological processes and stress responses. In particular, the cyanogenic potential of sorghum is reported to greatly increase under abiotic stresses (drought, salinity, freezing, insufficient light, and nutrient deficiency) and herbivore and insect attack [36]. In the case of MT, sorghum was probably subjected to overfertilization, as the very high nitrogen supply demonstrates (Table 2). In fact, it was proved that dhurrin biosynthetic enzymes are induced by nitrate availability [14].

A high content of dhurrin is toxic to animals [37,38] because of the release of HCN. Considering the fact that, together with grain, leaves and stems of sorghum are also generally used as forage, it is important to monitor and keep the level of this metabolite low in these organs also. This can be facilitated by the detection of environmental factors and practices correlated to the increase of this metabolite in sorghum.

In this work, metabolomic analysis was coupled with the assessment of crop and environmental parameters. This integrated approach allowed us to identify the most significant features related to sorghum metabolomic variations (Figure 9).

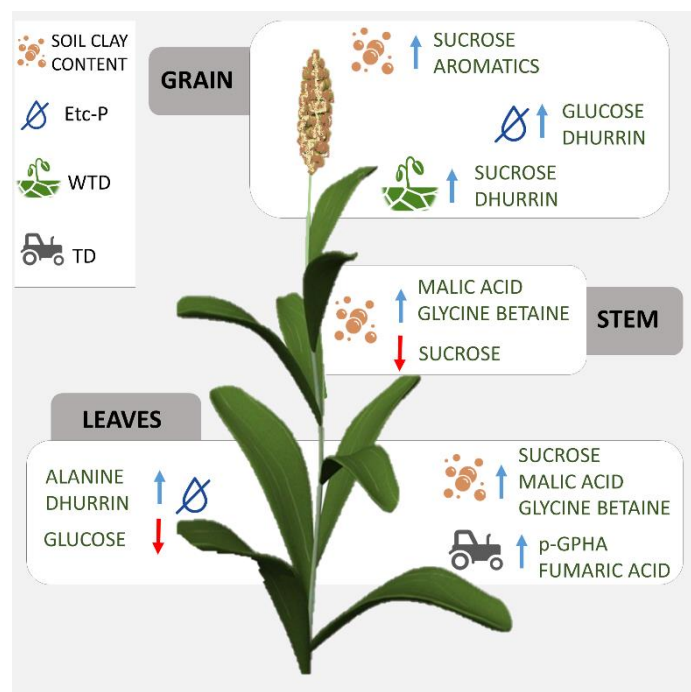


Figure 9. Schematic representation of the main agro-meteorological variables affecting the metabolite composition in sorghum at Sr. TD = tillage depth; WTD = depth of the shallow water table in July; $ET_C - P$ = difference between crop evapotranspiration and precipitation. WTD and $ET_C - P$ are related to water deficit.

Several soil features were proved to be important for the diversification of sorghum metabolome at different plant stages (Figure S6). In particular, clay content was correlated to the metabolite variations in all plant organs at Sr, as shown by the *S*-plots of the developed OPLS models reported in Figure 7. Specifically, highest clay was correlated with an increase of sucrose in Sr leaves and a decrease of the same metabolite in Sr stems and grain. Clay content was also positively correlated to malic acid and glycine betaine (a marker of drought resistance in plants) in both the stems and leaves at Sr and to the increasing aromatic compounds in grain, whereas it did not affect the dhurrin content in any plant organ.

Another influencing parameter for Sr leaves was TD; indeed, it directly correlated to the increasing concentration of *p*-GPHA and fumaric acid, in addition to a slight increase in dhurrin concentration.

Difference in $ET_C - P$ had an impact on the metabolomes of both leaves (at Sv and Sr) and grain, whereas WTD affected the grain selectively.

In leaves at Sr, increasing $ET_C - P$ (which reflects the water deficit) was highly related to increasing dhurrin content, together with alanine. This effect is consistent with

the findings of Wheeler *et al.* [39], who reported that a prolonged exposure to chronic water deficit induces higher cyanide potentials in sorghum plants. Our results also support the findings of Burke *et al.* [40], who demonstrated that the leaf dhurrin content is a quantitative measure of the level of pre- and post-flowering drought tolerance in sorghum.

The overall water deficit (increasing $ET_C - P$ and decreasing WTD) also determined a slight increase of dhurrin in grain.

Carbohydrate levels have also been associated with water supply variation in sorghum varieties [41]. According to our results, the sucrose level in grain was increased by higher WTD, whereas an opposite trend was shown for glucose. $ET_C - P$ increase was correlated to a lower glucose accumulation in leaves at Sr, and it was associated to a higher glucose content in grain (Figure S6).

Regarding grain yield, the strong variation in sorghum behavior and final yield is not surprising even in a relatively small region under a similar course of weather in a specific year. Although sorghum has lower water requirement than maize [42], it is affected by long dry periods, as those experienced in the 12 fields in 2017. Together with the impact on the metabolome, this factor leads to a reduced yield, overall, and stronger variation among the cultivation sites; the almost 1:4 yield ratio between the worst and best cases (Table 1) supports this point. However, grain yield, which is the ultimate goal for the farmer, was neither significantly correlated with the two parameters ($ET_C - P$ and ET_C/P) (Table 2), expressing water deficit in the whole crop cycle, nor with any of the four stages (initial, development, mid, and late) in which the crop cycle is subdivided for computing ET_C [19] (data not shown). This means that other factors must have played a major role, as the occurrence of a shallow water table contributing to sorghum water supply. Interactions with $ET_C - P$ and ET_C/P are, nevertheless, not excluded.

Although commercial sorghum grain is allowed to contain a low quantity of dhurrin, a better quality grain, especially for human consumption, is out of doubt dhurrin-free.

Our study highlighted that three sorghum fields (BG, BR, and SH) yielded grain still containing traces of dhurrin; among them, SH also showed the lowest antioxidant activity. Dhurrin content in sorghum grain generally decreases with ripening. Notably, in the case of BR and BG, the delay in ripening was prospected at Ss by their metabolomic profiles having a high content of dhurrin. Farmers commonly harvest sorghum under the

influence of the weather or other crop management urgencies. This practice may lead to premature harvesting, which, according to our results, determines lower quality grain as in the case of BR and BG.

To conclude, metabolomics combined with the surveyed agronomic parameters through multivariate data analysis turned out to be a valid tool to develop smart agriculture practices, enabling predictions on sorghum development trend since the seedling stage. This could provide information on the most appropriate agricultural practices since the early stage of crop management, in order to obtain better grain quality, together with residual plant organs (leaves and stems) better suited for feeding livestock. The models obtained represent a useful starting point for implementing further studies on sorghum, which are ongoing.

Supporting Information:

The Supporting Information is available free of charge at <https://pubs.acs.org/doi/10.1021/acs.jafc.0c06533>.

Abbreviations: BCB, β -carotene bleaching assay; DW, dry weight; ET₀, reference evapotranspiration; ETC, crop evapotranspiration; ETC–P, difference between crop evapotranspiration and precipitations; H-ini, soil humidity at the beginning of the sorghum growth season; H-mid, soil humidity at the middle of the sorghum growth season; H-late, soil humidity at the end of the sorghum growth season; OC, organic carbon content at 0–30 cm depth; p-GPA, p-glycosyloxyphenyl-acetic acid; p-GPHA, p-glucosyloxy-2-hydroxyphenylacetic acid; p-HMN, phydroxymandelonitrile; p-HBA, p-hydroxybenzaldehyde; Sr, ripening stage; Ss, seedling stage; Sv, advanced vegetative stage; TD, tillage depth; WTD, depth of the shallow water table in July.

References

1. Herrero, M.; Thornton, P. K.; Notenbaert, A. M.; Wood, S.; Msangi, S.; Freeman, H. A.; Bossio, D.; Dixon, J.; Peters, M.; van de Steeg, J.; Lynam, J.; Rao, P. P.; Macmillan, S.; Gerard, B.; McDermott, J.; Seré, C.; Rosegrant, M.; Lynam, J. Smart investments in sustainable food production: revisiting mixed crop-livestock systems. *Science* **2010**, *327*, 822–825.
2. Beddington, J. Food security: contributions from science to a new and greener revolution. *Philos. Trans. R. Soc., B* **2010**, *365*, 61–71.
3. Kamilaris, A.; Kartakoullis, A.; Prenafeta-Boldú, F. X. A review on the practice of big data analysis in agriculture. *Comput. Electron. Agr.* **2017**, *143*, 23–37.
4. Prashant, G.; Rao, E. V. S. P. Smart and sustainable agriculture through weather and climate informatics and multi-scale modelling. *CAB Rev.* **2015**, *10*, 1–13.
5. Wolfender, J.-L.; Marti, G.; Thomas, A.; Bertrand, S. Current approaches and challenges for the metabolite profiling of complex natural extracts. *J. Chromatogr. A* **2015**, *1382*, 136–164.
6. Ali, K.; Iqbal, M.; Yuliana, N. D.; Lee, Y.-J.; Park, S.; Han, S.; Lee, J.-W.; Lee, H.-S.; Verpoorte, R.; Choi, Y. H. Identification of bioactive metabolites against adenosine A1 receptor using NMR based metabolomics. *Metabolomics* **2013**, *9*, 778–785.
7. Mandrone, M.; Coqueiro, A.; Poli, F.; Antognoni, F.; Choi, Y. Identification of a collagenase-inhibiting flavonoid from *Alchemilla vulgaris* using NMR-based metabolomics. *Planta Med.* **2018**, *84*, 941–946.
8. Salomé-Abarca, L. F.; Mandrone, M.; Sanna, C.; Poli, F.; van der Hondel, C. A. M. J. J.; Klinkhamer, P. G. L.; Choi, Y. H. Metabolic variation in *Cistus monspeliensis* L. ecotypes correlated to their plant-fungal interactions. *Phytochemistry* **2020**, *176*, 112402.
9. Sherman, E.; Coe, M.; Grose, C.; Martin, D.; Greenwood, D. R. Metabolomics approach to assessing the relative contributions of the volatile and non-volatile composition to expert quality ratings of pinot noir wine quality. *J. Agric. Food Chem.* **2020**, *68*, 13380–13396.
10. Callao, M. P.; Ruisánchez, I. An overview of multivariate qualitative methods for food fraud detection. *Food Control* **2018**, *86*, 283–293.
11. Dahlberg, J.; Berenji, J.; Sikora, V.; Latkovic, D. Assessing sorghum [*Sorghum bicolor* (L.) Moench] germplasm for new traits: food, fuels & unique uses. *Maydica* **2011**, *56*, 85–92.
12. Pontieri, P.; De Vita, P.; Boffa, A.; Tuinstra, M. R.; Bean, S. R.; Krishnamoorthy, G.; Miller, C.; Roemer, E.; Alifano, P.; Pignone, D.; Massardo, D. R.; Giudice, L. D. Yield and morpho-agronomical evaluation of food-grade white sorghum hybrids grown in Southern Italy. *J. Plant Interact.* **2012**, *7*, 341–347.
13. Tuinstra, M. R. Food-grade sorghum varieties and production considerations: A review. *J. Plant Interact.* **2008**, *3*, 69–72.
14. Busk, P. K.; Møller, B. L. Dhurrin synthesis in sorghum is regulated at the transcriptional level and induced by nitrogen fertilization in older plants. *Plant Physiol.* **2002**, *129*, 1222–1231.
15. Rete del Sistema Informativo Nazionale Ambientale. Territorial data. <http://www.sinanet.isprambiente.it/it/sia-ispra/downloadmais/dem20/view> (accessed February 10, 2020).
16. Istituto Nazionale di Statistica. Territorial data of Emilia-Romagna region (year 2016, more detailed version). <https://www.istat.it/it/archivio/222527> (accessed February 10, 2020).
17. Arpae Emilia-Romagna. Meteorological data from regional meteorological stations. <https://www.arpae.it/index.asp?idlivello=1504> (accessed October 23, 2018).
18. Regione Emilia-Romagna website. Regional maps reporting soil features. https://geo.regione.emilia-romagna.it/cartpedo/carte_tematiche.jsp?tem=1#tem1 (accessed October 23, 2018).
19. Allen, R. G.; Pereira, L. S.; Raes, D.; Smith, M. Crop evapotranspiration. In Guidelines for Computing Crop Water Requirements; Irrigation and Drainage Paper 56; FAO: Rome, **1998**.
20. Hargreaves, G. H.; Samani, Z. A. Reference crop evapotranspiration from temperature. *Appl. Eng. Agric.* **1985**, *1*, 96–99.
21. Verpoorte, R.; Choi, Y. H.; Kim, H. K. NMR-based metabolomics at work in phytochemistry. *Phytochem. Rev.* **2007**, *6*, 3–14.
22. Mandrone, M.; Antognoni, F.; Aloisi, I.; Potente, G.; Poli, F.; Cai, G.; Faleri, C.; Parrotta, L.; Del Duca, S. Compatible and incompatible pollen-styles interaction in *Pyrus communis* L. show different transglutaminase features, polyamine pattern and metabolomics profiles. *Front. Plant Sci.* **2019**, *10*, 741.

23. Mandrone, M.; Scognamiglio, M.; Fiorentino, A.; Sanna, C.; Cornioli, L.; Antognoni, F.; Bonvicini, F.; Poli, F. Phytochemical profile and α -glucosidase inhibitory activity of Sardinian *Hypericum scruglii* and *Hypericum hircinum*. *Fitoterapia* **2017**, *120*, 184–193.
24. Malzert-Fréon, A.; Hennequin, D.; Rault, S. Partial least squares analysis and mixture design for the study of the influence of composition variables on lipidic nanoparticle characteristics. *J. Pharm. Sci.* **2010**, *99*, 4603–4615.
25. Bagnouls, F.; Gaussen, H. Saison sèche et indice xérothermique. *Bull. Soc. Hist. Nat. Toulouse* **1953**, *88*, 193–239.
26. Cornara, L.; Xiao, J.; Burlando, B. Therapeutic potential of temperate forage legumes: A review. *Crit. Rev. Food Sci. Nutr.* **2016**, *56*, S149–S161.
27. Leavesley, H. B.; Li, L.; Prabhakaran, K.; Borowitz, J. L.; Isom, G. E. Interaction of cyanide and nitric oxide with cytochrome c oxidase: implications for acute cyanide toxicity. *Toxicol. Sci.* **2008**, *101*, 101–111.
28. Tattersall, D. B.; Bak, S.; Jones, P. R.; Olsen, C. E.; Nielsen, J. K.; Hansen, M. L.; Høj, P. B.; Møller, B. L.; et al. Resistance to an herbivore through engineered cyanogenic glucoside synthesis. *Science* **2001**, *293*, 1826–1828.
29. Zagrobelny, M.; Bak, S.; Rasmussen, A. V.; Jørgensen, B.; Naumann, C. M.; Lindberg Møller, B. Cyanogenic glucosides and plant-insect interactions. *Phytochemistry* **2004**, *65*, 293–306.
30. Nielsen, L. J.; Stuart, P.; Pičmanová, M.; Rasmussen, S.; Olsen, C. E.; Harholt, J.; Møller, B. L.; Bjarnholt, N. Dhurrin metabolism in the developing grain of *Sorghum bicolor* (L.) Moench investigated by metabolite profiling and novel clustering analyses of time-resolved transcriptomic data. *BMC Genomics* **2016**, *17*, 1021.
31. Møller, B. L. Functional diversifications of cyanogenic glucosides. *Curr. Opin. Plant Biol.* **2010**, *13*, 337–346.
32. Castric, P. A.; Farnden, K. J. F.; Conn, E. E. Cyanide metabolism in higher plants: V. The formation of asparagine from β -cyanoalanine. *Arch. Biochem. Biophys.* **1972**, *152*, 62–69.
33. Piotrowski, M.; Schönfelder, S.; Weiler, E. W. The *Arabidopsis thaliana* isogene NIT4 and its orthologs in tobacco encode β -cyano-L-alanine hydratase/nitrilase. *J. Biol. Chem.* **2001**, *276*, 2616–2621.
34. Laursen, T.; Borch, J.; Knudsen, C.; Bavishi, K.; Torta, F.; Martens, H. J.; Silvestro, D.; Hatzakis, N. S.; Wenk, M. R.; Dafforn, T. R.; Olsen, C. E.; Motawia, M. S.; Hamberger, B.; Møller, B. L.; Bassard, J.-E. Characterization of a dynamic metabolon producing the defense compound dhurrin in sorghum. *Science* **2016**, *354*, 890–893.
35. Kundu, A.; Vadassery, J. Chlorogenic acid-mediated chemical defence of plants against insect herbivores. *Plant Biol.* **2019**, *21*, 185–189.
36. Sun, Z.; Zhang, K.; Wu, Y.; Georgiev, M. I.; Zhang, X.; Lin, M.; Zhou, M. Biosynthesis and regulation of cyanogenic glycoside production in forage plants. *Appl. Microbiol. Biotechnol.* **2018**, *102*, 9–16.
37. Haskins, F. A.; Gorz, H. J.; Johnson, B. E. Seasonal variation in leaf hydrocyanic acid potential of low and high dhurrin sorghum. *Crop Sci.* **1987**, *27*, 903–906.
38. Pandey, A. K.; Pusuluri, M.; Bhat, B. V. Down-regulation of CYP79A1 gene through antisense approach reduced the cyanogenic glycoside dhurrin in [*Sorghum bicolor* (L.) Moench.] to improve fodder quality. *Front. Nutr.* **2019**, *6*, 122.
39. Wheeler, J.; Mulcahy, C.; Walcott, J.; Rapp, G. Factors affecting the hydrogen cyanide potential of forage sorghum. *Aust. J. Agric. Res.* **1990**, *41*, 1093–1100.
40. Burke, J. J.; Chen, J.; Burow, G.; Mechref, Y.; Rosenow, D.; Payton, P.; Xin, Z.; Hayes, C. M. Leaf dhurrin content is a quantitative measure of the level of pre- and postflowering drought tolerance in sorghum. *Crop Sci.* **2013**, *53*, 1056–1065.
41. Ogbaga, C. C.; Stepien, P.; Dyson, B. C.; Rattray, N. J. W.; Ellis, D. I.; Goodacre, R.; Johnson, G. N. Biochemical analyses of sorghum varieties reveal differential responses to drought. *PLoS One* **2016**, *11*, No. e0154423.
42. Brauer, D.; Baumhardt, R. L. Future prospects for sorghum as a water-saving crop. In *Sorghum: State of the Art and Future Perspectives*; Ciampitti, I., Prasad, V., Eds.; *Agronomy Monographs* 58; ASA and CSSA: Madison, WI, **2016**.

2.2. Effects of LED supplemental lighting on the growth and metabolomic profile of *Taxus baccata* cultivated in a smart greenhouse

Ilaria Chiocchio, Alberto Barbaresi*, Lorenzo Barbanti, Manuela Mandrone, Ferruccio Poli, Daniele Torreggiani, Mattia Trenta, Patrizia Tassinari

This article has been submitted to an academic journal.

Abstract

Light emitting diode (LED) lamps are increasingly being studied in cultivation of horticultural, ornamental and medicinal plants as means to increase yield, quality, stress resistance, and bioactive compounds content. Enhancing the production of metabolites for medicinal or pharmaceutical use by regulating LED intensity and spectra is a challenging subject, where promising results have been achieved. Nevertheless, some species have been poorly investigated, despite their interest as a source of medicinally active substances, with particular reference to LED effects at the plant cultivation level. This study evaluates the effects of supplementary top-light LED treatments on *Taxus baccata*, one of the main sources of taxane precursors. Blue, red and mixed red-and-blue spectra were tested at $100 \mu\text{M m}^{-2} \text{s}^{-1}$. Moreover, 50 and $150 \mu\text{M m}^{-2} \text{s}^{-1}$ intensities were tested for the mixed spectrum. All treatments were set for 14 hours a day and were tested against natural light, in a controlled environment, from 19 August to 9 December 2019. A smart monitoring and control system powered by environmental and proximal sensors was implemented to assure homogeneity of environmental conditions, including base natural light for all the treatments. It resulted in negligible deviations from expected values and reliable exclusion of confusing factors. Biometric measurements and $^1\text{H-NMR}$ based metabolomic analysis were performed to investigate growth and phytochemical profile throughout the trial. One-way ANOVA showed that supplemental LED lighting increased plant height and number of sprouts, with a growing trend up to $100 \mu\text{M m}^{-2} \text{s}^{-1}$. Plant vigor also increased, after the early growth stages. LED lights including blue appeared to perform the best. According to the metabolomic analysis, treated plants at 28 DAT were characterized by the highest content of sucrose and aromatic compounds. Signals of a putative taxane were detected in the $^1\text{H NMR}$ profiles of plants, which were compared to the spectrum of baccatin III standard. However, the intensity of these spectral signals was not affected by the treatment, while they increased only slightly during time. Light at $150 \mu\text{M m}^{-2} \text{s}^{-1}$ induced the strongest variation in the metabolome. Conversely, light composition did not induce significant differences in the metabolome.

Introduction

LEDs for indoor cultivation mainly emit useful radiation, namely radiation able to enhance productivity by acting on the morphological and metabolic responses of plants. Since the maximum absorption of light by photoreceptors occurs in two wavelength ranges of the electromagnetic spectrum (650-665 nm and 450-470 nm, corresponding to the red and blue regions of the visible spectrum), the useful radiation for plants coincides with the wavelength range between 400 and 700 nm (PAR, photosynthetically active radiation). Photoreceptors sensitive to blue light (cryptochromes) and red light (phytochromes) stimulate transduction signals that act on plant morphology and physiology via different mechanisms of action [1,2]. Red light appears to be related to a stimulus to flowering in long-day species [3], and internode elongation [4], while blue light appears to be related to plant phototropism [5] and stomata opening [6].

Given these premises, and due to their physical characteristics (narrow spectral bands, non-thermal photon emission, longer life, energy saving), LED lamps with a combined red and blue spectrum are currently the most widely used light source to optimize growth and metabolism of plants in a controlled environment [7–9]. The physical properties of LEDs make them suitable for use both in intra-canopy (aka, inter-lighting) and top-lighting systems [10], and both in horticulture and ornamental plants production, allowing reductions in energy consumption while maintaining optimal photon flux values of the incident radiation; for this reason, they are a valid source of light energy in greenhouse environments, especially during the winter season, exerting positive effects on crop quality, disease resistance, and bioactive compounds content [7]. Supplemental LED inter-lighting, relevant in particular for high-wire vegetable cultivations, has proven to increase yield and improve fruit quality in various all-year round greenhouse crops [11]. Supplemental top-lighting has proved to be beneficial in improving plant growth, morphology and quality of ornamental greenhouse-grown plants, with different results depending on spectral composition [12].

The applications of LED lighting to the cultivation of plants for both horticultural and medicinal use are numerous, and their effectiveness is widely demonstrated. Exposure to spectra of variable composition (blue, red and white light) showed effects on the organoleptic characteristics (color, aroma and flavor) in pepper cultivars (*Capsicum*

annuum L.) [13] and on yield and characteristics (such as crispness, sweetness, shape, color, and accumulation of chlorophylls, carotenoids, soluble proteins and sugars, and nitrates) in different species of leaf crops (*Lactuca sativa* L., *Spinacia oleracea* L., also in hydroponic cultivation), and aromatic and medicinal plants (*Mentha arvensis* L., *Glycyrrhiza uralensis* Fisch. ex DC.) (14,15). Blue light, in particular, showed effects on production of metabolites with nutritional properties (carotenoids and other pigments, glycosinolates, minerals) [16]. Exposure to appropriate LED spectra can also trigger the synthesis of antioxidants and bioactive compounds which in turn contribute to the improvement of the nutritional properties of the species used in horticulture; it can directly increase nutrient content, reduce microbial contamination, induce systemic resistance to fungal pathogens, affect the post-harvest ripening times of fruit and vegetables [9].

Besides the huge research effort focused on the use of LEDs to promote indoor/hydroponic cultivation of edible and ornamental plants, an increasing attention has been paid to the study of the use of LEDs in medicinal and aromatic plants. It is acknowledged that medicinal and aromatic plants are influenced by micro-climatic conditions, namely light. This includes not only plant growth and development, but also secondary metabolite production [17]. However, the way and degree in which light intensity, duration and spectral composition influence plant behavior and the yield of secondary metabolites vary from species to species, and no univocal trend may be outlined. LED technology has been used to stimulate plant growth and production of metabolites for medicinal or pharmaceutical use in numerous species; monochromatic light or spectral combinations of two or more wavelengths were used, either administered in place of natural light or as additional lighting, both on crops in a controlled environment and on tissue cultures.

Fukuyama et al. [18–20] have shown that there are optimal frequencies and intensities of LED light (both red monochromatic and combined red-blue-UVA) capable of stimulating, increasing and optimizing the production of the monoterpenoid alkaloids vindoline and catharanthin, precursors of anticancer vinblastine and vincristine, in plants and leaf tissue of *Catharanthus roseus* (L.) G. Don. In the same species, Molchan et al. [21] determined the optimal PPF values for increase in dry weight and for alkaloid synthesis.

Supplemental night lighting with blue LEDs (440-540 nm, peak at 469 nm) showed positive effects both on main growth parameters and production of secondary metabolites of pharmacological interest (mainly flavonoids and polyphenols with antitumor activity) in plants of *Anoectochilus roxburghii* (Wall.) Lindl. grown in greenhouses [22].

In cultures of root apices of *Artemisia annua* L. exposed to red light (660 nm) higher biomass values and a higher artemisinin content were measured compared to crops exposed to white light [23]. In cell cultures of *Artemisia absinthium* L., both a higher frequency of growth and higher total phenol and flavonoid values were observed under white light compared to other spectra [24].

There are studies on the effects of treatment with LED spectra on conifers, focusing on growth parameters, on the physiology of gas exchange and on the induction of gene expression in seedlings of species of forest interest (*Picea abies* (L.) H. Karst. and *Pinus sylvestris* L.) [25,26]. Despite the great interest in the *Taxus* genus as a source of substances with antitumor activity, studies on the effects of LEDs for medicinal purposes in *Taxus* spp. are still in the initial phase.

Su et al. [27] report a study with light spectra obtained through colored filters on *Taxus yunnanensis* WCC Cheng & LKFu (synonymous with *Taxus wallichiana* Zucc. var. *wallichiana*): the blue and red filters in different combinations confirmed positive effects on growth, physiology and synthesis of metabolites of pharmacological interest, but experiments using LEDs have largely been performed on tissue cultures.

In the latest years, the agri-food sector has been showing an increasing interest in smart monitoring and modelling systems powered by ICT (Information and Communications Technology) and IoT (Internet of Things), since their application has set the premise for an efficient, sustainable and traceable management of agricultural systems, with positive impact on the market also due to the risen awareness of the consumers. Applications concerning the monitoring of field and indoor environmental conditions (for plant growing, livestock raising and food processing structures) represent a crucial part of those systems [28,29]. Moreover, spectral vegetation indices based on remote and proximal sensing have been widely used to estimate and analyze the vigor and phenology of plants, their reaction to stress conditions, degree in vegetation greenness, variation of canopy chlorophyll content [30,31]. Among them, the normalized difference vegetation index (NDVI) [32] is the vegetation index most widely used and

one of the most reliable [33,34]. Recently, specific developments proposed solutions to check and monitor several metrics from crops and animal conditions to the food quality. Moreover, the possibility to send, receive and store data in real time and the potentialities of big data analysis, allowed the precision and efficacy of the monitoring to be enhanced [35–38]. These systems also determine a dramatic improvement in the accuracy of plant cultivation experiments in controlled environments (such as greenhouses), based on the analysis of the spatial and temporal variability/homogeneity of environmental conditions affecting crop development, growth, quantitative and qualitative characteristics. These systems provide control of the designed conditions, record of the variable trends, identification and prevention of undesired conditions that could endanger or bias the trial. Moreover, monitored data could be helpful to define additional findings in research [39]. In particular, in studies aimed to assess the effect of one variable only, the homogeneity of other variables across all the treatments is a fundamental requirement.

European yew, *Taxus baccata* L., is considered one of the main sources of taxane precursors currently usable in the pharmacological field.

Based on the poor knowledge available about the effects of targeted lighting on this species grown in single plant pots, and the new opportunities opened by smart monitoring systems in the agricultural sector, this study aims at evaluating the effects of supplementary LED light treatments on *Taxus baccata* plants, both in terms of growth and metabolomic profile of the plants. Plants were grown in pots in a smart greenhouse, in order to maintain proper environmental conditions and ensure homogeneity among all the treatments, and ¹H NMR based metabolomic analysis was performed to investigate *T. baccata* metabolome and its response under different LED light treatments.

Besides the goal of contributing to the advancement of knowledge for this plant species under specific light spectra, this experiment paves the way for further studies, not only in order to improve the cultivation of this plant and the production of metabolites, but also to deepen the study of biosynthetic pathways.

Materials and Methods

Setting of environmental conditions and environmental monitoring system design

Due to the research aims, the trial was performed in a greenhouse in order to maintain proper environmental conditions as well as ensure their homogeneity among the treatments.

The trial took place in the experimental greenhouses of the Imola District of the University of Bologna (40 km South-East of Bologna) between the 19th of August 2020 and the 9th of December 2020. The greenhouse (see Figure 1) is divided into three spans and the trial was performed in the central one that covers an area of 8 m x 8 m; the height of the ceiling is between 4 and 5.5 m (measured respectively at eave and ridge). The facility is NE oriented (main axis azimuth 55°). Each span is provided with heating and cooling systems able to keep the temperature within the set range. Moreover, automatic openings help the temperature control and the air circulation. Finally, the greenhouse is provided with moveable shading screens useful to reduce the solar gain, to keep the indoor temperature and homogenize the indoor illumination. For the purposes of this experiment, according to Ellenberg [40], the heating and cooling systems were set to keep the temperature within 15°C and 25°C and the screens were kept throughout the whole trial.

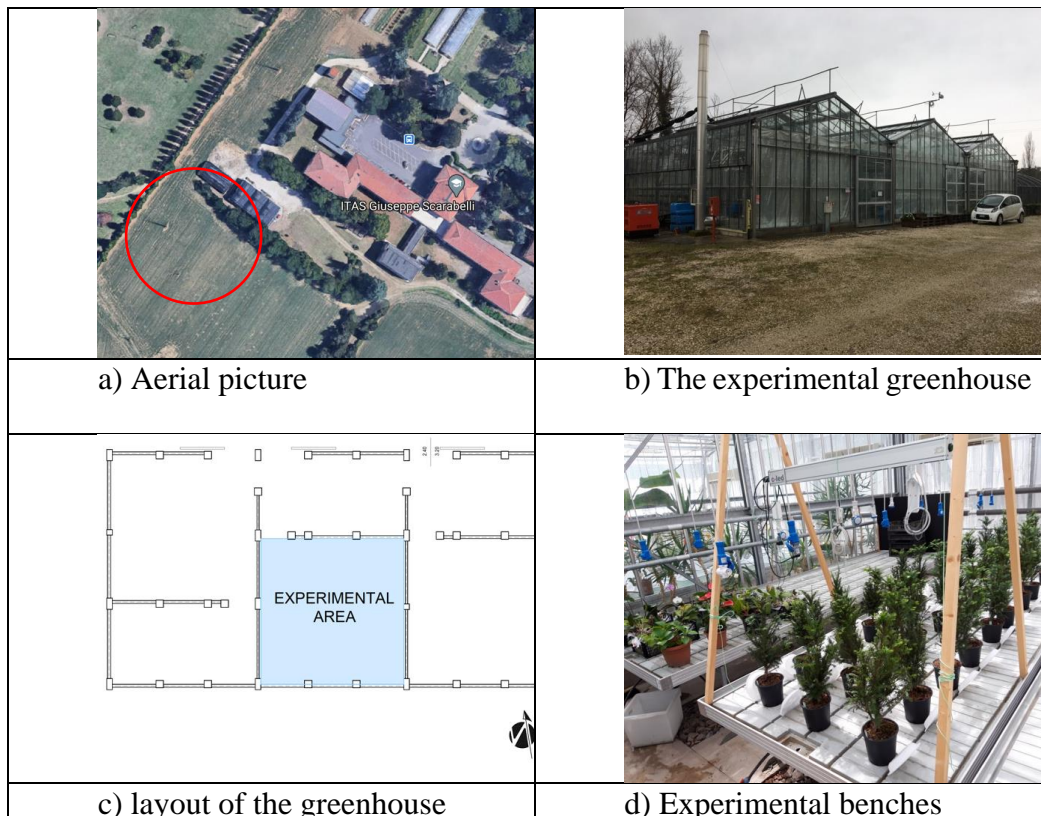


Figure 1 - University of Bologna Experimental greenhouse

To ensure the homogeneity of environmental conditions, specific tests were carried out before and during the trial. These tests allowed us to prove that the only difference in environmental conditions among the treatments was caused by the LED lamps in terms of intensity (PAR, Photosynthetically Active Radiation) and/or spectrum (red/blue ratio); tests were also intended to provide information on the environmental conditions during the experiment.

It is worth to recall that the LED lights were added as a supplement to the natural light, so the first test was designed to ensure that each treatment spot would receive the same amount of natural light. Considering that the artificial light was provided during the daylight hours, the test on the natural light was performed before the trial started (August 2019), when the lamps were off. In a 5-day campaign, illuminance in each spot was measured every day, three times a day (at 9 am, 1 pm and 6 pm). Sensors recorded values between 500 and 6500 lux; these values are higher than the compensation point for *T. baccata* [40]. Differences between the values on the spots and the average were lower than 5% for each set of measures. Therefore, the natural light could be considered uniform for all spots. Under this light, the illuminance recorded by the sensor placed in the control spot could be assumed as the natural light in the whole greenhouse span at the experiment level (70 cm above the floor level).

The artificial light was produced by five LED lamps with three emission spectra: blue (B), red (R) and mixed red and blue light (M) (see the “Light treatments” 2.3 section for more details). To produce the intensity required by the design of the trial, the lamp height was set in order to achieve the desired values 45 cm above the bench surface (average height of plants + pot at the beginning of the trial). Once the heights were set, the illuminance of each lamp was measured at foliage/canopy level for each treatment in total absence of natural light. Results are shown in Table 1.

Table 1 - LED Light characterization for each treatment

	Treatment 1	Treatment 2	Treatment 3	Treatment 4	Treatment 5	Treatment 6
LED Lamp	M	M	M	R	B	0
PAR [PPFD]	150	100	50	100	100	0
Illumin [lx]	2270	1870	1390	1830	1170	0

Unlike illuminance, temperature and relative humidity are not affected by the artificial light (a preliminary test proved that the heat generated by the lamp was negligible), therefore we were able to monitor their values throughout the whole trial.

The analysis of recorded data allowed us to characterize the trial environmental conditions as well.

To run the monitoring, besides the facility system, an additional monitoring equipment was placed in the greenhouse during the trial. This equipment – specifically designed and built for this experiment – was constituted by six nodes and a gateway (central unit) depicted in Figure 2.

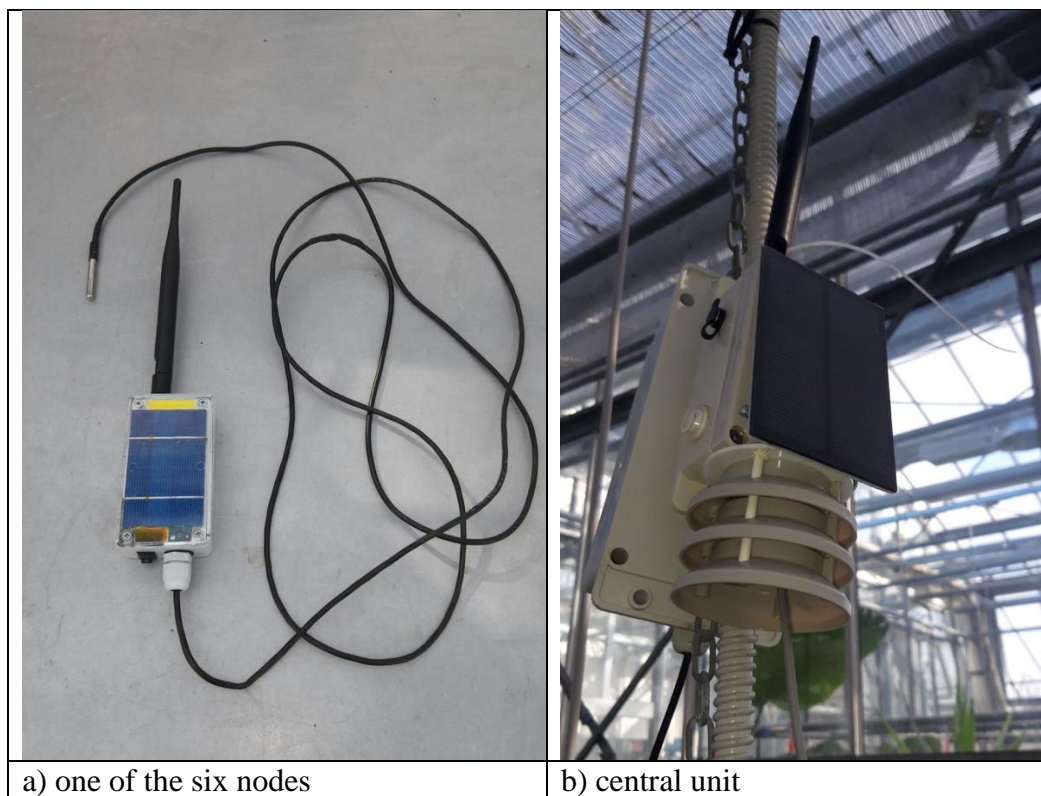


Figure 2 - Node and central unit of the monitoring system

Each node was placed in each treatment spot and measured temperature, relative humidity and illuminance every 3 minutes throughout the whole trial. The collected data were wirelessly sent to the gateway that uploaded data in a server with an internet connection allowing the experimental conditions to be checked remotely and in real time. Finally, data were stored and analyzed.

The sensor data characteristics and specification are reported in the Table 2.

Table 2 - Resolution and accuracy of the sensors used for the monitoring activity

Sensor	Resolution	Accuracy
Temperature	0.04 °C	± 0.3 °C
Relative Humidity	0.7 %	± 2 %
Illuminance	1 lx	± 1%

The homogeneity analysis was based on Barbaresi et al. [41], who designed a method to divide a room in zones with same temperature and humidity. The proposed method was later implemented to assess the homogeneity of indoor conditions in a subsequent work [42].

The above-mentioned paper assesses the homogeneity of environmental conditions by comparing data collected in a monitoring campaign with two reference parameters, IRV and ARV. The IRV – Identity Reference Value – is calculated on the sensor characteristics and is used to define when temperatures and humidity values can be considered identical. The second – the Acceptable Reference Value – is based on the purposes of the specific research and is used to define when differences in environmental conditions can be considered acceptable; in other words, when we can assume that the zones monitored by the sensors are in the same environmental conditions.

In accordance with the two above-mentioned studies, the IRVs are set as the sum of sensors' resolution and accuracy. On the other side, the ARVs are defined according to Ellenberg [40] and to the heating and cooling systems performances. Then, for the purpose of this study, IRV and ARV were set as follows (see Table 3):

Table 3 - Values of temperature and relative humidity assumed as thresholds for the uniformity of greenhouse environmental conditions

	IRV	ARV
Temperature	0.7 °C	2 °C
Relative Humidity	4.7 %	5 %

It is worth to note that the ARVs are remarkably lower than differences that can occur in *T. baccata* natural sites. According to the methods reported in [41], the following procedure was applied to temperature and humidity records:

- temperature and relative humidity in each treatment were monitored every 3 minutes for the whole trial;
- Data collected in a treatment were cleaned and compared to data collected in the other treatments, and difference were calculated for every record;

- The value $z_{ij} = (m_{ij} - \bar{m}) / sd_{ij}$ was calculated for every pair of sensors, where i and j are two sensors out of the six, m the mean and sd the standard deviation of the differences;
- The z values were finally compared to IRV and ARV. In order to state if all the treatment were under the same environmental conditions, all the z values for both temperature and humidity should be lower than ARV.

Plant material

Forty European yew (*Taxus baccata* L.) plants were purchased from a nursery and used for the trial in the experimental greenhouse. In the nursery, the plants had been individually grown from seed in black plastic pots (height 15 cm, superior internal diameter 16 cm, approx. 15x15 cm) with standard substrate. Their individual morphology was rather heterogeneous, as well as their height and shape.

Experimental design

Each plant was randomly labelled, and its weight, height, and number of sprouts were measured. Prior to weighing, the plants were well watered and let drain in order to minimize differences due to disparity in substrate humidity. Taking into account the differences for the three measured parameters, 36 plants were distributed into 6 groups so that the internal heterogeneity of each group was similar, making the groups comparable. The resulting group composition was as follows:

Group 1: plants n. 1, 2, 18, 19, 28, 33

Group 2: plants n. 3, 21, 22, 23, 31, 32

Group 3: plants n. 16, 24, 25, 26, 34, 36

Group 4: plants n. 11, 12, 20, 27, 29, 30

Group 5: plants n. 5, 7, 8, 9, 13, 14

Group 6: plants n. 4, 6, 10, 15, 17, 35

The four remaining plants were sampled for chemical analysis at time zero (T0; 19 August 2019), shortly before the start of LED lighting.

Light treatments

Each group of six plants was exposed to a top-light LED lamp emitting a different combination of light spectrum and intensity (PPFD, Photosynthetic Photon Flux Density), as follows:

Group 1: R/B/Fr LED (2/3 red, 1/3 blue), PPFD 150 $\mu\text{M m}^{-2} \text{s}^{-1}$ (R/B/Fr 150)

Group 2: R/B/Fr LED (2/3 red, 1/3 blue) PPFD 100 $\mu\text{M m}^{-2} \text{s}^{-1}$ (R/B/Fr 100)

Group 3: R/B/Fr LED (2/3 red, 1/3 blue) PPFD 50 $\mu\text{M m}^{-2} \text{s}^{-1}$ (R/B/Fr 50)

Group 4: Red LED, PPFD 100 $\mu\text{M m}^{-2} \text{s}^{-1}$ (R 100)

Group 5: Blue LED, PPFD 100 $\mu\text{M m}^{-2} \text{s}^{-1}$ (B 100)

Group 6: natural light control (Ctrl)

(R=Red, B=Blue, Fr=Far Red)

Plants cultivation

Plants were grown under treatment from 19 August to 9 December 2019. The supplemental lighting had the same light period of 14 hours per day for all LED treatments. The natural light varied according to the season (see tab. Table 6), while the indoor temperature, and consequently relative humidity, varied always within the set range. Watering was done when needed; since European yew is a slow-growing plant, no fertilization was given during the trial, in order to exclude morphophysiological responses due to factors other than LED light treatment. Moreover, in order to give each plant canopy a uniform light exposure, all plants were rotated a quarter turn every three days.

Chemicals

Deuterium oxide (D_2O , 99.90% D), CD_3OD (99.80% D) were purchased from Eurisotop (Cambridge Isotope Laboratories, Inc, France). Standard 3-(trimethylsilyl)-propionic-2,2,3,3- d_4 acid sodium salt (TMSP), sodium phosphate dibasic anhydrous and sodium phosphate monobasic anhydrous and all the other chemicals and solvents were purchased from Sigma-Aldrich Co. (St. Louis, MO, USA).

Biometric surveys and sampling for metabolomic analysis

Morphometric/biometric surveys were performed once every 28 days at 0, 28, 56, 84 and 112 days after treatment (DAT), spanning from 19 August to 9 December 2019.

At each survey three pictures per plant were taken for canopy shape evaluation, and the following parameters were measured:

- plant height: measured from the crown to the tip of the main stem; branches occasionally taller than the main stem were not considered;
- sprout number: number of young sprouts having pale green color;
- NDVI (Normalized Difference Vegetation Index), which is defined as the ratio between the difference and the sum of reflectance values in the near-infrared and red spectrum, was selected as indicator of plant growth status. It was determined with the portable GreenSeeker reader (Trimble Inc., Sunnyvale, CA; USA), holding the instrument horizontally 50 cm above plant tips.

Metabolomic analysis

For metabolomic analysis samples from each plant were collected every 28 days by cutting 3 representative branches per individual. The samples were dried at 40°C and powdered using an electrical grinder (IKA, A11 basic, Merck, Italy).

Plants extracts were prepared according to Mandrone et al. [43] with slight modifications. Briefly, thirty mg of each sample were extracted with 1 mL of mixture (1:1) of phosphate buffer (90 mM; pH 6.0) in H₂O-*d*₂ (containing 0.01% TMSP) and MeOH-*d*₄ by ultrasonication (TransSonic TP 690, Elma, Germany) for 20 minutes. After this procedure, samples were centrifuged for 10 min (17000 x *g*), then 700 µL of supernatant were transferred into NMR tubes.

NMR measurement

¹H NMR spectra were recorded at 25°C on a Varian Inova 600 MHz NMR instrument (600 MHz operating at the ¹H frequency) equipped with an indirect triple resonance probe. Methanol-*d*₄ was used for internal lock. Each ¹H-NMR spectrum consisted of 256 scans (corresponding to 16 min) with the relaxation delay (RD) of 2 s, acquisition time 0.707 s, and spectral width of 9595.8 Hz (corresponding to δ 16.0). A presaturation sequence (PRESAT) was used to suppress the residual water signal at δ 4.83 (power = -6dB, presaturation delay 2 s). The spectra were manually phased and baseline corrected, and calibrated to the internal standard trimethyl silyl propionic acid sodium salt (TMSP) at δ 0.0 using Mestrenova software (Mestrelab Research, Spain). For

metabolomic analysis, the regions of δ 5-4.5 and δ 3.34-3.30 were excluded because of the residual solvent signals. Then spectral intensities were reduced to integrated regions of equal width (δ 0.04) corresponding to the region from δ 0.0 to 10.0, and normalized by total area.

The spectrum of baccatin III was recorded in methanol- d_4 .

Data management and multivariate data analysis

Biometric data were split between two treatment sub-groups: one at different light intensity, composed by Ctrl, R/B/Fr 50, R/B/Fr 100 and R/B/Fr 150; and another at different light quality, composed by R 100, B 100 and R/B/Fr 100. In the two sub-groups, data were submitted to one-way ANOVA at each of the five surveys, using the STATISTICA v.10.0 software (StatSoft, Tulsa, OK, USA). For selected traits, the time trends of the treatments and their 95% confidence bands were traced, using the SigmaPlot 10 software (Systat Software Inc., San José, CA, USA).

The SIMCA software (v. 16.0, Umetrics, Sweden) was used for multivariate data analysis. In particular data were subjected to Pareto scaling and supervised models were evaluated by the goodness of fit (R^2_x (cum) and R^2_y (cum)) and goodness of prediction (Q^2 (cum)), together with the parameters given by cross validation tests: permutation test (performed using 200 permutations) and CV-ANOVA.

Results

For temperature and humidity characterization, the method described in Section 2.1 was applied and data measured by the sensors for each experimental treatment were compared. Table 4 and Table 5 show the results.

Table 4 - Analysis of the temperatures measured in each treatment. Data are expressed in Celsius degree

Treatment	Mean	St.dev.	m +sd
T1 vs T2	0.314	0.960	1.274
T1 vs T3	0.242	1.030	1.272
T1 vs T4	0.271	0.296	0.567
T1 vs T5	0.285	0.618	0.903
T1 vs T6	0.650	0.518	1.169
T2 vs T3	-0.071	0.301	0.372

T2 vs T4	-0.009	0.980	0.989
T2 vs T5	-0.025	0.464	0.489
T2 vs T6	0.320	0.785	1.105
T3 vs T4	0.067	1.095	1.161
T3 vs T5	0.049	0.569	0.618
T3 vs T6	0.437	0.834	1.271
T4 vs T5	-0.004	0.648	0.651
T4 vs T6	0.324	0.528	0.852
T5 vs T6	0.353	0.530	0.882

Table 5 - Analysis of the relative humidity measured in each treatment. Data are expressed in percentage

Treatment	Mean	St.dev.	m +sd
T1 vs T2	-0.196	2.845	3.041
T1 vs T3	-0.911	3.017	3.927
T1 vs T4	-1.106	1.687	2.793
T1 vs T5	-0.753	2.076	2.830
T1 vs T6	-1.440	2.426	3.867
T2 vs T3	-0.768	1.442	2.210
T2 vs T4	-1.037	2.612	3.650
T2 vs T5	-0.589	1.677	2.267
T2 vs T6	-1.137	2.315	3.452
T3 vs T4	-0.276	3.004	3.280
T3 vs T5	0.169	1.853	2.021
T3 vs T6	-0.435	2.566	3.001
T4 vs T5	0.348	2.183	2.531
T4 vs T6	-0.229	2.421	2.650
T5 vs T6	-0.592	1.942	2.534

The results show that the mean of differences were very low, even under the IRV in some cases and in general confirm the homogeneity of temperature and humidity. Under this light, to characterize the environmental conditions of the trial, the average temperature and humidity of the six treatments were retained to define the environmental conditions for all the treatments.

As reference, Table 6 reports the significant environmental conditions that characterized four periods during the trial. Each period is defined as the time between a

morphometric/biometric survey and the following one: Period 1 (19/08 – 16/09), Period 2 (17/09 – 14/10), Period 3 (15/10 – 11/11) and Period 4 (12/11 – 09/12).

Table 6 - Characterization of temperature, relative humidity and natural light (average values) measured in the four periods of the experiment

	Period 1		Period 2		Period 3		Period 4	
	day	night	day	night	day	night	Day	Night
T [°C]	23.65	21.44	22.87	20.05	20.55	16.61	19.42	15.04
rH [%]	58.07	70.03	63.62	70.78	70.00	77.77	56.47	64.71
Nat. light [lx]	1495	-	518	-	299	-	1280	-

Growth analysis

In the light intensity sub-group, plant height described a different trend across the 112 DAT (Figure 3.a). Plants under natural light (Ctrl group) only modestly increased in height, whereas plants at increasing light intensity (R/B/Fr 50, 100 and 150 $\mu\text{M m}^{-2} \text{s}^{-1}$) increased to a larger extent: the two upper levels (100 and 150 $\mu\text{M m}^{-2} \text{s}^{-1}$) were practically superimposed, while the lower level (50 $\mu\text{M m}^{-2} \text{s}^{-1}$) traced an intermediate trend between Ctrl and the two upper levels.

The number of sprouts per plant remained very low under natural light, whereas it was strongly enhanced by the LED treatments in the early phase (28 and 56 DAT) (Figure 3.b). The lower light intensity (50 $\mu\text{M m}^{-2} \text{s}^{-1}$) showed slightly lower data than the two upper light intensities (100 and 150 $\mu\text{M m}^{-2} \text{s}^{-1}$) only at 56 DAT. In the later growth phase (84 and 112 DAT), the stimulus to sprouting ceased, and all treatments fell very close to zero sprouting.

The NDVI exhibited non-significant differences among light intensity levels until 28 DAT (Figure 3.c). Thereafter, treatment differences became statistically significant, indicating that the Ctrl treatment was always below the three LED treatments. No further difference was shown among these latter.

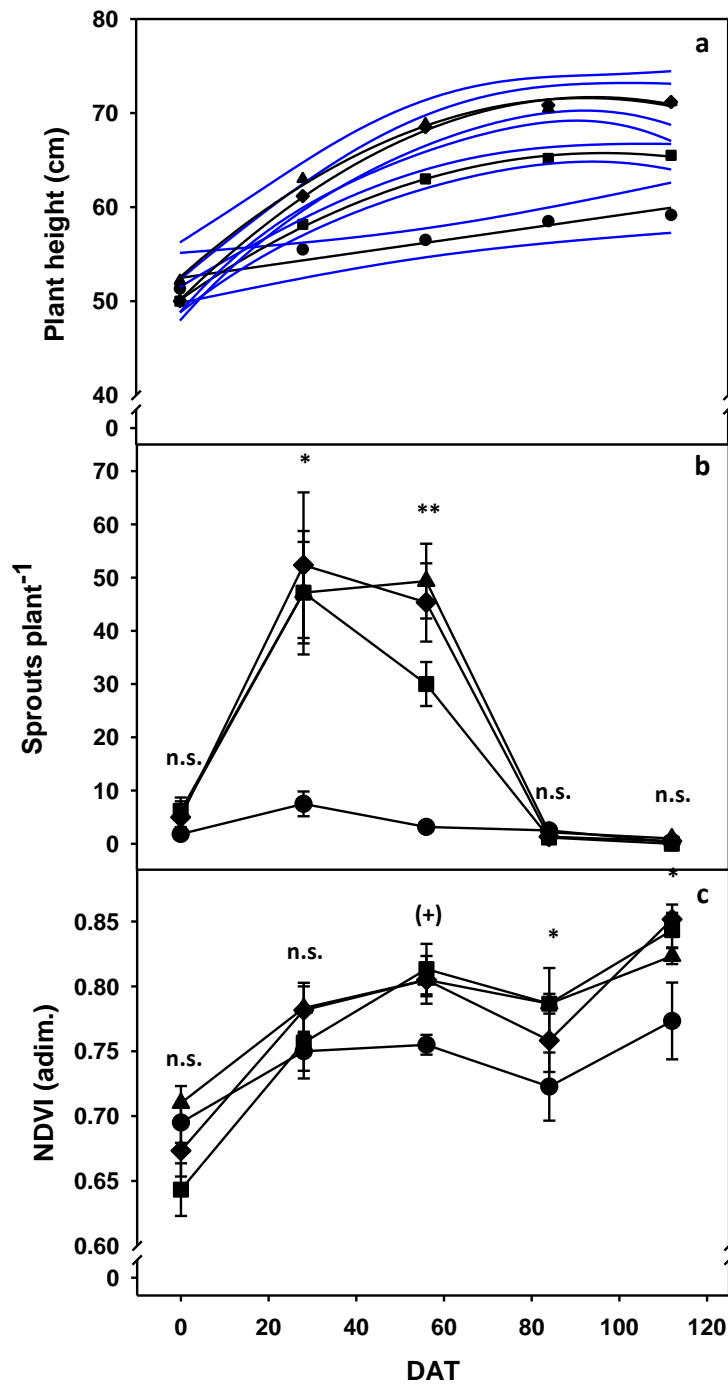


Figure 3 - Plant height (a), number of sprouts per plant (b), and normalized difference vegetation index (NDVI) (c) at various days after treatment (DAT) in *Taxus baccata* exposed to different light intensity. Circles, squares, diamonds and triangles indicate the control and the R/B/Fr LED lamps at 50, 100 and 150 $\mu\text{M m}^{-2} \text{s}^{-1}$, respectively. In plant height, the 95% confidence bands for the time trends of the four treatments are shown; in the other two traits, vertical bars indicate \pm SE (n=6); n.s., (+), * and ** indicate non-significant and significant at $P \leq 0.10$, $P \leq 0.05$ and $P \leq 0.01$, respectively.

In the light quality sub-group, no significant difference in the three biometric traits was evidenced, apart from the number of sprouts at 84 DAT. In general, a slight beneficial influence is perceived for the blue light, alone or in combination with the red and far red (B 100 and R/B/Fr 100), over the red light (R 100) in sprouts per plant (Table 8), whereas in plant height (Table 7) and NDVI (Table 9) this effect is unperceivable.

Table 7 - Plant height (cm) at various days after treatment (DAT) in *Taxus baccata* exposed to different light quality (R, red; B, blue; Fr, far red) at 100 $\mu\text{M m}^{-2} \text{s}^{-1}$. Data are means \pm SE (n=6).

DAT	0	28	56	84	112
R 100	55.7 \pm 0.9	60.3 \pm 1.4	65.0 \pm 2.0	66.2 \pm 1.2	66.7 \pm 1.0
B 100	56.7 \pm 2.0	61.7 \pm 1.9	67.0 \pm 1.9	69.7 \pm 2.0	70.3 \pm 2.3
R/B/Fr 100	50.0 \pm 2.3	61.2 \pm 4.6	68.5 \pm 5.1	70.8 \pm 5.4	71.2 \pm 5.2
Stat. signif.	n.s.	n.s.	n.s.	n.s.	n.s.

Table 8 – Number of sprouts per plant at various days after treatment (DAT) in *Taxus baccata* exposed to different light quality (R, red; B, blue; Fr, far red) at 100 $\mu\text{M m}^{-2} \text{s}^{-1}$. Data are means \pm SE (n=6).

DAT	0	28	56	84	112
R 100	1.5 \pm 1.0	25.2 \pm 6.4	28.0 \pm 4.4	3.7 \pm 0.3 a	1.0 \pm 0.4
B 100	2.0 \pm 0.7	57.3 \pm 10.5	34.8 \pm 4.3	1.2 \pm 0.7 b	0.2 \pm 0.2
R/B/Fr 100	5.0 \pm 0.9	52.3 \pm 13.7	45.3 \pm 7.4	1.3 \pm 0.5 b	0.5 \pm 0.5
Stat. signif.	n.s.	n.s.	n.s.	**	n.s.

Table 9 – Normalized difference vegetation index (adim.) at various days after treatment (DAT) in *Taxus baccata* exposed to different light quality (R, red; B, blue; Fr, far red) at 100 $\mu\text{M m}^{-2} \text{s}^{-1}$. Data are means \pm SE (n=6).

DAT	0	28	56	84	112
R 100	0.67 \pm 0.02	0.78 \pm 0.03	0.81 \pm 0.01	0.75 \pm 0.01	0.83 \pm 0.01
B 100	0.68 \pm 0.02	0.77 \pm 0.02	0.84 \pm 0.01	0.74 \pm 0.03	0.83 \pm 0.02
R/B/Fr 100	0.67 \pm 0.02	0.78 \pm 0.02	0.81 \pm 0.02	0.76 \pm 0.02	0.85 \pm 0.01
Stat. signif.	n.s.	n.s.	n.s.	n.s.	n.s.

The pictures in Fig. 4 allow morphological differences to be detected among under the different light treatments. No significant evidence of systematic differences was found. Individual variability within each group was as high as variability between different groups.

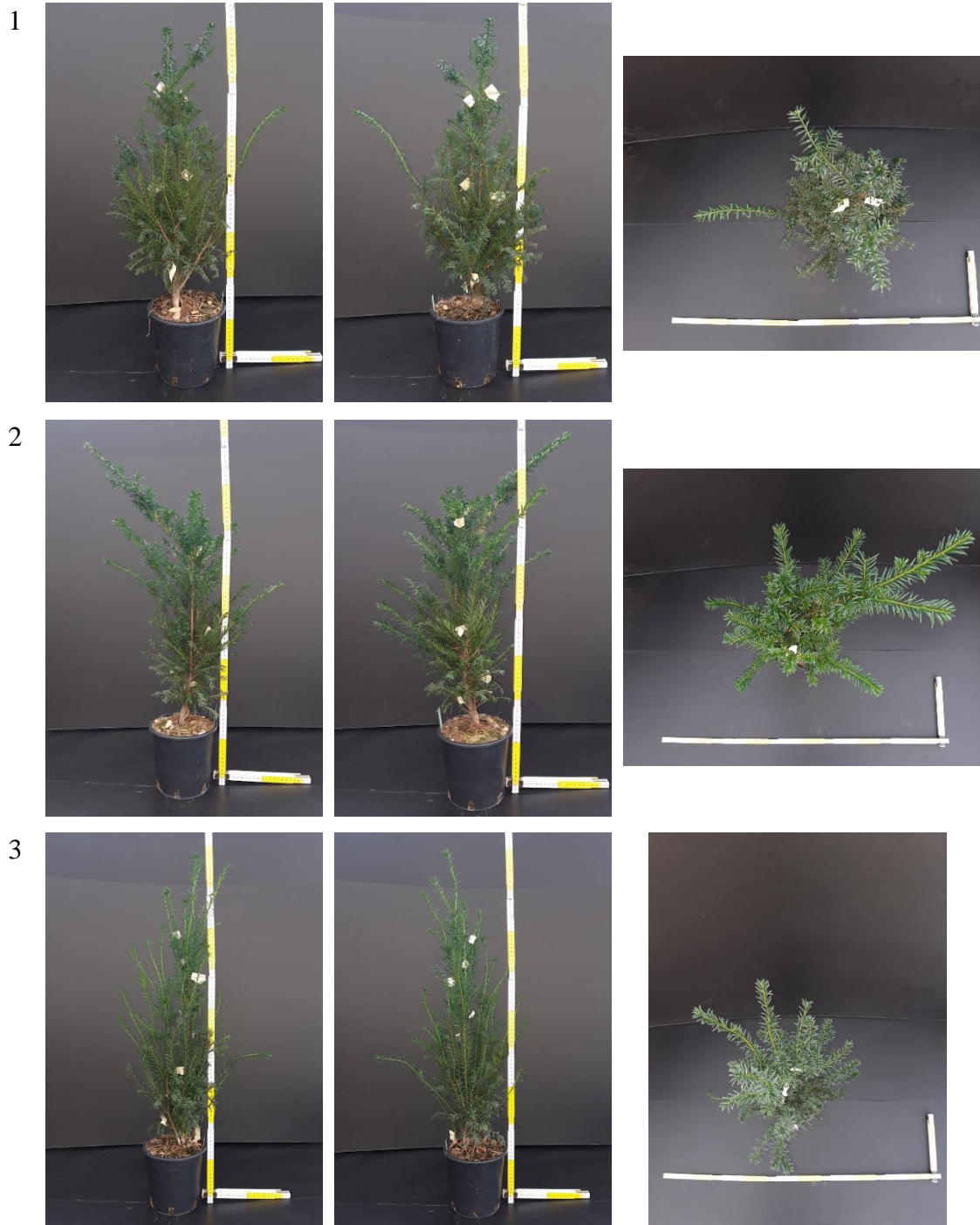


Figure 4 - Front, rear and above views of a plant from Control (1), R/B/Fr 100 (2), B 100 (3) treatments on December 2019

Metabolomic analysis

In order to detect eventual variations in the metabolome of the samples at 28 DAT, Principal Component Analysis (PCA) was performed on bucketed ^1H NMR spectra, used as x variables of the model. As shown by the score scatter plot (Fig. 5A), samples of the control group (NL) were clustered in the upper left quadrant (negative component $t[1]$ and positive component $t[2]$).

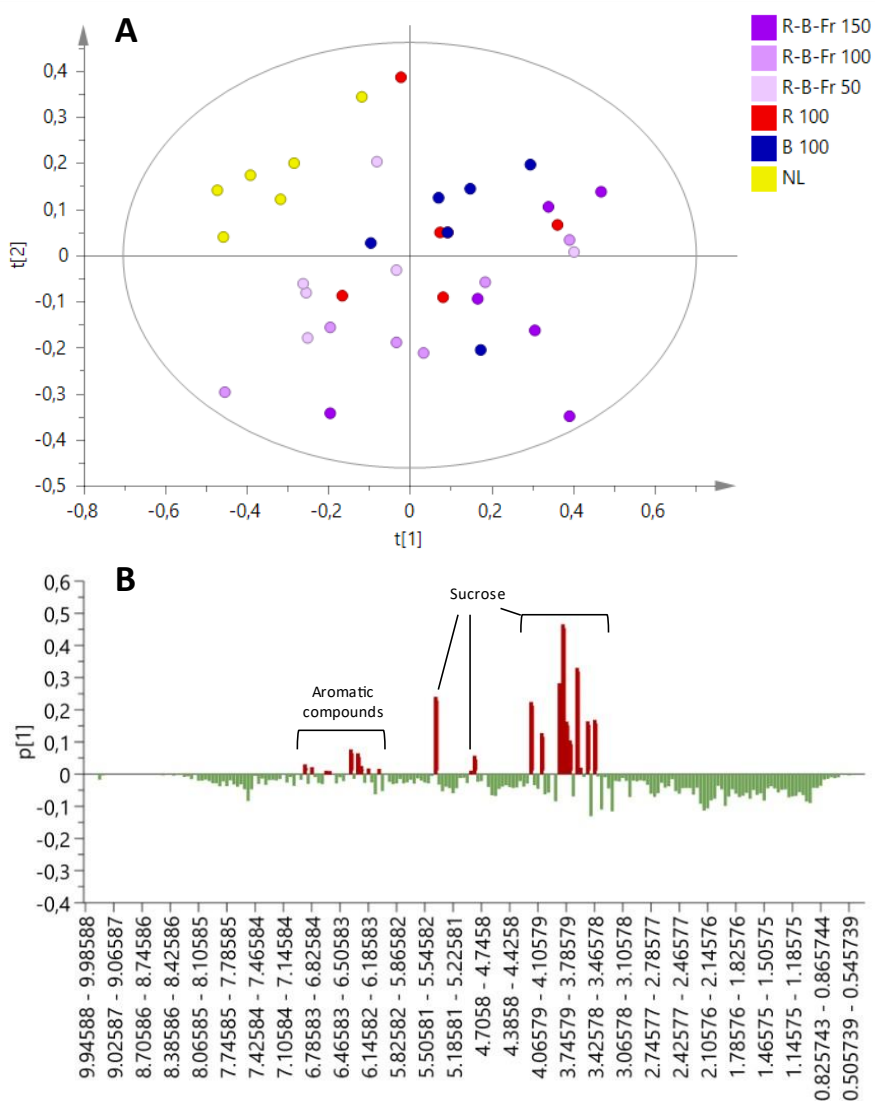


Figure 5 - ^1H NMR based Principal Component Analysis of *T. baccata* samples under different LED light treatments. A) Score scatter plot B) Loading column plot. $R^2(\text{cum})= 0.552$, $Q^2(\text{cum})=0.442$.

As shown by the loading plot (Fig. 5B), some spectral signals, resonating in the aromatics and carbohydrates regions, were particularly intense in the treated samples, determining a shift along the positive component $t[1]$ of these latter in the PCA score scatter plot (Fig. 5A). In fact, it was evident from the ^1H NMR spectra that treated samples were characterized by an increase in sucrose concentration compared to the control group. In addition, some spectral signals resonating at δ 6.26, 6.34, 6.78, 6.86 (aromatic region) were found characteristic of the treated samples. Even though the plants belonging to the same group showed individual responses to the treatment, group 1 (treatment R/B/Fr $150 \mu\text{M m}^{-2} \text{s}^{-1}$) resulted the most different from the control group (natural light, NL), while group 3 (treatment R/B/Fr $50 \mu\text{M m}^{-2} \text{s}^{-1}$) resulted more similar to the control.

According to the results of the metabolomic analysis on samples at 56 DAT, in this stage the treated plants were no longer different from the control group, suggesting an adaptive behavior of *T. baccata* metabolome to prolonged treatment. The PCA model built on the bucketed ^1H NMR spectra of both 28 DAT and 56 DAT (Fig. 6A), showed that all samples at 56 DAT were close to the control group at 28 DAT. Only the treated samples at 28 DAT showed evident differences compared to the controls.

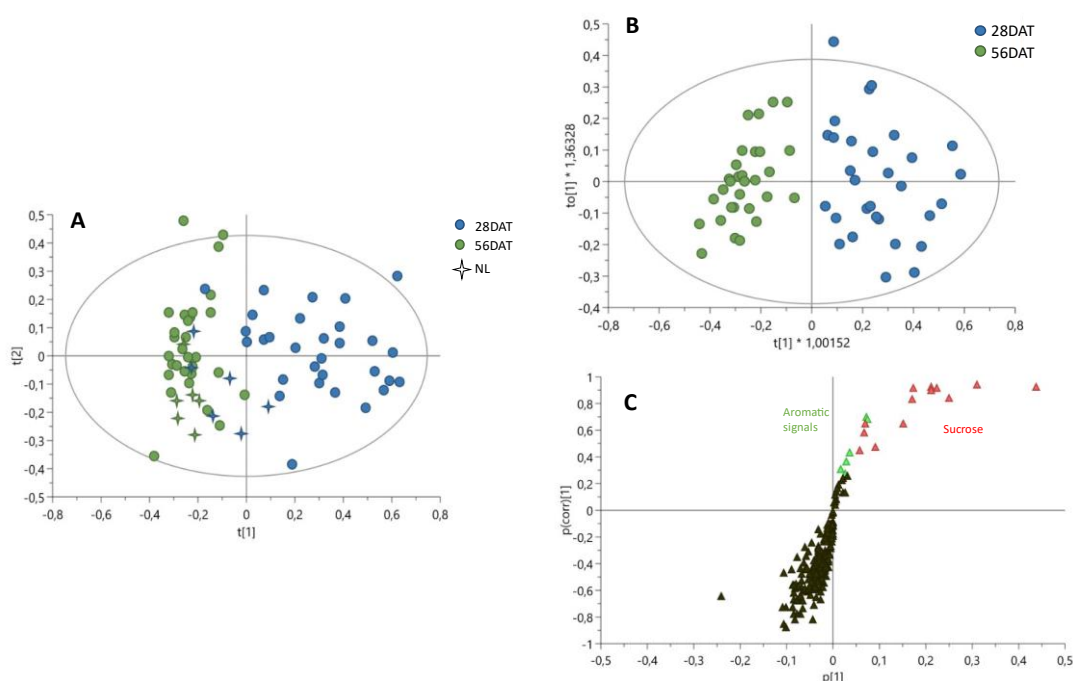


Figure 6 - A) ^1H NMR based PCA of *T. baccata* samples under different LED light treatments at 28 days and 56 days since treatments started. $R^2(\text{cum})= 0.871$, $Q^2(\text{cum})=0.674$. B) Score scatter plot of OPLS-DA model using sampling time as discriminant classes. C) S-plot of OPLS-DA model.

In order to obtain more information on the metabolites responsible for the separation of the treated samples at the different time points, OPLS-DA (Orthogonal Partial Least Squares-Discriminant Analysis) was carried out on bucketed ^1H NMR spectra of treated plants, using as discriminant classes the two time points of sampling (control plants were excluded from the analysis) (Fig. 6B-C). The model found a perfect fit to the response using two components, with goodness of fit ($R^2y(\text{cum})$) of 82% and goodness of prediction ($Q^2(\text{cum})$) of 71%. The model was evaluated by permutation test (performed using 200 permutations), which gave $R^2(\text{cum})$ of 83% and intercept on y axis of R -line was 0.16, and $Q^2(\text{cum})$ of 71% and intercept on y axis of Q -line was -0.29. Moreover, the significance of the model was tested by the ANOVA of cross-validated residuals (CV-ANOVA) giving $p = 2.1 \times 10^{-14}$ and $F = 34$. The results showed by the S -plot of this model (Fig. 6C) were consistent with the results of the PCA, confirming that at 28 DAT the treatments determined an increase in sucrose and aromatic compounds. In addition, from this plot it resulted that all the other metabolites were more abundant at 56 DAT.

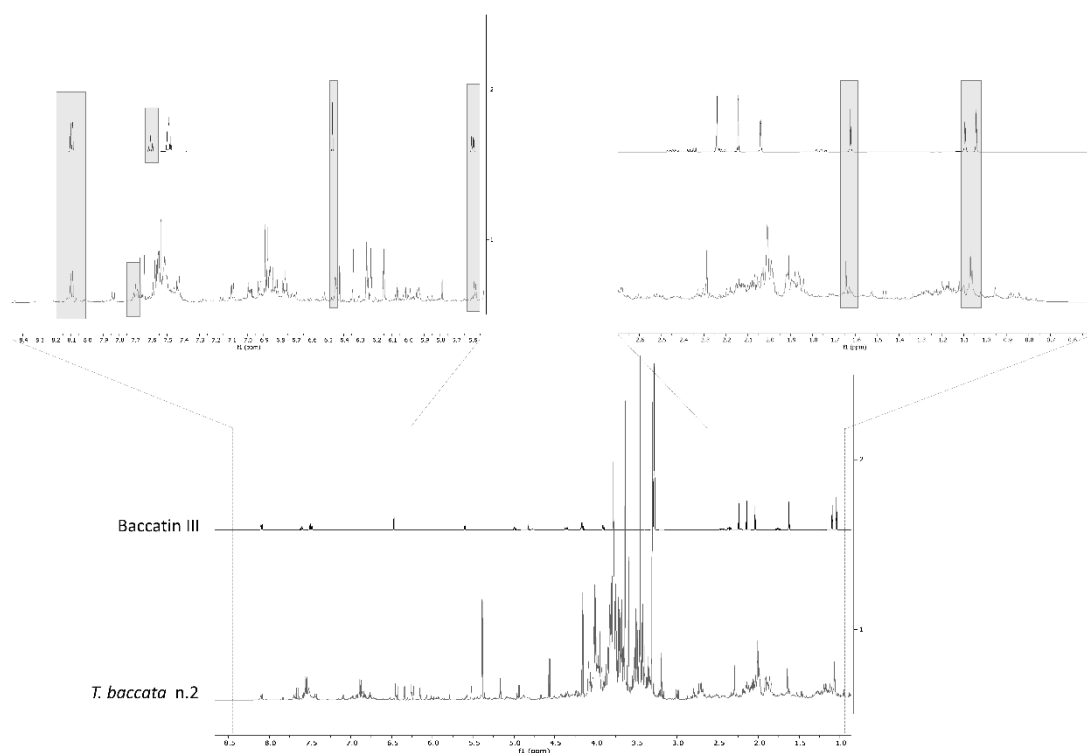


Figure 7 - Comparison between ^1H NMR spectra of baccatin III and plant number 2 at 56 DAT. On top are given extended regions from δ 0.6 to 2.6 and from δ 5.5 to 8.4.

Spectral signals ascribable to taxanes were also found in the ^1H NMR profiles of the experimental plants, which were compared to the ^1H NMR spectrum of baccatin III, a precursor of taxol [44].

(Fig. 7). These signals were scarcely affected by the treatment. However, from the S-plot of the OPLS-DA, it was possible to detect a slight increase of the putative taxane in plants at 56 DAT (Fig. 8).

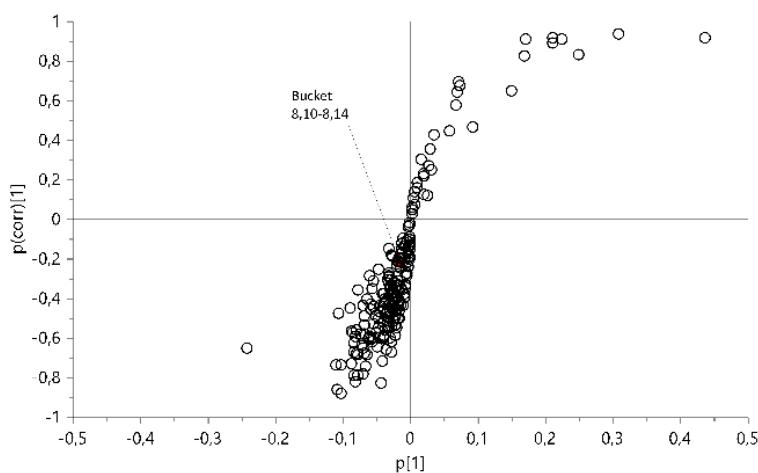


Fig. 8 - S-plot of OPLS-DA model where the bucket containing a signal ascribable to taxane (δ 8.10 - 8.14) was highlighted showing a slight increase in plants at 56 DAT

Discussion

To our best knowledge, the above results on *Taxus baccata* morphology, growth and metabolomic profile in response to differential LED treatments are the first to show up in the literature. In fact, coniferous plants are seldom surveyed among medicinal and aromatic plants, as a recent review demonstrates [17]. Still to our best knowledge, the only *Taxus* species having been focused in a previous LED experiment was *Taxus chinensis* [45], and in this case only plant growth and net photosynthetic rate were assessed in response to LED supplementation during the winter time.

In this paucity of information, despite a relatively short experiment and the intrinsically slow growth of this species, supplemental LED illumination of moderate intensity (up to $150 \mu\text{M m}^{-2} \text{s}^{-1}$) was able to determine increased plant height, enhanced sprouting in the early growth phase, and somewhat better growth status (Figure 3). The temporal phase and the extent to which LED determined the above effects varied

depending on light intensity ($0 - 150 \mu\text{M m}^{-2} \text{ s}^{-1}$ of supplemental PAR) as well as quality (R, B and R/B/Fr), thus indicating that additional work is needed to better circumstantiate suitable plant conditions leading to consistent benefits from LED use.

However, the generally good effects obtained with LED lighting in both quantitative (plant height and number of sprouts) and qualitative (NDVI as indicator of vigor) growth, are the premise for sustained growth over the medium to long term, potentially leading to higher production of valuable metabolites. These effects increased when light intensity rose, although beyond $100 \mu\text{M m}^{-2} \text{ s}^{-1}$ these effects faded, indicating that effective growth stimulus can be triggered by a small LED supplementation.

At the focal light intensity of $100 \mu\text{M m}^{-2} \text{ s}^{-1}$, LEDs including the blue wavelength in their spectra (B and B/R/Fr) were shown to be slightly more effective than the monochromatic red light (R). This circumstance is not consistently echoed in the literature on LED use, although it should be born in mind that no specific work has so far addressed *Taxus baccata*.

Both the combination of natural and LED light, and the low intensity of supplementary lighting require to be carefully managed in order to exclude any confounding factor. Therefore, besides an accurate design of the light supplementation and environmental control systems, this study paid special attention to assure and prove the uniformity of environmental conditions throughout the experiment. A system capable of monitoring temperature, relative humidity, and illuminance, allowed us to map and characterize every experimental slot with a high spatial and time resolution. The analysis of collected data allowed us to confirm that the different plant responses had to be attributed only to LED light supplementation.

The metabolomic analysis showed that one of the most prominent effects exerted by LEDs on *T. baccata* was to determine an increase in the sucrose content. This is explained by the stimulation of the photosynthetic activity due to the additional lighting. Moreover, treated plants showed higher content of aromatic compounds, indicating that light exposure might have triggered the synthesis of photoprotective compounds such as phenols and flavonoids, which are generally found in *Taxus* genus [46,47].

The treatment at $50 \mu\text{M m}^{-2} \text{ s}^{-1}$ was not sufficient to induce a strong variation in the most abundant metabolites produced by *T. baccata*. On the contrary, according to the PCA, plants treated with the highest intensity LEDs were the most diversified from the

control group, indicating that light intensity has a strong impact on plant metabolome. Moreover, varying the light composition (red, blue and red/blue/far red) at intermediate intensity ($100 \mu\text{M m}^{-2} \text{s}^{-1}$) did not determine significant differences in plant growth and morphology (Table 7). However, it may not be excluded that by varying some conditions, e.g., increasing light intensity, differences in light spectral composition might result in beneficial differences in plant behaviour.

The OPLS-DA model built using the ^1H NMR data collected at two different time points highlighted that treated plants become more similar to the control group at 56 DAT, and by S-plot it was possible to observe a general increase of metabolite content during plant growth. Although the treatment was not affecting the putative taxane concentration, it was increasing the number of sprouts and height of the plants. According to this data, the treatment of taxus with LED lights, might lead to obtain a higher amount of plant material with a consequent increase in the recovery of the metabolites of interest.

Conclusions

Studying the effects of supplemental LED lighting on the growth of medicinal plants and the production of secondary metabolites of pharmacological interest is a topical and challenging subject, which is gaining interest by many scholars across the globe. Nevertheless, it still needs further investigations, with particular reference to conifers, on which the effects of LED treatments have mostly been studied for forest tree species, focusing on growth and physiology, and have largely been performed on tissue cultures when the target feature was the production of metabolites of pharmaceutical interest.

Therefore, this study addressed the challenge of investigating the effects of both quality and intensity of supplemental LED lighting on both growth and metabolism of *Taxus baccata*, known for being a source of substances with antitumor activity.

The research focused on a cultivation environment which exploits natural light, allowing lower LED lighting intensities to be used, compared to those that would be needed in indoor farming. This was made possible thanks to a continuous monitoring and control of environmental parameters, which allowed us to assure homogeneous conditions of base natural light, temperature, and humidity, and thus to refer the differences in plant growth and metabolism only to the different supplemental light treatments.

Supplemental LED treatments showed clear effects on plant growth, in particular in terms of increased plant height, number of sprouts, and plant vigor. Both unsupervised (PCA) and supervised (OPLS-DA) analysis were performed on ¹H NMR profiles of samples, showing that sucrose and aromatic compounds were significantly higher in treated plants. The increment in sucrose production is likely reflecting the increased photosynthetic activity of plants exposed to LED lighting [48]. In addition, the increase of aromatic compounds might represent a photoprotective strategy [49]. An overall increase of the most abundant metabolites, including the detected putative taxane, was observed during plant growth. These results highlight the importance of paying attention to plant growth stage and treatment duration when setting greenhouse cultivation. The study allowed us to identify 100 $\mu\text{M m}^{-2} \text{s}^{-1}$ as the light intensity threshold above which no significant benefits can be obtained, and to detect that LED spectra including both red and blue show better results. However, further research is needed to better investigate the effects of different light spectra, also in combination with different light intensities.

Acknowledgments

C-Led s.r.l. (Imola, Italy) is gratefully acknowledged for the collaboration in designing and realizing LED lamps for the specific needs of this research.

References

1. Mitchell, A. K. Acclimation of Pacific yew (*Taxus brevifolia*) foliage to sun and shade. *Tree physiology*, **1998**, *18*(11), 749–757.
2. Schafer, E., & Nagy, F. Physiological basis of photomorphogenesis. In *Photomorphogenesis in Plants and Bacteria* **2006** (pp. 13–23). Springer, Dordrecht.
3. Deitzer, G. F., Hayes, R., & Jabben, M. Kinetics and time dependence of the effect of far red light on the photoperiodic induction of flowering in Wintex barley. *Plant physiology*, **1979**, *64*(6), 1015–1021.
4. Morgan, D. C., & Smith, H. A systematic relationship between phytochrome-controlled development and species habitat, for plants grown in simulated natural radiation. *Planta*, **1979**, *145*(3), 253–258.
5. Blaauw, O. H., & Blaauw-Jansen, G. Third positive (c-type) phototropism in the *Avena* coleoptile. *Acta botanica neerlandica*, **1970**, *19*(5), 764–776.
6. Schwartz, A., & Zeiger, E. Metabolic energy for stomatal opening. Roles of photophosphorylation and oxidative phosphorylation. *Planta*, **1984**, *161*(2), 129–136.
7. Hasan, M., Bashir, T., Ghosh, R., Lee, S. K., & Bae, H. An overview of LEDs' effects on the production of bioactive compounds and crop quality. *Molecules*, **2017**, *22*(9), 1420.
8. Yeh, N., & Chung, J. P. High-brightness LEDs—Energy efficient lighting sources and their potential in indoor plant cultivation. *Renewable and Sustainable Energy Reviews*, **2009**, *13*(8), 2175–2180.
9. Stutte, G. W. Commercial transition to LEDs: A pathway to high-value products. *HortScience*, **2015**, *50*(9), 1297–1300.
10. Kowalczyk, K., Olewnicki, D., Mirgos, M., & Gajc-Wolska, J. Comparison of selected costs in greenhouse cucumber production with LED and HPS supplemental assimilation lighting. *Agronomy*, **2020**, *10*(9), 1342.
11. Joshi, N. C., Ratner, K., Eidelman, O., Bednarczyk, D., Zur, N., Many, Y., ... & Charuvi, D. Effects of daytime intra-canopy LED illumination on photosynthesis and productivity of bell pepper grown in protected cultivation. *Scientia Horticulturae*, **2019**, *250*, 81–88.
12. Collado, C. E., & Hernández, R. Effects of Light Intensity, Spectral Composition, and Paclobutrazol on the Morphology, Physiology, and Growth of Petunia, Geranium, Pansy, and Dianthus Ornamental Transplants. *Journal of Plant Growth Regulation*, **2021**, 1–18.
13. Gangadhar, B. H., Mishra, R. K., Pandian, G., & Park, S. W. Comparative study of color, pungency, and biochemical composition in chili pepper (*Capsicum annuum*) under different light-emitting diode treatments. *HortScience*, **2012**, *47*(12), 1729–1735.
14. Goto, E. Plant production in a closed plant factory with artificial lighting. In *VII International Symposium on Light in Horticultural Systems 956*, **2012**, October, 37–49.
15. Lin, K. H., Huang, M. Y., Huang, W. D., Hsu, M. H., Yang, Z. W., & Yang, C. M. The effects of red, blue, and white light-emitting diodes on the growth, development, and edible quality of hydroponically grown lettuce (*Lactuca sativa* L. var. capitata). *Scientia Horticulturae*, **2013**, *150*, 86–91.
16. Kopsell, D. A., Sams, C. E., & Morrow, R. C. Blue wavelengths from LED lighting increase nutritionally important metabolites in specialty crops. *HortScience*, **2015**, *50*(9), 1285–1288.
17. Thakur, M., & Kumar, R.. Microclimatic buffering on medicinal and aromatic plants: A review. *Industrial Crops and Products*, **2020**, 113144.
18. Fukuyama, T., Ohashi-Kaneko, K., Ono, E., & Watanabe, H. Growth and alkaloid yields of *Catharanthus roseus* (L.) G. Don cultured under red and blue LEDs. *Journal of Science and High Technology in Agriculture*, **2013**, *25*(4), 175–182.
19. Fukuyama, T., Ohashi-Kaneko, K., & Watanabe, H. Estimation of optimal red light intensity for production of the pharmaceutical drug components, vindoline and catharanthine, contained in *Catharanthus roseus* (L.) G. Don. *Environmental Control in Biology*, **2015**, *53*(4), 217–220.
20. Fukuyama, T., Ohashi-Kaneko, K., Hirata, K., Muraoka, M., & Watanabe, H. Effects of ultraviolet A supplemented with red light irradiation on vinblastine production in *Catharanthus roseus*. *Environmental Control in Biology*, **2017**, *55*(2), 65–69.
21. Molchan O, Privalov V, Petrinchik V, Astasenko N. Effects of led light on the growth and secondary metabolite production in catharanthus roseus medicinal plants under artificial cultivation. *Khimija Rastit Syrja*. **2017**;3.
22. Wang, W., Su, M., Li, H., Zeng, B., Chang, Q., & Lai, Z. Effects of supplemental lighting with different light qualities on growth and secondary metabolite content of *Anoectochilus roxburghii*. *PeerJ*, **2018**, *6*, e5274.

23. Wang, Y., Zhang, H., Zhao, B., Yuan, X. Improved growth of *Artemisia annua* L hairy roots and artemisinin production under red light conditions. *Biotechnol Lett.* **2001**, 23(23):1971–3.
24. Tariq, U., Ali, M., & Abbasi, B. H. Morphogenic and biochemical variations under different spectral lights in callus cultures of *Artemisia absinthium* L. *Journal of Photochemistry and Photobiology B: Biology*, **2014**, 130, 264–271.
25. Riikonen, J., Kettunen, N., Gritsevich, M., Hakala, T., Särkkä, L., & Tahvonen, R. Growth and development of Norway spruce and Scots pine seedlings under different light spectra. *Environmental and experimental botany*, **2016**, 121, 112–120.
26. Alakärppä, E., Taulavuori, E., Valledor, L., Marttila, T., Jokipii-Lukkari, S., Karppinen, K., ... & Häggman, H. Early growth of Scots pine seedlings is affected by seed origin and light quality. *Journal of plant physiology*, **2019**, 237, 120–128.
27. Su, J., Zang, C., Liu, W., Li, S., & Zhang, Z. Effect of light quality on growth and taxanes contents of *Taxus yunnanensis*. *Forest Research, Beijing*, **2012**, 25(4), 419–424.
28. Fronimos, T., Koutsoubelias, M., Lalis, S., & Bartzanas, T. A Service-Based Approach for the Uniform Access of Wireless Sensor Networks and Custom Application Tasks Running on Sensor Nodes. In *Integration, Interconnection, and Interoperability of IoT Systems* **2018** (pp. 77–101). Springer, Cham.
29. Bovo, M., Benni, S., Barbaresi, A., Santolini, E., Agrusti, M., Torreggiani, D., & Tassinari, P. (2020, November). A smart monitoring system for a future smarter dairy farming. In *2020 IEEE International Workshop on Metrology for Agriculture and Forestry (MetroAgriFor)* (pp. 165–169). IEEE.
30. Myneni, R. B., Hall, F. G., Sellers, P. J., & Marshak, A. L. The interpretation of spectral vegetation indexes. *IEEE Transactions on Geoscience and Remote Sensing*, **1995**, 33(2), 481–486.
31. Sellers, P. J. Canopy reflectance, photosynthesis and transpiration. *International journal of remote sensing*, **1985**, 6(8), 1335–1372.
32. Rouse, J. W., Haas, R. H., Schell, J. A., & Deering, D. W. Monitoring vegetation systems in the Great Plains with ERTS. *NASA special publication*, 351(1974), 309.
33. Hatfield, J. L., Asrar, G., & Kanemasu, E. T. Intercepted photosynthetically active radiation estimated by spectral reflectance. *Remote sensing of Environment*, **1984**, 14(1–3), 65–75.
34. Wiegand, C. L., Maas, S. J., Aase, J. K., Hatfield, J. L., Pinter Jr, P. J., Jackson, R. D., ... & Lapitan, R. L. Multisite analyses of spectral-biophysical data for wheat. *Remote Sensing of Environment*, **1992**, 42(1), 1–21.
35. Barbaresi, A., Bibbiani, C., Bovo, M., Benni, S., Santolini, E., Tassinari, P., ... & Torreggiani, D.. A Smart Monitoring System for Self-sufficient Integrated Multi-Trophic AquaPonic. In *2020 IEEE International Workshop on Metrology for Agriculture and Forestry (MetroAgriFor)*, **2020**, November (pp. 175–179). IEEE.
36. Pezzuolo, A., Milani, V., Zhu, D., Guo, H., Guercini, S., & Marinello, F. On-barn pig weight estimation based on body measurements by structure-from-motion (SfM). *Sensors*, **2018**, 18(11), 3603.
37. Da Borso, F., Chiumenti, A., Sigura, M., & Pezzuolo, A. Influence of automatic feeding systems on design and management of dairy farms. *Journal of Agricultural Engineering*, **2017**, 48(s1), 48–52.
38. Barbaresi, A., Agrusti, M., Ceccarelli, M., Bovo, M., Tassinari, P., & Torreggiani, D. A method for the validation of measurements collected by different monitoring systems applied to aquaculture processing plants. *Biosystems Engineering* **2021**.
39. Barbaresi, A., Santolini, E., Agrusti, M., Bovo, M., Accorsi, M., Torreggiani, D., & Tassinari, P. Microventilation system improves the ageing conditions in existent wine cellars. *Australian Journal of Grape and Wine Research*, **2020**, 26(4), 417–426.
40. Ellenberg H. *Vegetation Ecology of Central Europe*. Cambridge University Press; **2009**. 756 p.
41. Barbaresi, A., Torreggiani, D., Benni, S., & Tassinari, P. Indoor air temperature monitoring: A method lending support to management and design tested on a wine-aging room. *Building and Environment*, **2015**, 86, 203–210.
42. Barbaresi, A., Dallacasa, F., Torreggiani, D., & Tassinari, P. Retrofit interventions in non-conditioned rooms: calibration of an assessment method on a farm winery. *Journal of Building Performance Simulation*, **2017**, 10(1), 91–104.
43. Mandrone, M., Chiochio, I., Barbanti, L., Tomasi, P., Tacchini, M., Poli, F. Metabolomic Study of Sorghum (*Sorghum bicolor*) to Interpret Plant Behavior under Variable Field Conditions in View of Smart Agriculture Applications. *J Agric Food Chem.* **2021**, 69(3):1132–45.
44. Onrubia, M., Moyano, E., Bonfill, M., Palazón, J., Goossens, A., Cusidó, R.M. The relationship between TXS, DBAT, BAPT and DBTNBT gene expression and taxane production during the development of *Taxus baccata* plantlets. *Plant Science* **2011**, 181(3), 282–287.

45. Wang, C., Hou, Y., Wang, W., & Wang, G. Effect of winter LED supplementary illumination on growing development of *Taxus chinensis* var. *mairei* Cheng et LK. *Medicinal Plant*, **2012**, 3(10), 17–19.
46. Gai, Q. Y., Jiao, J., Wang, X., Liu, J., Fu, Y. J., Lu, Y., ... & Xu, X. J. Simultaneous determination of taxoids and flavonoids in twigs and leaves of three *Taxus* species by UHPLC-MS/MS. *Journal of pharmaceutical and biomedical analysis*, **2020**, 189, 113456.
47. Edreva, A. The importance of non-photosynthetic pigments and cinnamic acid derivatives in photoprotection. *Agriculture, ecosystems & environment*, **2005**, 106(2-3), 135–146.
48. Chen, X.L., Wang, L.C., Li, T., Yang, Q.C., Guo, W.Z. Sugar accumulation and growth of lettuce exposed to different lighting modes of red and blue LED light. *Scientific reports* **2019**, 9(1), 1–10.
49. Yang, L., Wen, K. S., Ruan, X., Zhao, Y. X., Wei, F., & Wang, Q. Response of plant secondary metabolites to environmental factors. *Molecules* **2018**, 23(4), 762

Chapter 3

Natural products research and chemodiversity as a base for biodiversity protection

A sustainable development cannot be achieved without a responsible management of the ecosystems which firstly requires ecosystems protection and halting the loss of biodiversity. Studying plants, their specialized metabolites, and their properties contributes to raise the awareness of their importance, and enhances biodiversity valorization and protection.

Moreover, natural products research highly benefits from studies conducted in areas characterized by high biodiversity generating, in turn, high chemodiversity. This chapter specifically addresses the topic of biodiversity and chemodiversity by investigating plants of local flora. In particular, the first study here reported investigated plants collected in Sardinia island, which is characterized by high number of endemic and exclusive species. These plants were studied, for their potential antiproliferative activity on human osteosarcoma cells, gaining also information about their phytochemical composition. Secondly, the topic of plant chemodiversity was deepened in cooperation with the Molecular Interaction Ecology research group of the German Center for Integrative Biodiversity Research by studying *Solanum dulcamara* chemotypes through a MS-based metabolomics approach.

3.1 Antitumor Potential and Phytochemical Profile of Plants from Sardinia (Italy), a Hotspot for Biodiversity in the Mediterranean Basin

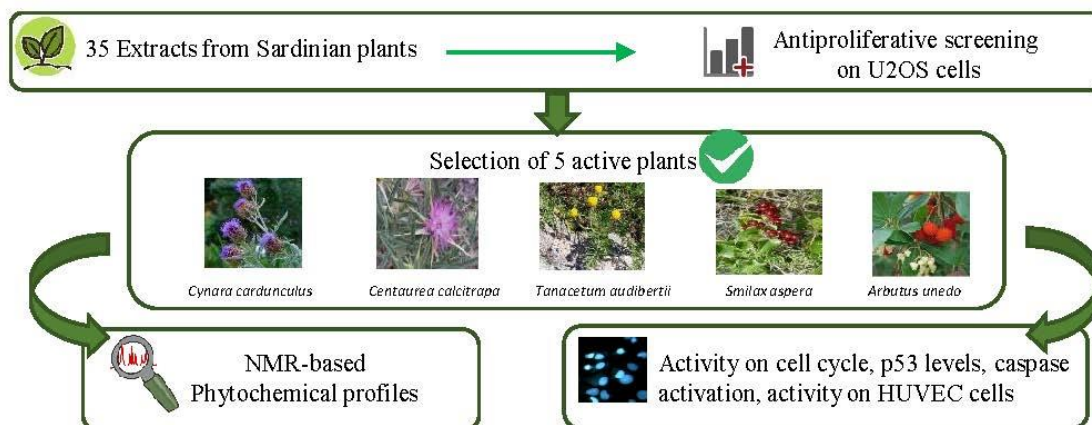
This article has been published in *Plants* Journal:

Cappadone, C., Mandrone, M., Chiocchio, I., Sanna, C., Malucelli, E., Bassi, V., Picone, G., Poli, F. (2020). Antitumor potential and phytochemical profile of plants from sardinia (Italy), a hotspot for biodiversity in the mediterranean basin. *Plants*, 9(1), 26. doi:10.3390/plants9010026

Keywords: Sardinian plants; antitumor activity; cell cycle; apoptosis; NMR profiling; sesquiterpene lactones

Abstract

Sardinia (Italy), with its wide range of habitats and high degree of endemism, is an important area for plant-based drug discovery studies. In this work, the antitumor activity of 35 samples from Sardinian plants was evaluated on human osteosarcoma cells U2OS. The results showed that five plants were strongly antiproliferative: *Arbutus unedo* (AuL), *Cynara cardunculus* (CyaA), *Centaurea calcitrapa* (CcA), *Smilax aspera* (SaA), and *Tanacetum audibertii* (TaA), the latter endemic to Sardinia and Corsica. Thus, their ability to induce cell cycle arrest and apoptosis was tested. All extracts determined cell cycle block in G2/M phase. Nevertheless, the p53 expression levels were increased only by TaA. The effector caspases were activated mainly by CyaA, TaA, and CcA, while AuL and SaA did not induce apoptosis. The antiproliferative effects were also tested on human umbilical vein endothelial cells (HUVEC). Except for AuL, all the extracts were able to reduce significantly cell population, suggesting a potential antiangiogenic activity. The phytochemical composition was first explored by ¹H NMR profiling, followed by further purifications to confirm the structure of the most abundant metabolites, such as phenolic compounds and sesquiterpene lactones, which might play a role in the measured bioactivity.



Introduction

Natural products (NP)-based drug discovery strongly benefits from research conducted in regions with high biodiversity and endemism [1,2]. In this context, Sardinia (Italy) deserves particular attention. This island is a hotspot for biodiversity, with a wide range of habitats and high degree of endemism, due to its geographical isolation and high geological and geomorphological diversification [3,4].

Sardinian flora consists of 2441 taxa [5], of which 295 taxa are endemic [6]. Among them, 189 are exclusive to Sardinia, 90 are Sardinian–Corsican endemics, and 16 taxa are also present in the Tuscan Archipelago [6]. Even though scientific evidence confirmed their interesting phytochemical and biological features [7,8,9,10], to date most Sardinian endemic plants remained scantily or not at all investigated.

In addition, plant-based traditional medicine is still widely practiced and documented in Sardinia (Table 1). Ethnobotany plays also an important role in NP-based drug discovery, providing precious information about plant properties and uses, thus, increasing the chances to individuate active natural products with a good safety profile.

Table 1. Ethnobotanical use of investigated plants in Sardinian traditional medicine. Up-to-date information on plants analyzed in this work. Traditional uses related to specific organs as well as preparation are reported.

Plant species	Plant Organ and label	Ethnobotanical use in Sardinia	Preparation
<i>Arbutus unedo</i> L.	Fruits (AuF)	Astringent [22, 23], blood circulation (atherosclerosis) [24]	Decoction
		Wound healing [25, 26]	Cataplasm
	Leaves (AuL)	Inflammations of intestine, kidney, bladder [25]	Decoction (together with fruits and roots)
		Antipyretic, diarrhea [26-28], intestinal pains, as a vulnerary [29], diuretic, against cystitis and nephritis [22], asthma and bronchitis [28]	Decoction
<i>Asphodelus ramosus</i> L. subsp. <i>ramosus</i>	Rhizome (ArRh)	Sore throat, skin diseases [24]	Decoction
	Leaves (ArL)	Skin disease (chilblain) [24, 29], hemorrhoids and impetigo [30]	Cataplasm
		Diuretic (not recommended for patient affected by rheumatisms) [22]	Decoction
<i>Carlina gummifera</i> (L.) Less.	Leaves (CgL)	Diuretic [27, 30], cholagogue, stomachic and diaphoretic [30]	Decoction and Infusion
<i>Centaurea calcitrapa</i> L.	Aerial parts (CcA)	Antipyretic, digestive, for constipation and diarrhea [22, 31]	Decoction
		Antiseptic [31]	Juice

<i>Centaurea horrida</i> Badarò ^a	Aerial parts (ChA)	N.D.*	-
<i>Centaurea napifolia</i> L.	Aerial parts (CnA)	Nutritional purposes: aerial parts are often included in the diet [32]	Direct ingestion
<i>Cistus monspeliensis</i> L.	Aerial parts (CmA)	Topically for wound healing [30]	Poultice obtained by pressing fresh leaves between two pieces of wood
<i>Cistus salvifolius</i> L.	Aerial parts (CsA)	N.D.*	-
<i>Cynara cardunculus</i> L.	Aerial parts (CycA)	Hepatoprotective, blood depurative, hypocholesterolemic, digestive, intestinal spasmolytic [24, 33]	Decoction
		Liver diseases [28]	Infusion
<i>Ferula arrigonii</i> Bocchieri ^b	Leaves (FaL)	N.D.*	-
	Roots (FaR)	N.D.*	-
<i>Galactites tomentosa</i> Moench	Aerial parts (GtA)	Nutritional purposes: aerial parts are often included in the diet [32]	Direct ingestion
<i>Genista corsica</i> (Loisel.) D ^b	Aerial parts, Flowers (GcA)	In Corse, flowers were used as disinfectant of wounds and abrasions [32]	Infusion
<i>Glechoma sardo</i> a (Bég.) Bég. ^b	Aerial parts (GsA)	Treatment of respiratory diseases, chronic catarrh, bronchitis, asthma and to heal wounds [22]	Infusion of steam and flowers in water or milk
<i>Hypericum hircinum</i> L. ssp <i>hircinum</i> ^c	Aerial parts (HhA)	Burns and wounds healing [22]	Macerate in olive oil
		For rheumatic and sciatic pains and for dislocations and sprains [22]	Macerated in olive oil and white wine, followed by evaporation of the wine
<i>Hypericum scruglii</i> Bacch., Brullo & Salmeri ^a	Aerial parts (HsA)	N.D.*	-
<i>Lavandula stoechas</i> L.	Aerial parts (LsA)	Against ringworm, skin diseases and wounds healing [22]	Maceration in spirit
		Treatment of migraine, vertigo, asthma, palpitation, whooping cough, laryngitis, bronchitis, rheumatism [22, 23], sedative and skin diseases [24]	Infusion
		Treatment of skin diseases [24]	Direct application of leaves
<i>Limonium morisianum</i> Arrigoni ^a	Aerial parts (LmA)	N.D.*	-
<i>Myrtus communis</i> L.	Fruits (McF)	Vulnerary, cough, sedative, digestive [21]	Decoction
		Against cough and catarrh [25] and eupeptic [30]	Decoction (together with leaves)
	Leaves (McL)	Digestive [25] Wound healing [30]	Macerated in spirit Dried and powdered for topical application

		Digestive and as an agent to treat respiratory ailments, as vulnerary, against hemorrhoids, to treat sweaty feet [22] catarrhal cough [26]	Infusion
		Digestive, treatment of respiratory inflammations and hemorrhoids [22]	Fresh leaves pack
		Vulnerary, cough, sedative, digestive [23] bronchitis and asthma [28]	Decoction
<i>Pistacia lentiscus</i> L.	Fruits (PIF)	Cutaneous inflammations [30]	Fresh-squeezed and heated for topical application
		Halitosis [22]	Fresh fruits
		Catarrhal cough, gingivitis, sore throat [30], stomachache [28]	Decoction
	Leaves (PIL)	Treatment of gingivitis, sore throat [30]	Decoction of fresh leaves to use as mouthwash
		Stomatitis, cough sedative, skin diseases [24]	Decoction
		Against ticks [25]	Fumigation
		Anti-catarrhal [22], against cough and against bad breath and as an anti-sudorific [29]	Infusion
<i>Pistacia terebinthus</i> L. ssp. <i>terebinthus</i>	Leaves (PtL)	Catarrhal cough [26]	Decoction
<i>Plagius flosculosus</i> (L.) Alavi & Heywood ^b	Aerial parts (PfA)	N.D.*	-
<i>Ptilostemon casabonae</i> (L.) Greuter ^d	Aerial parts (PcA)	Antispasmodic [32]	Direct ingestion
<i>Rosmarinus officinalis</i> L.	Aerial parts (RoA)	Stomachache [30], cholagogue, general tonic, against common cold, hair loss [25], inappetence, digestive, diuretic, sedative, headache, pruritus [21]	Infusion
		Hepatic [24], diarrhea [30], mucolytic, anti-inflammatory, tooth care, colic, tonic for blood pressure, joint pains [33], antitussive, antispasmodic, migraine, digestive [25], taenifuge, asthma, bronchitis. Stomachic [28]	Decoction
		Anti-rheumatic [28]	Cataplasm
<i>Santolina corsica</i> Jord. & Fourr ^b	Aerial parts (ScA)	N.D.*	
<i>Scolymus hispanicus</i> L. subsp. <i>hispanicus</i>	Aerial parts (ShA)	Nutritional purposes: young stems are often included in the diet [32]	Direct ingestion
<i>Silybum marianum</i> (L.) Gaertn.	Aerial parts (SmA)	Treatment of bleeding, diuretic, hypotensive, sudorifer in case of pneumonia and chronic catarrh [22]	Decoction (together with the seeds)
<i>Smilax aspera</i> L.	Aerial parts (SaA)	Treatment of rheumatisms, skin diseases [24], hemorrhoids [28]	Cataplasm
		Sudorific and blood cleanser [24, 27]	Decoction
		Toothache [28]	Drops of fresh-squeezed juice applied on the gums
<i>Stachys glutinosa</i> L. ^c	Aerial parts (SgA)	Antiseptic, antispasmodic [32]	Infusion
		Cholagogue, diuretic and hepatoprotective [27], common cold [28]	Decoction
<i>Tanacetum audibertii</i> (Req.) DC ^c	Aerial parts (TaA)	Digestive, vermifuge, anti-arthritis and to treat menstrual disorders [30]	Decoction

<i>Thymus herba barona</i> Loisel. ^e	Aerial parts (ThA)	Antitussive, expectorant, antispasmodic, collutory [22], anthelmintic, treatment of stomachache [24], sore throat, common cold, tonic and anti anaemic, diuretic [28]	Decoction or infusion
		Against foot perspiration and urticaria [25]	Powder obtained crushing aerial parts
		Rheumatisms [24]	Cataplasm
		Catarrhal, antipyretic [24] Lung diseases [24]	Macerated in wine Vaporization

^a Endemic species of Sardinia; ^b endemic to Sardinia and Corsica; ^c endemic to Sardinia, Corsica, and Tuscan Archipelago; ^d endemic to Sardinia (Italy), Corsica, and the Hyères islands (France); ^e endemic to Sardinia, Corsica, and Majorca (Spain); * N.D. = Not documented, there are no published data on the ethnobotanical use of these plants.

Several studies have demonstrated the role of medicinal plants in prevention and treatment of cancer [11], one of the leading causes of morbidity and mortality worldwide, responsible for one in eight deaths worldwide [12]. Chemotherapy and radiotherapy, routinely used for cancer treatment, are not devoid of their own intrinsic problems, such as the scarce selectivity toward cancer cells or the onset of drug resistance, requiring further research and treatment development. Next to common targets for tumor therapy, such as cell cycle inhibitors or proapoptotic agents, there are often angiogenesis modulators, especially in combined treatments [13]. The solid tumors, in fact, require an increased blood supply to support their growth, thus, angiogenesis is critical for the initiation, growth, and metastasis of these tumors [14].

As previously mentioned, in cancer treatment, the contribution of natural drugs has been both historically and currently remarkable [11,15]. Moreover, the preventive or antitumor activity of plant extracts was explored, attributing the result to the combined action of various phytochemicals rather than a single molecule [16,17]. Epidemiological studies also established associations between certain dietary patterns and reduced cancer risk [18,19], and significant results were obtained in vitro and in vivo on different food secondary metabolites such as carotenoids, phenolic, and organosulfur compounds [20,21].

On this basis, this work aimed at exploring the in vitro anticancer potential of a wide number of Sardinian plants, investigating the mechanisms of activity and the phytochemical profiles of the most active ones.

Results and Discussion

Plant Traditional Uses and Screening of Antiproliferative Effect

Firstly, a literature survey on uses in traditional Sardinian medicine of all the analyzed plants was conducted. The results are reported in Table 1.

Out of 30 plants, 18 resulted in being widely and commonly used for medicinal or nutritional purposes, while 13 are endemic and little known. For five of them (*Centaurea horrida*, *Ferula arrigonii*, *Hypericum scruglii*, *Limonium morisianum*, and *Plagius flosculosus*), there are no literature data available on their uses in traditional medicine, probably because of their rarity. They were included in the study for their importance as endemic species of Sardinia.

As a first line of screening, all plant extracts underwent MTT, 3-(4,5-dimethylthiazol-2-yl)-2,5-diphenyltetrazolium bromide assay to evaluate their growth inhibition activity on U2OS cells. Cells were treated for 24 h with plant extracts at two fixed concentrations (50 and 100 µg/mL), and the extracts which reduced cell growth by at least 20% were considered promisingly active and selected for further investigations. On this basis, five extracts significantly reduced osteosarcoma cell viability, namely: *Arbutus unedo* (AuL), *Centaurea calcitrapa* (CcA), *Cynara cardunculus* (CycA), *Smilax aspera* (SaA), *Tanacetum audibertii* (TaA) (Figure 1A).

determined a block of cell population in G2/M phase, even though of different entities, and as a consequence a variation of cell percentage in G0/G1 and S phases. In particular, the increase of cell percentage in G2/M phase became more consistent after treatment with CycA and TaA, reaching values above 50% (Figure 2A).

Several anticancer agents induce cell cycle arrest involving the pathway of the tumor suppressor p53 [34]; thus, the expression levels of this protein were analyzed by immunofluorescence after treatment with CycA and TaA. The TaA extract significantly affected p53 levels: the fluorescence mean channel went from 18 to 30 on a logarithmic scale, corresponding to an increase of the protein levels by 60% compared to the controls. On the contrary, CycA did not involve the p53 protein, as its levels in the treated cells were comparable to those of the controls (Figure 2B). Therefore, the two extracts exerted their effects through different mechanisms, involving various targets and signal transduction pathways. It is well known that many proapoptotic agents, including natural compounds and chemotherapeutics drugs, are able to induce apoptosis without any changes in p53 levels [35,36]. In particular, it is reported that doxorubicin-induced apoptosis on p53-null human osteosarcoma cells was characterized by an increase of ROS production, suggesting that ROS might act as the signal molecules even in the absence of p53 upstream cell death process [37].

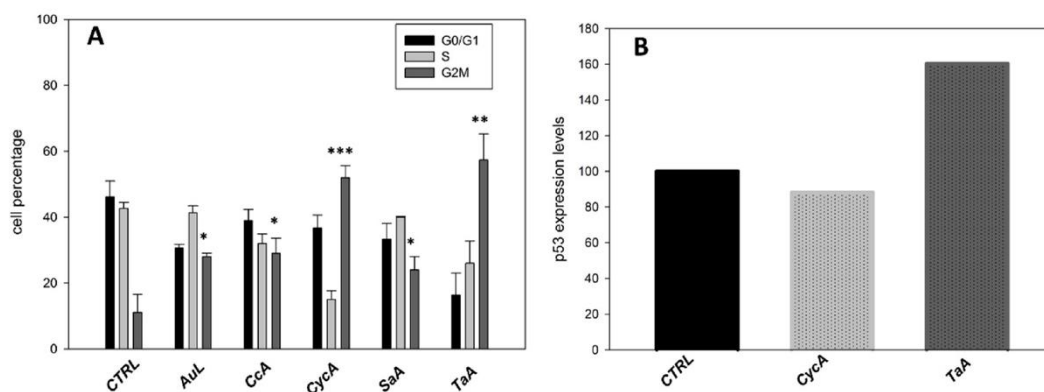


Figure 2. Effects of most potent plant extracts on cell cycle progression and p53 levels. (A) Cell cycle distribution of U2OS after 48 h of treatment with the plant extracts. Data are presented as means \pm SD of three different experiments. Differences were considered significant when $p \leq 0.05$ (* $p \leq 0.05$; ** $p \leq 0.05$; *** $p \leq 0.001$). (B) Flow cytometric analysis of p53 protein levels after CycA or TaA treatment. The histograms represent the protein expression levels with respect to the control taken arbitrarily as 100%. Results shown are representative data from three similar experiments.

Assessment of Apoptotic Effect of Selected Extracts

To give some insights into the biological effects of the active extracts, it was determined whether they induced apoptosis. Firstly, the morphology of the treated cells was evaluated. As expected, a significant reduction of adherent cells was visible as well as many floating cells, especially with CycA and TaA extracts (Figure 3A). Cells were stained with HOECHST nuclear probe to discriminate between apoptotic and necrotic death: the typical nuclear fragmentation of apoptotic cells, associated with the higher fluorescence intensity, was evident in treated samples, confirming the more prominent cytotoxicity of the CycA and TaA extracts (Figure 3B).

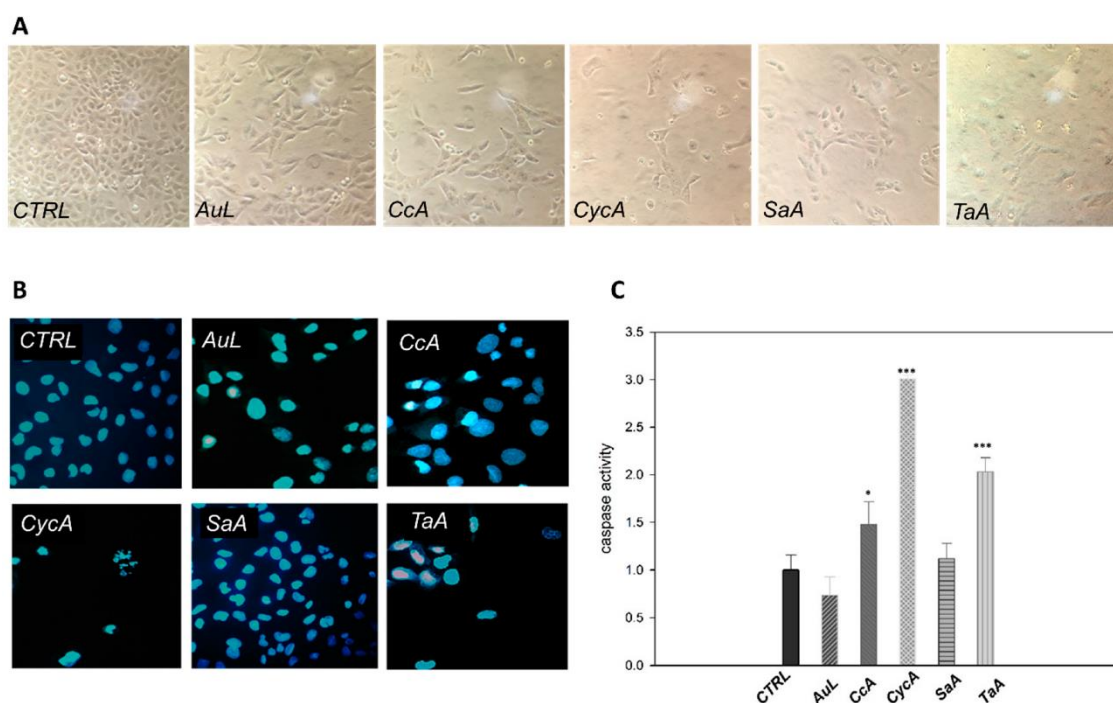


Figure 3. Apoptotic effects on U2OS cells treated for 48 h with the selected extracts: morphological changes and caspase activity. **(A)** Images acquired by optical microscope. **(B)** Images acquired by fluorescence microscope after HOECHST staining. (All the images were taken at the same magnification and depict microscopic fields representative of the whole cell population.) **(C)** Caspase activity assay (fold change of protein activity was calculated by taking untreated cells as a control = 1). Bar graphs represent means ± SD determined from at least three independent experiments. Differences were considered significant when $p \leq 0.05$ (* $p \leq 0.05$; *** $p \leq 0.001$).

It is well known that activation of effector caspases represents a clear marker of apoptotic cell death [38]. Hence, to evaluate the apoptotic effect of the selected extracts on osteosarcoma cells, the caspase-3 activity was determined. The histogram in Figure 3C shows that three plants triggered a significant caspase activation, although with different degrees. However, the higher induction was observed with CycA, followed by TaA and finally by CcA extracts. On the contrary, the antiproliferative effects of AuL and SaA extracts did not culminate in apoptotic events and these latter can be considered cytostatic rather than cytotoxic agents.

Comparison of the Selected Plants' Effects on U2OS and HUVEC Cells

A growing number of research has shown that angiogenesis is a hallmark of tumor development, becoming an attractive target for anticancer chemotherapy [39,40]. Furthermore, inhibiting angiogenesis before it starts (angio-prevention) allows blocking the expansion of hyperplastic foci and subsequent tumor development at the premalignant stage. Endothelial cell proliferation and migration are the key steps of the angiogenic process. Therefore, we investigated the effects of the most active extracts on the proliferation of human endothelial vein cells. As previously stated for Figure 1, a reduction of cell viability of at least 20% was considered significant. The data obtained clearly showed that four out of five tested extracts induced a marked cytotoxicity also in endothelial cells. In particular, CcA and CycA reduced the cell viability by 90% at both 50 $\mu\text{g/mL}$ and 100 $\mu\text{g/mL}$ concentrations. SaA and TaA reduced the viability by 30% and 50%, respectively, only at 100 $\mu\text{g/mL}$ concentration, similarly to osteosarcoma U2OS cells. Although this preliminary result requires further investigations, our findings suggest additional activity of these extracts, useful to contrast tumor growth. On the other hand, the lack of toxicity of AuL against HUVEC cells makes this extract interesting for the selectivity toward tumor cells (Table 2).

Table 2. Effects of five most active plant extracts on U2OS and HUVEC cell viability. Cells were treated at 50 and 100 $\mu\text{g/mL}$ concentrations for 24 h. Data are presented as means \pm SD of three replicated experiments and represent the percentage of viable cells with respect to the control taken arbitrarily as 100%.

Extracts	U2OS cells		HUVEC cells	
	50 $\mu\text{g/mL}$	100 $\mu\text{g/mL}$	50 $\mu\text{g/mL}$	100 $\mu\text{g/mL}$
AuL	79.6 \pm 7.7	56 \pm 5.5	111.8 \pm 0.63	104.7 \pm 4.6
CcA	90 \pm 2	50 \pm 6.5	6.5 \pm 0.29	6.4 \pm 0.05
CycA	45 \pm 1.4	29 \pm 9.9	6.5 \pm 0.02	7.7 \pm 0.37
SaA	85.4 \pm 5.5	68.3 \pm 0.7	114.2 \pm 0.08	77.3 \pm 1.11
TaA	96.9 \pm 12.9	56.9 \pm 3.9	98.9 \pm 0.07	50.4 \pm 1.5

Phytochemical Analyses

Since the results showed that *Arbutus unedo* (leaves) (AuL), *Cynara cardunculus* (aerial parts) (CycA), *Centaurea calcitrapa* (aerial parts) (CcA), *Smilax aspera* (aerial parts) (SaA), and *Tanacetum audibertii* (aerial parts) (TaA) were promising for their biological activities, they were subjected to further phytochemical investigations. Three of them (CycA, CcA, TaA) belong to the Asteraceae family and, among them, *T. audibertii* is endemic to Sardinia and Corsica.

Firstly, ^1H NMR profiling was performed to acquire a preliminary overview of the main metabolites present in the extracts (Figure 4). Both secondary and primary metabolites (such as amino acids, carbohydrates, and organic acids) were detected in the extracts (diagnostic ^1H NMR signals are listed in Table S2 in SI). The content of the main metabolites was then determined, on the basis of the internal standard TMSP, as reported in Table 3.

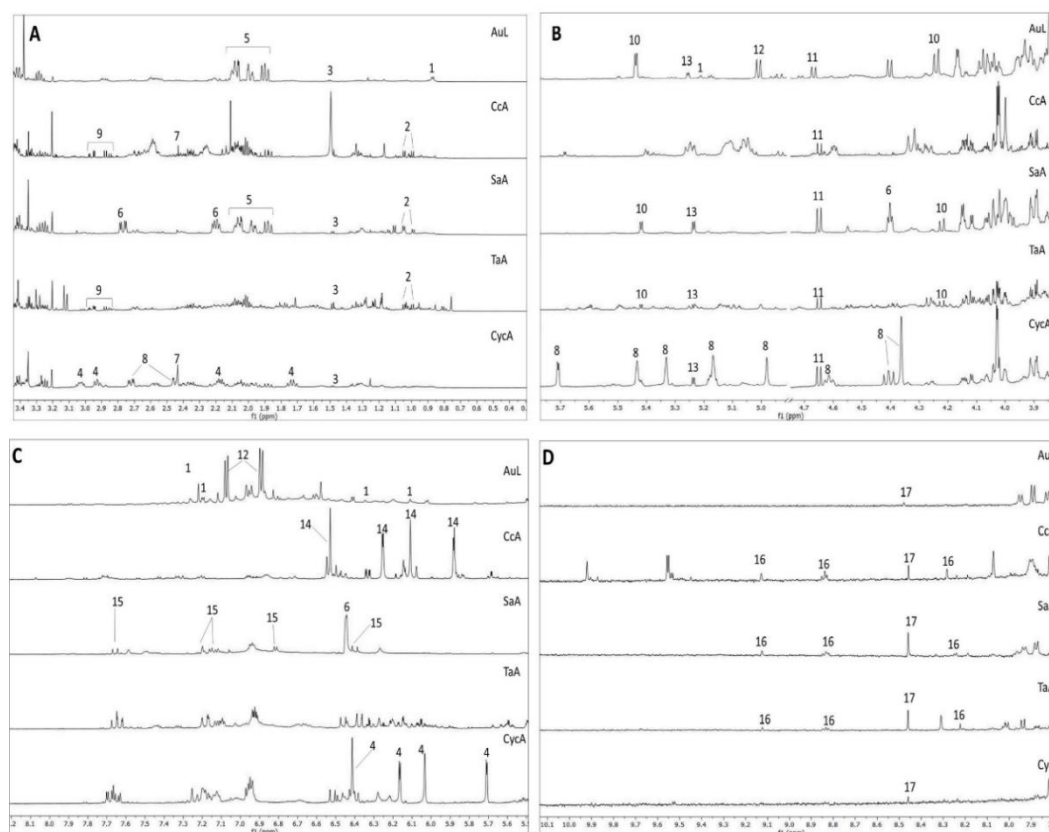


Figure 4. ^1H NMR extended spectral regions of AuL; CcA; SaA; TaA; CycA (from top to bottom). (A) region from δ 0.4 to 3.4; (B) from δ 3.4 to 5.4; (C) from δ 5.4 to 8.1; (D) from δ 7.8 to 10.00. Numbers indicate diagnostic signals of the most abundant metabolites: *O*-rhamnosyl flavonoid (1), valine (2), alanine (3), cynaropicrin (4), quinic acid (5), shikimic acid (6), succinic acid (7), malic acid (8), aspartic acid (9), sucrose (10), β -glucose (11), arbutin (12), α -glucose (13), sesquiterpene lactone-derivative (14), caffeic acid (15), trigonelline (16), formic acid (17). Spectra were measured in D_2O -buffer (pH 6.0) using TMS $^+$ as standard, residual water signal has been removed.

Table 3. Estimated amount of metabolites by ^1H NMR analysis.

Metabolite	Diagnostic ^1H NMR signal (δ) used for the quantification and number of underlying proton/s (in brackets)	Metabolite quantity in the extract ($\mu\text{g}/\text{mg}$ of extract)				
		AuL	CycA	CcA	TaA	SaA
alanine	1.48 (3H)	1.4	2.0	-	8.9	3.7
arbutin	7.07 (2H)	75	-	-	-	-
aspartate	2.96 (1H)	-	-	17	33	-
caffeic acid	7.62 (1H)	-	-	-	-	13
cynaropicrin	6.16 (1H)	-	159	-	-	-
α -glucose	5.2 (1H)	22	24	-	-	40
β -glucose	4.59 (1H)	36	49	-	34	88
isoleucine	1.06 (3H)	-	-	-	-	19
quinic acid	1.87 (1H)	142	43	-	-	193
shikimic acid	6.45 (1H)	-	-	-	-	141
sucrose	5.4 (1H)	138	-	-	45	79

Regarding secondary metabolites, AuL showed a high concentration of arbutin, a glycoside hydroquinone which is considered the main active principle of this plant [41]. The NMR profiling highlighted also the presence of O-rhamnosyl flavonoid, showing typical signals of α -rhamnose, namely the doublet of the methyl group resonating around δ 0.89. Both arbutin and flavonoids might play a role in the measured biological activities [42,43].

Since, in the first screening, both leaves (AuL) and fruits (AuF) of *Arbutus unedo* were tested, and only leaves were found active, the ^1H NMR-based phytochemical profiles of these two samples were also compared. The profile of AuF lacked both arbutin and rhamnosyl flavonoid signals (Figure S1), supporting the importance of these compounds for the bioactivity of AuL.

From the ^1H NMR profile of CycA, the guaiaine-type sesquiterpene lactone cynaropicrin resulted in being the most abundant metabolite (see Table A1 and Figure S2 for structure elucidation).

Interestingly, despite its high lipophilicity, this compound was found highly concentrated (159.4 $\mu\text{g}/\text{mg}$ of extract) in the extract solubilized in D_2O -buffer. This phenomenon is quite common in natural products chemistry, since the inclusion of a lipophilic compound in a complex mixture of metabolites, such as a plant extract, often increases its solubility in water [44]. The discrete concentration of cynaropicrin found in the water medium is interesting also because CycA is traditionally prepared in the form of a decoction or infusion (Table 1).

Cynaropicrin is potentially one of the most important active principles responsible for the bioactivity of CycA [45]. Similarly to CycA, the bioactivity of the other plants belonging to Asteraceae might be due to sesquiterpene lactones, which are typical of this plant family, and are reported to possess antitumor potential [46]. Moreover, several studies report the ability of these plant extracts to inhibit the proliferation mainly of breast cancer cells, but also of hematological cancer [47,48].

Regarding CcA, the ^1H NMR profile clearly presented signals ascribable to sesquiterpene lactones [48]. In particular, the geminal protons of the double bond in position 13 on the γ -lactone were clearly visible in the CcA profile. They showed two doublets with chemical shift of δ 6.05 and 5.59 and coupling constant of 3.23 Hz

(calculated by J-res experiment), with HSQC correlation to the carbon at δ 119.24, and HMBC and COSY correlation to carbon at δ 52.72 and proton at δ 3.08, respectively, which are characteristic chemical shifts of position 7 of this nucleus. The latter carbon, in turn, showed HMBC correlation to a proton resonating at δ 2.50 (linked to carbon at δ 51.41), which is typical of position 5 of the molecule (Figures S3 and S4). High antioxidant and cytotoxicity activities on HeLa and Vero cell lines were reported for *Centaurea calcitrapa* [49]. Our results confirm the capability of the hydroalcoholic plant extract to inhibit cell proliferation on another cell type, highly proliferating and undifferentiated such as the U2OS cell line.

Interestingly, in this work, two other species of *Centaurea* were tested (CnA and ChA) showing no relevant bioactivity. The ^1H NMR profiles of all three *Centaurea* species were recorded and compared. In the ChA profile, no signals ascribable to γ -lactone were visible, while in CnA, they were present, showing a lower intensity compared to the CcA profile (Figure S5 in SI). This data might support the importance of these compounds for the measured bioactivity.

The phytochemical profile of SaA showed a high quantity of shikimic acid and quinic acid, together with caffeic acid. There are very few studies on potential antiproliferative of *Smilax aspera*. It is reported that steroidal saponins and anthocyanins have been isolated from this plant, and that some of these compounds exhibit cytotoxic activity against human normal amniotic and human lung carcinoma cell lines [50,51]. We demonstrated that it induces cytostatic effects on osteosarcoma cells.

Moreover, flavonoid and phenolic content of the five selected plants were determined, and the results were compared by one-way ANOVA test (Figure S6). The phenolic content ranged from 76.97 to 25.68 mg GAE/g of extract, with the following order of concentration: AuL > SaA > TaA > CycA > CcA. Total flavonoid content ranged from 52.3 to 16.09 mg RE/g of extract. No significant differences were found among the samples, with the exception of TaA, which resulted as the extract with the highest content of flavonoids. It is noteworthy that samples treated with this latter extract showed a marked apoptosis induction, characterized by significant G2/M arrest and increased p53 level. The high phenolic content could explain the clear proapoptotic effect, as it is well known that this class of compounds is able to induce apoptosis via the p53 pathway [39].

Our work demonstrated for the first time the antitumor potential of *Tanacetum audibertii*, as only antifungal properties have been documented in the literature [52].

Materials and Methods

Chemicals

All reagents were purchased from Sigma Aldrich (Milano, Italy), except the deuterated solvents, which were purchased by Eurisotop (Cambridge, UK).

Plant Material

All plants were collected at the flowering stage. Species were botanically identified by Dr. Cinzia Sanna and voucher specimens were deposited at the General Herbarium of the Department of Life and Environmental Sciences, University of Cagliari (Table 4). Regarding selected endemic species, they are not protected by local or international regulations. Furthermore, the locations where they were harvested are not included in national or local parks or any other natural protected areas. Therefore, no specific permission was required for their collection.

Table 4. List of the plants analyzed in this work. Plant name, family, considered plant organ and adopted label, harvesting date and GPS coordinates, and voucher number are reported.

Plant name	Family	Plant organ and sample label in brackets	GPS coordinates	Harvesting date	Voucher
<i>Arbutus unedo</i> L.	Ericaceae	Fruits (AuF)	39°45'37.8"N 9°30'31.0"E	December 2017	Herbarium CAG 878
		Leaves (AuL)	39°45'37.8"N 9°30'31.0"E	December 2017	
<i>Asphodelus ramosus</i> L. subsp. <i>ramosus</i>	Asphodelaceae	Rhizome (ArRh)	39°10'38.7"N 9°22'50.3"E	April 2017	Herbarium CAG 1405
		Leaves (ArL)	39°10'38.7"N 9°22'50.3"E	April 2017	
<i>Carlina gummifera</i> (L.) Less.	Asteraceae	Leaves (CgL)	39°45'44.2"N 9°40'16.9"E	July 2018	Herbarium CAG 770
<i>Centaurea calcitrapa</i> L.	Asteraceae	Aerial parts (CcA)	39°18'02.3"N 8°53'39.4"E	June 2017	Herbarium CAG 781
<i>Centaurea horrida</i> Badarò*	Asteraceae	Aerial parts (ChA)	40°57'51.6"N 8°12'05.0"E	June 2017	Herbarium CAG 777
<i>Centaurea napifolia</i> L.	Asteraceae	Aerial parts (CnA)	39°16'51.5"N 8°56'01.5"E	June 2017	Herbarium CAG 784
<i>Cistus monspeliensis</i> L.	Cistaceae	Aerial parts (CmA)	39°45'44.2"N 9°40'16.9"E	April 2018	Herbarium CAG 135

<i>Cistus salvifolius</i> L.	Cistaceae	Aerial parts (CsA)	39°45'44.2"N 9°40'16.9"E	April 2018	Herbarium CAG 135/C
<i>Cynara cardunculus</i> L.	Asteraceae	Aerial parts (CycA)	39°18'02.3"N 8°53'39.4"E	April 2017	Herbarium CAG 790
<i>Ferula arrigonii</i> Bocchieri**	Apiaceae	Leaves (FaL)	39°51'37.9"N 8°26'05.2"E	April 2017	Herbarium CAG 612/A
		Roots (FaR)	39°51'37.9"N 8°26'05.2"E	April 2017	
<i>Galactites tomentosa</i> Moench	Asteraceae	Aerial parts (GtA)	39°46'16.7"N 9°30'41.6"E	September 2018	Herbarium CAG 789
<i>Genista corsica</i> (Loisel.) DC**	Fabaceae	Aerial parts (GcA)	39°49'35.0"N 9°20'27.5"E	May 2017	Herbarium CAG 286
<i>Glechoma sardoa</i> (Bég.) Bég**	Lamiaceae	Aerial parts (GsA)	39°57'33.5"N 9°19'13.3"E	June 2017	Herbarium CAG 1104
<i>Hypericum hircinum</i> L. ssp <i>hircinum</i> ⁺	Hypericaceae	Aerial parts (HhA)	39°46'55.8"N 9°30'52.5"E	June 2018	Herbarium CAG 232
<i>Hypericum scruglii</i> Bacch., Brullo & Salmeri*	Hypericaceae	Aerial parts (HsA)	39°45'57.4"N 9°30'41.8"E	June 2018	Herbarium CAG 239/C
<i>Lavandula stoechas</i> L.	Lamiaceae	Aerial parts (LsA)	39°45'44.2"N 9°40'16.9"E	April 2017	Herbarium CAG 1067
<i>Limonium morisianum</i> Arrigoni*	Plumbaginaceae	Aerial parts (LmA)	39°54'33.3"N 9°24'41.0"E	December 2017	Herbarium CAG 909/G
<i>Myrtus communis</i> L.	Myrtaceae	Fruits (McF)	39°45'44.2"N 9°40'16.9"E	December 2018	Herbarium CAG 514
		Leaves (McL)	39°08'22.2"N 8°58'08.9"E	April 2018	
<i>Pistacia lentiscus</i> L.	Anacardiaceae	Fruits (PIF)	39°45'44.2"N 9°40'16.9"E	December 2017	Herbarium CAG 280
		Leaves (PIL)		December 2017	
<i>Pistacia terebinthus</i> L. ssp. <i>terebinthus</i>	Anacardiaceae	Leaves (PtL)	39°47'38.8"N 9°30'38.3"E	June 2018	Herbarium CAG 279
<i>Plagius flosculosus</i> (L.) Alavi & Heywood**	Asteraceae	Aerial parts (PfA)	39°21'45.2"N 8°32'24.1"E	July 2017	Herbarium CAG 743
<i>Ptilostemon casabonae</i> (L.) Greuter**	Asteraceae	Aerial parts (PcA)	39°53'52.7"N 9°26'31.8"E	June 2018	Herbarium CAG 796
<i>Rosmarinus officinalis</i> L.	Lamiaceae	Aerial parts (RoA)	40°34'10.1"N 8°22'57.0"E	May 2017	Herbarium CAG 1091
<i>Santolina corsica</i> Jord. & Fourr**	Asteraceae	Aerial parts (ScA)	40°32'30.6"N 9°36'09.4"E	November 2017	Herbarium CAG 732/A
<i>Scolymus hispanicus</i> L. subsp. <i>hispanicus</i>	Asteraceae	Aerial parts (ShA)	39°03'25.9"N 8°58'46.3"E	June 2018	Herbarium CAG 812
<i>Silybum marianum</i> (L.) Gaertn.	Asteraceae	Aerial parts (SmA)	39°16'51.5"N 8°56'01.5"E	May 2017	Herbarium CAG 801
<i>Smilax aspera</i> L.	Smilacaceae	Aerial parts (SaA)	39°10'38.7"N 9°22'50.3"E	May 2017	Herbarium CAG 1414
<i>Stachys glutinosa</i> L. ⁺	Lamiaceae	Aerial parts (SgA)	39°55'46.1"N 9°27'10.7"E	June 2017	Herbarium CAG 1099
<i>Tanacetum audibertii</i> (Req.) DC**	Asteraceae	Aerial parts (TaA)	40°02'07.9"N 9°17'59.1"E	August 2018	Herbarium CAG 737/A

<i>Thymus herba barona</i> Loisel [§]	Lamiaceae	Aerial parts (ThA)	39°56'01.2"N 9°19'56.9"E	June 2017	Herbarium CAG 1065
--	-----------	--------------------	-----------------------------	-----------	--------------------

* Endemic species of Sardinia

** Endemic to Sardinia and Corsica

⁺ Endemic to Sardinia, Corsica and Tuscan Archipelago

⁺⁺ Endemic to Sardinia (Italy), Corsica and the Hyères islands (France)

[§] Endemic to Sardinia, Corsica and Balearic Islands (Spain)

Preparation of Plant Extracts for Bioactivity Tests and for ¹H NMR Profiling

A total of 30 mg of dried and powdered plant material were extracted by sonication for 30 min using 1.5 mL of MeOH/H₂O (1:1). Subsequently, samples were centrifuged (1700× g) for 20 min and the supernatant was separated from the pellet and dried, firstly in vacuum concentrators (speedVac SPD 101b 230, Savant, Italy) for 2 h to remove MeOH, then the residual extracts were freeze-dried overnight to completely remove the residual H₂O, finally yielding the crude extracts. This extraction procedure is ideal to prepare a small quantity of extracts for in vitro bioactivity tests, thus for screenings of a high number of plants, allowing a minimal consumption of both solvents and plant material. The choice of the extraction solvents was based on metabolomics works [53,54], where MeOH/H₂O (1:1) turned out as the best choice for first-line extraction of generic plant material, having obtained a broad spectrum of compounds.

Extracts were solubilized in H₂O to prepare stock solution at a concentration of 1 mg/mL, which was centrifuged for 10 min (1700× g) and used for testing the biological activities.

For ¹H NMR profiling, 4 mg of freeze-dried extracts were solubilized in 1 mL of phosphate buffer (90 mM, pH 6.0) in D₂O containing standard 0.01% trimethylsilylpropionic-2,2,3,3-d₄ acid sodium salt (TMSP). Samples were centrifuged for 10 min (1700× g) and 700 μL of the supernatant were transferred into NMR tubes for the analysis.

Fractionation and Cynaropicrin Identification

To better characterize predominant secondary metabolites from CycA and AuL, further purification procedures were carried out. The amount of 1 g of CycA was extracted

in 50 mL of MeOH/H₂O (1:1), sonicated for 30 min, and centrifuged for 15 min in 50 mL tubes. The supernatant was dried in a rotary evaporator, yielding 92 mg of extract, which was solubilized in 25 mL of H₂O and subjected to liquid/liquid partition with CHCl₃ (25 mL for three times). The organic phases were collected, anhydricated using Na₂SO₄ anhydrous, filtered, and dried in the rotary evaporator. Cynaropicrin was identified by NMR experiments (¹H NMR; HMBC, HSQC, COSY, J-res) (Figure S2 and Table A1) from the CHCl₃ fraction (yield equal to 21 mg) solubilized in CD₃OD at a concentration of 4 mg/mL.

NMR Measurement and Analysis

¹H NMR spectra, J-resolved (J-res), ¹H-¹H homonuclear, and inverse detected ¹H-¹³C correlation experiments were recorded at 25 °C on a Varian Inova 600 MHz NMR instrument (600 MHz operating at the ¹H frequency) equipped with an indirect triple resonance probe. D₂O was used for internal lock for ¹H NMR profiling and CD₃OD for the other measurements.

For all ¹H NMR analyses, relaxation delay was 2.0 s, observed pulse 5.80 μs, number of scans 256, acquisition time 16 min, and spectral width 9595.78 Hz (corresponding to δ 16.0). For ¹H NMR profiling, a presaturation sequence (PRESAT) was used to suppress the residual H₂O signal at δ 4.83 (power = -6dB, presaturation delay 2 s).

Spectra were processed by Mestrenova software (Mestrelab Research, Santiago de Compostela, Spain), and the analysis of ¹H NMR profiles of extracts was performed based on an in-house library and comparison with literature [55,56]. Estimation of metabolites amount in the crude extracts was calculated by comparison of diagnostic signals and TMSP (internal standard) resonating at δ 0.

Phenolic and Flavonoid Content

The assays were performed in a Spectrophotometer Jasco V-530 as described by Mandrone et al. (2019) [8]. Analyses were performed in triplicate.

Cell Culture and Treatment

Human osteosarcoma cells U2OS were cultured in RPMI 1640 medium, supplemented with 10% fetal bovine serum and 2 mM L-glutamine, at 37 °C in a humidified atmosphere containing 5% CO₂.

Cells were plated at 1×10^4 cells/cm² in Petri dishes and treated with plant extracts after 24 h for all experiments.

Human umbilical vein endothelial cells (HUVEC) were plated on gelatin-coated tissue culture dishes and maintained in phenol red-free basal medium M200 (Life Technologies, Waltham, Massachusetts) containing 10% FBS and growth factors (LSGS, Life Technologies, Waltham, Massachusetts) at 37 °C with 5% CO₂. Cells from passages 3 to 7 were actively proliferating (70%–90% confluent) when samples were harvested and analyzed. Dried extracts were dissolved in ultrapure water at 1 mg/mL and added to cell medium at the appropriate concentration and for the required time depending on the experiments.

MTT Assay

The cells were seeded in a 96-well plate and treated for 24 and 48 h with extracts under test in quadruplicate; controls were treated with an equal volume of water.

A total of 20 µL of tetrazolium salt (2.5 mg/mL) in PBS was added to culture medium for 4 h, then the medium was removed and 100 µL isopropanol was added to each well. The absorbance at 570 nm of the solubilized formazan salt was determined by microplate reader (VICTOR3, PerkinElmer Life and Analytical Sciences, Milan, Italy).

EC₅₀ refers to the concentration of extract which results in a 50% reduction of cell growth, and values for different extracts were obtained by dose–response curve interpolation, using Sigma Plot 10.0 software.

Cell Cycle Analysis

DNA profiles were obtained by cytofluorimetric analysis. After 48 h of treatment, 1×10^6 cells were pelleted and suspended in trisodium citrate 0.1% (*m/v*), RNase 0.1 mg/L, Igepal 0.01% (*v/v*), propidium iodide (PI) 50 mg/L. After 30 min at 37 °C in the dark, cells were analyzed by Bryte HS Biorad cytometer, equipped with Xe-Hg lamp. PI fluorescence was collected on a linear scale at 600 nm and the DNA distribution was analyzed by the Modifit 5.0 software.

Analysis of p53 Expression Levels by Flow Cytometry

The cells were harvested, washed twice with PBS, fixed with 3% paraformaldehyde, washed with 0.1 M glycine in PBS, and permeabilized in 70% ice-cold ethanol. After

fixing, the cells were washed with 1% BSA in PBS and incubated overnight with 1:200 anti-p53 monoclonal antibody (Upstate, MA, USA) in blocking buffer. Then, the cells were washed three times and incubated for 1 h at room temperature in 1:1000 FITC labeled secondary antibody (Sigma Aldrich, Milan, Italy). Finally, the samples were analyzed by flow cytometry. FITC green fluorescence was analyzed at 525 nm on a logarithmic scale by WinDMI 2.8 software.

Caspase Activity Assay

The enzymatic activity of caspase 3 was evaluated by using the colorimetric CaspACE assay system (Promega), according to the manufacturer's instructions. Briefly, treated and control cells were detached, centrifuged, and resuspended in lysis buffer at 5×10^7 cells/mL concentration. Cells were lysed by three freeze–thaw cycles. Cell lysates were centrifuged and supernatant fraction was collected. In a 96-well plate were added Caspase Assay Buffer (32 μ L), DMSO (2 μ L), DTT 100 mM (10 μ L), deionized water to final volume (98 μ L), and 2 μ L of caspase substrate (DEVD-pNA) in each well. After 4 h of incubation at 37 °C, the absorbance at 405 nm was measured and the caspase activity was obtained.

Fluorescence Microscopy

The cells were seeded onto slides and treated with plant extracts. After 24 h of incubation, they were marked with fluorescent dye Hoechst 33,432 0.1 mg/mL for 30 min at 37 °C. Then, the samples were washed twice with PBS and fixed with 4% para-formaldehyde in PBS for 20 min at room temperature in the dark. After two washes in glycine-PBS, samples were embedded in Mowiol and analyzed by a Nikon Eclipse fluorescence microscope.

Statistical Analysis

Values are expressed as the mean \pm SD of three independent experiments (each one performed in triplicate). Statistical analyses were performed using Graph Pad Prism 4 software (La Jolla, CA, USA). For biological assays, the statistical significance of differences among treatment groups was determined by paired Student's T-test. For flavonoids and phenolic content, samples were compared by one-way analysis of

variance (ANOVA), followed by Tukey's honestly significant difference (HSD) post hoc test, considering significant differences at p values <0.05 .

Conclusions

Thirty-five extracts from Sardinian plants were screened for their antitumor potential against U2OS cells. The results showed five plants were endowed with high activity, namely: *Arbutus unedo* (AuL), *Cynara cardunculus* (CycA), *Centaurea calcitrapa* (CcA), *Smilax aspera* (SaA), and *Tanacetum audibertii* (TaA), this latter endemic to Sardinia and Corsica and still scantily investigated. The antiproliferative activity and the phytochemical profiles of these five plants were further investigated. All five extracts caused a block of cell cycle in G2/M phase, and treating with CycA and TaA, the percentage of cells in this phase was higher than 50%. The activity of TaA significantly affected p53 expression levels, while CycA activity did not involve this protein. A significant caspase activation was observed especially for CycA, followed by TaA and CcA. On the contrary, AuL and SaA did not induce apoptotic cell death, suggesting cytostatic rather than cytotoxic effects.

Except for AuL, the other four extracts produced a marked cytotoxicity also on human endothelial vein cells, making them interesting for the additional potential to contrast angiogenesis development. On the other hand, the complete inactivity of AuL on the viability of HUVEC cells indicates its selectivity. The phytochemical analysis revealed a high presence of arbutin and flavonoids in this plant, which might be important for the measured bioactivity. Interestingly, three out of five active plants (CcA, CycA, and TaA), belong to the Asteraceae family, which is renowned for producing bioactive sesquiterpene lactones; in fact, these compounds were detected by NMR analysis.

This study highlighted the potential use of these plants as active ingredients to develop functional food for chemoprevention or adjuvants in cancer therapy. Further phytochemical and biological studies are ongoing.

Supplementary Materials: available online at <https://www.mdpi.com/2223-7747/9/1/26/s1>

Appendix A

Table A1. NMR spectral references for cynaropicrin. Spectra of the purified fraction were measured in CD₃OD. Splitting patterns and coupling constants were determined by J-res experiment.

Position	¹ H (δ; J)	¹³ C (δ)	HMBC	COSY
1	3.00 (ddd; J=11.53; 10.65 Hz; 6.84)	46.22	39.78; 51.32; 74.18; 118.11; 142.84	2.09; 1.74; 2.88
2a	2.09 (ddd; J=13.14; 7.50; 6.84 Hz)	39.78	46.22; 51.32; 74.18; 142.84	1.74; 3.00; 4.49
2b	1.74 (ddd; J=13.14; 11.53; 8.80 Hz)	39.78	46.22; 74.18; 152.92	2.09; 3.00; 4.49
3	4.49 (dd; J=8.80; 7.60 Hz)	74.18	152.92	2.09; 1.74; 5.43; 5.64
4	-	152.92	-	-
5	2.88 (ddd; J=10.65; 9.21 Hz)	51.32	79.81	3.00; 4.33; 4.91; 5.33
6	4.33 (dd; J=11.06; 8.89 Hz)	79.81	75.15	2.88; 3.27
7	3.27 (m)	41.48	ov.	4.33; 5.15; 6.12 5.64
8	5.15 (m)	75.15	ov.	3.27
9a	2.73 (dd; J=14.65; 5.26 Hz)	37.14	118.11; 142.84	2.40; 4.91; 5.15
9b	2.40 (dd; J=14.65; 3.50 Hz)	37.14	118.11; 142.84	2.73; 4.91; 5.15
10	-	142.84	-	-
11	-	138.77	-	-
12	-	170.01	-	-
13a	6.12 (d; J=3.30 Hz)	121.96	41.48; 138.77; 170.01	3.27; 5.64
13b	5.64 (d; J=3.30 Hz)	121.96	41.48; 138.77; 170.01	3.27; 6.12
14a	5.14 (d; J=2.09 Hz)	118.11	37.14; 46.22; 142.84	2.40; 2.73; 4.91
14b	4.91 (d; J=2.09 Hz)	118.11	37.14; 46.22; 142.84	2.40; 2.73; 5.14
15a	5.43 (d; J=1.97 Hz)	122.36	51.32; 74.18; 152.92	2.88; 4.49; 5.33
15b	5.33 (d; J=1.97 Hz)	122.36	51.32; 74.18; 152.92	2.88; 4.49; 5.43
1'	-	165.28	-	-
2'	-	140.80	-	-
3'a	6.30 (d; J=1.40 Hz)	125.70	61.73; 140.80; 165.28	4.30; 5.97
3'b	5.97 (d; J=1.40 Hz)	125.70	61.73; 140.80; 165.28	4.30; 6.30
4'	4.30 (s)	61.73	125.70; 140.80; 165.28	5.97; 6.30

References

1. Bolzani da Silva, V.; Valli, M.; Pivatto, M.; Viegas, C. Natural products from Brazilian biodiversity as a source of new models for medicinal chemistry. *Pure Appl. Chem.* **2012**, *84*, 1837–1846.
2. Henrich, C.J.; Beutler, J.A. Matching the power of high throughput screening to the chemical diversity of natural products. *Nat. Prod. Rep.* **2013**, *30*, 1284–1298.
3. Cañadas, E.; Giuseppe, F.; Peñas, J.; Lorite, J.; Mattana, E.; Bacchetta, G. Hotspots within hotspots: Endemic plant richness, environmental drivers, and implications for conservation. *Biol. Conserv.* **2014**, *170*, 282–291.
4. Fois, M.; Fenu, G.; Cañadas, E.M.; Bacchetta, G. Disentangling the influence of environmental and anthropogenic factors on the distribution of endemic vascular plants in Sardinia. *PLoS ONE* **2017**, *12*, e0182539.
5. Bartolucci, F.; Peruzzi, L.; Galasso, G.; Albano, A.; Alessandrini, A.; Ardenghi, N.M.G.; Astuti, G.; Bacchetta, G.; Ballelli, S.; Banfi, E.; et al. An updated checklist of the vascular flora native to Italy. *Plant Biosyst.* **2018**, *152*, 179–303.
6. Fenu, G.; Fois, M.; Cañadas, E.M.; Bacchetta, G. Using endemic-plant distribution, geology and geomorphology in biogeography: The case of Sardinia (Mediterranean Basin). *Syst. Biodivers.* **2014**, *12*, 181–193.
7. Cagno, V.; Sgorbini, B.; Sanna, C.; Cagliero, C.; Ballero, M.; Civra, A.; Donalisio, M.; Bicchi, C.; Lembo, D.; Rubiolo, P. In vitro anti-herpes simplex virus-2 activity of *Salvia desoleana* Atzei & V. Picci essential oil. *PLoS ONE* **2017**, *12*, e0172322.
8. Mandrone, M.; Bonvicini, F.; Lianza, M.; Sanna, C.; Maxia, A.; Gentilomi, G.A.; Poli, F. Sardinian plants with antimicrobial potential. Biological screening with multivariate data treatment of thirty-six extracts. *Ind. Crop. Prod.* **2019**, *137*, 557–565.
9. Sanna, C.; Scognamiglio, M.; Fiorentino, A.; Corona, A.; Graziani, V.; Caredda, A.; Cortis, P.; Montisci, M.; Ceresola, E.; Canducci, F.; et al. Prenylated phloroglucinols from *Hypericum scruglii*, an endemic species of Sardinia (Italy), as new dual HIV-1 inhibitors effective on HIV-1 replication. *PLoS ONE* **2018**, *13*, e0195168.
10. Sanna, C.; Rigano, D.; Corona, A.; Piano, D.; Formisano, C.; Farci, D.; Franzini, G.; Ballero, M.; Chianese, G.; Tramontano, E.; et al. Dual HIV-1 reverse transcriptase and integrase inhibitors from *Limonium morisianum* Arrigoni, an endemic species of Sardinia (Italy). *Nat. Prod. Res.* **2019**, *33*, 1798–1803.
11. Roy, A.; Ahuja, S.; Bharadvaja, N. A review on medicinal plants against cancer. *J. Plant. Sci. Agric. Res.* **2017**, *2*, 1008.
12. Moten, A.; Schafer, D.; Ferrari, M. Redefining global health priorities: Improving cancer care in developing settings. *J. Glob. Health* **2014**, *4*.
13. Mokhtari, R.B.; Homayouni, T.S.; Baluch, N.; Morgatskaya, E.; Kumar, S.; Das, B.; Yeger, H. Combination therapy in combating cancer. *Oncotarget* **2017**, *8*, 38022–38043.
14. Zuazo-Gatzelu, I.; Casanovas, O. Unraveling the role of angiogenesis in cancer ecosystems. *Front. Oncol.* **2018**, *8*, 248.
15. Sun, L.R.; Zhou, W.; Zhang, H.M.; Guo, Q.S.; Yang, W.; Li, B.J.; Sun, Z.H.; Gao, S.H.; Cui, R.J. Modulation of multiple signaling pathways of the plant-derived natural products in cancer. *Front. Oncol.* **2019**, *9*, 1153.
16. Dutta, R.; Khalil, R.; Green, R.; Mohapatra, S.S.; Mohapatra, S. *Withania somnifera* (Ashwagandha) and withaferin A: Potential in integrative oncology. *Int. J. Mol. Sci.* **2019**, *20*, 5310.
17. Remadevi, V.; Mohan Lathika, L.; Sasikumar Sujatha, A.; Sreeharshan, S. Ficus extract—A promising agent for antimammary tumorigenesis: A review on current status and future possibilities. *Phytother. Res.* **2019**, *33*, 1597–1603.
18. Chen, P.; Li, C.; Li, X.; Li, J.; Chu, R.; Wang, H. Higher dietary folate intake reduces the breast cancer risk: A systematic review and meta-analysis. *Br. J. Cancer* **2014**, *110*, 2327–2338.
19. Toledo, E.; Salas-Salvadó, J.; Donat-Vargas, C.; Buil-Cosiales, P.; Estruch, R.; Ros, E.; Corella, D.; Fitó, M.; Hu, F.B.; Arós, F.; et al. Mediterranean diet and invasive breast cancer risk among women at high cardiovascular risk in the PREDIMED Trial: A randomized clinical trial. *JAMA Intern. Med.* **2015**, *175*, 1752–1760.

20. Crew, K.D.; Brown, P.; Greenlee, H.; Bevers, T.B.; Arun, B.; Hudis, C.; McArthur, H.L.; Chang, J.; Rimawi, M.; Vornik, L.; et al. Phase IB randomized, double-blinded, placebo-controlled, dose escalation study of polyphenon E in women with hormone receptor-negative breast cancer. *Cancer Prev. Res. (Phila)* **2012**, *5*, 1144–1154.
21. Hui, C.; Qi, X.; Qianyong, Z.; Xiaoli, P.; Jundong, Z.; Mantian, M. Flavonoids, flavonoid subclasses and breast cancer risk: A meta-analysis of epidemiologic studies. *PLoS ONE* **2013**, *8*, e54318.
22. Ballero, M.; Floris, R.; Poli, F. Le piante utilizzate nella medicina popolare nel territorio di Laconi (Sardegna centrale). *Boll. Soc. Sarda Sci. Nat.* **1997**, *31*, 207–229.
23. Loi, M.C.; Maxia, L.; Maxia, A. Ethnobotanical Comparison between the Villages of Escolca and Lotzorai (Sardinia, Italy). *J. Herbs Spices Med. Plants* **2005**, *11*, 67–84.
24. Ballero, M.; Poli, F.; Sacchetti, G.; Loi, M.C. Ethnobotanical research in the territory of Fluminimaggiore (south-western Sardinia). *Fitoterapia* **2001**, *72*, 788–801.
25. Ballero, M.; Sacchetti, G.; Poli, F. Plants in folk medicine in the territory of Perdasdefogu (Central Sardinia, Italy). *Allonia* **1997**, *35*, 57–164.
26. Bruni, A.; Ballero, M.; Poli, F. Quantitative ethnopharmacological study of the Campidano Valley and Urzulei district, Sardinia, Italy. *J. Ethnopharmacol.* **1997**, *57*, 97–124.
27. Loi, M.C.; Frailis, L.; Maxia, A. Le piante utilizzate nella medicina popolare nel territorio di Gesturi (Sardegna centro-meridionale). *Atti. Soc. Tosc. Sci. Nat. Mem. Ser. B* **2002**, *109*, 167–176.
28. Loi, M.C.; Poli, F.; Sacchetti, G.; Selenu, M.B.; Ballero, M. Ethnopharmacology of Ogliastra (Villagrande Strisaili, Sardinia, Italy). *Fitoterapia* **2004**, *75*, 277–295.
29. Leonti, M.; Casu, L.; Sanna, F.; Bonsignore, L. A comparison of medicinal plant use in Sardinia and Sicily-De Materia Medica revisited? *J. Ethnopharmacol.* **2009**, *121*, 255–267.
30. Ballero, M.; Bruni, A.; Sacchetti, G.; Poli, F. Le piante utilizzate nella medicina popolare nel comune di Tempio Pausania (Sardegna settentrionale). *Acta Phytother.* **1997**, *1*, 23–29.
31. Ballero, M.; Poli, F. Plants used in folk medicine of Monteleone (Northern Sardinia). *Fitoterapia* **1998**, *69*, 52–64.
32. Atzei, A.D. *Le Piante Nella Tradizione Popolare Della Sardegna*; Carlo Delfino: Sassari, Italy, 2003.
33. Palmese, M.T.; Manganelli, R.E.; Tomei, P.E. An ethno-pharmacobotanical survey in the Sarrabus district (south-east Sardinia). *Fitoterapia* **2001**, *72*, 619–643.
34. Hientz, K.; Mohr, A.; Bhakta-Guha, D.; Efferth, T. The role of p53 in cancer drug resistance and targeted chemotherapy. *Oncotarget* **2016**, *8*, 8921–8946.
35. Sharma, K.; Vu, T.; Cook, W.; Naseri, M.; Zhan, K.; Nakajima, W.; Harada, H. p53-independent Noxa induction by cisplatin is regulated by ATF3/ATF4 in head and neck squamous cell carcinoma cells. *Mol. Oncol.* **2018**, *12*, 788–798.
36. Gupta, K.; Thakur, V.S.; Bhaskaran, N.; Nawab, A.; Babcook, M.A.; Jackson, M.W.; Gupta, S. Green Tea Polyphenols Induce p53-Dependent and p53-Independent Apoptosis in Prostate Cancer Cells through Two Distinct Mechanisms. *PLoS ONE* **2012**, *7*, e52572.
37. Tsang, W.P.; Chau, S.P.Y.; Kong, S.K.; Fung, K.P.; Kwok, T.T. Reactive oxygen species mediate doxorubicin induced p53-independent apoptosis. *Life Sci.* **2003**, *73*, 2047–2058.
38. Shalini, S.; Dorstyn, L.; Dawar, S.; Kumar, S. Old, new and emerging functions of caspases. *Cell Death Differ.* **2015**, *22*, 526–539.
39. Folkman, J. Fighting cancer by attacking its blood supply. *Sci. Am.* **1996**, *275*, 150–154.
40. Wu, J.-G.; Ma, L.; Lin, S.; Wu, Y.; Yi, J.; Yang, B.; Wu, J.-Z.; Wong, K. Anticancer and anti-angiogenic activities of extract from *Actinidia eriantha* Benth root. *J. Ethnopharmacol.* **2017**, *203*, 1–10.
41. Morgado, S.; Morgado, M.; Plácido, A.I.; Roque, F.; Duarte, A.P. *Arbutus unedo* L.: From traditional medicine to potential uses in modern pharmacotherapy. *J. Ethnopharmacol.* **2018**, *225*, 90–102.
42. Curti, V.; Di Lorenzo, A.; Dacrema, M.; Xiao, J.; Nabavi, S.M.; Daglia, M. In vitro polyphenol effects on apoptosis: An update of literature data. *SeminCancer Biol.* **2017**, *46*, 119–131.
43. Jiang, L.; Wang, D.; Zhang, Y.; Li, J.; Wu, Z.; Wang, Z.; Wang, D. Investigation of the pro-apoptotic effects of arbutin and its acetylated derivative on murine melanoma cells. *Int. J. Mol. Med.* **2018**, *41*, 1048–1054.
44. Choi, Y.H.; van Spronsen, J.; Dai, Y.; Verberne, M.; Hollmann, F.; Arends, I.W.C.E.; Witkamp, G.-J.; Verpoorte, R. Are natural deep eutectic solvents the missing link in understanding cellular metabolism and physiology? *Plant Physiol.* **2011**, *156*, 1701–1705.
45. Lepore, S.M.; Maggisano, V.; Lombardo, G.E.; Maiuolo, J.; Mollace, V.; Bulotta, S.; Russo, D.; Celano, M. Antiproliferative effects of cynaropicrin on anaplastic thyroid cancer cells. *Endocr. Metab. Immune* **2019**, *19*, 59–66.

46. Bruno, M.; Bancheva, S.; Rosselli, S.; Maggio, A. Sesquiterpenoids in subtribe Centaureinae (Cass.) Dumort (tribe Cardueae, Asteraceae): Distribution, (13) C NMR spectral data and biological properties. *Phytochemistry* **2013**, *95*, 19–93.
47. Genovese, C.; Brundo, M.; Toscano, V.; Tibullo, D.; Puglisi, F.; Raccuia, S. Effect of *Cynara* extracts on multiple myeloma cell lines. *Acta Hort.* **2016**, *1147*, 113–118.
48. Ramos, P.A.B.; Guerra, Á.R.; Guerreiro, O.; Santos, S.A.O.; Oliveira, H.; Freire, C.S.R.; Silvestre, A.J.D.; Duarte, M.F. Antiproliferative effects of *Cynara cardunculus* L. var. *altilis* (DC) lipophilic extracts. *Int. J. Mol. Sci.* **2016**, *18*, 63.
49. Erol-Dayi, Ö.; Pekmez, M.; Bona, M.; Aras-Perk, A.; Arda, N. Total phenolic contents, antioxidant activities cytotoxicity of three *Centaurea* species: *C. calcitrapa* subsp. *calcitrapa*, *C. ptosimopappa*, *C. spicata*. *Free Radic. Antiox.* **2011**, *1*, 31–36.
50. Ivanova, A.; Mikhova, B.; Batsalova, T.; Dzhambazov, B.; Kostova, I. New furostanol saponins from *Smilax aspera* L. and their *in vitro* cytotoxicity. *Fitoterapia* **2011**, *82*, 282–287.
51. Longo, L.; Vasapollo, G. Extraction and identification of anthocyanins from *Smilax aspera* L. berries. *Food Chem.* **2006**, *94*, 226–231.
52. Maxia, A.; Sanna, C.; Piras, A.; Porcedda, S.; Danilo, F.; Gonçalves, M.; Cavaleiro, C.; Salgueiro, L. Chemical composition and biological activity of *Tanacetum audibertii* (Req.) DC. (Asteraceae), an endemic species of Sardinia Island, Italy. *Ind. Crop. Prod.* **2015**, *65*, 472–476.
53. Kim, H.K.; Choi, Y.H.; Verpoorte, R. NMR-based metabolomic analysis of plants. *Nat. Protoc.* **2010**, *5*, 536–549.
54. Mandrone, M.; Coqueiro, A.; Poli, F.; Antognoni, F.; Choi, Y.H. Identification of a collagenase-inhibiting flavonoid from *Alchemilla vulgaris* using NMR-based metabolomics. *Planta Med.* **2018**, *84*, 941–946.
55. Mandrone, M.; Scognamiglio, M.; Fiorentino, A.; Sanna, C.; Cornioli, L.; Antognoni, F.; Bonvicini, F.; Poli, F. Phytochemical profile and α -glucosidase inhibitory activity of Sardinian *Hypericum scruglii* and *Hypericum Hircinum*. *Fitoter* **2017**, *120*, 184–193.
56. Mandrone, M.; Antognoni, F.; Aloisi, I.; Potente, G.; Poli, F.; Cai, G.; Faleri, C.; Parrotta, L.; Del Duca, S. Compatible and incompatible pollen-styles interaction in *Pyrus communis* L. show different transglutaminase features, polyamine pattern and metabolomics profiles. *Front. Plant. Sci.* **2019**, *10*, 741.

3.2. A metabolomic study of leaves and adventitious roots of *Solanum dulcamara* chemotypes

Ilaria Chiocchio, Redouan Adam Anaia, Fredd Vergara, Nicole M. van Dam

Ongoing research

Background and aim of the work

In addition to the production of primary metabolites, directly involved in normal growth, development and reproduction, plants also synthesize compounds known as secondary metabolites. It has been predicted that plant intraspecific phytochemical diversity (i.e. chemodiversity) accounts for at least 1.060.000 metabolites [1]. However, only 200.000 plant secondary metabolites have been identified so far [2]. These metabolites play a variety of functions, governing the interaction with the environment and other organisms [3]. Secondary metabolites may vary qualitatively and quantitatively among individuals of the same plant species giving rise to chemotypes. Intraspecific chemodiversity has been observed in many plant species within and among populations. For example, *Artemisia annua*, one of the most studied medicinal plant, displayed two contrasting chemotypes: one producing high amount of the antimalarial principle ‘artemisinin’, and the other one producing significantly lower quantity of the same metabolite [4]. It is postulated/assumed that chemical diversity is the results of adaptation to the abiotic environment [5] and co-evolutionary processes between plants, and their interaction partners such as herbivores and pathogens [6]. Chemodiversity also affects plant ecology, since specialized metabolites serve as defense against predators and attractant for pollinators [7]. For instance, Tewes and Müller [8] have recently reported how different *Bunias orientalis* chemotypes shown different resistance to fungal pathogens. However, the current knowledge about chemodiversity and its effects on plant biodiversity and ecology is still incomplete.

The huge diversity of secondary metabolites has fascinated scientists for decades, especially for their pharmaceutical properties. Yet, questions about the biological role of secondary metabolites in plants, and about the origin of plant chemodiversity, are still unanswered [9]. A consequence of chemodiversity, is its impact on the biological or pharmacological activity of a plant extract [10]. Thus, many efforts have been made in order to phytochemically characterize chemotypes and to develop analytical techniques for quality control in plants with relevant economic profit [11].

Solanum dulcamara L., also known as ‘bittersweet nightshade’, is among the herbaceous species which display intraspecific chemodiversity. It belongs to the Solanaceae family and is considered a good model plant to study, since it can host pathogens of other commercially important Solanaceae, such as tomato or potato [12].

Differently to domesticated and widely cultivated nightshades, *S. dulcamara* is a wild species found in contrasting habitats, from relatively dry sandy areas to regularly inundated floodplains [13].

As described since the late '70s [14], *S. dulcamara* produces diverse steroidal glycosides that differ in the presence of nitrogen or oxygen in the nucleus, saturation degree, number and type of conjugated sugars. More recently, it was reported that this structural diversity influences herbivores preference, suggesting the involvement of steroidal glycosides in plant defense [15,16].

Although *S. dulcamara* intra-specific variation in steroidal glycoside composition is already reported, little is known about the chemical variation among ontogenetic stages and among organs.

A crossing scheme carried out by the Molecular Interaction Ecology research group (MIE) of the German Centre for Integrative Biodiversity Research (Leipzig, Germany) allowed to select chemotypes differing for their leaf steroidal glycoalkaloids composition, detected by Liquid Chromatography coupled with Mass Spectrometry (LC-MS). In particular, two chemotypes showing steroidal glycoalkaloids differing in the saturation degree, one labeled as “U” (unsaturated) and the other one labeled as “S” (saturated).

In this framework, the present work examines *S. dulcamara* “S” and “U” chemotypes with the aim of characterizing the phytochemical profiles of different organs across two developmental stages, namely vegetative and generative (flowering).

Methods

Plant material

Solanum dulcamara seeds were collected in two contrasting environments in The Netherlands, coastal dunes (Zandvoort Dry 4 - ZD04) and island wetlands (Texel Wet 12 - TW12) [15]. Knowing that the leaves of TW12 contain saturated glycoalkaloids, while ZD04 produces predominantly unsaturated glycoalkaloids, accessions of both types were used to produce reciprocal hybrids. Here, progeny of the cross TW12 x ZD04 (TW12 maternal genome, TW12 pollen donor) was preliminarily analyzed by liquid chromatography-quadrupole-time of flight-mass spectrometry (LC-QTOF-MS) and classified into two groups on the basis of the leaf chemotype. Stem cuttings were taken from two lines of each group and propagated in order to obtain enough material for the

experiment. Plants were grown in greenhouse and after 6 weeks, leaves and roots samples were collected and immediately frozen in liquid nitrogen in order to obtain samples for the vegetative stage. Simultaneously, stem cuttings were taken to grow new plants, which were kept under the same greenhouse conditions until they reached the generative (flowering) stage. As soon as the plants flowered for at least 7 days a second sampling was carried on at this growth stage, collecting also flowers and stems in addition to leaves and roots. Frozen samples were freeze-dried, ground with a Ball mill (Mixer Mill MM 400, Retsch GmbH, Haan, Germany), and stored at -80°C in the dark.

Extraction and metabolomic analysis

Plant material was extracted and analyzed by LC-qToF-MS (Impact HD, Bruker GmbH, Bremen, Germany XXX) following the metabolomics protocol developed by the MIE group [15] with slight modifications. Briefly, 20 mg of leaf material per sample and 10 mg of root material per sample were extracted in 1 mL of solvent. Hence, leaves extracts were diluted 1:10 while root extracts were diluted 1:5 and then analyzed. Data were processed using Metaboscape (Bruker GmbH, Bremen, Germany) and multivariate data analysis was carried out in SIMCA 16 (Umetrics, Umeå, Sweden).

Preliminary results and future perspectives

The Principal Component Analysis based on MS data of the vegetative stage (Fig.1) showed three separate groups (Fig.1A): two groups of leaves samples and one of roots samples.

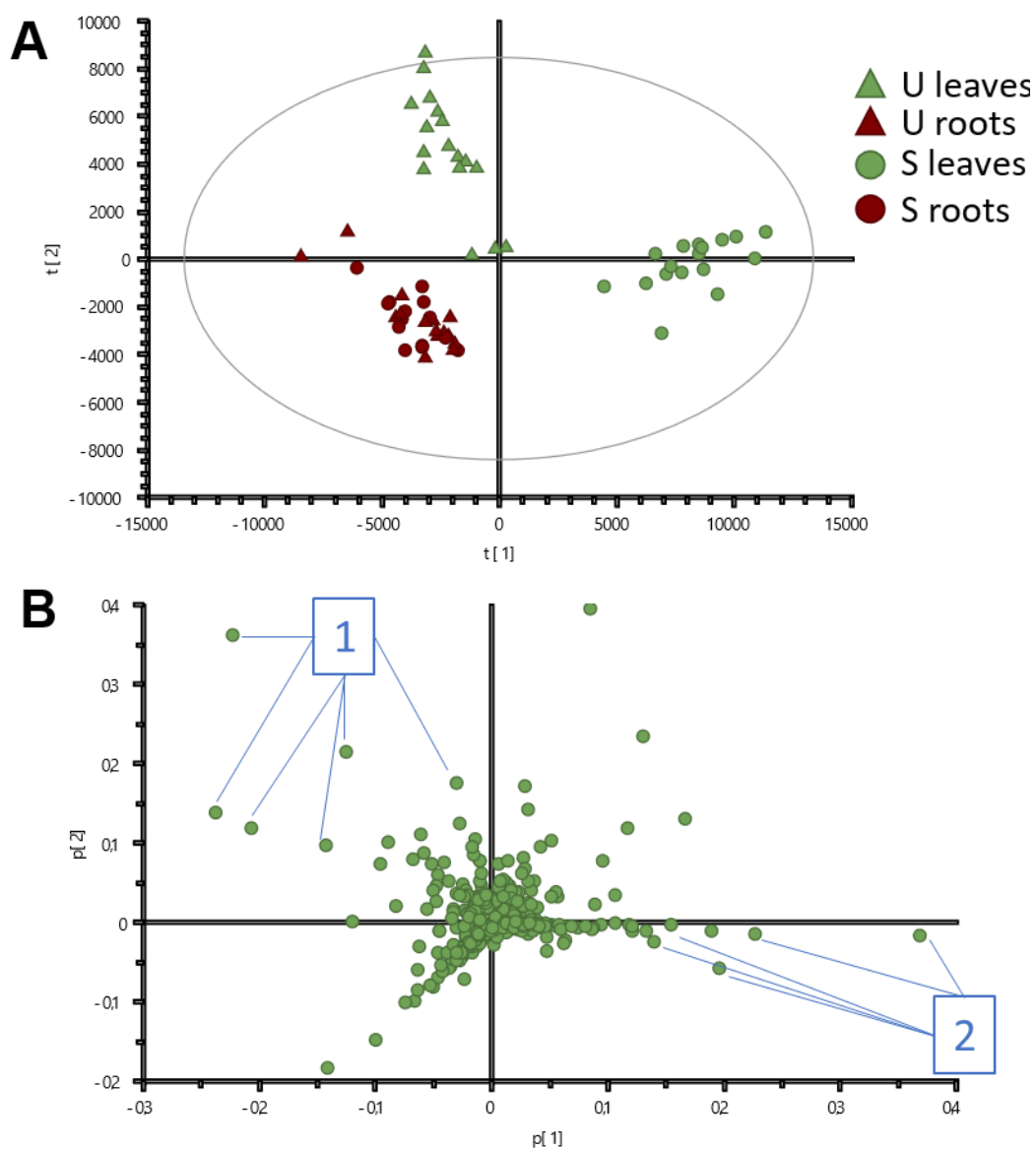


Fig. 1. PCA of LC-qToF-MS based metabolomic data of plants at vegetative stage. A) Score scatter plot; B) Loading scatter plot, 1- steroidal glycoalkaloids having aglycone whose m/z value is 414.33, 2- steroidal glycoalkaloids having aglycone whose m/z value is 416.35.

This result confirmed that the leaves belonging to two different chemotypes had different metabolomic profiles. In particular, the chemotype labeled as “S” contained steroidal glycoalkaloids having diagnostic m/z value equal to 416.35. The other chemotype, labeled as “U”, showed steroidal glycoalkaloids having m/z value equal to 414.33. Both these peaks are ascribable to the aglycone (eluting at retention time from minute 5 to minute 6.6) and since they differ from each other by 2 Da they likely have different saturation degree. This was already expected and is consistent with the upstream

broad chemotyping. However, the metabolomic analysis also highlighted other features important for the separation and ascribable to more polar compounds (eluting at retention time from minute 1 to minute 4) that still need to be characterized. For example m/z values 183.68, 120.68, and 163.03 are important in the separation between “S” and “U” leaves, while 138.05, 142.12, and 84.08 are among the peaks which leads the clustering between roots and leaves.

Interestingly, roots of both S and U chemotype clustered together and separately from the leaves. This result showed that *S. dulcamara* chemodiversity is differently expressed in roots and leaves. From the inspection of the roots mass spectra it emerged that, independently of the chemotype, they contain both types of steroidal glycoalkaloids.

Transcriptomic analysis has been planned in order to clarify the molecular mechanisms underling these chemical differences. Moreover, clones of the experimental plants were grown in fields with the aim of investigating the interactions among plants and above-belowground herbivores.

References

1. Afendi, F. M., Okada, T., Yamazaki, M., Hirai-Morita, A., Nakamura, Y., Nakamura, K., ... & Saito, K. KNApSAcK family databases: integrated metabolite–plant species databases for multifaceted plant research. *Plant and Cell Physiology* **2012**, *53*(2), e1–e1.
2. Kessler, A., & Kalske, A. Plant secondary metabolite diversity and species interactions. *Annual Review of Ecology, Evolution, and Systematics* **2018**, *49*, 115–138.
3. Pagare, S., Bhatia, M., Tripathi, N., Pagare, S., & Bansal, Y. K. Secondary metabolites of plants and their role: Overview. *Current Trends in Biotechnology and Pharmacy* **2015**, *9*(3), 293–304.
4. Czechowski, T., Larson, T. R., Catania, T. M., Harvey, D., Wei, C., Essome, M., ... & Graham, I. A. Detailed phytochemical analysis of high-and low artemisinin-producing chemotypes of *Artemisia annua*. *Frontiers in plant science* **2018**, *9*, 641.
5. Defosse, E., Pitteloud, C., Descombes, P., Glauser, G., Allard, P. M., Walker, T. W., ... & Rasmann, S. Spatial and evolutionary predictability of phytochemical diversity. *Proceedings of the National Academy of Sciences* **2021**, *118*(3).
6. Whitehead, S. R., Bass, E., Corrigan, A., Kessler, A., & Poveda, K. Interaction diversity explains the maintenance of phytochemical diversity. *Ecology Letters* **2021**, *24*(6), 1205–1214.
7. Demain, A. L., & Fang, A. The natural functions of secondary metabolites. In *History of modern biotechnology I* (pp. 1–39) **2000**. Springer, Berlin, Heidelberg.
8. Tewes, L. J., & Müller, C. Interactions of *Bunias orientalis* plant chemotypes and fungal pathogens with different host specificity in vivo and in vitro. *Scientific reports* **2020**, *10*(1), 1–11.
9. Saito, K. The Origin of Plant Chemodiversity–Conceptual and Empirical Insights. *Frontiers in Plant Science* **2020**, *11*.
10. Mkindi, A. G., Tembo, Y., Mbega, E. R., Medvecky, B., Kendal-Smith, A., Farrell, I. W., ... & Stevenson, P. C. Phytochemical analysis of *Tephrosia vogelii* across East Africa reveals three chemotypes that influence its use as a pesticidal plant. *Plants* **2019**, *8*(12), 597.
11. György, Z., Incze, N., & Pluhár, Z. Differentiating *Thymus vulgaris* chemotypes with ISSR molecular markers. *Biochemical Systematics and Ecology* **2020**, *92*, 104118.

12. Flier, W. G., Van den Bosch, G. B. M., & Turkensteen, L. J. Epidemiological importance of *Solanum sisymbriifolium*, *S. nigrum* and *S. dulcamara* as alternative hosts for *Phytophthora infestans*. *Plant Pathology* **2003**, 52(5), 595–603.
13. Calf, O.W., and Van Dam, N.M. Bittersweet bugs: The Dutch insect community on *Solanum dulcamara*. *Entomologisch Berichten* 72 **2012**, 193–197.
14. Máthé I., Máthé I. Data to the European area of the chemical taxa of *Solanum dulcamara* L. *Acta Botanica Academica Scientiarum Hungaricae* **1973**, 19: 441–451.
15. Calf, O. W., Huber, H., Peters, J. L., Weinhold, A., & van Dam, N. M. Glycoalkaloid composition explains variation in slug resistance in *Solanum dulcamara*. *Oecologia* **2018**, 187(2), 495–506.
16. Calf, O. W., Huber, H., Peters, J. L., Weinhold, A., Poeschl, Y., & van Dam, N. M. Gastropods and insects prefer different *Solanum dulcamara* chemotypes. *Journal of chemical ecology* **2019**, 45(2), 146–161.

Conclusions

This thesis connects the study of plant specialized metabolites to Sustainable Developmental Goals through three main research lines: circular economy, sustainable agriculture, and biodiversity valorization.

The first aim of this work was to valorize plant neglected matrices for circular economy. Knowing that plants are endowed with numerous bioactive compounds, this aim was achieved by analyzing the phytochemical profile and the bioactivity of several wastes and by-products of plant origin. In particular, neglected plant matrices including agricultural residues, pest plants, and by-products from herbal and food industries were tested to assess their antioxidant and antibacterial activities against plant pathogens. Twenty-three neglected matrices proved to exert *in vitro* antioxidant activity and notably, residues of aromatic plants after distillation showed antibacterial activity against the Gram-positive bacterium *Clavibacter michiganensis* subsp. *nebraskense*. Some of the detected compounds were rosmarinic acid, shikimic acid, sclareol, and hydroxycinnamic acids. This result supports the use of by-products from herbal industry in phytoprotection, and this is particularly interesting since, from the literature review conducted for this thesis, it emerged that only poor studies suggesting the exploitation of plant specialized metabolites in agriculture were found.

Moreover, by-products of chestnut cultivation (spiny burs and leaves) were evaluated for their potential neuroprotective properties in BV-2 microglia cells. This research line allowed several bioactive samples to be found and the ¹H NMR profiling provided preliminary information about their chemical composition. In addition, flavonoids, such as astragalín, isorhamnetin glucoside, and myricitrin were identified in *Castanea sativa* leaves through NMR and MS experiments.

These results support the valorization of waste and by-products of plant origin through their use in several sectors, such as nutraceutical and agrochemical, and contribute to the circular economy.

The second research line aimed at achieving a deeper knowledge of plant-environment interactions in view of sustainable agriculture. In this framework, two research projects were carried out, the first one was focused on *Sorghum bicolor* grown in field and subjected to different environmental and anthropic conditions. Metabolomics

coupled to agrometeorological survey revealed interesting information about sorghum crop allowing to identify dhurrin as biomarker of quality and crop development. In addition, environmental features such as water supply and soil composition proved to influence sorghum metabolome providing important insights for its cultivation. The second project was a greenhouse experiment on *Taxus baccata* exposed to different LED lighting. NMR-based metabolomics contributed to monitor *T. baccata* growth in a smart greenhouse and showed that LED light supplementation enhances the synthesis of sucrose and aromatic compounds especially at the highest tested intensity ($150\mu\text{M m}^{-2} \text{ s}^{-1}$).

The third aim was the investigation of spontaneous plants in order to enhance biodiversity valorization. Hence, 35 samples from Sardinian plants, including also endemic species, were investigated for their antitumor activity on human osteosarcoma cells U2OS. Five plants resulted endowed with promising bioactivity namely, *Arbutus unedo*, *Cynara cardunculus*, *Centaurea calcitrapa*, *Smilax aspera*, and *Tanacetum audibertii*. Mono- and two-dimensional NMR experiments were carried out to investigate the phytochemical composition of the active samples allowing the identification of the most abundant metabolites, such as phenolics and sesquiterpene lactones. This work supports other evidence about the potential of highly biodiverse region and their related chemodiversity to favor the discovery of bioactive compounds. Finally, a study of *Solanum dulcamara* chemodiversity was also carried out. In this case, different organs of two selected chemotypes were investigated through an MS-based metabolomics approach. Steroidal glycoalkaloids in the leaves resulted involved in the discrimination between the two chemotypes, while the same was not observed in the roots. This result laid the basis for future investigations aimed at clarifying the molecular mechanisms underlying the observed chemodiversity and its ecological consequences.

In conclusion, the results reported in this thesis highlighted the importance of natural products chemistry and metabolomics to promote sustainable development in many different ways. Plant specialized metabolites represent an endless resource to be explored and the study of these molecules, both as bioactive agents and for their importance in plant-environment interactions, offers great opportunities to enhance circular economy, sustainable agriculture, and to valorize biodiversity. In this context, the metabolomics approach, providing the base to build databases, make predictions, and favor data sharing, is particularly suitable.